

Al-Dabbagh, A. G. A (2015) Use of microarray technology for the detection of a range of RNA viruses in clinical samples. PhD thesis, University of Nottingham.

**Access from the University of Nottingham repository:**

<http://eprints.nottingham.ac.uk/29356/1/USE%20OF%20MICROARRAY%20TECHNOLOGY%20FOR%20THE%20DETECTION%20OF%20A%20RANGE%20OF%20RNA%20VIRUSES%20IN%20CLINICAL%20SAMPLES.pdf>

**Copyright and reuse:**

The Nottingham ePrints service makes this work by researchers of the University of Nottingham available open access under the following conditions.

This article is made available under the University of Nottingham End User licence and may be reused according to the conditions of the licence. For more details see:  
[http://eprints.nottingham.ac.uk/end\\_user\\_agreement.pdf](http://eprints.nottingham.ac.uk/end_user_agreement.pdf)

**A note on versions:**

The version presented here may differ from the published version or from the version of record. If you wish to cite this item you are advised to consult the publisher's version. Please see the repository url above for details on accessing the published version and note that access may require a subscription.

For more information, please contact [eprints@nottingham.ac.uk](mailto:eprints@nottingham.ac.uk)



The University of  
**Nottingham**

UNITED KINGDOM • CHINA • MALAYSIA

Faculty of Medicine and Health Sciences

School of Molecular Medical Science

**USE OF MICROARRAY TECHNOLOGY FOR  
THE DETECTION OF A RANGE OF RNA  
VIRUSES IN CLINICAL SAMPLES**

by

**Ayman Ghanim Ameen AL-Dabbagh**

B.Sc., M.Sc.

Thesis Submitted to the University of Nottingham for  
The degree of Doctor of Philosophy

May 2015

## **DECLARATION OF ORIGINALITY**

**Title of Thesis:** Use of Microarray Technology for the Detection of  
a Range of RNA Viruses in Clinical Samples

This is to declare that I am the sole author of this thesis, that the original work is my own, unless otherwise referenced and indicated, and that this thesis has not been submitted for a higher degree to any other institution or university.

Author's Name: **AYMAN GHANIM AMEEN AL-DABBAGH**

Signature: Ayman Aldabbagh

Date: 29/06/2015

## **Abstract**

There are many RNA virus pathogens of humans including influenza, parainfluenza, enteroviruses, parechoviruses, coronaviruses, pneumoviruses, and metapneumoviruses. These commonly invade and infect the respiratory and gastrointestinal tracts, giving rise to acute and chronic respiratory tract infections, and some may also reach the central nervous system (CNS) either via haematogenous or neural routes resulting in a variety of clinical presentations, (e.g. meningitis, encephalitis) which may lead to severe irreparable damage such as poliomyelitis especially in young children. Early correct diagnosis of viral infections is indispensable in order to prevent potential outbreaks which threaten the public health worldwide and might lead to high morbidity and some with significant mortality.

Several laboratory techniques such as virus isolation, direct visualization of viral particles, detection of viral antigens and/or nucleic acids, and detection of host immune response (e.g. anti-viral antibodies) to infection, are available for diagnosis, but may have significant drawbacks such as time-inefficiency, cost and certain individual limitations. Microarray technology offers one way to overcome some of these limitations.

In this study, a microarray chip containing 7967 oligonucleotides (probes) covering the whole genomes of human enteroviruses, rhinoviruses, respiratory syncytial viruses, metapneumoviruses and influenza viruses was designed and constructed using both OligoArray and Agilent eArray software, to allow simultaneous detection of any of the above viruses present in any clinical specimen.

This virochip was tested against positive controls and clinical samples known to contain RNA nucleic acids of these viruses. Viral RNA was reverse transcribed, and amplified. Considerable effort was expended in trying to optimise a multiple displacement amplification (MDA) protocol for whole genome amplification, and in addition, long-range PCR was also utilised. Amplification products were fragmented, labelled and loaded into a hybridization reaction with the designed viral probes printed on the virochip. The results revealed (i) a number of technical problems associated with MDA; (ii) that some probes either failed to recognise their intended targets, or produced cross-reactive signals with non-intended targets; (iii) that many of the designed probes hybridized to their relevant viral nucleic acids and generated hybridization signals of high fluorescent intensity offering an opportunity to develop this probe array in order to be used for the identification of a wide variety of virus species up to the serogroup level or beyond (if required) specifically those causing CNS and respiratory tract infections.

## **Thesis related publication**

- 1- The School of Molecular Medical Sciences Postgraduate Research Day (MOL-PG Research Day) at University of Nottingham, Nottingham, 26<sup>th</sup> June 2012.
- 2- East Midlands Universities Postgraduate Student Research (EMU) conference at University of Nottingham/Sutton Bonington campus, Nottingham, 5th July, 2012.
- 3- 7<sup>th</sup> VACCINE & ISV congress at Sitges, Barcelona, Spain, 27<sup>th</sup> - 29<sup>th</sup> October 2013.

## **Acknowledgments**

First and foremost, I would like to thank Allah almighty, the Lord of the universe for all his uncounted bounties bestowed upon me which one of them was granting me this opportunity for a PhD study at the University of Nottingham; one of the globally reputable universities.

I take this opportunity to acknowledge the Iraqi Ministry of Higher Education and Scientific Research represented by the Iraqi Cultural Attach in London for providing the financial support for my PhD study.

I would like to express my sincerest gratitude and deepest appreciation to Professor William Irving for his supervision, patience, constant guidance and unlimited support throughout my PhD journey. I will never ever forget his painstaking efforts in proofreading the chapter drafts which have attributed greatly to improve my thesis.

I would also like to express my heartfelt thankfulness and respectful to Dr Paddy Tighe; the genius of Molecular Biology and Bioinformatics for his supervision, continuous encouragement, invaluable scientific and technical mentorship and moral support. I gained a lot from his vast knowledge, expertise and proficiency.

I am also extremely indebted to Professor Peter Simmonds, Dr Taha Yusri, Dr. Zoie Aiken and Katrina Levi who made this study possible through providing the control and clinical samples. I gratefully acknowledge Dr. Mohammed Abdel-Hakeem and Dr. Ola Nigm for their guidance and generous assistance during my research. I will forever be grateful to my closest friend Dr. Omar Akram who was at all times willing to help and offer his best suggestions for a lot of problems even if he was busy with his PhD study, I really miss him now.

Many thanks go to Colin Nicholson for his excellent technical assistance especially in using Agilent Bioanalyzer machine and the GenePix 4200AL autoloader scanner. Thanks also to all my colleagues in Immunology department in the University of Nottingham.

I would like to express my deep sense of appreciation to the University of Nottingham for all the invaluable support offered by many of the academic and administrative staff especially in the last few months during writing my thesis when I was very concern on my family and relatives in my city Mosul, in Iraq due to the turmoil there. I would like to extend my appreciation to Leanne Mitchell, Ian Kerr and Ruth Hudson who they had clear imprints and unforgettable roles in my years of PhD study. Special thanks to the professors Kusai Alchalabi, Basima Abdulla, Yahya Alneimy, Saad Ghanim and Sahi Dahi for their support during the application process for the PhD study.

I will not forget my mother, my deceased father and my father and mother in law who they deserve my sincere gratitude and profound appreciation for their unconditional love, support and encouragement during all my life. My acknowledgement is also extended to my brothers (Bashar, Ammar and Mohammad), sister (May) and brothers (Ghassan, Marwan and Raied) and sister (Alaa) in law who they provided assistance and moral support.

## **Special acknowledgment**

My special acknowledgements and gratitude go to my beloved wife Mafaz who was like a candle, burn to light up my road since the first day of our marriage. She dedicated her life and shouldered all the responsibilities of our family



without caring about her health to provide the suitable atmosphere to complete my PhD study. She was a model of selfless in her patience, support and love. My thanks to my beloved son Hassan who was waiting my return to house in the window every night during my study. He was always cheering me up through his genius in school especially in maths and power point. I also would like to thank my sweet little daughter Basma who added moments of funny and excitement during the stress time of my thesis writing. I am indebted to all of them more than they know.

## ABBREVIATIONS

A	Adenine
APTS	Aminopropyltriethoxysilane ethanol
ARI	Acute respiratory illness
BBB	Blood brain barrier
BLAST	Basic Local Alignment Search Tool
β-ME	B-mercaptoethanol
BSA	Bovine serum albumin
C	Cytosine
CBS	Centre for Biomolecular Sciences
cDNA	Complementary DNA
CDS	Coding sequences
CNS	Central nervous system
CPE	Cytopathic effect
CSF	Cerebrospinal fluid
Ct	Threshold cycle
Cy3	Cyanine 3
Cy5	Cyanine 5
DMF	Dimethylformamide
DNA	Deoxyribonucleic acid
DOL	Degree of labelling
DOP-PCR	Degenerate oligonucleotide-primed-PCR
dsDNA	Double stranded deoxyribonucleic acid
dT	Deoxythymine
dUTP	Deoxyuridine triphosphate
EDTA	Ethylenediaminetetraacetic acid
EIA	Enzyme Immunoassay
EM	Electron microscopy
FW-primer	Forward primer
G	Guanine
GAL	GenePix array list
HA	Hemagglutinin

HEF	Hemagglutinin esterase fusion
HHVs	Human herpesviruses
HIV	Human immunodeficiency virus
HMPV	Human metapneumovirus
HPRT	Hypoxanthine-guanine phosphoribosyltransferase
HRSV	Human respiratory syncytial virus
HSV	Herpes simplex virus
ICTV	International Committee on Taxonomy of Viruses
IF	Immunofluorescence technique
IG	Immunoglobulin
IME	Immunolectron microscopy
IUPAC	International Union of Pure and Applied Chemistry
KB	Kilo base
L	Large polymerase subunit
LRT	Lower respiratory tract
M	Matrix protein
MDA	Multiple displacement amplification
MEGA	Molecular evolutionary genetics analysis
MPV	Metapneumovirus
N	Nucleocapsid
NA	Neuraminidase
NCBI	National Centre for Biotechnology Information
NEP	Nuclear export protein
NEP	Nuclear export protein
NGS	Next generation sequencing
NH4Ac	Ammonium acetate
NHS	N-hydroxysuccinimide
NP	Nucleocapsid protein
NS1	Non-structural 1
NT	Nucleotide
ORF	Open reading frame
P	Phosphoprotein
PA	Polymerase acid

Pb	Base pair
PB1	Polymerase basic 1
PB2	Polymerase basic 2
PBS	Phosphate buffered saline
PCR	Polymerase chain reaction
PMT	Photo-multiplier tube
QMC	Queen's Medical Centre
QPCR	Quantitative real time PCR
RIA	Radioimmunoassay
RNA	Ribonucleic acid
rNTPs	Ribonucleoside triphosphates
rRNA	Ribosomal ribonucleic acid
RSV	Respiratory syncytial virus
RT-PCR	Reverse transcriptase-PCR
RV-primer	Reverse primer
SARS	Sever acute respiratory syndrome
SDS	Sodium dodecyl sulphate
SH	Small hydrophobic
SNP	Single nucleotide polymorphisms
SSC	Saline sodium citrate
T	Thymine
TAE	Tris-acetic acid-EDTA
TAS	Total Array System
TBST	Tris buffered saline 0.01% tween
TEAC	Tetraethylammonium chloride
tRNA	Transfer ribonucleic acid
ULS	Universal linkage system
UPGMA	Unweighted pair group method with arithmetic mean
URT	Upper respiratory tract
UTRs	Untranslated regions
UV	Ultraviolet
VZV	Varicella zoster virus
WGA	Whole genome amplification

## Contents:

<b>1</b>	<b>General Introduction</b> .....	<b>1</b>
1.1	Diagnoses of viral infections: .....	3
1.1.1	Cell Culture:.....	4
1.1.2	Electron microscopy: .....	5
1.1.3	Antigen detection technique: .....	8
1.1.4	Detection of viral genetic material: .....	10
1.1.5	Indirect detection methods:.....	13
1.2	Central nervous system viral infections:.....	14
1.2.1	Pathogenesis of the CNS viral infections.....	15
1.2.2	The neurotropic viruses .....	16
1.3	Respiratory tract viral infections.....	22
1.3.1	Pathogenesis of the respiratory viral infections .....	23
1.3.2	Respiratory viruses .....	23
1.4	Microarray-based technology .....	34
1.5	Aim of the study .....	41
1.5.1	Objectives .....	41
<b>2</b>	<b>Designing multiple hybridization probes for the selected RNA viruses</b> .....	<b>42</b>
2.1	Introduction.....	43
2.2	Aims.....	43
2.3	Methods .....	44
2.3.1	Downloading viral genome sequences .....	44
2.3.2	Viral sequence analysis.....	55
2.3.3	Multiple viral probes design .....	57
2.3.4	Testing the specificity of the designed probes:.....	59
2.3.5	Printing the designed probes.....	59
2.4	Results .....	60
2.4.1	Phylogenetic analysis results of the human enterovirus genomic sequences .....	60
2.4.2	Alignment results of the viral genomes sequences .....	69
2.4.3	Generation of the consensus sequences .....	71
2.4.4	Probe design.....	73
2.4.5	Probe printing .....	77
2.5	Discussion.....	78

<b>3</b>	<b>Application of the multiple displacement amplification technique for testing the specificity of the designed viral microarray</b> .....	<b>81</b>
3.1	Introduction.....	82
3.2	Aims.....	84
3.3	Materials and methods .....	84
3.3.1	Specimens .....	84
3.3.2	Samples preparation.....	85
3.3.3	Amplification of the whole viral RNA .....	96
3.3.4	Labelling the samples amplicons .....	99
3.3.5	Manufacturing experimental microarrays.....	106
3.3.6	Manual hybridization of the experimental microarrays.....	113
3.3.7	Quantification of the pTZ18R amplicons using microplate fluorescence assay	116
3.3.8	Quantitative real time PCR (QPCR).....	117
3.4	Results .....	120
3.4.1	MDA results.....	120
3.4.2	Amplicon fragmentation results.....	121
3.4.3	HPRT-PCR results.....	122
3.4.4	Labelling results.....	123
3.4.5	Hybridization results of the experimental enterovirus microarray ....	125
3.4.6	Optimizing MDA/hybridization process using pTZ18R plasmid.....	126
3.4.7	Target amplification using GenomePlex complete WGA kit: .....	141
3.4.8	Quantitative real time PCR (QPCR) results: .....	144
3.5	Discussion:.....	149
3.5.1	Sample preparation: .....	149
3.5.2	cDNA synthesis: .....	150
3.5.3	Amplification of the viral cDNA: .....	151
3.5.4	Fragmenting viral amplicons .....	153
3.5.5	Labelling viral amplicons .....	154
3.5.6	Hybridizing viral amplicons: .....	154
<b>4</b>	<b>Application of the Polymerase Chain Reaction for testing the specificity of the designed viral microarray</b> .....	<b>156</b>
4.1	Introduction.....	157
4.2	Aims.....	158
4.3	Materials and methods .....	158
4.3.1	Samples.....	158
4.3.2	Amplification of the samples nucleic acids using PCR technique.....	159

4.3.3	Fragmenting and Labelling the PCR products.....	168
4.3.4	Manual hybridization experiments .....	169
4.4	Results .....	174
4.4.2	Experimental hybridization results of the VZV, pTZ18R and enterovirus long-PCR products.....	184
4.4.3	Hybridization results using virochip.....	186
4.4.4	Description of the virochip .....	189
4.5	Discussion.....	253
5	<b>General Discussion</b> .....	258
5.1	Conclusion .....	260
5.2	Limitations of study .....	261
5.3	Future work.....	261
6	<b>REFERENCES</b> .....	263

## List of figures:

<b>Figure 1-1:</b> Routes of viral entry to the central nervous system. ....	16
<b>Figure 1-2:</b> Schematic diagram shows the size and organization of the human enterovirus genome.....	21
<b>Figure 1-3:</b> The common clinical syndromes of the URT and LRT caused by the different types of viruses. ....	26
<b>Figure 1-4:</b> Schematic diagram of influenza virus particle showing the arrangement of the viral genome segments, and their functions.....	30
<b>Figure 1-5:</b> Schematic diagram of the genomic maps of the HRSV, HMPV and their viral particle.....	33
<b>Figure 1-6:</b> Shows the schematic drawing of multivirus chip. ....	35
<b>Figure 1-7:</b> Schematic diagram shows the working principle of Phi 29 DNA polymerase during MDA process. ....	40
<b>Figure 2-1:</b> Phylogenetic analysis of the aligned 5'UTR nucleic acid sequences of the Human enterovirus A strains. ....	61
<b>Figure 2-2:</b> Phylogenetic analysis of the aligned CDS nucleic acids sequences of the Human enterovirus A strains. ....	62
<b>Figure 2-3:</b> Phylogenetic analysis of the aligned 3'UTR nucleic acids sequences of the Human enterovirus A strains.....	62
<b>Figure 2-4:</b> Phylogenetic analysis of the aligned 5'UTR nucleic acid sequences of the Human enterovirus B strains. ....	64
<b>Figure 2-5:</b> Phylogenetic analysis of the aligned CDS nucleic acid sequences of the Human enterovirus B strains. ....	65
<b>Figure 2-6:</b> Phylogenetic analysis of the aligned 3'UTR nucleic acid sequences of the Human enterovirus B strains. ....	66
<b>Figure 2-7:</b> Phylogenetic analysis of the aligned 5'UTR nucleic acid sequences of the Human enterovirus C strains. ....	67
<b>Figure 2-8:</b> Phylogenetic analysis of the aligned CDS nucleic acid sequences of the Human enterovirus C strains. ....	68
<b>Figure 2-9:</b> Phylogenetic analysis of the aligned 3'UTR nucleic acid sequences of the Human enterovirus C strains .....	68
<b>Figure 2-10:</b> Phylogenetic analysis of the aligned 5'UTR, CDS and 3'UTR nucleic acid sequences of the Human enterovirus D strains.....	69
<b>Figure 2-11:</b> Part of the multiple sequence alignment of the 5'UTR nucleic acid of a group of the closely relative stains of the Human enterovirus C.....	70



<b>Figure 2-12:</b> Part of the multiple sequence alignment of the nucleic acid sequences of the HA genomic segment of the H1N1 subtypes.....	71
<b>Figure 2-13:</b> Nucleic acid consensus sequence of cluster 1 of the phylogenetic tree of the aligned 5'UTR of the Human enterovirus A.....	72
<b>Figure 2-14:</b> Schematic drawing of the printed chip containing 8 arrays of the designed viral probes. ....	77
<b>Figure 3-1:</b> Schematic diagram showing the linearization process of the pTZ18R plasmid.....	90
<b>Figure 3-2:</b> Schematic drawing showing the working principle of the universal linkage system used for labelling nucleic acids.....	103
<b>Figure 3-3:</b> Schematic drawing of the amplicons bands blotting. ....	105
<b>Figure 3-4:</b> Schematic drawing of the experimental enterovirus microarray. ....	109
<b>Figure 3-5:</b> Schematic drawing of the experimental pTZ18R-enterovirus microarray .....	112
<b>Figure 3-6:</b> Metal 24 wells hybridization cassette.....	114
<b>Figure 3-7:</b> Loading of the standard, unknown and NTC samples into the QPCR microplate wells.....	119
<b>Figure 3-8:</b> Thermal profile used in QPCR .....	119
<b>Figure 3-9:</b> Agarose gel electrophoresis of the amplified enteroviral cDNA generated by MDA technique for 1.5 hour at 30 oC.....	121
<b>Figure 3-10:</b> Agarose gel electrophoresis of the fragmented enteroviral amplicons.....	122
<b>Figure 3-11:</b> Agarose gel electrophoresis of the HPRT PCR products. ....	123
<b>Figure 3-12:</b> Example of the nanodrop plots of the HPRT amplicon labelled with dyomics 547 fluorescent dye. ....	124
<b>Figure 3-13:</b> Hybridization reaction results of the labelled amplified products with the experimental enterovirus microarray as seen on the GenePix laser scanner. ....	126
<b>Figure 3-14:</b> Agarose gel electrophoresis of the digested pTZ18R plasmid. ....	128
<b>Figure 3-15:</b> Electropherogram generated from analysis of the plasmid RNA using Agilent 2100 Bioanalyzer .....	129
<b>Figure 3-16:</b> Agarose gel electrophoresis of the amplified pTZ18R plasmid and enteroviral RNA using Whole transcriptome kit. ....	131
<b>Figure 3-17:</b> Agarose gel electrophoresis of the unpurified amplicons generated from MDA of the pTZ18R plasmid and enteroviral RNA using Whole transcriptome kit.....	132
<b>Figure 3-18:</b> Hybridization reaction results of the labelled amplified products with the experimental plasmid-enterovirus microarray as seen on the GenePix laser scanner. ....	134

<b>Figure 3-19:</b> Agarose gel electrophoresis of the pTZ18R products generated from the fragmentation process using DNase I at different times.....	136
<b>Figure 3-20:</b> Agarose gel electrophoresis of the biotinylated amplicons blotted on a nylon membrane as seen under infrared scanner. ....	138
<b>Figure 3-21:</b> Microplate fluorescence assay calibration results of the products generated from MDA.....	141
<b>Figure 3-22:</b> Schematic diagram showing the amplification steps of the target nucleic acids using GenomePlex complete WGA kit. ....	142
<b>Figure 3-23:</b> Agarose gel electrophoresis of the amplified materials generated from amplification process using GenomePlex complete WGA kit. ....	144
<b>Figure 3-24:</b> Standard curve of the enterovirus QPCR.....	146
<b>Figure 3-25:</b> Amplification plots of the enterovirus QPCR.....	148
<b>Figure 3-26:</b> Schematic diagram showing the steps used for optimizing hybridization process using the experimental microarrays. ....	155
<b>Figure 4-1:</b> Schematic drawing of the experimental HHVs-pTZ18R-enterovirus microarray.....	172
<b>Figure 4-2:</b> Agilent Microarray Hybridization Chamber Kit used for holding the microarray slide. ....	173
<b>Figure 4-3:</b> Agarose gel electrophoresis of the pTZ18R cDNA and VZV DNA generated from Long-range PCR amplification reaction.....	175
<b>Figure 4-4:</b> Agarose gel electrophoresis of Long-range PCR amplification of enteroviral cDNA.....	176
<b>Figure 4-5:</b> Agarose gel electrophoresis of the clinical enterovirus amplicons generated from Long-range PCR reaction using temperature gradient. ....	177
<b>Figure 4-6:</b> Agarose gel electrophoresis of HMPV amplicons generated from Long-range PCR amplification process.....	178
<b>Figure 4-7:</b> Agarose gel electrophoresis of HRSV amplicons generated from Long-range PCR amplification process.....	179
<b>Figure 4-8:</b> Schematic diagram shows the size and position of the amplified and the unamplified parts of the HMPV and HRSV genomes generated from long-range PCR amplification process. ....	180
<b>Figure 4-9:</b> Agarose gel electrophoresis of the products of HA and NA genomic segments of H1N1 and H3N2 subtypes generated from Long-range PCR amplification process. ....	182
<b>Figure 4-10:</b> Schematic diagram shows the size of the amplified and unamplified products generated from long-range PCR amplification process of the HA and NA segments of the H1N1 and H3N2 subtypes of the human influenza virus A. ....	183

<b>Figure 4-11:</b> Hybridization reaction results of the labelled VZV, pTZ18R and enterovirus amplicons generated from Long-range PCR amplification process with the experimental HHVs-pTZ18R-enterovirus microarray as seen on the GenePix laser scanner.....	185
<b>Figure 4-12:</b> Schematic diagram shows the loading sequence of the labelled amplicons into the chambers of the Agilent gasket slide.....	188
<b>Figure 4-13:</b> Scanned image of the virochip after hybridization reactions with the labelled amplicons of the enteroviruses, HMPV, HRSV and human influenza virus A.....	189
<b>Figure 4-14:</b> Signals generated from the hybridization reactions of four of the human enterovirus amplicons with the probes designed specifically for the human enteroviruses using OligoArray software. ....	193
<b>Figure 4-15:</b> Signals generated from the hybridization reactions of four of the enterovirus amplicons with the probes designed specifically for the human enteroviruses using Agilent eArray software.....	196
<b>Figure 4-16:</b> Signals of cross hybridization generated between the human enterovirus probes and the HMPV amplicons.....	202
<b>Figure 4-17:</b> Signals of cross hybridization generated between the human enterovirus probes and the HRSV amplicons.....	203
<b>Figure 4-18:</b> Signals of cross hybridization generated between the human enterovirus probes and the amplicons of the H1N1 and H3N2. ....	203
<b>Figure 4-19:</b> Signals generated from the hybridization reactions of four of the HMPV amplicons with the probes designed specifically for the HMPV using OligoArray software. ....	206
<b>Figure 4-20:</b> Signals of cross hybridization generated between the HMPV probes and the human enterovirus amplicons. ....	213
<b>Figure 4-21:</b> Signals of cross hybridization generated between the HMPV probes and the HRSV amplicons. ....	214
<b>Figure 4-22:</b> Signals of cross hybridization generated between the HMPV probes and the amplicons of the H1N1 and H3N2.....	214
<b>Figure 4-23:</b> Signals generated from the hybridization reactions of four of the HRSV amplicons with the probes designed specifically for the HRSV using OligoArray software. ....	217
<b>Figure 4-24:</b> Signals generated from the hybridization reactions of the HRSV-1 amplicon with the probes designed specifically for the HRSV using Agilent eArray software. ....	218

<b>Figure 4-25:</b> Signals of cross hybridization generated between the HRSV probes and the human enterovirus amplicons. ....	233
<b>Figure 4-26:</b> Signals of cross hybridization generated between the HRSV probes and the HMPV amplicons. ....	234
<b>Figure 4-27:</b> Signals of cross hybridization generated between the HRSV probes and the amplicons of the H1N1 and H3N2.....	235
<b>Figure 4-28:</b> Signals generated from the hybridization reactions of four of the human influenza virus A amplicons with the probes designed specifically for the HA and NA genomic segments of the H1N1 and H3N2 using OligoArray software.....	238
<b>Figure 4-29:</b> Signals generated from the hybridization reactions of four of the human influenza virus A amplicons with the probes designed specifically for the HA and NA genomic segments of the H1N1 and H3N2 using Agilent eArray software. ....	240
<b>Figure 4-30:</b> Signals of cross hybridization generated between the H1N1and H3N2 probes and the human enterovirus amplicons.....	251
<b>Figure 4-31:</b> Signals of cross hybridization generated between the H1N1and H3N2 probes and the HMPV amplicons. ....	252
<b>Figure 4-32:</b> Signals of cross hybridization generated between the H1N1and H3N2 probes and the HRSV amplicons. ....	252

## List of Tables:

<b>Table 1-1:</b> Shows the important DNA and RNA viruses causing CNS infections. ....	17
<b>Table 1-2:</b> Viruses causing respiratory tract infections .....	24
<b>Table 2-1:</b> Shows the strains of the Human enterovirus A and their NCBI accession numbers. ....	46
<b>Table 2-2:</b> Shows the strains of the Human enterovirus B and their NCBI accession numbers. ....	47
<b>Table 2-3:</b> Shows the strains of the Human enterovirus C and their NCBI accession numbers. ....	50
<b>Table 2-4:</b> Shows the strains of the Human enterovirus D and their NCBI accession numbers. ....	51
<b>Table 2-5:</b> Shows the strains of the human rhinoviruses and their NCBI accession numbers . ....	52
<b>Table 2-6:</b> Shows strains of HMPV and their NCBI accession numbers .....	53
<b>Table 2-7:</b> Shows strains of HRSV and their NCBI accession numbers .....	53
<b>Table 2-8:</b> Shows the selected genomic segments of the human influenza viruses A, B and C, their size and the subtype numbers.....	55
<b>Table 2-9:</b> The code of the degenerate nucleotides used at the mismatches positions of the aligned viral nucleic acid sequences. ....	73
<b>Table 2-10:</b> Characteristics of the probes designed for the consensus sequence of the 5' UTR nucleic acid sequences of the Human coxsackievirus A4, 14, 6 and 16 which were clustered together in cluster-1 in the 5'UTR phylogenetic tree of the Human enterovirus A strains. ....	74
<b>Table 2-11:</b> Shows the number of the probes designed for each species or subtype of the selected RNA viruses, using OligoArray and Agilent eArray software .....	75
<b>Table 3-1:</b> Features of the primers used for HPRT-PCR.....	95
<b>Table 3-2:</b> The optimal cycling programme used for HPRT-PCR amplification .....	96
<b>Table 3-3:</b> Sequences of the enterovirus probes used for printing the experimental enterovirus microarray.....	108
<b>Table 3-4:</b> Sequence of the HPRT probe used as internal positive control in the experimental microarrays. ....	108
<b>Table 4-1:</b> Characteristics of the primers used for PCR amplification of the viral groups. ....	165
<b>Table 4-2:</b> Sequences of the HHVs probes used for printing the experimental microarray.....	170

<b>Table 4-3:</b> Shows the amplification methods and fluorescent dyes used for amplifying and labelling the viral samples used for validating the designed viral probes.....	187
<b>Table 4-4:</b> Shows the number of the probes designed for each species or subtype of the selected RNA viruses, using OligoArray and Agilent eArray software .....	190
<b>Table 4-5:</b> Characteristics of the human enterovirus OligoArray and Agilent eArray probes which showed higher fluorescent intensities with the amplicons of the echovirus 7, coxsackievirus A-21 and clinical enterovirus .....	198
<b>Table 4-6:</b> Characteristics of the HMPV OligoArray probes which showed higher fluorescent intensities with the HMPV amplicons .....	207
<b>Table 4-7:</b> Characteristics of the HRSV OligoArray and Agilent eArray probes which showed higher fluorescent intensities with the HRSV amplicons. ....	220
<b>Table 4-8:</b> Characteristics of the OligoArray and Agilent eArray probes of the HA and NA genomic segments of the human influenza virus A which showed higher fluorescent intensities with the H1N1 and H3N2 amplicons.....	242

# **1 General Introduction**

Viruses are the plural of virus, a Latin word which means poison or venom. They are described as simple, acellular and tiny particles which have the ability to pass through the finest filters that retain mycoplasma, the smallest type of bacteria. Nanometre (1 nm =  $10^{-9}$  m) is the most appropriate unit used to measure their diminutive size. Therefore, they are very difficult to be seen even with the light microscope (Carter and Saunders, 2007, Condit, 2013). Viruses have been divided according to their genomic nature into two groups: deoxyribonucleic acid (DNA) viruses and ribonucleic acid (RNA) viruses (Willey et al., 2008).

The argument concerning the living nature of these agents is still continuing since their early description and then their first naming as viruses in 1898 by Martinus Beijerinck. Most scientists agree that viruses are non-living because there is no evidence to confirm their ability to reproduce independently, which is considered as one of the main features of life. They must attack and parasitize the cells of all living beings such as humans, animals, plants, yeasts and fungi which are known as eukaryotes. These organisms all possess a nucleus, an enveloped organelle surrounding their genetic materials, normally deoxyribonucleic acid (DNA). Even prokaryotes, those primitive unicellular microorganisms that lack a nucleus, such as bacteria, are invaded by viruses. Therefore, viruses are generally known as obligate intracellular parasites which control the metabolic activities and genetic functions of living cells and direct them towards their benefits; reproduction and existence. Viral parasitism damages the host cells which mostly appear as symptoms of disease indicating viral infection (Collier and Oxford, 2000, Wagner and Hewlett, 2008, Flint et al., 2009).



## 1.1 Diagnoses of viral infections:

Viruses are the common causative agents of different types of human infections which may lead to significant morbidity and a considerable rate of mortality (Kannangai et al., 2010). Early correct diagnosis of viral infections is indispensable in order to prevent their potential outbreaks which threaten the public health worldwide and might lead to high morbidity and some with significant mortality, and allows for introduction of appropriate antiviral therapy (e.g. acyclovir, ganciclovir, foscarnet and neuraminidase inhibitors), and decreases the potential cost and toxicity of inappropriate therapy (Storch, 2000, Morshed et al., 2007, Mizutani et al., 2007, Kannangai et al., 2010).

Some of these infections are asymptomatic whereas others are diverse in their clinical signs. Accurate diagnosis of these infections requires demonstration of the virus or at least its components in appropriate clinical samples ideally by using highly sensitive laboratory methods within a short time, or of a host immune response to infection. Different techniques have been used in order to fulfil these purposes either directly or indirectly through developments in the immunological, biotechnological and molecular fields, such as virus isolation, direct visualization of viral particles, detection of viral antigens and/or nucleic acids, and detection of host immune response (e.g. anti-viral antibodies) to infection (Muir et al., 1998, Boriskin et al., 2004, Lodes et al., 2007, Rabenau et al., 2007, Kannangai et al., 2010).

### 1.1.1 Cell Culture:

Success in propagating human cells in vitro at the beginning of 20<sup>th</sup> century, was the starting point for the isolation and growing of viruses in the laboratory. Embryonated eggs and laboratory animals were firstly used and then replaced by cell culture techniques which utilize isolated cells separated from either human or animal trypsinized tissues (Freshney, 2000). This method is the only one able to generate viable isolate of virus which can be employed to investigate characteristics such as virulence, pathogenicity and antiviral susceptibility in more detail (Charlton et al., 2009). An additional major advantage of cell culture was the ability to generate effective viral vaccines, some of which are still commercially produced in this way (Dwyer et al., 2006). However, it is difficult to detect every possible virus which might be present in any clinical sample by using one type of cell culture because the latter will be unable to supply all the requirements necessary for the growth of all medically related viruses. Thus, diagnostic laboratories would use various types of cell culture such as cell lines derived from monkey kidney in addition to those obtained from human fibroblast and epithelial cells in order to enhance the range of viruses which could be isolated and identified (Chonmaitree et al., 1989, Leland and Ginocchio, 2007).

The presence of a virus within a cell culture can be recognized by the production of a cytopathic effect (CPE). This term describes pathological effects of viruses on their host cells including alteration in cell morphology, formation of multinucleated giant cells, or syncytia, through fusion between two or more singular cells, cell vacuolation and cell lysis. These effects can be typically detected by light microscopy (Lodes et al., 2007).

This technique, however, has a number of disadvantages:

- 1- Potential high cost of the different types of cell culture and their maintenance in-house, such that not all types may be available in all diagnostic laboratories (Hsiung, 1984).
- 2- It requires technical expertise to examine the probable viral CPE every couple of days for more than one week of incubation period in order to confirm viral diagnosis.
- 3- Many viruses are slow-growing in tissue culture, meaning that diagnosis by this technique may take up to two weeks. This is exacerbated when there are low titres of virus in the starting material.
- 4- There are health and safety issues associated with working with live viruses in the laboratory (Storch, 2000, Leland and Ginocchio, 2007, Charlton et al., 2009).
- 5- Not all viruses can be isolated in tissue culture e.g. hepatitis C virus and human papilloma viruses are extremely difficult to culture in this way.

### **1.1.2 Electron microscopy:**

Electron microscopy (EM) has been used in the diagnosis of viral infections since 1939, eight years after its early discovery by Ernest Ruska, who was also the first to visualize tobacco mosaic virus (a plant pathogen). Subsequently, EM was applied in the differentiation and diagnosis of smallpox and chickenpox infections, and provided the first image of poliovirus, contributing to the discovery of enteroviruses (Nagler and Rake, 1948, Van Rooyen and Scott, 1948, Melnick and Phillips, 1970). Current knowledge of the accurate morphological and structural features of viruses as well as their mechanisms of

attachment and replication was obtained by electron microscopy. This information was very beneficial and led to an early scheme of viral classification, determination of viral types parasitizing humans and contributed to the development of vaccines and antiviral therapy (Hazelton and Gelderblom, 2003).

Detection of viral particles by means of this technique mainly depends on the negative staining principle by use of phosphotungstic acid. This stain is unable to penetrate virus particles which therefore appear as white spots against a dark field. Therefore, it does not necessitate use of any particular reagents which makes it faster and easier than some other methods such as cell culture, which requires use of specific nutrition media in order to maintain the viability of the cultured cells which are still difficult to produce as commercial kits. Therefore, EM is preferred to diagnose viruses which cannot be cultivated, and has been commonly used in the surveillance systems of detection and identification of any strange emerging pathogens especially viruses (Collier and Oxford, 2000). Electron microscopy is efficient in the detection of both viable and unviable isolates of viruses even those which were stored for decades e.g. variola (Goldsmith and Miller, 2009).

On the other hand, diagnosis of viral infections by EM is accompanied with some difficulties which are:

- 1- Due to its high equipment cost, it is not available in all diagnostic laboratories, and even where it is available, it is not widely used for routine screening of a great number of specimens (Hazelton and Gelderblom, 2003).

- 2- Lack of sensitivity. EM can only detect virus particles present at a minimal concentration of  $10^6 \text{ ml}^{-1}$ , therefore, it is hard to diagnose any clinical sample which may contain less than this concentration. In this case, it is recommended to add virus-specific antibodies to the samples in order to cluster viral particles and facilitate their detection. This process is termed immunoelectron microscopy (IME), but this adds an extra cost to the technique (Collier and Oxford, 2000, Murray et al., 2009).
- 3- Fluid specimens may require concentration via centrifugation especially those in small amounts (e.g. cerebrospinal fluid samples), which necessitate use of an ultracentrifuge (e.g. at 100,000 xg) in order to concentrate viral particles which have low density mass (Goldsmith and Miller, 2009).
- 4- An experienced microscopist is required in order to provide a reliable diagnosis (Collier and Oxford, 2000).
- 5- It is not recommended for specimens which require inoculation in viral transport media e.g. swabs, in order to maintain the viability of suspected viruses especially influenza and respiratory syncytial viruses, since this results in dilution of virus-titre (Jensen and Johnson, 1994, Hazelton and Gelderblom, 2003).
- 6- It can only identify viruses at the family level. For that reason, other methods are required for further identification of specific isolates beyond this taxonomic stage (Goldsmith and Miller, 2009).
- 7- It requires a high standard of cautiousness to deal with risky infectious samples.

### 1.1.3 Antigen detection technique:

Viruses produce abundant amounts of proteins and enzymes during their replication. These viral particles accumulate inside the infected host cell and behave as antigens to stimulate the immune system to generate specific protein factors called antibodies against them in order to neutralize their pathogenic effect, which leads to the formation of large insoluble complexes of antigen-antibody. Viruses can be identified through the detection of viral proteins (antigens) which can be secreted or leak out from the injured host cells into body fluids, or are expressed on cell membrane surfaces or within the cell (Grandien, 1996, Murray et al., 2009).

Liu in 1956 was the first one who tried to diagnose influenza infections by using an immunofluorescence technique (IF) as a specific tool for direct identification of viral antigens in clinical samples. The principle of this method is based on utilizing laboratory prepared antiviral antibody which is attached covalently to a fluorescent molecule (e.g. fluorescein-isothiocyanate-labelled rabbit antiviral antibody) in order to facilitate the detection of the viral antigen-antibody complex by using ultraviolet (UV) light. Enzyme immunoassay (EIA) is another means for the indirect detection of viral antigens, but the antibody is conjugated to a particular enzyme e.g. horseradish peroxidase or alkaline phosphatase, which can catalyse the conversion of a chromophore compound in order to mark the presence of antigen (Grandien, 1996, Storch, 2000, Murray et al., 2009).

Antigen detection techniques may be improved for both identification and estimation purposes of the viral antigen by using antibodies labelled with radioactive reagents such as iodine-125. During this radioimmunoassay (RIA),

the probable viral antigens which are suspected in the patient's specimen, are captured by the radiolabelled antibodies. Then, the complexes of antigen-antibody are precipitated to measure their radioactivity. Advantages of antigen detection techniques include:

- 1- Rapidity. Staining and visualisation can be completed within 2 hours of receipt of specimen.
- 2- It is highly flexible-in principle it can be used to diagnose any virus for which a poly- or mono-clonal antibody is available. Amongst other applications, detection of viral antigens is a useful method for the diagnosis of virus infections of the respiratory tract, the gastrointestinal tract, and vesicular skin lesions.
- 3- It does not require the presence of viable isolates as the recognition process is immunological.

Disadvantages include:

- 1- Some viruses (e.g. enteroviruses and rhinoviruses) cannot be identified by this technique due to their extensive antigenic heterogeneity as well as the absence of cross reacting antigens.
- 2- Body fluids such as cerebrospinal fluid (CSF) contain low concentrations of causative viruses which may result in missing the detection of the above viruses and lead to false negative results (Chonmaitree et al., 1989, Storch, 2000).
- 3- It requires preparation of large number of animal antisera which should be kept on hand (Chonmaitree et al., 1989, Grandien, 1996).
- 4- The required dilutions of the reagents which are used in this method in addition to the interference of the clinical samples' peroxidases diminish its

sensitivity to about 44% (Leland and Ginocchio, 2007, Chonmaitree et al., 1989, Linde et al., 1997, Charlton et al., 2009).

5- It requires technical expertise. Weak fluorescent signals may arise from use of strong UV light or from improper mounting (Grandien, 1996), giving rise to difficult-to-interpret or even false negative results.

6- Performance of commercial kits may vary considerably between manufacturers, meaning that results from different laboratories may not be comparable.

#### **1.1.4 Detection of viral genetic material:**

Detection and analysis of the viral genome in clinical samples is mainly based on the molecular biological methods which have been widely used over the past two decades as powerful emerging tools in clinical diagnostic laboratories for routine diagnoses of viral infections. These methods improved the poor sensitivity and specificity, and time-inefficiency of the traditional means by using nucleic acid amplification techniques which opened a novel strategy to overcome the problem of very low quantity of viral genetic materials and produce more detectable concentration directly from any clinical samples especially those unculturable or slow-growing viruses (Tang et al., 1997, Kittler et al., 2002, Morshed et al., 2007). Polymerase chain reaction (PCR) is one of the most common utilized techniques, which was invented during the early 1980s by Kary Mullis to produce millions of copies of the target sequence of genome in vitro within a few hours (Mullis, 1990, Murray et al., 2009). This enzymatic technique involves use of complementary synthetic oligonucleotides which bind covalently to a specific region of nucleic acid



sequence (usually DNA), and act as primers for a thermostable polymerase enzyme to synthesize new copies of target DNA through approximately 30-50 repeated thermal cycles. Each cycle starts with nucleic acid denaturation at around 94°C, followed by annealing of the primers to their complementary target at around 50 °C and ends with primer elongation at around 70°C which leads to doubling the quantity of the nucleic acids (Lu et al., 2002).

This process is mainly used to amplify DNA viruses, but reverse transcriptase (RT)-PCR was devised to amplify the genomic materials of RNA viruses which firstly should be converted to the complementary sequence of DNA (cDNA) by employing a reverse transcriptase enzyme. Other types of PCR were developed to enhance the sensitivity of the conventional one. Nested PCR was designed to detect the diminutive quantities of the target nucleic acids by using two different sets of primers through dual amplification steps (Poggio et al., 2000). Multiplex PCR was developed and applied for the amplification of more than one target sequence in specimens throughout a single PCR run. Contamination is the major problem of PCR assay technique especially the nested-amplification mode, which arises during the transferring period of the amplification products from the first round to the second one. However, this hitch was solved either by utilizing a layer of wax or oil in order to separate the two mixtures of amplification or by using sets of designed primers appropriate for annealing in different temperatures. In general, it is recommended to locate PCR machines in specific cabinets which should be provided with independent sets of micropipettes equipped with filtered tips, sterile tubes and batch of reagents inside isolated laboratories away from the analyzing area of amplified products (Tang et al., 1997, Casas et al., 1999, Lu et al., 2002).

The applicable combination between the chemistry of PCR and fluorescent detection of the amplified products in one vessel, led to a new generation of PCR-based assay known as Real-time PCR which revolutionized the clinical microbiology fields (Nissen and Sloots, 2002). It is faster than the conventional PCR due to its simultaneous amplification and detection of the target nucleic acids. Furthermore, it is more sensitive and specific than all other conventional methods, and valuable in the analysis of large numbers of clinical specimens as it can be performed in a 96 microwell format. Real-time (PCR) has been adopted in many clinical diagnostic laboratories since its application became easier (semi-automatically) now due to the availability of its reagents (primers and enzymes) as commercial kits, and robotic machines to perform the various stages of the assay. Furthermore, decreasing of the amplicons' contamination risk in addition to accurate detection of the copy number of the target nucleic acid were the enormous benefits of real-time PCR since both amplification and detection steps of the target nucleic acids can be achieved in one closed vessel (Niesters, 2002, Espy et al., 2006).

In spite of the significant role of PCR techniques in the detection of viral nucleic acids in clinical samples, it has some difficulties:

- 1- The required expertise which is limited to special referral laboratories.
- 2- Samples should be collected and analyzed at definite periods of infection.

Any delay in these two processes might affect the sensitivity of PCR due to the reduction of the viral concentration which can be lost and lead to false negative results. False negative results are also attributed to the existence of polymerase inhibitors such as hairpin or endonucleases in the clinical samples (Koskiniemi et al., 2002, Debiassi and Tyler, 2004).

- 3- The high cost of the instrument as well as its reagents and probe detection requirements. Moreover, it necessitates suitable physical space.
- 4- The reliability of the results mainly depends on the efficient extraction processes of the nucleic acids from variant clinical specimens (Niesters, 2002).
- 5- It requires highly conserved sequence of the target nucleic acids for efficient reaction with the primers (Yolken et al., 1989).
- 6- Serotyping or subclassification of some viruses (e.g. enteroviruses) is quiet difficult (Muir et al., 1998).

However, the overall advantages of using PCR in the diagnosis of human viral infections through the amplification of viral nucleic acids presented in clinical samples outweighs its disadvantages.

### **1.1.5 Indirect detection methods:**

Serological techniques which detect the host humoral immune response can be used for the diagnosis of some viral infections. It is recommended when other means of viral detection such as virus isolation or antigen detection are unavailable or their results are negative (Dwyer et al., 2006). It is helpful for the identification of acute (or recent) infection, through the detection of specific viral immunoglobulin (Ig)-M antibodies in serum samples. The detection of this type of antibody which reaches its peak concentration during the first 2-3 weeks of viral infections indicates the acute recent primary infection. On the other hand, recognition of antiviral specific –IgG indicates a past infection (Murray et al., 2009). However, serological techniques also have a number of potential drawbacks due to:

- 1- Possible false negative and false positive results.
- 2- Some viruses (e.g. mumps and parainfluenza) possess related antigens and lead to serological cross reaction, confusing identification of the accurate pathogen. While others viruses such as rhinoviruses have too specific antibodies which are unable to recognize other members of the same family.
- 3- Antigenic composition of different viruses cannot be identified by this procedure.
- 4- Most patients hold some pre-existing antibodies for some particular viral infections (e.g. influenza) therefore; it is difficult to recognize the recent infection (Dwyer et al., 2006, Murray et al., 2009).

This thesis will be concerned with the development of molecular assays for the diagnosis of central nervous system (CNS) and respiratory tract viral infections. These particular infections are therefore reviewed in the following sections.

## **1.2 Central nervous system viral infections:**

Although, the central nervous system is protected by the skull, bony cage, thick dura mater and blood brain barrier (BBB) represented by cerebral capillaries, it is vulnerable for infection by more than 100 different viruses. These viruses might invade and infect the spinal cord, the brain stem, the cerebellum or the cerebrum causing myelitis, rhomboencephalitis, cerebellitis and encephalitis respectively as well as aseptic meningitis (Lu et al., 2002, Debiassi and Tyler, 2004, Irani, 2008). Some of these viral infections (e.g. viral meningitis) are

widespread in clinical practice and responsible for considerable rates of morbidity and mortality throughout the world especially in the United States, Europe, Japan and Southeast Asia (Tyler, 2009, Big et al., 2009). More than 12,700 cases of aseptic meningitis were reported every year to the Centres for Disease Control during the period from 1973 to 1983. This infection is responsible for approximately 5-15 cases per 100,000 cases of annual hospital admission in the United Kingdom (Chonmaitree et al., 1989, Chadwick, 2005). On the other hand, focal infections which are accompanied by viral myelitis can be confused with those of non-infectious origin.

### **1.2.1 Pathogenesis of the CNS viral infections**

Viruses usually reach the CNS by either haematogenous or neuronal route. Through the haematogenous route; viruses are transmitted by the blood from their portal of entry and initial multiplication sites in the mucosal surfaces of the respiratory tract, gut and lymph nodes throughout the body towards the secondary multiplication sites (extraneural sites) in the spleen, liver muscles and vascular tissues, and then cross the BBB towards the CNS via the infected leukocytes, cerebral capillary endothelial cells or choroid plexus (figure 1-1). The peripheral nerves and/or the olfactory nerve represent the possible conduits for certain viruses to reach and infect the CNS through the neuronal route (Kaslow and Evans, 1997, Pokorn, 2003, Cassady and Whitley, 2004, Sundaram et al., 2011, Heise and Virgin, 2013).

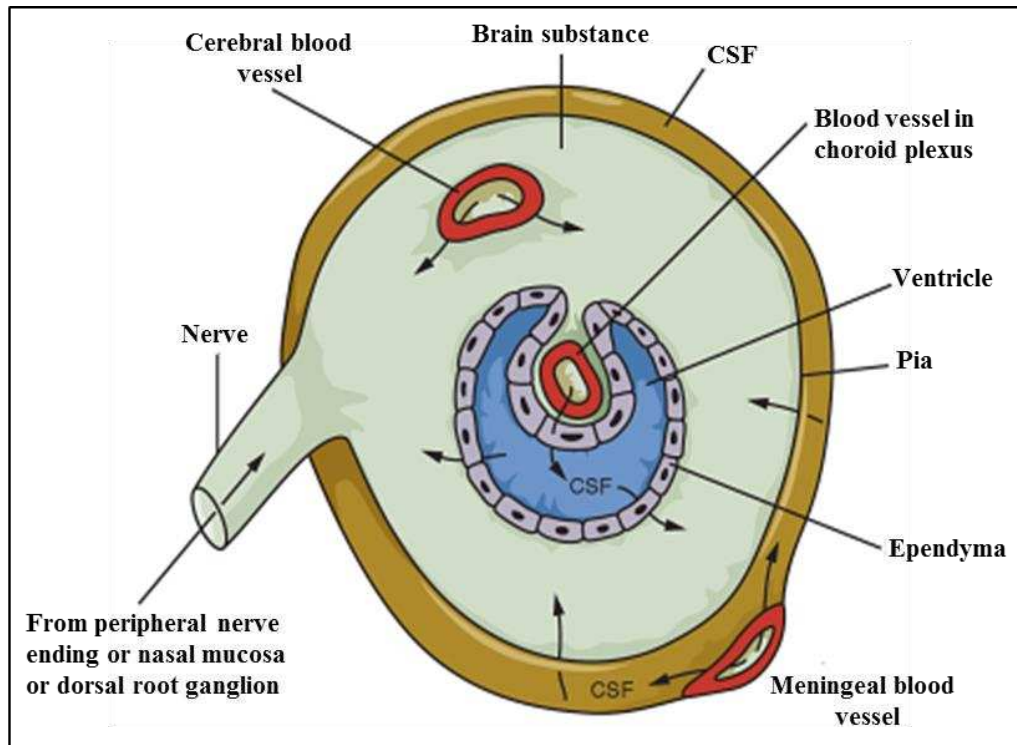


**Figure 1-1: Routes of viral entry to the central nervous system.**

Adopted from (Cassady and Whitley, 2004).

### 1.2.2 The neurotropic viruses

Many types of viruses including DNA and RNA viruses have been identified as neurotropic viruses due to their ability to colonize and infect the nerve cells, and causing CNS viral infections (table 1-1). Some of these neurotropic viruses have caused outbreaks of CNS viral infections during the past decades (e.g. West Nile virus encephalitis in the 90s) and since that time the researches were directed toward diagnosis of CNS viral infections.

Table 1-1: Shows the important DNA and RNA viruses causing CNS infections, and their invasion routes.

	Family	Genus	Species	Route to CNS	CNS infection
<b>DNA viruses</b>	Adenoviridae	Mastadenovirus	Human mastadenovirus A-G	Haematogenous	- Meningitis - Encephalitis
	Herpesviridae	Simplexvirus	Human herpesvirus 1	Neuronal	- Encephalitis - Meningitis - Meningoencephalitis
			Human herpesvirus 2		
		Varicellovirus	Human herpesvirus 3	- Haematogenous - Neuronal	- Cerebellitis - Encephalitis - Meningitis - Myelitis
		Lymphocryptovirus	Human herpesvirus 4	Haematogenous	- Encephalitis - Meningitis - Myelitis
		Cytomegalovirus	Human herpesvirus 5	Haematogenous	- Encephalitis
	Roseolovirus	Human herpesvirus 6	?		
Poxviridae	Orthopoxvirus	Vaccinia virus	Haematogenous	- Encephalomyelitis	
<b>RNA viruses</b>	Arenaviridae	Arenavirus	Lymphocytic choriomeningitis virus	Haematogenous	- Meningitis - Encephalitis
	Bunyaviridae	Orthobunyavirus	California encephalitis virus		
	Reoviridae	Coltivirus	Colorado tick fever virus		
	Togaviridae	Alphavirus	Eastern equine encephalitis virus		
	Retroviridae	Lentivirus	Human immunodeficiency virus 1	Haematogenous	- Encephalopathy - Encephalitis
	Rhabdoviridae	Lyssavirus	Rabies virus	Neuronal	- Encephalitis - Encephalomyelitis

	Family	Genus	Species	Route to CNS	CNS infection
<b>RNA viruses</b>	Picornaviridae	Enterovirus	Nonpolio enteroviruses: - Coxsackieviruses - Echoviruses	Haematogenous	- Meningitis - Myelitis
			Polioviruses	- Haematogenous - Neuronal	- Meningitis - Meningoencephalitis - Myelitis
	Flaviviridae	Flavivirus	West Nile virus	Haematogenous	- Meningitis - Encephalitis
			Japanese encephalitis virus		
			St. Louis encephalitis virus		
			Murray Valley encephalitis virus	Haematogenous	Encephalitis
			Tick-born encephalitis virus	Haematogenous	- Meningitis - Encephalitis
			Western equine encephalitis virus Venezuelan equine encephalitis virus		
	Paramyxoviridae	Morbillivirus	Measles virus	Haematogenous	- Encephalitis - Subacute sclerosing panencephalitis
		Rubulavirus	Mumps virus	Haematogenous	- Meningitis - Encephalitis - Myelitis
Orthomyxoviridae	Influenza viruses	Influenza A, B virus	Haematogenous	- Encephalitis	

Adapted from (Cassady and Whitley, 2004).



### 1.2.2.1 Human enteroviruses

Human enteroviruses are the prominent etiological agents of many of the human diseases every year which associated with different clinical manifestations ranging from asymptomatic to mild or severe infections which may threaten patient life (Hyoty and Taylor, 2002, Diaz-Horta et al., 2011). Human enteroviruses belong to the Picornaviridae family, and include more than 100 different viral serotypes which are the major invaders of the CNS (Simmonds, 2006, Michos et al., 2007). Nonpolio human enteroviruses which include various serotypes of coxsackieviruses, echoviruses and enterovirus types 68 to 71 are classified into four species: Enterovirus A, B, C and D are the causative agents of more than 90% of viral meningitis and encephalitis which are the reason for approximately 10% of mortality rates in the neonates (Irani, 2008, Tebruegge and Curtis, 2009). Euscher and his colleagues ((Euscher et al., 2001) reported that the neurodevelopmental delays in the newborn is a consequence of the enterovirus infections during pregnancy. Polioviruses comprise three additional serotypes of the human enteroviruses and are classified within the Enterovirus C, which can infect the spinal cord and causing paralytic poliomyelitis (Chonmaitree et al., 1989, Chadwick, 2005, Rhoades et al., 2011). Commonly, children are at high risk of enteroviral CNS infections especially during the summer/autumn of their first year of age in tropical and subtropical countries. Generally, polio viral infections are now controlled worldwide, except in the Middle East region. These infections might lead to a severe unrepairable damage of the nervous tissues such as poliomyelitis (Redington and Tyler, 2002).

### 1.2.2.1.1 Structure of human enteroviruses

Human enteroviruses are spherical particles consist of non-enveloped, icosahedral capsid of 27-30 nm in diameter containing the viral genome which consists of single strand RNA of approximately 7400 nucleotides having the same sense as mRNA which can be immediately translated into viral proteins by the host cell. Therefore, it is referred to such viruses as positive sense single stranded RNA viruses. The genomic RNA of the human enteroviruses consists of a single long open reading frame (ORF) encodes an individual viral polyprotein which comprises three units (P1 to P3) of approximately 2200 amino acids, flanked by the 5' and 3' untranslated regions (UTRs). The translated viral polyprotein units are cleaved by viral proteases in order to generate four structural proteins (VP4, VP2, VP3 and VP1) from P1 unit, and seven nonstructural proteins (2A to 2C and 3A to 3D) from both P2 and P3 units (figure 1-2). The four viral structural proteins are assembled together in order to form the enterovirus capsid, while the nonstructural viral proteins are involved in viral replication and RNA synthesis (Oberste et al., 2004, Agol, 2006, Nakashima and Ishibashi, 2010, Boros et al., 2011, Diaz-Horta et al., 2011, Rhoades et al., 2011, Racaniello, 2013).

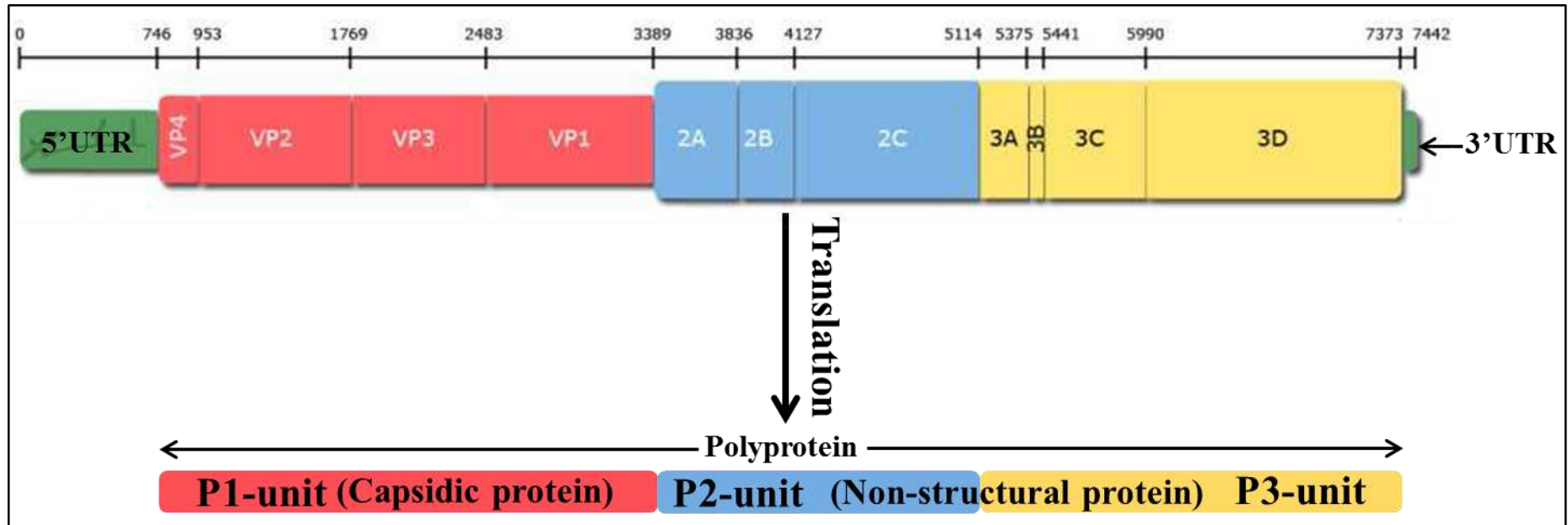


Figure 1-2: Schematic diagram shows the size and organization of the human enterovirus genome.

Adopted from ((Diaz-Horta et al., 2011, Racaniello, 2013).

### 1.3 Respiratory tract viral infections

Infectious diseases were controlled at least to a degree for much of the twentieth century in Western human populations, but since 1980s many viral infections have emerged as well as those previously identified which were thought to be under control (Kuiken et al., 2003). Respiratory tract infections are common and caused by multiple different types of pathogens, but viruses are responsible for more than 85% of these infections (Chiu et al., 2008). Seasonal outbreaks of viral respiratory tract infections are the major causes of illness, loss of individuals' productivity and hospitalization which add further burden on the budgets of the national health care (Bertino, 2002, Gillim-Ross and Subbarao, 2006). In general most infants and children suffer from a common cold-like illness 3-8 times each year which increases by 30% in developing countries (Bertino, 2002, Bharaj et al., 2009). These respiratory tract infections are also considered to be a major problem in immunocompromised and elderly people (Garbino et al., 2004).

The respiratory system includes upper respiratory tract (URT) which consists of each of the nasal cavity, pharynx, larynx and trachea, and lower respiratory tract (LRT) which comprises of the bronchi, bronchioles and lungs. The organs of both URT and LRT except lungs are lined with a layer of ciliated epithelial cells covered with a layer of mucus secreted by specific glandular cells scattered among the epithelial cells, called goblet cells. This mucociliary structure represents a physical barrier responsible for the protection of the respiratory system against microbial pathogens through ciliary movement and continuous mucus flow which end up with expelling such pathogens. Alveolar macrophages play an important role in eliminating pathogens that can evade

the mucociliary structure, and reach the lungs (Rubins, 2003, Manjarrez-Zavala et al., 2013).

### **1.3.1 Pathogenesis of the respiratory viral infections**

Most viruses enter the URT carried by aerosols and droplets produced by sneezing and/or coughing of other patients. Some viruses especially those of a large size which are trapped in the turbinates and sinuses may colonize these sites and then spread to other adjacent organs causing upper respiratory tract infections. Other viruses of a smaller size which are able to avoid the mucociliary action of the URT can spread downwards via the bronchi and bronchioles, reach the alveoli inside the lungs and cause lower respiratory tract infections (Andersen, 1998, Flint et al., 2009).

### **1.3.2 Respiratory viruses**

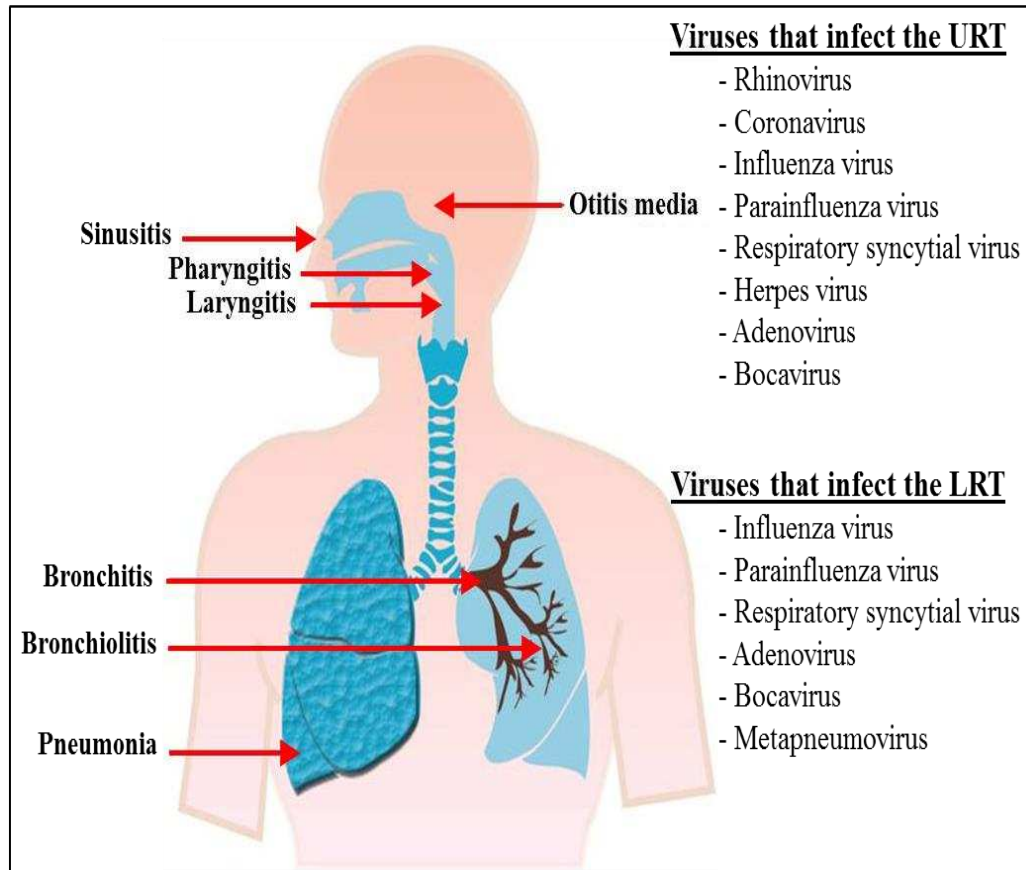
Several types of viruses have been isolated from the respiratory tract of patients at different ages, which are belonging to different families (table 1-2). Many of these viruses have been identified as etiological agents of both URT and LRT infections (figure 1-3), while few other viruses enter the respiratory tract in order to move to other organs (Mackie, 2003, Peiris and Madeley, 2009, Manjarrez-Zavala et al., 2013).

Table 1-2: Viruses causing respiratory tract infections

	<b>Family</b>	<b>Genus</b>	<b>Species</b>	
DNA viruses	Adenoviridae	Mastadenovirus	Human mastadenovirus A-G	
	Herpesviridae	Simplexvirus	Human herpesvirus 1	
				Human herpesvirus 2
		Varicellovirus	Human herpesvirus 3	
		Lymphocryptovirus	Human herpesvirus 4	
	Cytomegalovirus	Human herpesvirus 5		
RNA viruses	Orthomyxoviridae	Influenzavirus A	Influenza A virus	
		Influenzavirus B	Influenza B virus	
		Influenzavirus C	Influenza C virus	
	Paramyxoviridae	Respirovirus		Human parainfluenza virus 1
				Human parainfluenza virus 3
		Rubulavirus		Human parainfluenza virus 2
				Human parainfluenza virus 4
				Mumps virus
		Metapneumovirus	Human metapneumovirus	
		Pneumoviruses	Human respiratory syncytial virus	
Morbillivirus	Measles virus			

	<b>Family</b>	<b>Genus</b>	<b>Species</b>
<b>RNA viruses</b>	Picornaviridae	Enteroviruses	Rhinovirus A, B, C
	Coronaviridae	Alphacoronavirus	Human coronavirus NL63
			Human coronavirus 229 E
		Betacoronavirus	Human coronavirus HKU1
			Sever acute respiratory syndrome -related coronavirus (SARS-CoV)
	Parvoviridae	Bocaparvovirus	Middle East respiratory syndrome coronavirus (MERS-CoV)
			Primate Bocaparvovirus 1
	Bunyaviridae	Hantavirus	Primate Bocaparvovirus 2
			Hantaan virus
			Bayou virus
			Black Creek Canal virus
New York virus			
		Sin Nombre virus	

Adapted from (Mackie, 2003, Peiris and Madeley, 2009).



**Figure 1-3: The common clinical syndromes of the URT and LRT caused by the different types of viruses.**

Adopted from (Manjarrez-Zavala et al., 2013).

### 1.3.2.1 Influenza viruses

Influenza viruses have been reported as significant dangerous causes of respiratory diseases, which may lead to high rates of morbidity and mortality especially in infants, elderly and immunocompromised people (Thompson et al., 2003). They have been classified into three genera within the family Orthomyxoviridae which include Influenzavirus A, B and C. Each genus contains only single species represented by Influenza A virus, Influenza B virus and Influenza C virus, respectively. The high continuous mutation rates of the influenza virus genes coding the two surface glycoproteins (hemagglutinin HA



and neuraminidase NA), change some amino acids in the antibody binding sites of these viral proteins and lead to new antigens each year which are able to evade the acquired immunity from the same previous infection (antigenic drift) (Fouchier et al., 2005). Therefore, the viruses of the influenza A type are further classified into subtypes based on the antigenicity of the HA and NA. Accordingly, Influenza A virus contains 17 HA subtypes and 9 NA subtypes which all of them have been found in wild bird (the natural hosts) (Wright et al., 2013). The subtypes H1, H2, H3 and N1 and N2 represent the most virulent human pathogens which were transmitted from wild aquatic birds, pigs and ferrets as a result of mutational alteration in the HA and/or NA genes of the influenza virus subtypes which is called genetic shift and usually associated with the pandemics (Garman and Laver, 2004, Mahony, 2008). In contrast, avian pathogenesis can cause fatal infections in human, affect many organs and can even cross the placental barrier which may affect the growing foetus (Korteweg and Gu, 2008).

H1N1, H2N2 and H3N2 are the common human virulent subtypes of influenzavirus A which caused major memorable pandemics of Spanish Flu in 1918, Asian Flu in 1957 and Hong Kong Flu in 1968, respectively. The most recent influenza pandemic was the Swine Flu in 2009 which was caused by a new strain of H1N1. These influenza pandemics resulted in more than 50 million, 2 million, 1 million and 18 thousand deaths worldwide, respectively according to the World health Organization. Influenza B and C viruses are predominantly circulating among humans causing less severe infections than influenza A viruses (Johnson and Mueller, 2002, Barry, 2004, Morens and

Fauci, 2007, Osterhaus, 2008, Taubenberger and Morens, 2008, <http://www.ictvonline.org/index.asp>, 2009, Sato et al., 2010).

#### **1.3.2.1.1 Structure of the influenza viruses**

Influenza viruses are mostly spherical particles of approximately 80-120 nm in diameter consist of viral genome inside a helically symmetric nucleocapsid, surrounded by a lipid envelope. Viral envelope is derived from the host cell membrane and consists of an inner layer of protein known as matrix protein (M1) which is spanned by a number of ion channels composed of M2 protein, and an outer layer of lipid. The HA and NA glycoproteins which consist of 500 rod-shaped spikes and 100 mushroom-shaped spikes, respectively project from this viral envelope (White and Fenner, 1994, Garman and Laver, 2005, Parija, 2009) (Figure 1-4).

The influenza virus genome is a single-stranded RNA which has a complementary sequence of the mRNA. Accordingly, it cannot be translated directly into viral protein; therefore it must be transcribed firstly into mRNA in order to start encoding influenza viral proteins. Thus, it is referred to such viruses as negative sense single stranded RNA viruses. The viral genome of influenza A and B viruses consists of eight separate segments while the genome of the influenza C viruses consists of seven segments; each segment encodes one of the influenza virus proteins (Fujii et al., 2003, Huang et al., 2009). The size of the segments is variable and ranges from 890 to approximately 2500 nucleotides (Steinhauer and Skehel, 2002). RNA polymerase complex which includes polymerase basic 2 (PB2) and 1 (PB1), and polymerase acid (PA), hemagglutinin (HA), nucleocapsid protein (NP),

neuraminidase (NA), matrix protein (M1) and (M2), and non-structural proteins (nuclear export protein NEP and NS2) represent the influenza viral proteins which are encoded by the genomic segments (1-8), respectively of both of influenza viruses A and B. The fourth genomic segment of the influenza virus C encodes for the hemagglutinin esterase fusion (HEF) protein which performs the functions of both HA and NA proteins (Porter et al., 1980, Webster et al., 1992, Steinhauer and Skehel, 2002, Palese and Shaw, 2013) (figure 1-4).

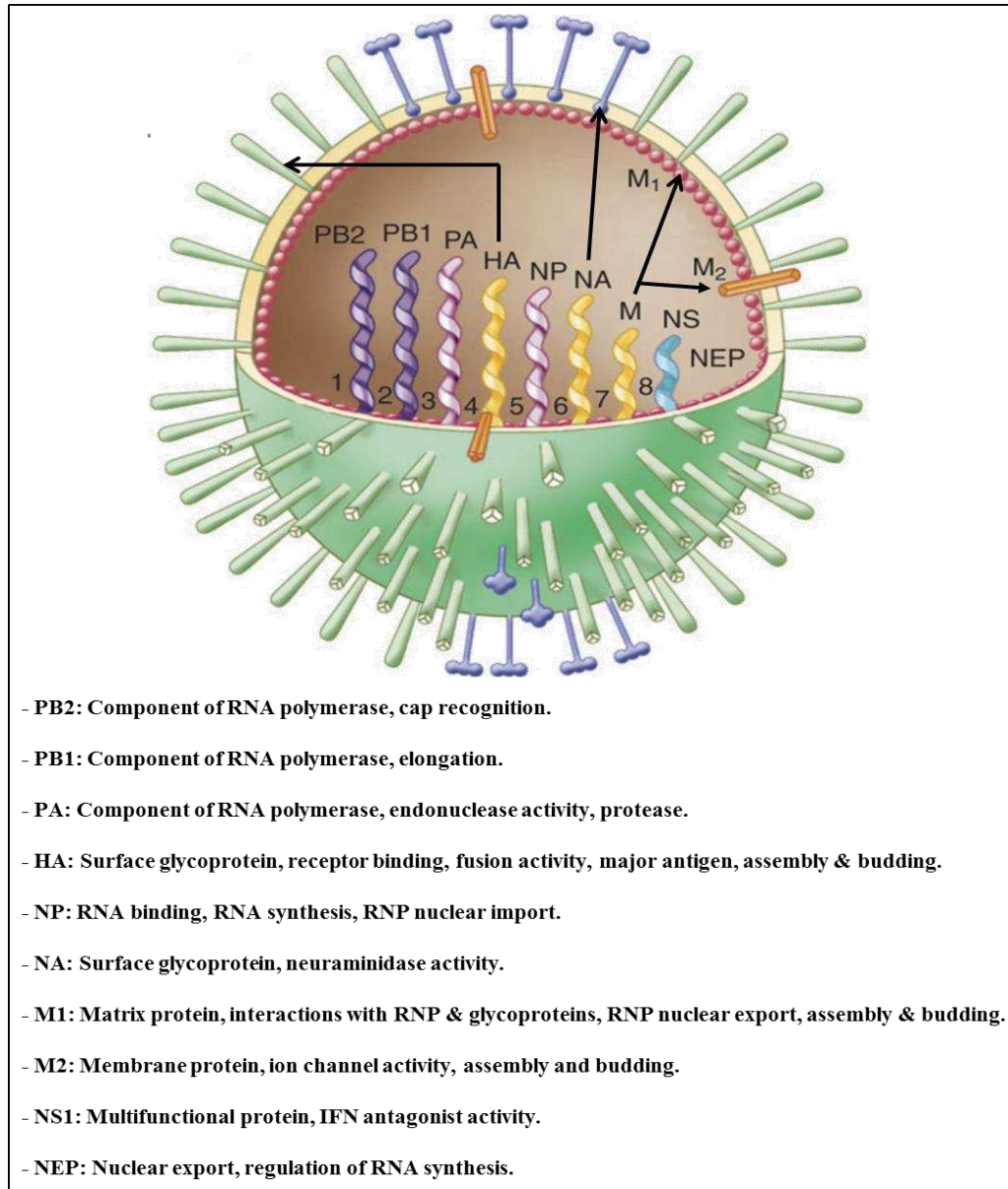


**Figure 1-4: Schematic diagram of influenza virus particle showing the arrangement of the viral genome segments, and their functions.**

Adapted from (Palese and Shaw, 2013).

### **1.3.2.2 Respiratory syncytial virus**

Respiratory syncytial virus (RSV) belongs to the genus Pneumovirus which represents one of the genera of the Paramyxoviridae family, and contains Human respiratory syncytial virus (HRSV); the major causative agent of pediatric lower respiratory tract illness (LRI) in babies. Young children especially those under 2 years old, elderly and immunosuppressed persons are more affected by HRSV. This virus infects epithelial cells of the LRT causing bronchiolitis and pneumonia which may be accompanied by serious complications such as breathing difficulties or apnoea especially in infants leading to high rates of hospitalization (Glezen et al., 1986, Tsai et al., 2001, Nokes et al., 2004, Hall et al., 2009). HRSV has the ability to infect many cells without leaving, which leads to form syncytia (multinucleated cells) and protects the virus against the antibody attack, therefore the vast majority of the first natural HRSV infections do not provide lifelong immunological protection (Manjarrez-Zavala et al., 2013). Accordingly, more than 90% of children are commonly reinfected by the same or different strain of HRSV during their second birthday, but without complications (Ohuma et al., 2012, Papenburg et al., 2012). The detailed structure of RSV genome is discussed in section 1.3.2.3.1.

### **1.3.2.3 Metapneumovirus**

Metapneumovirus (MPV) represents other genus of the Paramyxoviridae family, which contains the species Human metapneumovirus (HMPV). The virus circulates among human populations mostly in children less than five years old. It was only identified as a causative agent of respiratory tract

infections in 2001 (van den Hoogen et al., 2001). This virus was reported in the Asia, Europe, Australia and North America causing recurrent respiratory diseases in both children and adults causing LRI similar to those caused by HRSV which also require hospitalization (Kuiken et al., 2003, Banerjee et al., 2007). Several studies reported that the HMPV are considered as the second cause of bronchiolitis and pneumonia during the early childhood after the HRSV infections (Kahn, 2006, Heikkinen et al., 2008). The detailed structure of MPV genome is discussed in section 1.3.2.3.1.

#### **1.3.2.3.1 Structure of the HRSV and HMPV**

Both HRSV and HMPV are spherical enveloped particles of approximately 100-350 nm in diameter, but the long filamentous form of 10  $\mu$ m in length and 60-200 nm in diameter is the predominant shape of these paramyxoviruses (Collins and Karron, 2013). Their genome consists of a single-stranded, nonsegmented negative sense RNA of approximately 15.2 and 13 kb, respectively, with similar but non identical genomic organization (Biacchesi et al., 2003). The genome of the HRSV consists of 10 genes encoding 11 viral proteins which are: non-structural 1 (NS1), NS2, nucleocapsid (N), phosphoprotein (P), Matrix (M), small hydrophobic (SH), attachment (G), fusion (F), transcription elongation factors (M2-1), RNA regulatory factor (M2-2) and large polymerase subunit (L). In contrast, the genome of the HMPV lacks the first two genes (NS1 and NS2), therefore it consists of 8 genes encode 9 viral proteins (figure 1- 5) (Mackie, 2003, Guerrero-Plata, 2013).

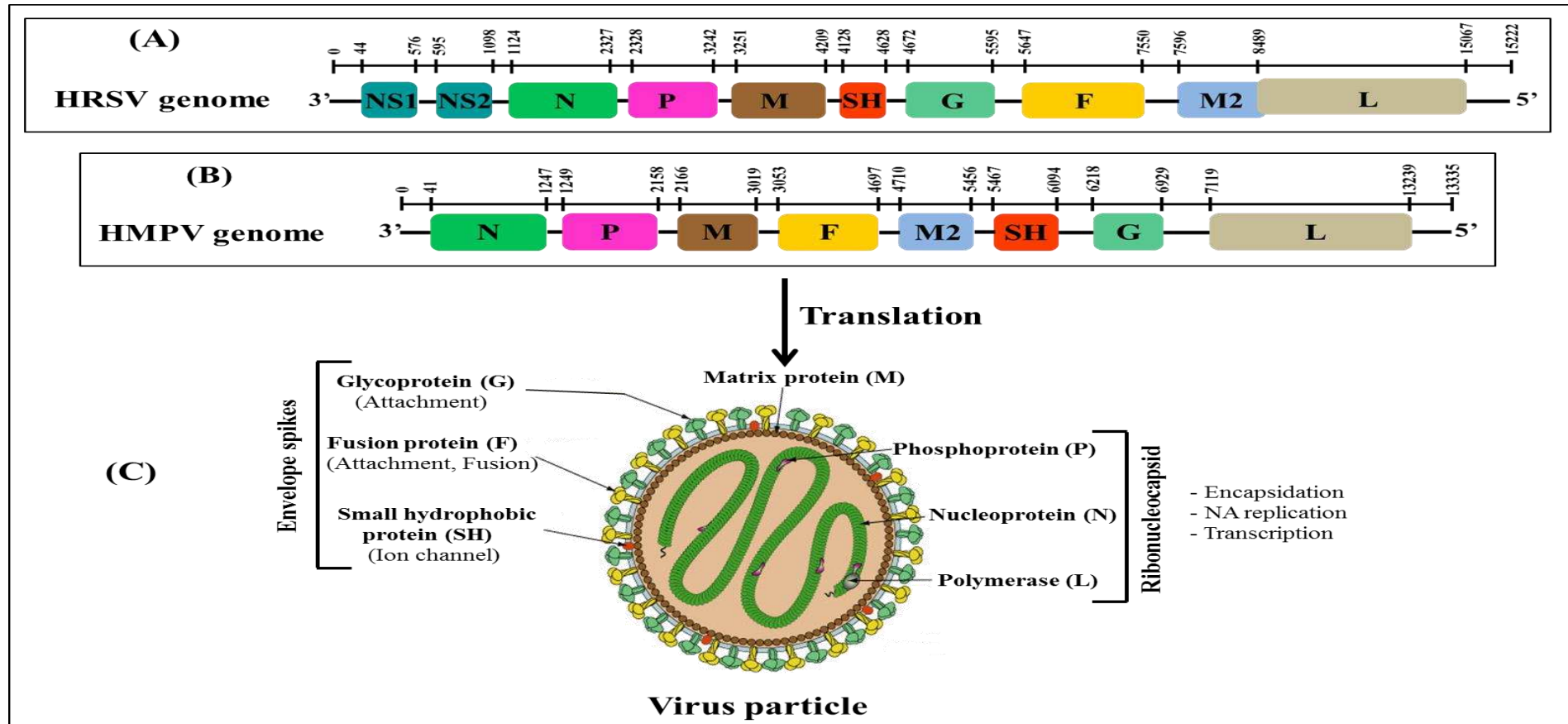


Figure 1-5: Schematic diagram of the genomic maps of the HRSV (figure A) and HMPV (figure B), and the viral particle (figure C) consisting of viral proteins generated from their genome translation.

Adapted from (Collins and Karron, 2013, Guerrero-Plata, 2013).

#### **1.3.2.4 Rhinoviruses**

Rhinoviruses represent other species of human pathogenic viruses which also belong to the genus enterovirus. This viral group include more than 100 serotypes which have been recently classified into three species, Rhinovirus A, B and C based on their genome sequence analysis, differential susceptibility to particular antiviral compounds in a given serum and receptor specificity (Oberste et al., 1999, Ledford et al., 2004, Lamson et al., 2006). These viruses are commonly associated with acute respiratory illness (ARI) especially in infants as well as elderly and immunosuppressed people, which include common cold, bronchiolitis and pneumonia. Several studies reported that more than half of the common cold cases caused by rhinoviruses may be exacerbated to wheezing and asthma especially in children of school age (Johnston et al., 1995, Chung et al., 2007). The capsid structures and the genome organization of the rhinoviruses are similar to those of enteroviruses, but they differ in their genome size which is approximately 7.2 kb. Therefore, it is thought that both enteroviruses and rhinoviruses diverged from the last ancestor (Gern and Palmenberg, 2013).

#### **1.4 Microarray-based technology**

Microarray technique has emerged as a new functional tool in genomic research and clinical laboratories (Peytavi et al., 2005). Figure 1-6 clarifies the principle of this nanoscale technique. It includes use of synthesized fragments of recombinant nucleic acids or oligonucleotides (probes) affixed on a specific chip which is either a nylon membrane or the surface of a glass slide. These probes are able to hybridize with complementary nucleic acid sequences.



Fluorescent labelling dyes (e.g. platinum compounds) can facilitate the detection of this type of hybridization (Shieh and Li, 2004). Based on its high capacity to accommodate hundreds to thousands of individual viral gene probes and allow simultaneous detection of any amplifiable pathogen present in a specimen, microarray technology is able to overcome the limitations of the conventional methods which are applied for the diagnoses of viral infections which are virus or pathogen specific.

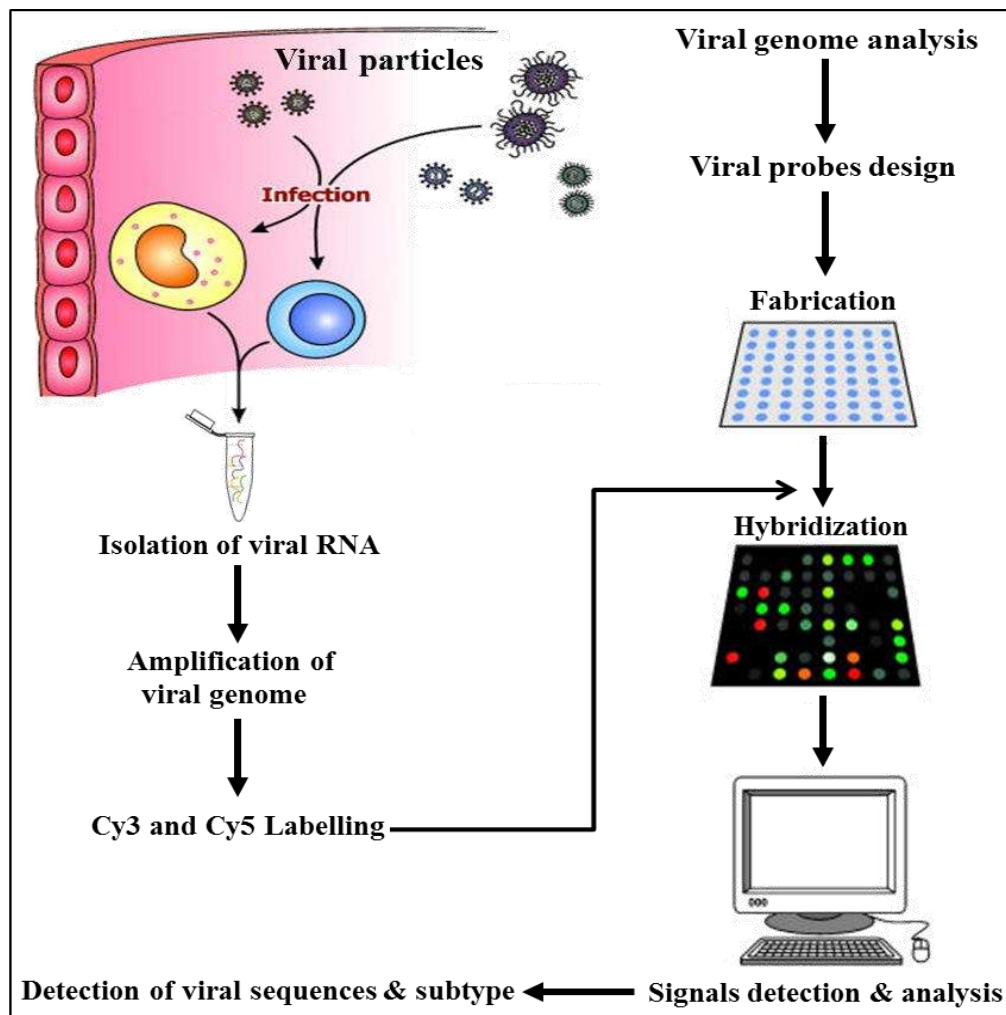


Figure 1-6: Shows the schematic drawing of multivirus chip.

Adopted from (Shieh and Li, 2004).

This technique has certain advantages over the conventional methods used for detection and identification of the microbial pathogens, which they are:

- 1- The complication rates of false positive results due to contamination are highly limited.
- 2- The microarray chip can be designed with high flexibility to detect all of the viral pathogens. It can be also rapidly modified to match the emergence of new viruses.
- 3- Viral gene expression as well as genotyping of viral isolates can be achieved by this process (Shieh and Li, 2004).
- 4- Many viruses can be identified by microarray at the same time. Therefore, it is highly recommended for the diagnosis of specimens which are suspected to contain multiple pathogenic viruses (Elnifro et al., 2000).

This technique has been employed together with PCR amplification for the simultaneous identification of several pathogens in only one process (Miller and Tang, 2009). A microarray viral system was firstly described by (Wang et al., 2002) aiming to identify the pathogens of severe viral respiratory infections. This chip contained about 1600 probes covering 140 viral genomes including the serotypes of RSV, parainfluenza, adenoviruses and human rhinoviruses. This was later developed into a pan-viral microarray by using approximately 10,000 highly conserved sequences of 70-mer oligonucleotides representing the full reference sequence of 1000 viral genomes from GeneBank in order to improve the identification possibility of both known and unknown members through cross-hybridization to this array of specific probes. A modified random PCR protocol was used to amplify viral genomes in clinical specimens. This procedure starts with the synthesis of first- and second strand

by using specific primer-A (5'- GTTTCCCAGTCACGATCNNNNNNNNN), this will be completed with 40 cycles of PCR amplification process with another specific primer-B (5'-GTTTCCCAGTCACGATC). Generally, this protocol includes three rounds of PCR (A, B and C). In round A, cDNA is synthesized using primer A. In round B, the generated templates (first and second strand cDNA) are then amplified using primer B. The amplification is completed in round C through incorporation of an additional group, which is either an amino allyl deoxyuridine triphosphate (dUTP) or a cyanine-dye-coupled nucleotide, using additional PCR cycles. More additional details are found at <http://dx.doi.org/10.1371/journal.pbio.0000002.sd002> (Wang et al., 2003). The virochip was applied globally to discover the virus associated with SARS (Ksiazek et al., 2003).

DNA microarray technology was devised by Boriskin and his group in 2004 for the detection of viral neuropathogens (e.g. VZV, HSV and enteroviruses) in persons with encephalitis and meningitis especially those very young and immunocompromised patients. Multiplex PCR was used to amplify viral genetic materials in clinical samples especially those with low quantities such as CSF. This array was able to identify up to 13 different viruses in one panel.

The Affymetrix GeneChip system was designed by (Malanoski et al., 2006) for the instantaneous identification of respiratory pathogens through resequencing the short oligonucleotides of the original platform which aided in the identification of new subtypes of influenza virus H5N1 and H1N1 in 2007 and 2009, respectively. GreenChipResp platform was designed later by (Quan et al., 2007) and utilized for the detection of subtypes of influenza-A viruses and other respiratory viruses, and was then developed for the identification of the

coronaviruses (Miller and Tang, 2009). MChips was created by (Dawson et al., 2006) and employed for the identification of the influenza-A in recent and historical specimens through the detection of the polymorphisms in their M gene. This MChip was also used for the identification of influenza-B in similar samples and those subtypes of both influenza A and B (H1N1, H3N2 and H5N1) which infect humans (Mikhailovich et al., 2008).

Simultaneous identification of seven human herpes viruses (HSV-1, HSV-2, VZV, EBV, CMV, HHV-6A and HHV-6B) in a single reaction was achieved by (Zheng et al., 2008) based on the conserved regions of DNA polymerase gene of the previous viruses which are used to develop a cheap DNA microarray chip.

Microarray technology was used as a novel approach to identify and quantify hepatitis B and C; and Human immunodeficiency virus type 1 (HIV-1) in the plasma specimens of donors (Khodakov et al., 2008).

Amplification process is necessary in microarray technology in order to amplify the minute amounts of viral genomes in clinical samples. PCR is the common method used for exponential amplification of nucleic acids, but this method can only generate fragments with maximum length 500 base pairs. Degenerate oligonucleotide primed-PCR (DOP-PCR) represents the recent technique used to amplify the entire genomes of different organisms from any source through using partially degenerate primers (primers containing few of the degenerate nucleotides shown in table 2-9) which can facilitate binding these primers to their complementary nucleic acid sequences in a PCR protocol with two different annealing temperatures (Fortina et al., 2001).

The successful isolation of the isothermal Phi 29 DNA polymerase from *Bacillus subtilis* bacteriophage Phi 29 which has the ability to replicate the target nucleic acid isothermally, opened the door for continuous nucleic acids amplification along the entire microbial genome using random hexamer primers in a productive isothermal process called whole genome amplification (WGA).

In this process, some molecules of the Phi 29 DNA polymerase start elongation of random hexamers annealed to the complementary sequences of the target denatured DNA without disassociation from the original template. At the same time, other molecules of the Phi-29 DNA polymerase partially displace the beginning of the new extending complementary strands, which provides new templates ready for more isothermal multiple displacement amplification (MDA) reactions. Continuous priming and strand displacement led to exponential amplification and generated high molecular weight of hyperbranched amplicons containing various lengths of linear dsDNA, ssDNA and some forks of nucleic acids. Therefore, MDA is being used as an appropriate method for WGA of nucleic acids in the absence of prior knowledge of organisms that may be present at a rate of more than  $(10^4)$  copies/ml (figure 1-7) (Lage et al., 2003, Monstein et al., 2005, Lovmar and Syvanen, 2006, Binga et al., 2008, Maragh et al., 2008, Wang et al., 2011, Zheng et al., 2011).

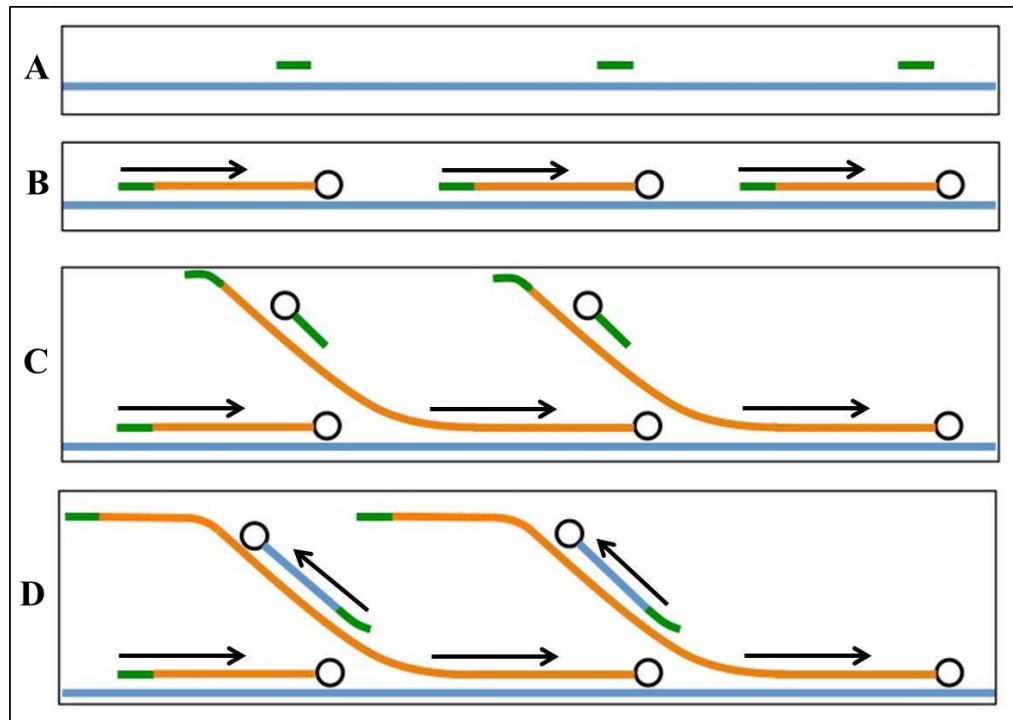


**Figure 1-7: Schematic diagram shows the working principle of Phi 29 DNA polymerase during MDA process.**

In figure A, the random hexamers primers represented by the short green lines anneal to the single strand DNA represented by the long blue line. In figure B, the Phi 29 DNA polymerase molecules represented by the black circles start extending the annealed random hexamers primers till reaching the newly synthesized complementary strands of DNA represented by the orange lines. In figure C, the Phi 29 DNA polymerase molecules displace the newly synthesized strands and continue the polymerization, at the same time more primers of random hexamers annealed to the newly synthesized complementary strand of DNA. In figure D, polymerization starts on the new strands, forming a hyperbranched structure. The black arrows show the direction of the new strands synthesis.

Adopted from (Spits et al., 2006).

In general, it has emerged as an ideal method for the extensive parallel identification and differentiation of various pathogens and their strains in clinical samples (Maughan et al., 2001).

## 1.5 Aim of the study

The study aims to provide a unique methodology-detection system through generating a probe array for simultaneous detection of a wide variety of virus species (specifically those causing CNS and respiratory tract infections).

### 1.5.1 Objectives

The main objects of this study were:

- Design single platform chip containing multiple specific independent hybridization probes of 28-30 bases covering the viral strains of each of human enteroviruses, human rhinoviruses, human metapneumoviruses, human respiratory syncytial viruses and influenza viruses (described in chapter 2). This specific length is preferred in order to avoid long time hybridization for the longer probes and omit nonspecific hybridization for the shorter probes.
- Optimize the steps used for validating the chip against some viral positive control and clinical samples, which includes amplifying the entire genome of the selected viruses, labelling and fragmenting the amplified viral nucleic acid, and hybridizing the labelled materials with the designed viral probes (described in chapter 3 and 4).
- Determine the properties of individual probes, and then select the optimal probes for constructing an optimal cheap virochip applicable to use in clinical laboratories for robust detection and identification of many RNA viruses up to subgroup level, directly from the clinical samples (described in chapter 4).

## **2 Designing multiple hybridization probes for the selected RNA viruses**



## **2.1 Introduction**

Designing probes is the cornerstone for constructing a nucleic acid microarray. These probes should be complementary to specific sequences of the target nucleic acid required to be detected or identified in order to facilitate their annealing together and forming the probe-target combination which is normally called a hybrid. Labelling of either the probes or the nucleic acid of interest with an appropriate detectable molecule can facilitate detection of the generated hybrid when it is formed (Call, 2001a, Li et al., 2002, de Muro, 2005, Jayapal and Melendez, 2006, Trevino et al., 2007). The availability of the nucleic acid sequences for the vast majority of organisms including viruses, in addition to the existence of many of free probe design programmes, makes it very easy to design the required probes for any specific gene or nucleic acid sequence of any organism in order to be used in a microarray technology. The designed probes can be synthesized and then printed on any supporting solid surface such as glass or nylon membrane using a microarray spotter (Hegde et al., 2000, Ehrenreich, 2006). Nowadays, nucleic acid microarrays can be synthesized in situ on a chip by many commercial companies like Agilent Technologies based on a principle called custom-made arrays which makes cost much lower than printing it in the laboratory using an expensive microarrayer (Hughes et al., 2001, Nordberg, 2005, Ehrenreich, 2006).

## **2.2 Aims**

Designing multiple specific probes of similar lengths targeting the entire sequence of each of the human enterovirus, human rhinoviruses, HMPV, HRSV and human influenza virus genomes using two of the free probe design

software programmes (OligoArray 2.1, [http://berry.engin.umich.edu/oligoarray2\\_1/](http://berry.engin.umich.edu/oligoarray2_1/) and Agilent Technologies eArray, <https://earray.chem.agilent.com/earray/>), was the first aim of this chapter. The second aim was to test in silico the specificity of the designed probes against the original sequences of the selected viral genomes using the Basic Local Alignment Search Tool (BLAST) software. Finally, the third aim was to select the most specific probes in order to be synthesised and spotted simultaneously on a chip by Agilent Technologies Company.

## **2.3 Methods**

### **2.3.1 Downloading viral genome sequences**

The 2009 virus taxonomy list of the International Committee on Taxonomy of Viruses (ICTV), [http://ictvonline.org/virusTaxonomy.asp?msl\\_id=25](http://ictvonline.org/virusTaxonomy.asp?msl_id=25) was used as a reference for the selected RNA viruses causing human viral infections which were: enteroviruses, metapneumoviruses, respiratory syncytial viruses and influenza viruses.

#### **2.3.1.1 Enterovirus genome sequence**

Enteroviruses contain several human pathogenic species including Human enterovirus A, Human enterovirus B, Human enterovirus C, Human enterovirus D, Human rhinovirus A, Human rhinovirus B and Human rhinovirus C (Racaniello, 2013). Full-length nucleotide sequences of viral genomes for each of the 16, 53, 15 and 3 strains of the Human enterovirus A, B, C and D species, respectively, were downloaded from the recent database of

the GeneBank at the National Centre for Biotechnology Information (NCBI) and saved in a FASTA format (tables-2-1 to 2-4). The genomes of the above human enteroviruses contain three regions: 5'untranslated region (5'UTR), coding sequences (CDS) and 3' untranslated region (3'UTR), respectively. Therefore, the nucleotide sequence of each one of the enteroviral genomes was split according to these three regions.

Complete viral genome sequences of only seventeen of the human rhinoviruses were also downloaded from the same above website of the NCBI and saved using the same mentioned FASTA format (table 2-5). These sequences were selected based on a previous study (Wang et al., 2008), as a preliminary step to use the microarray assay for the diagnosis of infections caused by rhinoviruses.

**Table 2-1: Shows the strains of the Human enterovirus A and their NCBI accession numbers, and genome size and regions.**

No	Serotype	Strain	Accession	Genome length (bp)	Genome regions' size		
					5'UTR	CDS	3'UTR
1-	Coxsackievirus A2	Fleetwood	AY421760	7398	1-742	743-7315	7316-7398
2-	Coxsackievirus A3	Olson	AY421761	7395	1-742	743-7312	7312-7395
3-	Coxsackievirus A4	High Point	AY421762	7434	1-747	748-7353	7354-7434
4-	Coxsackievirus A5	Swartz	AY421763	7400	1-741	742-7317	7318-7400
5-	Coxsackievirus A6	Gdula	AY421764	7434	1-745	746-7351	7352-7434
6-	Coxsackievirus A7	Parker	AY421765	7404	1-742	743-7321	7322-7404
7-	Coxsackievirus A8	Donovan	AY421766	7396	1-743	744-7313	7314-7396
8-	Coxsackievirus A10	Kowalik	AY421767	7409	1-744	745-7326	7327-7409
9-	Coxsackievirus A12	Texas	AY421768	7404	1-745	746-7321	7322-7404
10-	Coxsackievirus A14	G-14	AY421769	7415	1-755	756-7334	7335-7415
11-	Coxsackievirus A16	G-10	U05876	7413	1-750	751-7332	7333-7413
12-	Enterovirus 71	BRCR	U22521	7408	1-743	744-7325	7326-7408
13-	Enterovirus 76	FRA91-10369	AY697458	7438	1-747	748-7344	7345-7438
14-	Enterovirus 89	BAN00-10359	AY697459	7429	1-747	748-7335	7336-7429
15-	Enterovirus 90	BAN99-10399	AY697460	7425	1-749	750-7331	7332-7425
16-	Enterovirus 91	BAN00-10406	AY697461	7427	1-745	746-7333	7334-7427

**Table 2-2: Shows the strains of the Human enterovirus B and their NCBI accession numbers, and genome size and regions.**

No	Serotype	Strain	Accession	Genome size	Genome regions' size		
					5'UTR	CDS	3'UTR
1-	Coxsackievirus A9	Grigs/Bozek	D00627	7452	1-743	744-7349	7350-7452
2-	Coxsackievirus B1	C0nn-5	M16560	7389	1-741	742-7290	7291-7389
3-	Coxsackievirus B2	Ohio-1	AF085363	7411	1-742	743-7306	7307-7411
4-	Coxsackievirus B3	Nancy	M16572	7396	1-740	741-7298	7299-7396
5-	Coxsackievirus B4	JVB	X05690	7395	1-743	744-7295	7296-7395
6-	Coxsackievirus B5	Faulkner	AF114383	7400	1-742	743-7300	7301-7400
7-	Coxsackievirus B6	Schmidt	AF105342	7398	1-743	744-7298	7296-7398
8-	Echovirus 1	Farouk	AF029859	7397	1-743	744-7298	7298-7397
9-	Echovirus 2	Cornelis	AY302545	7435	1-741	742-7335	7336-7435
10-	Echovirus 3	Morrisey	AY302553	7428	1-743	744-7328	7329-7428
11-	Echovirus 4	Pesascek	AY302557	7394	1-742	743-7294	7295-7394
12-	Echovirus 5	Noyce	AF083069	7433	1-742	743-7333	7334-7433
13-	Echovirus 6	D'Amori	AY302558	7418	1-742	743-7318	7319-7418
14-	Echovirus 7	Wallace	AY302559	7427	1-742	743-7327	7327-7427
15-	Echovirus 9	Hill	X84981	7420	1-739	740-7321	7322-7420
16-	Echovirus 11	Gregory	X80059	7438	1-751	752-7339	7340-7438
17-	Echovirus 12	Travis	X79047	7501	1-741	742-7323	7324-7501
18-	Echovirus 13	Del Carmen	AY302539	7410	1-742	743-7309	7310-7410
19-	Echovirus 14	Tow	AY302540	7450	1-741	742-7350	7351-7450
20-	Echovirus 15	CH96-51	AY302541	7437	1-743	744-7337	7338-7437

No	Serotype	Strain	Accession	Genome size	Genome regions' size		
					5'UTR	CDS	3'UTR
21-	Echovirus 16	Harrington	AY302542	7437	1-742	743-7333	7334-7433
22-	Echovirus 17	CHHE-29	AY302543	7416	1-743	744-7316	7317-7416
23-	Echovirus 18	Metcalf	AF317694	7410	1-740	741-7310	7311-7410
24-	Echovirus 19	Burke	AY302544	7433	1-742	743-7333	7334-7433
25-	Echovirus 20	JV-1	AY302546	7394	1-742	743-7294	7295-7394
26-	Echovirus 21	Farina	AY302547	7426	1-741	742-7326	7327-7426
27-	Echovirus 24	DeCamp	AY302548	7433	1-742	743-7333	7334-7433
28-	Echovirus 25	JV-4	AY302549	7426	1-741	742-7326	7327-7426
29-	Echovirus 26	Cornel	AY302550	7424	1-741	742-7323	7324-7424
30-	Echovirus 27	Bacon	AY302551	7412	1-744	745-7311	7312-7412
31-	Echovirus 29	JV-10	AY302552	7427	1-742	743-7327	7328-7427
32-	Echovirus 30	Bastianni	AF162711	7440	1-750	751-7335	7336-7440
33-	Echovirus 31	Caldwell	AY302554	7432	1-741	742-7332	7333-7432
34-	Echovirus 32	PR-10	AY302555	7420	1-732	733-7320	7321-7420
35-	Echovirus 33	Toluca-3	AY302556	7394	1-742	743-7294	7295-7394
36-	Enterovirus 69	Toluca-1	AY302560	7411	1-744	745-7311	7312-7411
37-	Enterovirus 73	CA55-1988	AF241359	7411	1-744	745-7311	7312-7411
38-	Enterovirus 74	USA/CA75-10213	AY556057	7410	1-742	743-7309	7310-7410
39-	Enterovirus 75	USA/OK85-10362	AY556070	7429	1-747	748-7329	7330-7429
40-	Enterovirus 77	CF496-99	AJ493062	7415	1-742	743-7315	7316-7415
41-	Enterovirus 79	USA/CA79-10384	AY843297	7430	1-745	746-7330	7331-7430
42-	Enterovirus 80	USA/CA67-10387	AY843298	7428	1-743	744-7328	7329-7428
43-	Enterovirus 81	USA/CA68-10389	AY843299	7415	1-739	740-7315	7316-7415

No	Serotype	Strain	Accession	Genome size	Genome regions' size		
					5'UTR	CDS	3'UTR
44-	Enterovirus 82	USA/CA64-10390	AY843300	7427	1-745	746-7333	7334-7427
45-	Enterovirus 83	USA/CA64-10392	AY843301	7394	1-742	743-7294	7295-7394
46-	Enterovirus 84	CIV2003-10603	DQ902712	7423	1-744	745-7323	7324-7423
47-	Enterovirus 85	BAN00-10353	AY843303	7418	1-742	743-7321	7322-7418
48-	Enterovirus 86	BAN00-10354	AY843304	7400	1-742	743-7300	7301-7400
49-	Enterovirus 87	BAN01-10396	AY843305	7422	1-743	744-7322	7323-7422
50-	Enterovirus 88	BAN01-10398	AY843306	7433	1-744	745-7332	7333-7433
51-	Enterovirus 97	BAN99-10355	AY843307	7413	1-742	743-7312	7313-7413
52-	Enterovirus 100	BAN2000-10500	DQ902713	7421	1-744	745-7320	7321-7421
53-	Enterovirus 101	CIV03 -10361	AY843308	7445	1-742	743-7345	7346-7445

**Table 2-3: Shows the strains of the Human enterovirus C and their NCBI accession numbers, and genome size and regions.**

No	Serotype	Strain	Accession	Genome size	Genome regions' size		
					5'UTR	CDS	3'UTR
1-	Coxsackievirus A1	Tompkins	AF499635	7397	1-711	712-7326	7327-7397
2-	Coxsackievirus A11	Belgium-1	AF499636	7453	1-746	747-7385	7386-7453
3-	Coxsackievirus A13	Flores	AF499637	7458	1-745	746-7390	7391 7458
4-	Coxsackievirus A15	G9	AF499638	7441	1-734	735-7373	7374-7441
5-	Coxsackievirus A17	G12	AF499639	7457	1-747	748-7389	7390-7457
6-	Coxsackievirus A18	G13	AF499640	7458	1-744	745-7389	7390-7458
7-	Coxsackievirus A19	8663	AF499641	7410	1-715	716-7339	7340-7410
8-	Coxsackievirus A20	IH35	AF499642	7436	1-744	745-7368	7369-7436
9-	Coxsackievirus A21	Kuykendall	AF546702	7406	1-713	714-7337	7338-7406
10-	Coxsackievirus A22	Chulman	AF499643	7406	1-715	716-7336	7337-7406
11-	Coxsackievirus A24	Joseph	EF026081	7459	1-745	746-7390	7391-7459
12-	Poliovirus 1	Brunhilde	AY560657	7445	1-746	747-7376	7377-7445
13-	Poliovirus 2	Lansing	M12197	7440	1-747	748-7371	7372-7440
14-	Poliovirus 3	Leon/37	K01392	7431	1-742	743-7363	7364-7431
15-	Enterovirus 96	Banoo-10488	EF015886	7478	1-746	747-7406	7407-7478



**Table 2-4: Shows the strains of the Human enterovirus D and their NCBI accession numbers, and genome size and regions.**

No	Serotype	Strain	Accession	Genome size	Genome regions' size		
					5'UTR	CDS	3'UTR
1-	Enterovirus 68	Fermon	AY426531	7367	1-732	733-7299	7300-7367
2-	Enterovirus 70	J670/71	D00820	7390	1-726	727-7311	7312-7390
3-	Enterovirus 94	E210	DQ916376	7364	1-714	715-7287	7288-7364

**Table 2-5: Shows the strains of the human rhinoviruses, their NCBI accession numbers and genome size.**

No	Serotype	Strain	Accession	Genome size
1-	Rhinovirus 1B	ATCC VR-1366	D00239	7133
2-	Rhinovirus 2	ATCC VR-482	X02316	7102
3-	Rhinovirus 8	ATCC VR-1118	FJ445113	7108
4-	Rhinovirus 9	ATCC VR-489	FJ445177	7132
5-	Rhinovirus 12	ATCC VR-1122	EF173415	7124
6-	Rhinovirus 14	ATCC VR-284	NC_001490	7212
7-	Rhinovirus 17	ATCC VR-1127	EF173420	7219
8-	Rhinovirus 32	ATCC VR-1142	FJ445127	7133
9-	Rhinovirus 39	ATCC VR-340	AY751783	7137
10-	Rhinovirus 50	ATCC VR-517	FJ445135	7118
11-	Rhinovirus 69	ATCC VR-1179	FJ445151	7211
12-	Rhinovirus 82	ATCC VR-1192	FJ445160	7123
13-	Rhinovirus 84	ATCC VR-1194	FJ445162	7201
14-	Rhinovirus 85	ATCC VR-1195	FJ445163	7140
15-	Rhinovirus 86	ATCC VR-1196	FJ445164	7213
16-	Rhinovirus 89	ATCC VR-1199	FJ445184	7152
17-	Rhinovirus 90	ATCC VR-1291	FJ445167	7124

### 2.3.1.2 Metapneumovirus genome sequence

Metapneumoviruses contain only one pathogenic species for the human which is (HMPV). Therefore, the full genome sequences of eleven serotypes of HMPV covering its two subtypes A and B (Biacchesi et al., 2003, van den Hoogen et al., 2004), were downloaded from the NCBI website and saved in a FASTA format (table 2-6).

**Table 2-6: Shows strains of HMPV, their NCBI accession numbers and genome size.**

No	Serotype	Strains	Accession	Genome size
1-	Human metapneumovirus	Jpn03-1	AB503857	13337
2-		BJ1887	DQ843659	13327
3-		BJ1816	DQ843658	13271
4-		TW05-00125	EF535506	13282
5-		HMPVgz01	GQ153651	13327
6-		CAN97-83	AY297749	13335
7-		CAN98-75	AY297748	13280
8-		00-1	AF371337	13350
9-		NL/00/17 type A2	FJ168779	13336
10-		NL/94/01 subtype B2	FJ168778	13282
11-		NL/1/99	AY525843	13293

**2.3.1.3 Human respiratory syncytial virus (HRSV) genome sequence**

HRSV represents another viral species causing viral infections of humans. The whole genome sequences of seven serotypes of HRSV covering its two subtypes A and B (Jafri et al., 2013) were obtained from the NCBI website and saved in a FASTA format (table 2-7).

**Table 2-7: Shows strains of HRSV, their NCBI accession numbers and genome size.**

No	Serotype	Strain	Accession	Genome size
1-	Human respiratory syncytial virus	98-25147-X	FJ948820	15223
2-		rA2cp	AF035006	15223
3-		cp52	AF013255	13933
4-		ATCC VR-26	AY911262	15226
5-		cpts 248	U50363	15222
6-		strain B1	AF013254	15225
7-		S2	U39662	15190

#### **2.3.1.4 Influenza virus genome sequences**

Influenza A virus, Influenza B virus and Influenza C virus are the human pathogenic species of the influenza viruses. Out of eight genomic segments of the human influenza viruses A and B, the full length sequences of the HA, NA and matrix protein (M) genomic segments of European origin were downloaded from the Influenza Virus Sequence Database of the NCBI. On the other hand the sequences of the hemagglutinin-esterase-fusion (HEF) and the matrix protein genomic segments of the human influenza virus C were selected from the seven segments of this virus genome also within European population and downloaded from the same database of the NCBI website. All the downloaded sequences were saved in a FASTA format, and then the identical sequences were collapsed (table 2-8). Searching the National Centre for Biotechnology Information (NCBI) website to download the nucleic acid sequences of the influenza viruses come with some subtypes of H7 that causing viral infection for human within Europe, therefore it was decided to include those subtypes belong to H7.

**Table 2-8: Shows the selected genomic segments of the human influenza viruses A, B and C, their size and the subtype numbers.**

Virus species	Genomic segment	Segment size (kb)	Virus subtype	Subtypes No.	Total
Influenza A virus	HA	~1.7	H1N1	1186	1667
			H1N2	9	
			H2N2	15	
			H3N2	453	
			H7N7	4	
	NA	~1.4	H1N1	711	1184
			H1N2	7	
			H2N2	21	
			H3N2	443	
			H7N7	2	
	MP	~0.98	H1N1	331	640
			H1N2	6	
			H2N2	21	
			H3N2	280	
H7N7			2		
Influenza B virus	HA	~1.8	HA	23	75
	NA	~1.4	NA	36	
	MP	~1.1	MP	16	
Influenza C virus	HEF	~1.9	HEF	24	25
	MP	~1.1	MP	1	
Total					3591

### 2.3.2 Viral sequence analysis

The genetic diversity among the strains and subtypes of the selected RNA viruses makes it very difficult if not impossible to design probes targeting all their sequences. Therefore, it was decided to analyse the genomic sequences of the selected viral strains or subtypes of each species in order to generate consensus sequences that could be used for designing specific probes for each viral species through the following steps:

### **2.3.2.1 Viral sequence alignment**

Nucleic acid sequence alignments for each of the three regions of each of the Human enterovirus A, B, C and D serotypes as well as the genomic sequences of those other serotypes of the human rhinovirus, HMPV and HRSV were implemented using CLUSTALW of the molecular evolutionary genetics analysis (MEGA) software version 4. The alignment was done in two steps: pairwise alignment and multiple alignment with the same alignment parameters which were adjusted on 15 for gap opening penalty and 6.66 for gap extension penalty. Multiple sequence alignments for each of the selected genomic segments of the human influenza virus A, B and C subtypes were carried out through the Influenza Virus Resource of the NCBI website.

### **2.3.2.2 Phylogenetic analysis of the human enteroviruses**

The aligned nucleic acid sequences of the 5'UTR, CDS and 3'UTR regions of each of the Human enterovirus A, B, C and D serotypes were saved in MEGA format and then the maximum-likelihood phylogenetic and molecular evolutionary analyses were also conducted by using the MEGA software version 4. Molecular evolution design and nucleotide-level tree for the above three regions of the human enterovirus strains were made by selecting the unweighted pair group method with arithmetic mean (UPGMA) within the phylogeny option of the software toolbar. More alignment trials were performed for the nucleic acid sequences of the human enterovirus strains based on their phylogenetic analysis outcome.

### **2.3.2.3 Generation of the viral consensus sequences**

Consensus sequences for each of the three genomic regions of the phylogenetically related strains of the human enteroviruses, in addition to the human rhinovirus, HMPV, HRSV strains and each of the selected genomic segments of the human influenza virus A, B and C subtypes were designed based on their nucleic acid sequence alignments, using MAC VECTOR software. The generated consensus sequences were saved in a FASTA format and then chopped into many segments; each segment contained 380 bases while the last segment contained the remaining nucleotides.

### **2.3.3 Multiple viral probes design**

Designing specific probes for the selected RNA viruses was performed using two software programs to maximize the yields of probes and to compare between the two methods, as follows:

#### **2.3.3.1 Probes design using OligoArray software**

The OligoArray software version 1 was used for designing specific multiple probes for each consensus sequence of the human enterovirus, human rhinovirus, HMPV and HRSV strains, and human influenza virus subtypes. The software required two files of nucleotide data: the input file and the custom database file. The target consensus sequences of the above viral strains and subtypes were loaded into the input file separately while the custom file should contain the full genome sequences of all viral strains and subtypes of interest. Both input and custom files should be loaded in a FASTA format.

OligoArray software was run 4 times for each consensus sequence. The parameters of the software in the first trial were set as follows:

Probe or Oligo length was 30-31 bases, Temperature range  $T_m$  was 60 °C to 80 °C, GC content ratio was 25-50%, Maximum temperature for a secondary structure was 65 °C, Minimum temperature to consider X-Hybrid was 50 °C , Maximum number of oligo was 50, Maximum distance between the 5' end of each probe and the 3' end of each target sequence was 1500 bases, The minimum distance between 2 oligos was 10 bases and the Prohibited sequences were CCCC, GGGG, AAAA, TTTT. The target consensus sequences were also loaded as prohibited sequences during each trial in order to avoid complete compatibility among the designed probes and these consensus sequences, which may interfere with the subsequent hybridization process. All these parameters were set similarly in the 4 trials except the Maximum temperature to consider X-hybrid was changed in the last three trials to be 55°C, 60°C and 65°C, respectively.

### **2.3.3.2 Probes design using Agilent Technologies eArray software**

The Agilent Technologies eArray software was also used for designing specific probes for each of the above viral strains and subtypes. A compressed folder containing the original full length nucleotide sequences of all of the viral strains and subtypes included in this study was uploaded in a FASTA format into this software while the probe details such as probe length and probe number per target were set to 30 bp and 10 respectively.



### **2.3.4 Testing the specificity of the designed probes:**

The designed OligoArray probes for the human entero-, influenza-, metapneumo- and respiratory syncytial viruses' serotypes were tested using the (BLAST) software of the GeneBank against the NCBI database in order to detect the binding specificity of these designed probes towards their related serotypes' sequences, and also to reveal any sequence homology among the designed viral probes and the human genomes, or other viral genome sequences.

### **2.3.5 Printing the designed probes**

All the probe sequences generated from the probe design process using both of the OligoArray and Agilent eArray software were synthesized and printed simultaneously on two chips (glass slide) by Agilent Technologies Company as mentioned in section 2.3.3. In addition, another group of probes designed by a previous PhD student (Abdel-Hakeem, 2010), were also printed on the same two chips. This group included 80 probes covering the sequences of human herpes viruses (HHV) and was used as a control for the probes design in the current study. Further details about some of these probes will be mentioned in section 4.3.4. The printed chips were stored in a vacuum desiccator in order to be used later for evaluating the performance of the designed probes against some of their target viral nucleic acids.

## **2.4 Results**

### **2.4.1 Phylogenetic analysis results of the human enterovirus genomic sequences**

The first trial of aligning the whole genomes of each of the Human enterovirus A, B, C and D strains revealed very short conserved sequences (up to 10 bp) among their nucleic acids due to the high genetic diversity especially at the 5'UTR and 3'UTR regions. Accordingly, the generated consensus sequence for each of the above human enterovirus species, included many sequences of degenerate nucleotides in order to avoid excluding the hypervariable regions of these generated consensus sequences, which can facilitate designing more probes covering the whole genome of the selected human enterovirus species. The probe design process using these generated consensus sequences will generate probes containing many degenerate nucleotides which may affect probe specificity towards their target viral nucleic acids. Therefore, it was decided to align the nucleic acids sequences of the 5'UTR, CDS and 3'UTR of each of the above human enterovirus strains, use the alignment results of the above regions for each of the Human enterovirus A, B, C and D strains in order to find the phylogenetic relationships among them and then align the nucleic acid sequences of those closely related strains which may generate more specific consensus sequences.

Based on the phylogenetic analysis of the aligned nucleic acid sequences of the three regions (5'UTR, CDS, 3'UTR) of the human enteroviruses, their strains clustered within several groups in a rooted phylogenetic tree specific for each species. The phylogenetic tree of the aligned 5'UTR sequences of the Human enterovirus A strains contains 6 clusters (figure 2-1) while only 3 clusters can

be noticed in the phylogenetic tree of the aligned CDS and 3'UTR sequences of the same strains, respectively (figures 2-2 and 2-3). It can be noticed that coxsackieviruses A 4, 14, 6, 16, 12, 3, 7, 5, 10, 2, 8 and enterovirus 71 strains are closely related to each other in their genetic structure in comparison to those of enteroviruses 76, 89, 90 and 91. However, Human coxsackievirus A6 as an example, clustered with Human coxsackievirus A4, 14 and 16 in one group in the aligned 5'UTR sequences while in the aligned CDS and 3'UTR sequences it clustered in another group with Human coxsackievirus A6, 10, 2, 12, 3, 8, 7 and Human enterovirus 71.

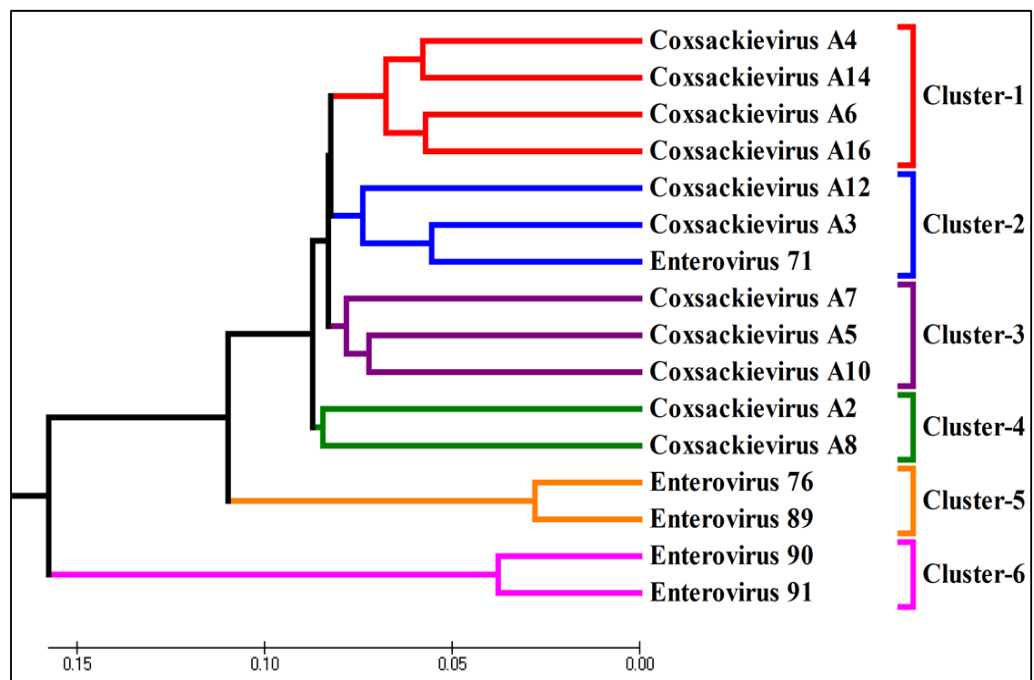


**Figure 2-1: Phylogenetic analysis of the aligned 5'UTR nucleic acid sequences of the Human enterovirus A strains using UPGMA of the MEGA software. The scale refers to percentage of differences among viral strains.**

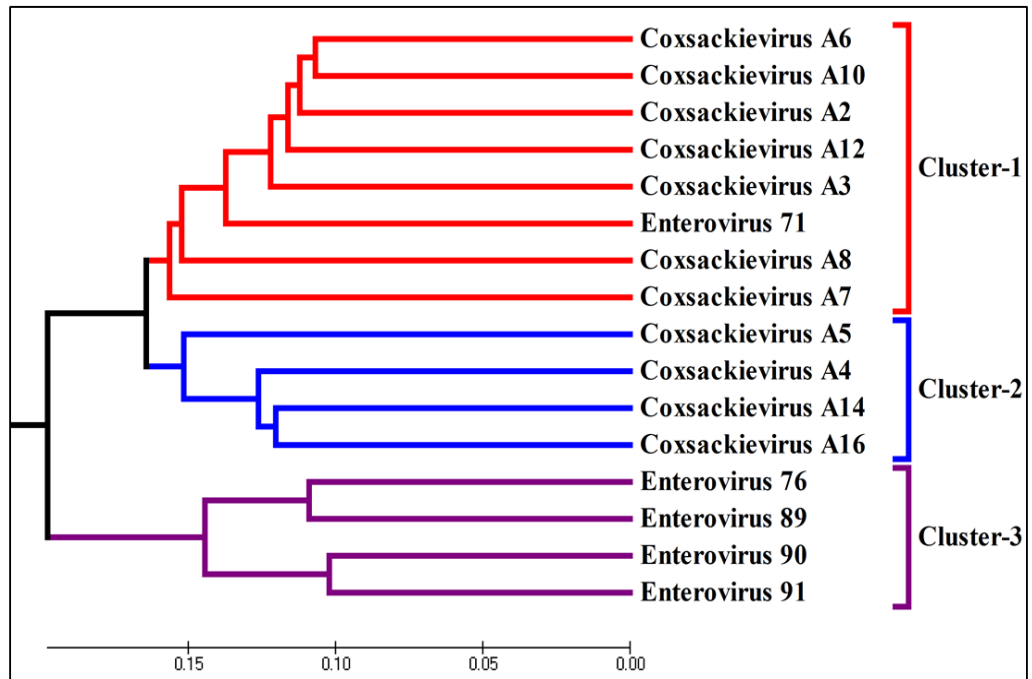


**Figure 2-2: Phylogenetic analysis of the aligned CDS nucleic acids sequences of the Human enterovirus A strains using UPGMA of the MEGA software. The scale refers to percentage of differences among viral strains.**

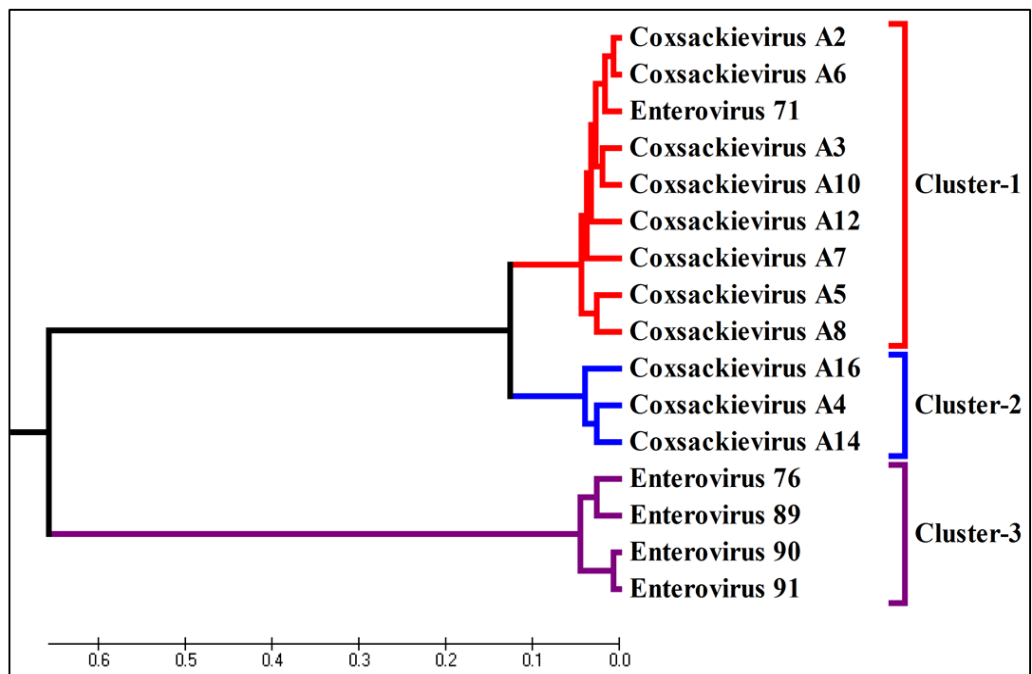


**Figure 2-3: Phylogenetic analysis of the aligned 3'UTR nucleic acids sequences of the Human enterovirus A strains using UPGMA of the MEGA software. The scale refers to percentage of differences among viral strains.**

On the other hand, three phylogenetic trees were generated from the phylogenetic analysis of the aligned 5'UTR, CDS and 3'UTR sequences of the Human enterovirus B strains. Figure 2-4 shows that 31 of these strains clustered together in cluster-1 and 20 strains grouped in cluster-2 while each one of the remaining two strains clustered alone in clusters 3 and 4. All these strains distributed differently into 5 and 8 clusters according to their aligned CDS and 3'UTR sequences as shown in figures 2-5 and 2-6, respectively. Based on the genetic relationships, it can be noticed that Human echovirus 12 as an example clustered alone in the aligned sequences of the 5'UTR region, in the aligned CDS sequences it clustered with 10 other strains (Human echovirus 3, 6, 14, 16, 25, 13, 26, 27, Human coxsackievirus B4 and 6) while it was related to 17 strains in the aligned 3'UTR sequences (Human echovirus 5, 20, 31, 2, 33, 12, 24, 17, 19, 3, 32, 7, 29, Human enterovirus 69, 73, and Human coxsackievirus B4 and A9).

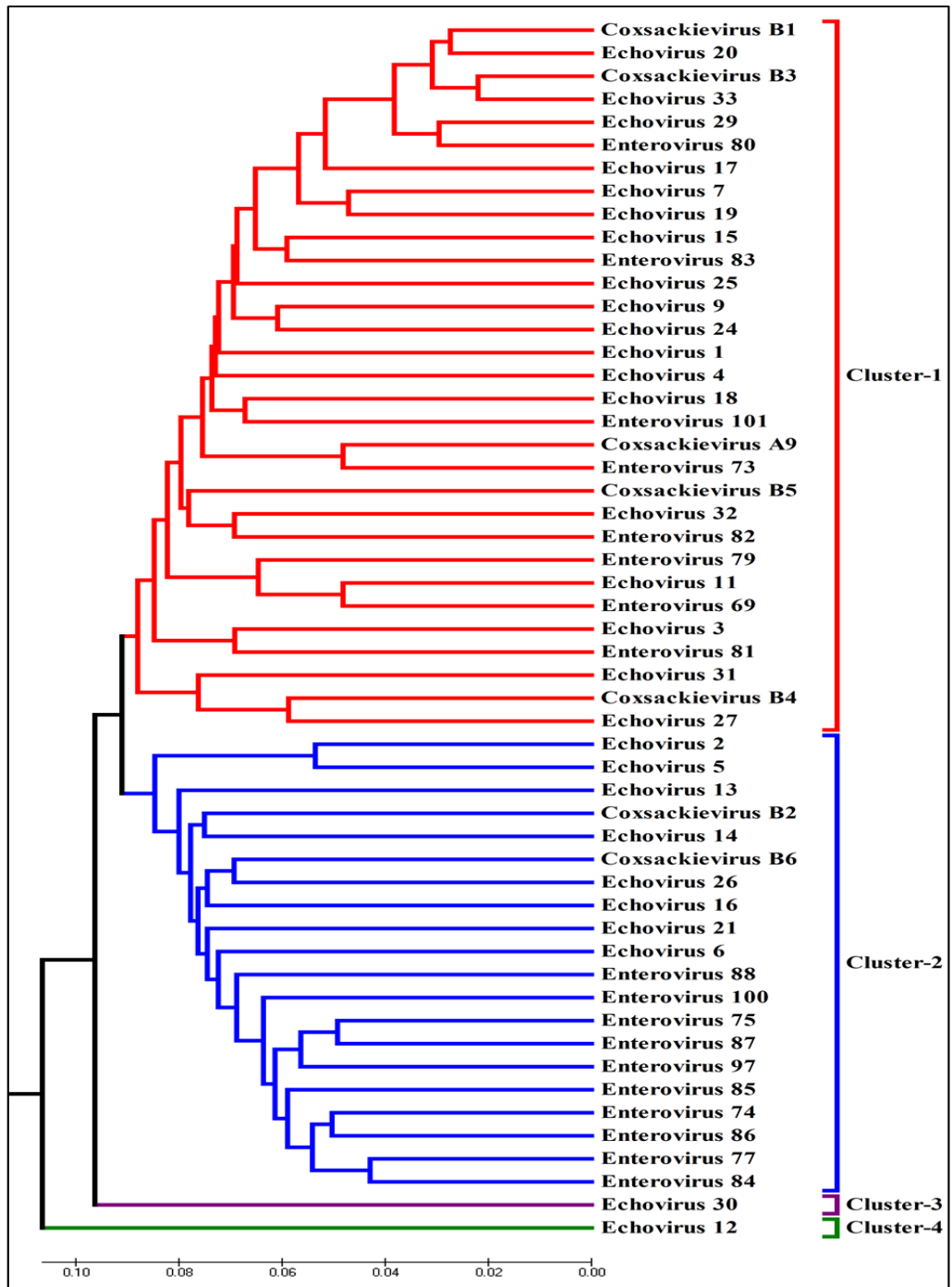


**Figure 2-4: Phylogenetic analysis of the aligned 5'UTR nucleic acid sequences of the Human enterovirus B strains using UPGMA of the MEGA software. The scale refers to percentage of differences among viral strains.**

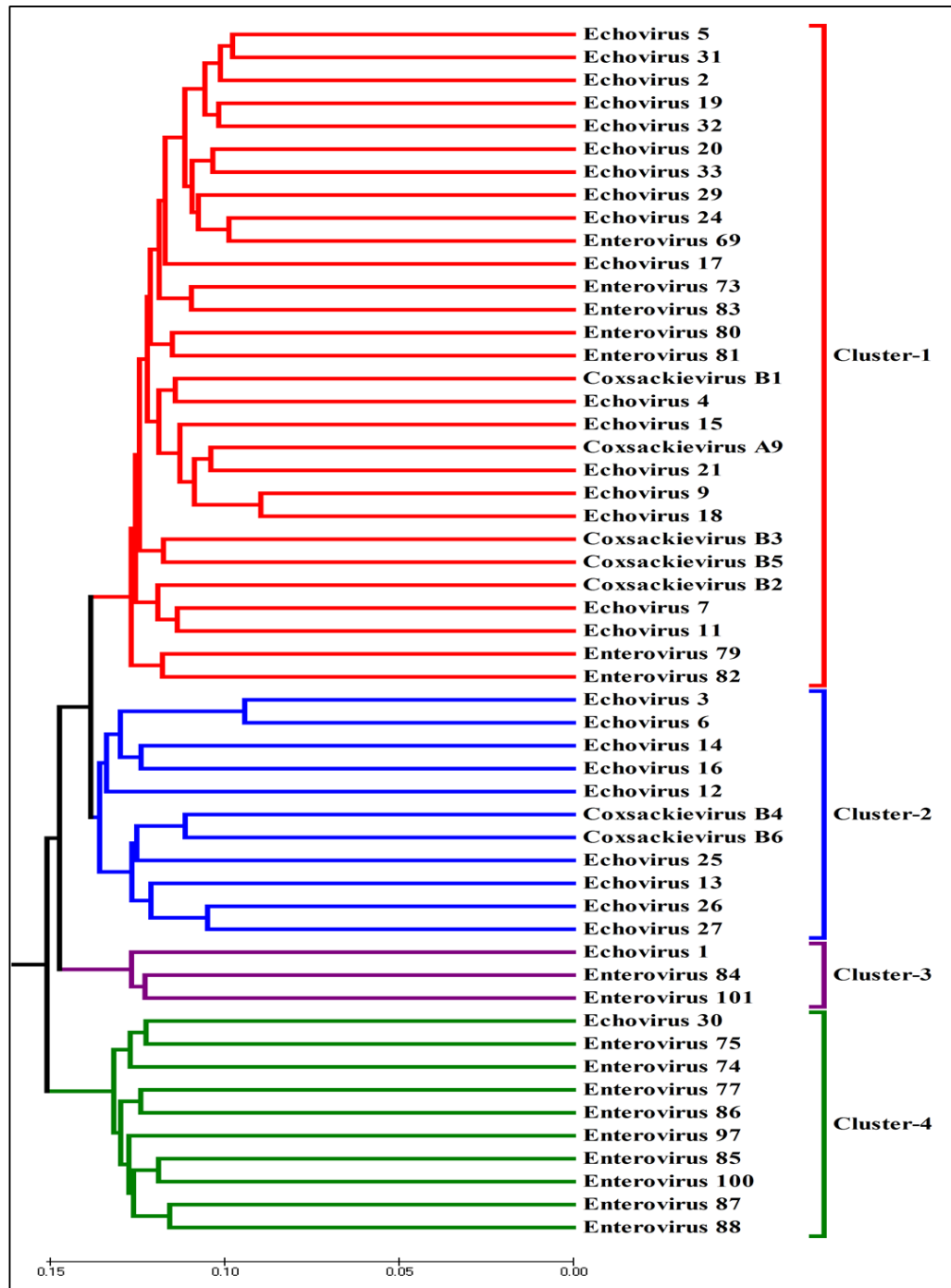


**Figure 2-5: Phylogenetic analysis of the aligned CDS nucleic acid sequences of the Human enterovirus B strains using UPGMA of the MEGA software. The scale refers to percentage of differences among viral strains.**

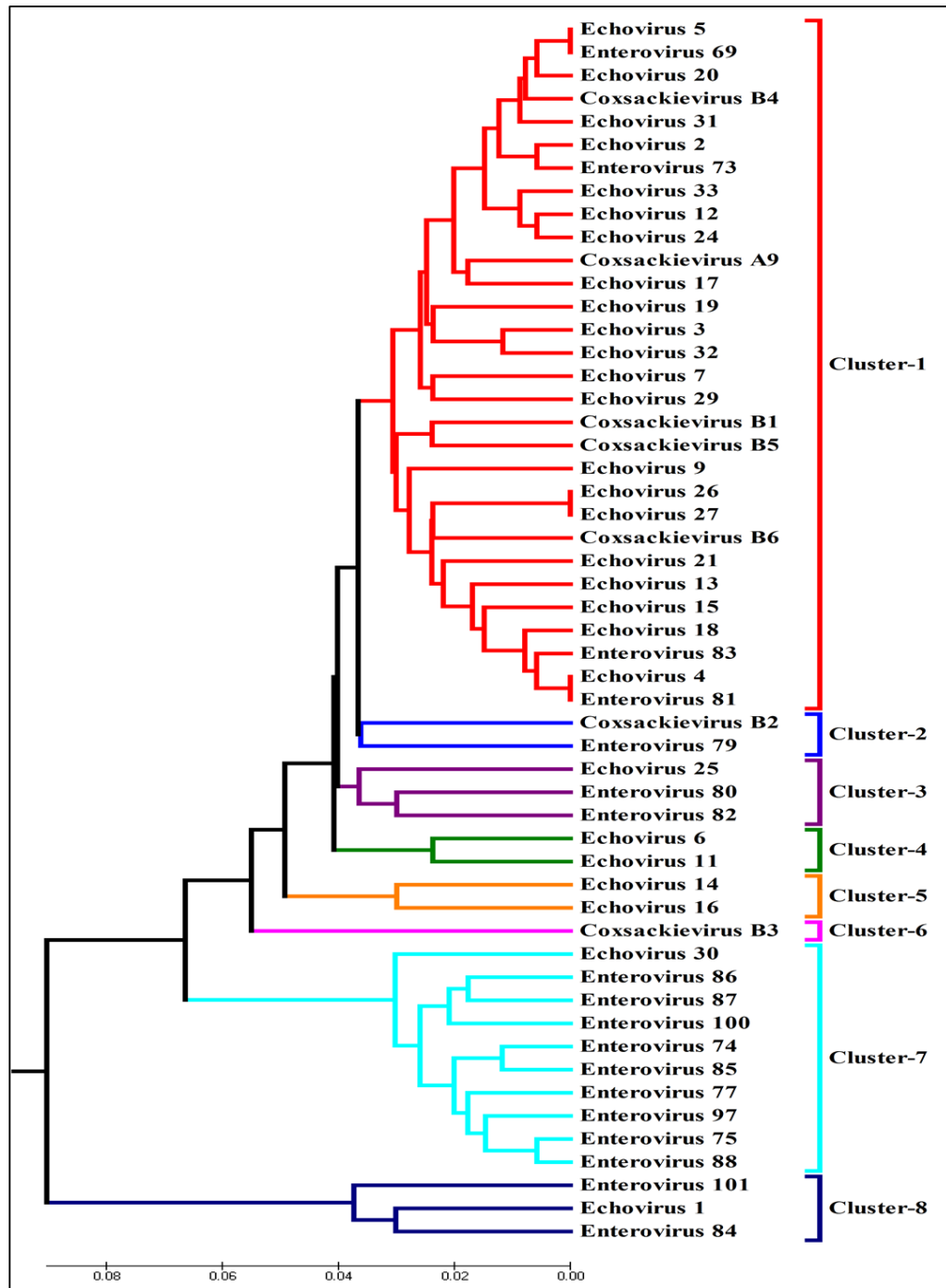


**Figure 2-6: Phylogenetic analysis of the aligned 3'UTR nucleic acid sequences of the Human enterovirus B strains using UPGMA of the MEGA software. The scale refers to percentage of differences among viral strains.**



The strains of Human enterovirus C were also clustered in three different phylogenetic trees based on the alignment of their 5'UTR, CDS and 3'UTR sequences, respectively (figures 2-7 to 2-9). Human enterovirus 96 as an example was genetically close to the Human coxsackievirus A18, 15, 11, 24, 17 and Human poliovirus 2 therefore it clustered with them in one group in the 5'UTR sequences (figure 2-7). However, it clustered alone in the phylogenetic tree of the aligned CDS sequences (figure 2-8), and with Human coxsackievirus A1 and 19 (figure 2-9) according to the alignment results of the nucleotide sequences of each of CDS and 3'UTR regions of the Human enterovirus C strains.

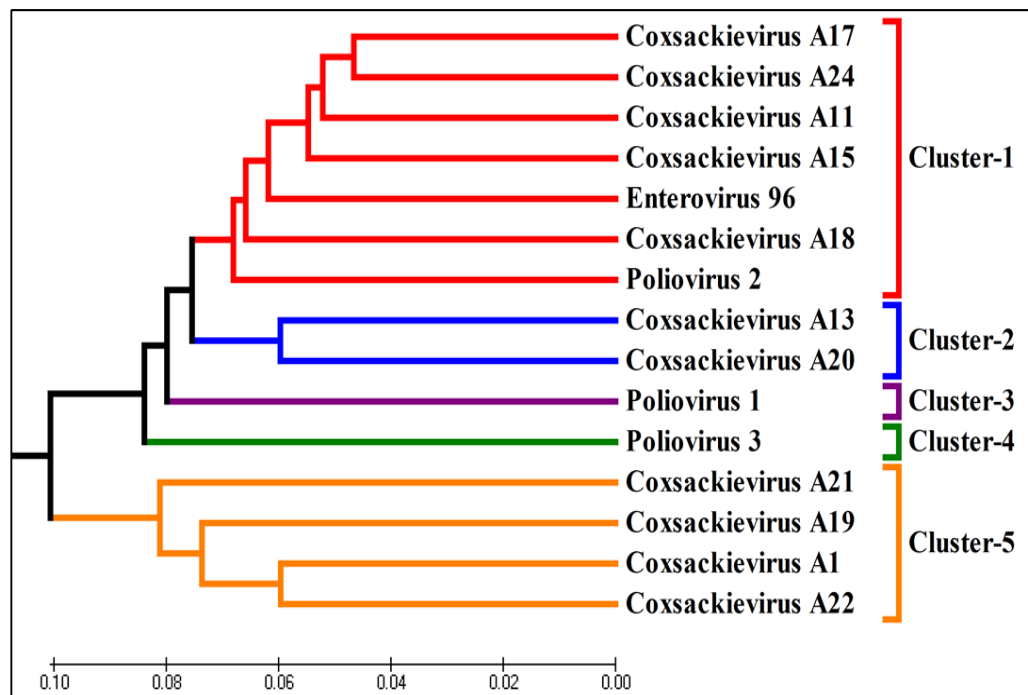


**Figure 2-7: Phylogenetic analysis of the aligned 5'UTR nucleic acid sequences of the Human enterovirus C strains using UPGMA of the MEGA software. The scale refers to percentage of differences among viral strains.**

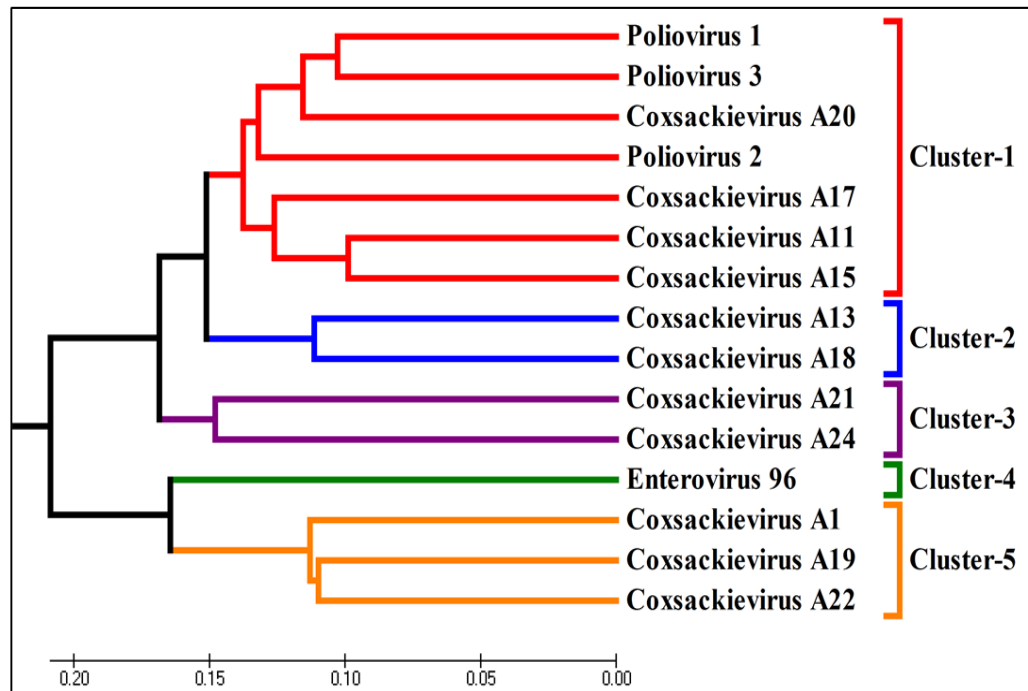


**Figure 2-8: Phylogenetic analysis of the aligned CDS nucleic acid sequences of the Human enterovirus C strains using UPGMA of the MEGA software. The scale refers to percentage of differences among viral strains.**

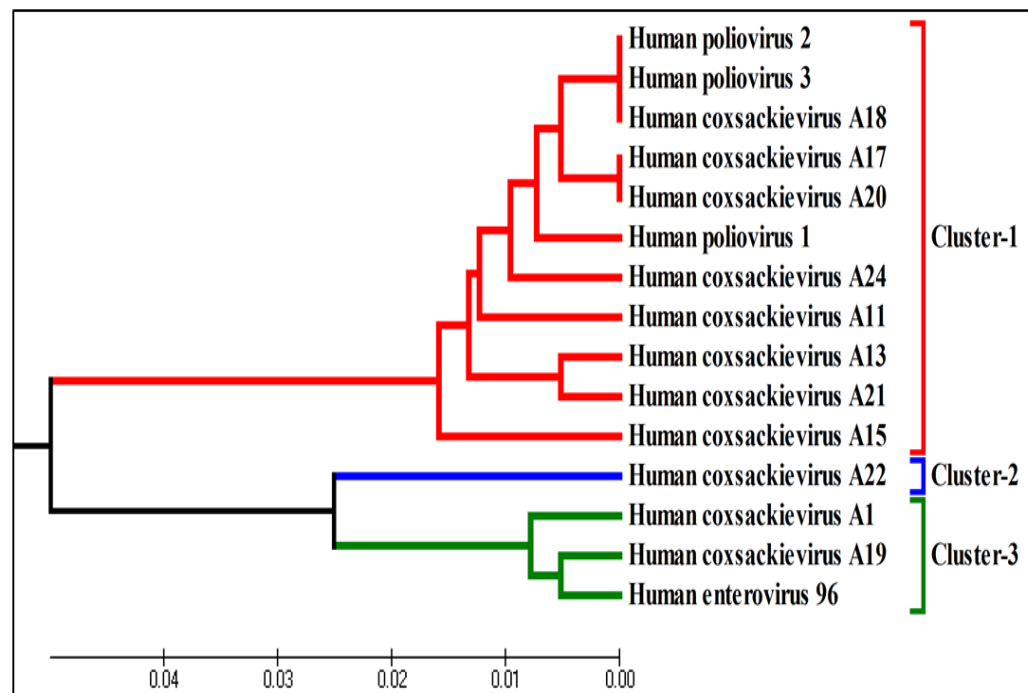


**Figure 2-9: Phylogenetic analysis of the aligned 3'UTR nucleic acid sequences of the Human enterovirus C strains using UPGMA of the MEGA software. The scale refers to percentage of differences among viral strains.**

Alignment results of the 5'UTR, CDS and 3'UTR sequences of the Human enterovirus D showed the same phylogenetic tree for three regions as the Human enterovirus 70 and 94 were close to each other in the alignment results of their 5'UTR, CDS and 3'UTR sequences therefore, they gathered together in one cluster while Human enterovirus 68 clustered alone in the phylogenetic trees (figure 2-10).

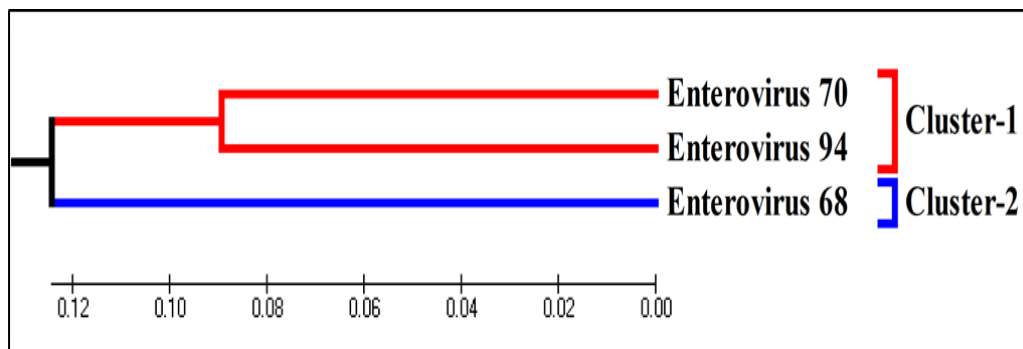


**Figure 2-10: Phylogenetic analysis of the aligned 5'UTR, CDS and 3'UTR nucleic acid sequences of the Human enterovirus D strains using UPGMA of the MEGA software. The scale refers to percentage of differences among viral strains.**

#### **2.4.2 Alignment results of the viral genomes sequences**

Nucleic acid sequence alignment results of the 5'UTR, CDS and 3'UTR regions of the closely related stains of each of the Human enterovirus A, B, C and D, and the human rhinovirus, HMPV and HRSV strains using the CLUSTALW of the MEGA software version 4 revealed many conserved regions among each of the above viral strains which were highlighted with stars (figure 2-11).



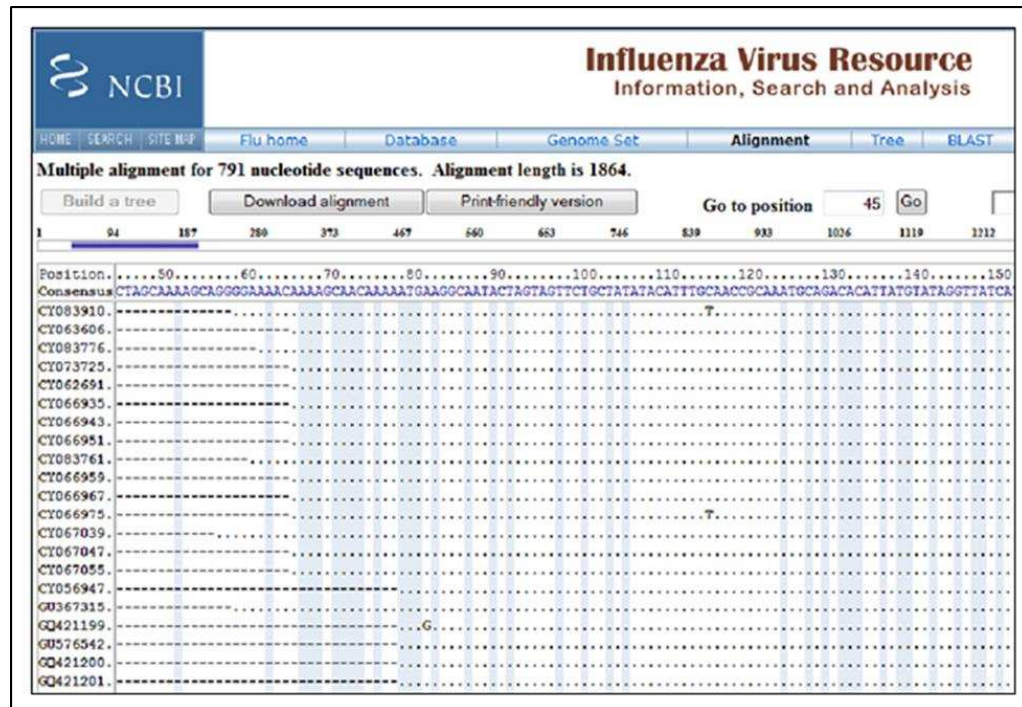


**Figure 2-12: Part of the multiple sequence alignment of the nucleic acid sequences of the HA genomic segment of the H1N1 subtypes showing the conserved regions.**

A=Adenine. G=Guanine. T=Thymine. C=cytosine.

(•) refers to the conserved nucleotides. (-) refers to the mismatch among the nucleotides.

### 2.4.3 Generation of the consensus sequences

Based on the phylogenetic analysis and alignment results of the 5'UTR, CDS and 3'UTR nucleic acid sequences of each of the Human enterovirus A, B, C and D strains, consensus sequence was generated for the closely related strains which were clustered together in one group using MAC VECTOR software. More consensus sequences were generated for each of the human rhinovirus, HMPV, HRSV strains, and each of the HA, NA, MP and HEF genomic segments of the human influenza subtypes in the same way based on the alignment results of their whole genome sequences.

The length of the generated consensus sequences varied as it depends on viral genome size. Any nucleotide mismatch among the aligned nucleic acid sequences of the above viral strains or subtypes was encoded by the MAC VECTOR software with one of the degenerate nucleotides shown in red colour letters in figure 2-13 indicating that the nucleotide at this mismatch position could be either A, T, C or G according to the International Union of Pure and Applied Chemistry (IUPAC) nucleotide ambiguity code shown in table 2-9.

```

NTTAAAACAGCCTGTGGGTTGYACCCACCCACAGGGCCCACTGGGCGCTAGCA
CACTGATTYTVCGGAATCYTTGTGCGCCTGTTTTATATCCCCTCCCCNAADCN
NNGTAACCTAGAAGHWTWVYACHTBWNYGACCADTAGCAGGCGTGRCGRC
CAGYCATGTCTTGGTCAAGCACTTCTGTTTCCCCGGACTGAGTATCAATAAACT
GCTCACGCGGTTGAAGGAGAAAACGTTTCGTTACCCGGCTAACTACTTCGAGAA
ACCTAGTACCACCATGAAAGTTGCTGAGTGTTTCGCTCAGCACTTCCCCCGTGT
AGATCAGGTCGATGAGTCACTGCAAGCCCCACGGGCGACCGTGGCAGTGGCTG
CGTTGGCGGCCTGCCTATGGGDYAACCCATRGGACGCTCTAATAYRGACATGG
TGTGAAGAGTCTATTGAGCTAGTTAGTAGTCCCTCCGGCCCCTGAATGCGGCTAA
TCCTAACTGCGGAGCACAYACCBCAAHCCAGGGGGCAGTGTGTCGTAACGGG
CAACTCTGCAGCGGAACCGACTACTTTGGGTGTCCGTGTTCCTTTTATTCTTAT
ABTGGCTGCTTATGGTGACAATTGARRATTGTTACCATATAGCTATTGGATTGG
CCATCCGGTGTVTAACAGAGCNATDATNTACYHTTTGTGRTTTTRTWCCACT
HACHYHYASHDNNNCHBTHGABACTCTANVTACATTCTWWAHTTGAACWCY
ARRAANNNNN

```

**Figure 2-13: Nucleic acid consensus sequence of cluster 1 of the phylogenetic tree of the aligned 5'UTR of the Human enterovirus A (coxsackievirus A4, 14, 6 and 16).**

**Table 2-9: The code of the degenerate nucleotides used at the mismatches positions of the aligned viral nucleic acid sequences (Cornish-Bowden, 1985).**

UPAC nucleotide code	Base
A	Adenine
C	Cytosine
G	Guanine
T	Thymine
R	A or G
Y	C or T
S	G or C
W	A or T
K	G or T
M	A or C
B	C or G or T
D	A or G or T
H	A or C or T
V	A or C or G
N	Any base

#### 2.4.4 Probe design

The generated consensus sequences were used as templates for probe design which was done in 4 trials by using OligoArray software. In order to acquire more probes within a shorter time, each consensus sequence was segmented into several fragments with 380 nucleotides for each segment except the last one which contained the remainder nucleotides of the consensus sequence. All these segments were loaded as input files into the OligoArray software which generated hundreds of 30 base probes for each of the selected RNA viruses. Since the consensus sequences which were used as templates for probe design included degenerate nucleotides, many of the probes designed using OligoArray software contained some of these degenerate nucleotides scattered along the probe length. Those OligoArray probes containing more than two degenerate nucleotides especially at their 3' end were excluded (table 2-10).

**Table 2-10: Characteristics of the probes designed for the consensus sequence of the 5' UTR nucleic acid sequences of the Human coxsackievirus A4, 14, 6 and 16 which were clustered together in cluster-1 in the 5'UTR phylogenetic tree of the Human enterovirus A strains (see figure 2-1).**

Probe 5'-3'	Position	Length	Tm °C
GGGT <b>Y</b> AACCCAT <b>R</b> GGACGCTCTAATACAGA	12-41	30	74.22
CCCAT <b>R</b> GGACGCTCTAATAY <b>R</b> GACATGGTG	19-48	30	76.2
TAGGACGCTCTAATA <b>Y</b> RGACATGGTGTGAA	23-52	30	75.14
TAATAAGGACATGGTGTGAAGAGTCTATTG	33-62	30	70.81
GGACATGGTGTGAAGAGTCTATTGAGCTAG	39-68	30	77.43
ATGGTGTGAAGAGTCTATTGAGCTAGTTAG	43-72	30	75.11
GGCGCTAGCACACTGATT <b>Y</b> T <b>V</b> CGGAATCCT	44-73	30	78.76
TGAAGAGTCTATTGAGCTAGTTAGTAGTCC	49-78	30	74.28
CACTGATT <b>Y</b> TACGGAATC <b>Y</b> TTGTGCGCCTG	54-83	30	77.95
<b>G</b> <b>C</b> <b>R</b> CCAG <b>Y</b> CATGTCTTGGTCAAGCACTTCT	156-185	30	78.69
GGACTGAGTATCAATAAACTGCTCACGCGG	194-223	30	79.77
TATA <b>B</b> TGGCTGCTTATGGTGACAATTGAAG	206-235	30	75.67
GCTTATGGTGACAATTGAA <b>RR</b> ATTGTTACC	216-245	30	72.5
ATTGAA <b>RR</b> ATTGTTACCATATAGCTATTGG	229-258	30	69.08
TTCGTTACCCGGCTAACTACTTCGAGAAAC	239-268	30	78.95
TACCATATAGCTATTGGATTGGCCATCCGG	242-271	30	78.94
TATTGGATTGGCCATCCGGTGT <b>V</b> TAACAGA	253-282	30	79.24
TCGAGAAACCTAGTA <b>R</b> CACCATGAAAGTTG	260-289	30	74.94
TAGTA <b>R</b> CACCATGAAAGTTG <b>C</b> <b>R</b> GAGTGTTT	270-299	30	73.32

Loading the original whole genome sequences of the human enterovirus, human rhinovirus, HMPV, HRSV, and HA, NA, MP and HEF genomic segments of the human influenza virus into the Agilent Technologies eArray software also generated hundreds of specific probes for each of the above viral strains or subtypes (table 2-11).



**Table 2-11: Shows the number of the probes designed for each species or subtype of the selected RNA viruses, using OligoArray and Agilent eArray software**

Family	Genus	Species	Subtype	Number of probes	
				OligoArray	Agilent eArray
Picornaviridae	Enterovirus	Human enterovirus-A	-----	703	142
		Human enterovirus-B		1081	439
		Human enterovirus-C		858	126
		Human enterovirus-D		310	30
		Human rhinovirus A and B		108	170
Paramyxoviridae	Pneumovirus	Human respiratory syncytial virus		649	42
	Metapneumovirus	Human metapneumovirus		473	66
Orthomyxoviridae	Influenzavirus A	Influenza A virus	HA-H1N1	63	302
			HA-H1N2	61	21
			HA-H2N2	66	25
			HA-H3N2	61	165
			HA-H7N7	93	20
			NA-H1N1	52	375
			NA-H1N2	57	11
			NA-H2N2	57	22
			NA-H3N2	57	212
NA-H7N7	62	10			

Family	Genus	Species	Subtype	Number of probes	
				OligoArray	Agilent eArray
Orthomyxoviridae	Influenzavirus A	Influenza A virus	MP-H1N1	28	143
			MP-H1N2	26	7
			MP-H2N2	27	19
			MP-H3N2	26	97
			MP-H7N7	42	15
	Influenzavirus B	Influenza B virus	HA	57	77
			NA	50	123
			MP	31	61
	Influenzavirus C	Influenza C virus	HEF	71	22
			MP	44	12
Total				5213	2754

### 2.4.5 Probe printing

The 7967 probes generated from the probe design process using both of the OligoArray and Agilent eArray software were printed as spots on two chips; each chip has 8 repeated arrays (figure 2-14). Each array contained duplicates of the 5213 OligoArray probes, 2754 Agilent eArray probes in addition to 45 copies of a specific single probe for HPRT and 80 specific probes for HHV which were designed by a previous PhD student (Abdel-Hakeem, 2010). As a result, each array has 16374 probes.

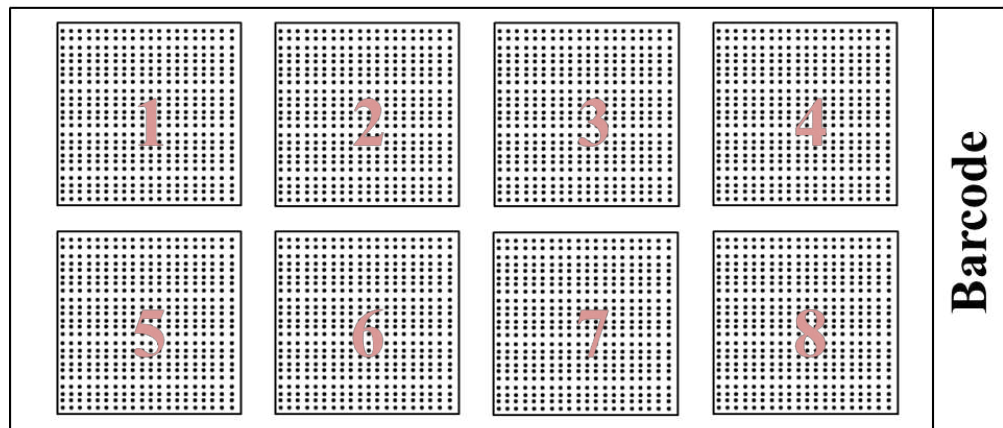


**Figure 2-14: Schematic drawing of the printed chip containing 8 arrays of the designed viral probes.**

## **2.5 Discussion**

Application of the nucleic acid microarrays for the diagnosis of viral infections is mainly based on the detection of the target viral nucleic acids suspected to be found in clinical samples through a hybridization reaction with complementary sequences of nucleic acid called probes spotted on a solid support surface. The definite identity and the spatial position of the probe which hybridizes with the target complementary viral nucleic acid will lead to uncover the identity of viruses in a clinical sample (Brown and Botstein, 1999, Russell, 2003). Double stranded DNA microarrays and Oligonucleotide DNA microarrays are the two common types of nucleic acid microarrays. Double stranded DNA probes or the so-called gene probes (single probe per one gene) generated from either gene clone process or PCR amplification process, are used for constructing double stranded DNA microarrays (Schena et al., 1995, Heller et al., 1997, Duggan et al., 1999). The long length of the gene probes (200-800 bp) enables incorporating more detectable molecules per each probe and increases their hybridization sensitivity and specificity which represents the advantage of this type of nucleic acid microarray in addition to their low production cost. Nevertheless, production of the gene probes requires long time and laborious work especially by using gene cloning method which is considered the main drawback of the double stranded DNA microarrays (Knight, 2001, de Muro, 2005, Ehrenreich, 2006). Oligonucleotide DNA microarrays are the most common type of nucleic acid microarrays used in different aspects of biomedical research, especially in the diagnosis of viral infections. They involve using synthetic oligonucleotide probes targeting specific nucleic acid sequences within the genes of any organism in order to be used for analyzing

and monitoring their expression. Different length of oligonucleotide probes were used for constructing this type of microarray. Short oligonucleotide probes (18-30 nt) were used for mutation detection among the influenza virus subtypes based on the single base mismatch among their nucleic acids sequences (Sengupta et al., 2003, Kessler et al., 2004). Chou and his colleagues used long oligonucleotide probes (60-70 nt) for detecting and identifying viral pathogens in clinical samples. Direct chemical synthesis of the oligonucleotide probes on a solid surface allows spotting up to 100 000 of these oligonucleotide probes on a one inch area. This type of nucleic acid microarray is called a high density oligonucleotide array and can be produced commercially by many companies (Lander, 1999, Hughes et al., 2001). Therefore, it was decided to use this type of nucleic acid microarray for designing a single microarray chip containing thousands of probes in order to be used for diagnosing of viral infections caused by four different groups of RNA viruses. The length of the designed probes was determined to be 30 nt as shorter probes may lack specificity while the longer probes require more time to hybridize with their target complementary nucleic acid sequences. All the probes were designed with a GC content ratio not more than 60% in order to avoid possible cross hybridization resulted from higher GC content ratio. Furthermore, the OligoArray and Agilent Technology eArray software were set to exclude probes containing complementary regions or long stretches sequences (> 4) of the same nucleotide in order to avoid forming secondary and/or hair pin structures which may inhibit their hybridization to the target nucleic acids (Keller et al., 1989).

Due to the short size of the oligonucleotide probes, they can easily attach to the solid substrate through covalent coupling and electrostatic attraction, but this attachment is not strong enough to keep them linked to the microarray surface as a considerable amount of them may be lost through the hybridization process and post-hybridization wash harshness (Rickman et al., 2001, Ehrenreich, 2006). Modifying the oligonucleotide probes by adding amino group at their 5' end, can enhance their covalent linkage to the microarray surface, but it may add some cost for constructing the oligonucleotide microarrays (Zammatteo et al., 2000, Call et al., 2001). Coating the supporting surface used for accommodating oligonucleotide probes with chemical compounds such as amino silane provides positively charged amine groups which can attach to the negatively charged phosphate groups of the oligonucleotide probes (Todt and Blohm, 2009, Maskos and Southern, 1992). Nitrocellulose (Nylon) membrane can be used for constructing nucleic acid microarrays, but its high autofluorescence and fragility in addition to their ability to release the probes during hybridization process limit its application for this purpose. On the contrary, glass slides have low inherent fluorescence and superior optical features for fluorescent scanning as well as being more resistant to break. Therefore, slides are more convenient for probe printing than the other types of membranes and it is considered as the perfect choice for microarray spotting (Chiu et al., 2003, de Muro, 2005).

**3 Application of the multiple  
displacement amplification technique  
for testing the specificity of the  
designed viral microarray**

### 3.1 Introduction

Microarray technology represents the latest invaluable method used widely in molecular biology laboratories for research purposes (Jayapal and Melendez, 2006). It was first used in immunological assays by Ekins in 1989 (Ekins, 1989, Howbrook et al., 2003). Kononen and his colleagues developed nucleic acid microarrays as a tool for comprehensive screening of gene expression of a large number of genes within a tumor in one experiment (Kononen et al., 1998). (Wang et al., 1998) designed a microarray chip for wide scale identification of human single nucleotide polymorphisms (SNP) responsible for many genetic diseases (Call, 2001b). Microarray has also been applied for identification of human and animal pathogens (Severgnini, 2011) and accordingly, many new drugs and therapeutic compounds have been discovered and validated for human use using the microarray technique in the Pharmacology field (Gerhold et al., 2002, Trevino et al., 2007, Khan, 2010).

Sachse and his colleagues used microarray for the identification of Chlamydia and Chlamydophila spp. (Sachse et al., 2005), while other researchers identified 11 bacterial- and 5 viral species using only a single microarray (Wilson et al., 2002). Many other research groups applied this technique for identification of human viral pathogens only (Wang et al., 2002, Sengupta et al., 2003, Klaassen et al., 2004, Nordstrom et al., 2005, Albrecht et al., 2006, Lopez-Campos et al., 2007, Baek et al., 2008).

Microarray consists of tiny spots (10-500 microns) of biomolecules, affixed in a grid pattern to a solid support platform which may be either silicon, plastic or glass surface, using a suitable robotic arrayer. Either the attached biomolecules or the target materials should carry a reporter molecule such as cyanine 3 (Cy-



3), Cy-5 or biotin in order to detect the fluorescent signals generated from their interaction using an appropriate reader (Call, 2001b, Zajac et al., 2007).

DNA microarray is the most common type of biological microarray used in the healthcare field not only for the diagnosis of infectious diseases, but also to define tumor genes. DNA microarrays may contain from a few dozen to many thousands of oligonucleotides (up to 50-mer) called probes, fabricated either covalently or noncovalently on the solid surface. The work principle of the DNA microarray mainly depends on the base pairing and hybridization reaction between the attached probes and complementary sequences of nucleic acids labelled with a detectable molecule. The resultant hybrids can be detected using a laser scanner.

DNA microarray became superior to other traditional techniques used for the same application such as Southern or Northern blots due to its ability to screen thousands of genes simultaneously (Heller, 2002, Trevino et al., 2007).

Both purity and concentration of the target genetic materials may affect the performance and success of the nucleic acids microarray. Using low concentrations of microbial biomass may inhibit the hybridization reaction between complementary sequences and make it difficult to apply nucleic acids microarray for the detection of microbial pathogens (Wu et al., 2006).

Therefore, it is highly recommended to amplify either the sample content of nucleic acids before starting microarray hybridization regardless of their available initial concentration, or amplify the generated signals after hybridization (Stears et al., 2000, Zhou and Thompson, 2002).

Difficulties associated with using conventional PCR based methods for amplification of microbial genome samples, such as probable bias during

amplification and/or the need to use many sets of primers for comprehensive amplification of each sample, urged researchers to think about using an alternative method for amplification of the nucleic acids (Vora et al., 2004).

WGA involves using of Phi 29 DNA polymerase enzyme which binds tightly to the DNA template and synthesizes several new complementary strands through MDA process (Kittler et al., 2002).

## **3.2 Aims**

There were two main aims for this chapter of the project. The first was to randomly amplify the entire genome of some human enteroviral nucleic acids extracted from clinical samples and tissue cultures using multiple displacement activity of the Phi 29 DNA polymerase. The second aim was to validate the hybridization behaviour of the viral amplicons against six specific probes for human enteroviruses which were designed and tested successfully by a previous PhD student (Abdel-Hakeem, 2010), before using these amplicons for testing the hybridization performance of the viral probes designed in chapter two.

## **3.3 Materials and methods**

### **3.3.1 Specimens**

Some samples including i) RNA transcripts for Human echovirus 30 , ii) clinical samples known to be positive for enteroviruses, iii) pTZ18R plasmid, iiiii) hypoxanthine-guanine phosphoribosyltransferase (HPRT) were used as a source for nucleic acids in order to optimize the microarray hybridization and test the designed microarray assay under real-world conditions.

The viral transcripts were comprised of  $10^6$  copies/ $\mu\text{l}$  of an extracted RNA for Human echovirus 30, and provided kindly by Professor Peter Simmonds, Centre of Infectious Diseases, University of Edinburgh, Summerhall, Edinburgh, UK. The clinical samples were provided from the clinical Virology laboratory, Queen's Medical Centre (QMC), Nottingham, UK.

### 3.3.2 Samples preparation

Different processing steps were used to prepare samples for hybridization experiment, as follow:

#### 3.3.2.1 Isolation of the ribonucleic acid (RNA)

$\mu\text{MACS}$  one-step cDNA kit (Miltenyi Biotec, Surry, UK) was used to extract RNA, which can also fulfil the reverse transcription of the viral mRNA which is normally called complementary DNA (cDNA) synthesis in a further step. This method was used only with enteroviruses, as their genomes harbour poly-A tail. The principle of this isolating method is to pull down RNA containing a poly-A tail by using microbeads coated with oligo-dT.

The enterovirus clinical sample was first lysed by adding 1 ml of lysis/binding buffer per 0.5 ml of the above sample and vortexing for 3-5 minutes. The sheared lysate was loaded into the provided lysate clear column and centrifuged at  $\geq 11800$  rpm for 3 minutes. Then, the eluate was mixed with 50  $\mu\text{l}$  of oligo-dT microbeads. The MACS micro column was positioned in the magnetic field of the provided thermoMACS separator and rinsed with 100  $\mu\text{l}$  of lysis/binding buffer. The magnetically labelled eluate was loaded on to the micro column matrix which retained the RNA-oligo-dT microbeads hybrid

while the eluate was passed through the micro column. The hybrid was washed twice with 200  $\mu$ l of lysis/binding buffer and four times with 100  $\mu$ l of wash buffer. cDNA synthesis proceeded directly on the same separating micro column which was rinsed twice with 100  $\mu$ l of the equilibration/wash buffer.

Immediately, the lyophilized reverse transcriptase was dissolved in 20  $\mu$ l of resuspension buffer and loaded on the column matrix. The column was incubated in the thermoMACS separator for 60 minutes at 42 °C to achieve reverse transcription process and generate cDNA. The column was rinsed twice with 100  $\mu$ l of the equilibration/wash buffer, followed by addition of 20  $\mu$ l of the cDNA release solution. After incubation for a further 10 minutes at 42 °C, the generated cDNA was eluted with 50  $\mu$ l of elution buffer.

### **3.3.2.2 Extraction of viral RNA from clinical samples**

Viral RNA was extracted from the clinical samples using the QIAamp Viral RNA Mini kit (Qiagen, west Sussex-UK). This method was used with viral types other than enteroviruses, which their genomes lack poly-A tail. Samples were first lysed using AVL buffer which contains guanidine thiocyanate. This highly denaturing buffer is necessary for the release of the viral RNA from the viral particles and infected human cells. Furthermore, it inactivates RNases and adjusting the buffering conditions to improve viral RNA binding to the QIAamp membrane.

According to the manufacturer's guideline, samples were lysed by mixing 560  $\mu$ l of AVL buffer containing 5.6  $\mu$ g of carrier RNA with 140  $\mu$ l of the clinical sample by pulse-vortexing for 15 seconds. After 10 minutes of incubation at room temperature, 560  $\mu$ l of absolute ethanol were added to the lysate. Then

the mixture was applied to a QIAamp Mini column and spun at >8000 rpm for 1 minute. Any further protein and salt contaminants were washed away from the bound RNA in the column membrane through centrifugation for 1 minute at >8000 rpm using 500 µl washing buffers AW1 and AW2, respectively. Finally, the viral RNA was eluted in 60 µl of elution buffer (AVE) after centrifugation for 1 minute at 8000 rpm.

### **3.3.2.3 Reverse transcription of the viral RNA**

SuperScript III First-Strand Synthesis SuperMix kit (provided by Invitrogen) was used as an additional method to generate viral cDNA from viral RNA. This step is required to generate the starting template for the initiation of viral nucleic acid amplification.

Six microliters of the total viral RNA were mixed with 1 µl of oligo-dT primers (50 pmol) and 1 µl of the annealing buffer in order to initiate and improve the primers annealing to the viral RNA target. After 5 minutes of incubation at 65 °C in a thermal cycler, the mixture was immediately chilled on ice for 1 minute and spun briefly. Generation of the cDNA was achieved by adding 10 µl of the 2X First-Strand Reaction Mix which contains 1mM of each dNTP, and 2 µl of the SuperScript III/ RNaseOut Enzyme mix containing the reverse transcriptase enzyme. The mixture was incubated at 50 °C for 30 minutes. The reaction was terminated by heating the mixture at 85 °C for 5 minutes. The generated viral cDNA was stored at -80 °C for further use.

### **3.3.2.4 Second strand synthesis of the viral cDNA**

NEBNext Second Strand Synthesis Module (New England Biolabs) was used to generate double stranded cDNA from the first strand viral cDNA, which may be more appropriate for amplification process using PCR.

The total 20  $\mu$ l of the reverse transcription reaction generated in section 3.3.2.3 were mixed with 48  $\mu$ l of nuclease free water, 8  $\mu$ l of 10X second strand synthesis reaction buffer and 4  $\mu$ l of second strand synthesis enzyme mix, and incubated at 16 °C for 2.5 hours.

### **3.3.2.5 Preparation of the pTZ18R plasmid**

The pTZ18R plasmid was introduced to amplification and subsequent hybridization steps. This allowed for comparing the effect of the fragile RNA on such processing and subsequent weak hybridization signals.

#### **3.3.2.5.1 Linearization of the pTZ18R**

The pTZ18R is a circular double stranded DNA plasmid with 2861 bp length. Therefore, the plasmid was digested by a restriction endonuclease in order to produce linear copies with sticky ends. This step enables binding of the linear chunks of the plasmid together through ligation of their resulted compatible ends to generate longer products which can improve the performance of the MDA process later.

SapI restriction enzyme supplied in 2000 units/ml by New England Biolabs was used to digest the pTZ18R. This enzyme will cut the pTZ18R plasmid at the recognition site 470-476 with the following sequence, and generates a linear product (figure 3-1).

$$5' \dots \text{GCTCTTC} \dots 3'$$
$$3' \dots \text{CGAGAAG} \dots 5'$$

According to the manufacturer's protocol, 1 µg of the circular plasmid was digested using 1 unit of SapI and 5 µl of 10X NE Buffer, the final reaction volume was adjusted to 50 µl using nuclease free water. The reaction mixture was incubated at 37 °C for 1 hour followed by heating to 65 °C for 20 minutes in order to inactivate the enzyme and stop the digestion reaction.

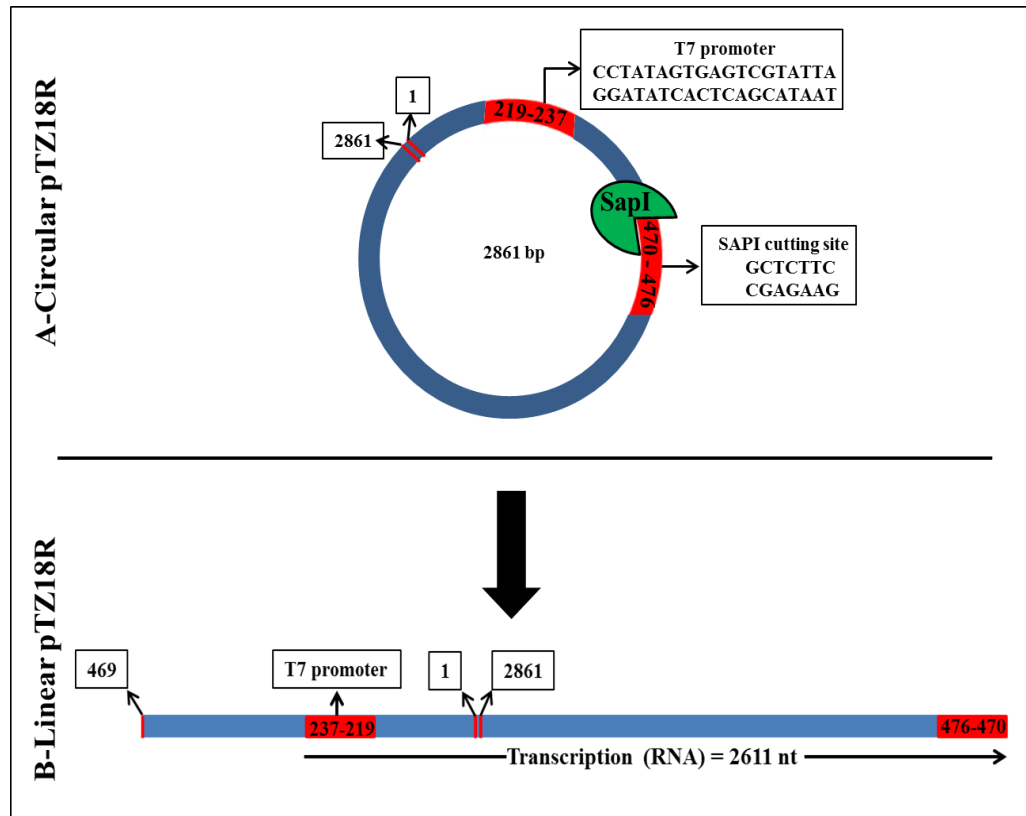


**Figure 3-1: Schematic diagram showing the linearization process of the pTZ18R plasmid.**

Figure (A) the circular shape of the plasmid showing the site, size and the sequence of each of the T7 promoter and the recognition site of the SapI. Figure (B) the linear shape of the plasmid showing the starting point and the direction of the plasmid transcription, and the length of the generated RNA.

### 3.3.2.5.2 Purification of the digested pTZ18R

A Qiaquick PCR purification kit (Qiagen, UK) was used to purify the digested plasmid. The combination between the spin column technique and the selective binding properties of the included silica membrane improves the kit purification performance.

High concentrations of chaotropic salts in addition to  $\text{pH} \leq 7.5$  will be required to facilitate and enhance the adsorption and capturing of the digested products of the plasmid ranging between 0.1 to 10 kb in size to the column's silica membrane when applying the digestion reaction mixture.



Any contaminants, oligonucleotides or enzymes will be washed away through the column by using the PE buffer. The clean digested products of the pTZ18R will be eluted using nuclease free water or elution buffer in the final step. Seventy five  $\mu$ l of Buffer PB were mixed with 15  $\mu$ l of the digestion reaction mixture, and then 10  $\mu$ l of 3M sodium acetate, pH 5 were added to the mixture to adjust the pH reaction below 7.5. The mixture was applied to the assembled spin column with its 2 ml collection tube, and centrifuged for 1 minute at 13000 rpm. After discarding the flow-through, the column was placed back in the tube and the digested products were washed with 750  $\mu$ l Buffer PE using centrifugation with the same above conditions. The flow-through was also discarded and the spin column was re-placed in the same collection tube to repeat centrifugation for an additional 1 minute to remove any residual ethanol from the washing step. The column was placed in a sterile eppendorf tube and the digested pTZ18R was eluted in 30  $\mu$ l elution buffer after spinning for 1 minute at the same above speed.

### **3.3.2.5.3 Agarose gel electrophoresis**

In order to detect the expected size of the digested products and compare it with the undigested plasmid, both samples were run on a 1% agarose gel (Invitrogen, Paisley, UK) using 1X Tris-acetic acid-EDTA (TAE) running buffer containing 0.2 ng/ml ethidium bromide (SIGMA-ALDRICH, UK). Five microliters of each plasmid sample were mixed with the DNA loading buffer and run on the gel for 45 minutes using 90 volts. Smear bands of the plasmid products were visualized using an ultraviolet light scanner, and their size was

compared to the 1 kb DNA Step Ladder (Fermentas life Sciences, UK) used as a size marker.

#### **3.3.2.5.4 Evaluating the digested plasmid products**

In order to determine the quantity and the quality of the digested products after purification, they were measured spectrophotometrically using the NanoDrop ND 1000 (Thermo Scientific). One microliter of the digested pTZ18R was uploaded to the machine and their optical absorbance was measured at two wavelengths 260 and 280 nm.

#### **3.3.2.5.5 Transcription of the digested pTZ18R**

Transcription of the plasmid was done in order to generate an RNA template comparable to the viral nucleic acids used in this study which can facilitate optimizing the processing steps for the successful hybridization between the selected viral nucleic acids and the probes designed in chapter 2.

The MEGAscript T7 kit (Life technologies) was used for plasmid transcription. According to the manufacturer's protocol, 0.25 µg of the linear plasmid was mixed with 2 µl of each of the ribonucleoside triphosphate (rNTPs), 2 µl of 10X reaction buffer and 2 µl of the enzyme-T7 RNA polymerase. The final volume of the reaction mixture was adjusted to 20 µl using nuclease free water. The transcription reaction proceeded via incubation of the mixture at 37 °C for 4 hours, followed by incubation at the same temperature for 15 minutes after adding 1µl of the Turbo DNase in order to remove the template DNA of the plasmid.

### 3.3.2.5.6 Purification of the pTZ18R RNA

The transcribed RNA was subjected to purification step before proceeding with any further preparation processes for the microarray hybridization as it may be inhibited by any residual of the enzymatic reaction such as plasmid DNA, rNTPs or enzymes especially RNases and RNA polymerase. Furthermore, any short segment of the RNAs less than 200 nucleotides such as ribosomal ribonucleic acid (rRNA) and transfer ribonucleic acid (tRNA) will be removed. RNeasy Plus Mini kit (Qiagen, west Sussex-UK) was used to purify the transcribed RNA which was mixed with 350  $\mu$ l of RLT buffer containing 0.01%  $\beta$ -mercaptoethanol ( $\beta$ -ME) and 250  $\mu$ l of absolute ethanol. Using the provided RNeasy spin column, the mixture was centrifuged for 15 seconds at 10000 rpm. The retained RNA was washed with 700  $\mu$ l of buffer RW1 followed by 500  $\mu$ l of buffer RPE using centrifugation with the same previous conditions. Final washing step was done using the same volume of buffer RPE with centrifugation at 10000 rpm for 2 minutes. The clean RNA was eluted in 50  $\mu$ l of nuclease free water. Based on the NanoDrop results, the final copy number of the transcribed RNA was determined per each microliter.

### 3.3.2.5.7 Analysis of the pTZ18R RNA

The quality of the RNA generated from the plasmid DNA transcription process was determined using the RNA 6000 Nano Assay Kit (Agilent Technologies) and the Agilent 2100 Bioanalyzer. By following the manufacture's guideline, the bioanalyzer electrode was cleaned with the RNase ZAP and rinsed with RNase free water using a nano chip electrode cleaner. Nine  $\mu$ l of the prepared gel-dye mixture were loaded into each one of the 3 wells of the RNA nano chip

marked with G. By the same way, 5  $\mu$ l of the Nano Marker (green) were added to each one of the remaining 13 wells. Finally, one microliter of the RNA 6000 ladder was denatured for 2 minutes at 70 °C and injected into the well which marked with the ladder symbol, while 1  $\mu$ l of the denatured RNA sample at the same previous conditions was loaded into the RNA sample well. Then, the RNA nano chip was placed in the Agilent 2100 Bioanalyzer and the RNA sample was analysed using the 2100 Expert Software (prokaryotic total RNA program) loaded on the machine.

### **3.3.2.6 Preparation of the HPRT sample to be used as an internal positive control**

HPRT is one of the housekeeping genes expressed in all human tissues and cells. Therefore it was selected to be an internal positive control as an indicator for the performance of the hybridization experiments. A sequence of steps was done to prepare the HPRT sample for hybridization test which included:

#### **3.3.2.6.1 Extraction of human DNA**

Nucleic acid DNA from human peripheral blood samples was extracted using the QIAamp DNA mini extraction kit (Qiagen, west Sussex-UK). In a 1.5 ml eppendorf tube, 200  $\mu$ l of the blood sample were mixed with 20  $\mu$ l of the Qiagen protease and 200  $\mu$ l AL buffer containing guanidinium hydrochloride solution in order to lyse the blood cells and release their nucleic acids. Two hundred microliters of absolute ethanol were added to the lysate after 10 minutes of incubation at 56 °C. The mixture was applied to the provided QIAamp mini spin column and centrifuged at 8000 rpm for 1 minute.

The DNA bound to the mini column was washed with 500  $\mu$ l of wash buffer 1 (AW1) and centrifuged at the same above conditions. The washing step was repeated using 500  $\mu$ l AW2 and centrifuged for 3 minutes at 14000 rpm. Finally, the pure DNA was eluted in 50  $\mu$ l elution buffer (AE) with centrifugation for 1 minute at 8000 rpm.

### 3.3.2.6.2 HPRT amplification

The isolated human DNA was subjected to PCR in order to amplify part of the HPRT gene with the accession number: NM\_000194 in the NCBI database. HotStarTaq DNA Polymerase kit (Qiagen, west Sussex-UK) was used for this purpose with a set of in-house 20-mer primers for PCR amplification of the HPRT (table 3-1).

**Table 3-1: Features of the primers used for HPRT-PCR**

(Adopted from (Abdel-Hakeem, 2010))

Primer ID	Sequence (5'→3')	Tm °C	GC%	Amplicon Size
HPRT-FW	GACCAGTCAACAGGGGACAT	55.9	55	160 bp
HPRT-RV	CGACCTTGACCATCTTTGGA	54.2	50	

FW=Forward primer, RV= Reverse primer

According to the manufacturer's guideline, 100  $\mu$ l of the PCR reaction mix containing 1X PCR buffer, 200  $\mu$ M of each dNTP, 0.2  $\mu$ M of each primer, 2.5 units of HotStarTaq DNA polymerase and 0.5  $\mu$ l of the extracted human DNA was prepared. The reaction mix was amplified using the thermal cycler (Techne TC-3000) with the cycling programme shown in table 3-2.

**Table 3-2: The optimal cycling programme used for HPRT-PCR amplification**

Stage		Temperature	Time	Cycles
Initial enzyme activation		95 °C	5 minutes	1
Amplification	Denaturation	94 °C	1 minute	35
	Annealing	58°C	1 minute	
	Extension	72 °C	1 minute	
Final extension		72 °C	10 minutes	1

### 3.3.2.6.3 HPRT Purification and measurement

The PCR products were purified using a Qiaquick PCR purification kit as described in section 3.3.2.5.2. The purified products were run on a 1% agarose gel as described in section 3.3.2.5.3 to determine their size, while their concentration was measured using the NanoDrop as described in section 3.3.2.5.4.

## 3.3.3 Amplification of the whole viral RNA

Amplification of viral nucleic acids may be necessary with viral samples containing a low copy number of the viral genomes in order to achieve detectable hybridization. Three different methods were used for this purpose:

### 3.3.3.1 MDA process

Viral cDNA was randomly amplified using a REPLI-g UltraFast mini kit (Qiagen, UK) utilizing Phi 29 DNA polymerase. This enzyme has the ability to replicate the viral genome isothermally in a technique called multiple displacement amplification (MDA) see chapter 1.

According to the manufacturer's recommendations, 1  $\mu$ l of the diluted denaturation buffer (1:7) was added to a tube containing 1  $\mu$ l of the viral cDNA template and incubated at room temperature. The denaturation process was stopped after 3 minutes by adding 2  $\mu$ l of the diluted neutralization buffer (1:9). Replication of the viral nucleic acids was completed by adding 16  $\mu$ l of a mixture containing 1  $\mu$ l of the Phi 29 DNA polymerase and 15  $\mu$ l of the reaction buffer containing dNTPs, and incubating at 30 °C for 1.5 hour in a thermal cycler. The amplification was stopped by heating the mixture for 3 minutes at 65 °C. A Parallel reaction was performed as a negative control by adding 1  $\mu$ l of nuclease free water instead of the viral cDNA. The amplified products were purified as described in section 3.3.2.5.2 followed by running the purified amplicon on agarose gel, and measuring their concentration using nanodrop as describe in sections 3.3.2.5.3 and 3.3.2.5.4, respectively.

### **3.3.3.2 Amplification of the RNA templates using QuantiTect whole transcriptome kit**

Based on the same principle of the MDA, QuantiTect whole transcriptome kit (Qiagen, west Sussex-UK) was used as an alternative kit for WGA of the pTZ18R RNA in parallel with enteroviral RNA. The kit is designed to synthesise a cDNA strand from its relevant RNA template and ligate the generated cDNA segments together to provide a longer template for a MDA step in three sequential reactions.

In this alternative kit, 5  $\mu$ l of the RNA template were added to 5  $\mu$ l of reverse transcription mix containing 1  $\mu$ l of T-script enzyme and 4  $\mu$ l of T-Script buffer. The cDNA synthesis process was started by incubation of the reaction

mixture at 37 ° C for 30 minutes and stopped by inactivation of the T-Script enzyme at 95 ° C for 5 minutes. Ten microliters of the ligation mix containing 6 µl of the ligation buffer, 2 µl of the ligation reagent and 1 µl of each of the ligation enzymes 1 and 2 were added to the cooled cDNA reaction mixture at 22 ° C, and incubated at the same temperature for 2 hours to initiate ligation of the generated cDNA together. The ligated cDNA was amplified by adding 29 µl of the REPLI-g midi reaction buffer and 1 µl of REPLI-g midi DNA polymerase, and incubated at 30 ° C for 2 hours. All incubation steps were performed using thermal cycler (Applied Biosystems). The amplified cDNA products were purified and run on 1% agarose gel to detect their bands as described in section 3.3.2.5.2 and 3.3.2.5.3, respectively.

### **3.3.3.3 Amplification of the target RNA using GenomePlex complete WGA kit**

A third approach to the amplification of the viral genome was to use the GenomePlex complete WGA kit (Sigma-Aldrich, UK). This technique generates nucleic acid fragments with the target size for microarray hybridization flanked by universal priming sites ready for amplification using universal primers in 3 sequential steps of one reaction.

With this kit, both of i) the first strand cDNA template prepared in section 3.3.2.3 and ii) double stranded cDNA generated in section 3.3.2.4 were amplified using this technique. The reaction was started with the fragmentation step which was achieved by adding 1 µl of 10X fragmentation buffer to 10 µl of the pTZ18R plasmid cDNA (1ng/µl) in a PCR tube. The mixture was heated for 5 minutes at 95 ° C followed by immediate cooling on ice. The mixture was



directly incubated with 2  $\mu$ l of 1X library preparation buffer and 1  $\mu$ l of library stabilization solution for 2 minutes at 95 °C for the initiation of the second step called library preparation. One  $\mu$ l of library preparation enzyme was added to the mixture after cooling it on ice, and incubated for 20 minutes at each of the following temperatures 16, 24, 37 °C, respectively, using a thermal cycler which also terminated this reaction by heating the mixture to 75 °C for 5 minutes.

The generated library molecules were amplified through the final step by adding 7.5  $\mu$ l of 10X amplification master mix, 47.5  $\mu$ l of nuclease free water and 5  $\mu$ l of WGA-DNA polymerase to the previous 15  $\mu$ l reaction mixture. After 3 minutes of initial denaturation at 95 °C 14 cycles of denaturation at 94 °C for 15 seconds and annealing/extension at 65 °C for 5 minutes, were used as a thermal profile. The generated products were purified and run on 1% agarose gel to detect their bands as described in section 3.3.2.5.2 and 3.3.2.5.3, respectively.

### **3.3.4 Labelling the samples amplicons**

Use of fluorescent dyes to label either the designed probes or the viral nucleic acids, is a common method used for the detection of any hybridization that may occur among them. Successful labelling requires the following steps:

#### **3.3.4.1 Amplicon fragmentation**

The optimal length of nucleic acids for successful hybridization is between 100-300 bp, while the typical size of the MDA product is >10 kb. This length of nucleic acid will lead to a high spotted background in in situ hybridization.

Therefore, the MDA amplicons were fragmented using the following fragmentation methods:

#### **3.3.4.1.1 Amplicons sonication**

The amplicons generated in section 3.3.3.1 were diluted to concentration of 20 ng/ $\mu$ l with 0.3 mM ethylenediaminetetraacetic acid (EDTA) and 10 mM Tris-HCl, pH 8.0 in total volume of 100  $\mu$ l. The MDA mixture was then sonicated for 3 cycles at amplitude 5 using the Soniprep 150 MSE sonicator in the Centre for Biomolecular Sciences (CBS)/University of Nottingham. Each cycle was run for 1 minute sonication with 5 seconds stopping intervals every 15 minutes of sonication, 1 minute incubation on ice and 5 seconds centrifugation. This method is fast, simple to conduct and with generally acceptable results. The main drawback of sonication is the generation of uneven fragments of nucleic acids that may affect the hybridization process.

#### **3.3.4.1.2 Amplicon fragmentation using DNase I**

The amplified products generated in section 3.3.3.2 were sheared using DNase I as an alternative fragmentation method to the sonication technique during the optimization steps of the microarray hybridization. DNase I was provided as a lyophilized enzyme containing 2000 units/mg by (Roche, USA).

According to the manufacturer's guideline, DNase I stock was prepared by dissolving 1 mg of the lyophilized DNase I in 1 ml of dilution buffer containing 5 mM NaAc pH 5.2, 1 mM CaCl<sub>2</sub> and 50% glycerol. The DNase I stock was diluted to a working concentration 0.0004 unit/ $\mu$ l by adding 1  $\mu$ l of

the DNase I stock to 5000  $\mu$ l of 1X nicking buffer containing 50 mM Tris-HCl pH7, 10mM CaCl<sub>2</sub> and 10 mM MgCl<sub>2</sub>.

The fragmentation process was performed by adding 3-5  $\mu$ l (0.0012 – 0.002 unit) of the diluted DNase I and 2.5  $\mu$ l of 10X nicking buffer per 1  $\mu$ g of the amplicons generated in section 3.3.5.3 in a total reaction volume of 25  $\mu$ l.

After 10 minutes of incubation at 37 °C for 10 minutes, the fragmentation reaction was stopped by placing the tube on ice.

This method generates a more regular length of nucleic acids than the sonication process. However, DNase I fragmentation requires extra time and effort for optimization which affect its application in research work.

#### **3.3.4.2 Fragments precipitation**

The nucleic acid fragments were then purified in order to re-concentrate them and to remove salts from the fragmentation step, which may affect their labelling efficiency. Ethanol precipitation was used to fulfil this purpose.

The sonicated solution was mixed with 1/10 of its volume with 3M sodium acetate (NaAc) and 2 volumes of 100% ethanol while the mixture of the products generated from amplicons digestion using DNase I were mixed with its ¼ volume of 10 M Ammonium acetate (NH<sub>4</sub>Ac) and 2.5 volumes of 100% ethanol. Both mixtures were incubated for 20 minutes at -80 °C followed directly by centrifugation at full speed (>15000 rpm) for 30 minutes at 4 °C. The supernatant was disposed and the pellet was washed with 70% ethanol and re-centrifuged for 15 minutes at the same above conditions. The nucleic acids sediment was eluted in 20  $\mu$ l nuclease free water after discarding the supernatant. The fragmented amplicons were run on 1% agarose gel to

determine their size as described in section 3.3.2.5.3. Due to the small size of the amplified HPRT product (160 bp), the fragmentation step was considered not necessary.

### **3.3.4.3 Labelling the fragmented amplicons**

The Platinum Bright Nucleic Acid Labelling Kit (Kreatech biotechnology) was used for labelling the viral nucleic acids in a one-step non-enzymatic fluorescent reaction. The principle of this kit is based on the presence of a universal linkage system (ULS) represented by the platinum complex which has the ability to bind to a fluorescein, dyomics 547 fluorescent dye or biotin as a marker or detectable group, through one of its two free binding sites.

The marker/platinum complex binds to nucleic acids through a stable coordinative bond between the N7 atom of guanine base and the leaving group which represents the other free site of the ULS/complex. The leaving group will be displaced after reaction with the target biomolecules in the presence of the detectable molecule (figure 3-2).

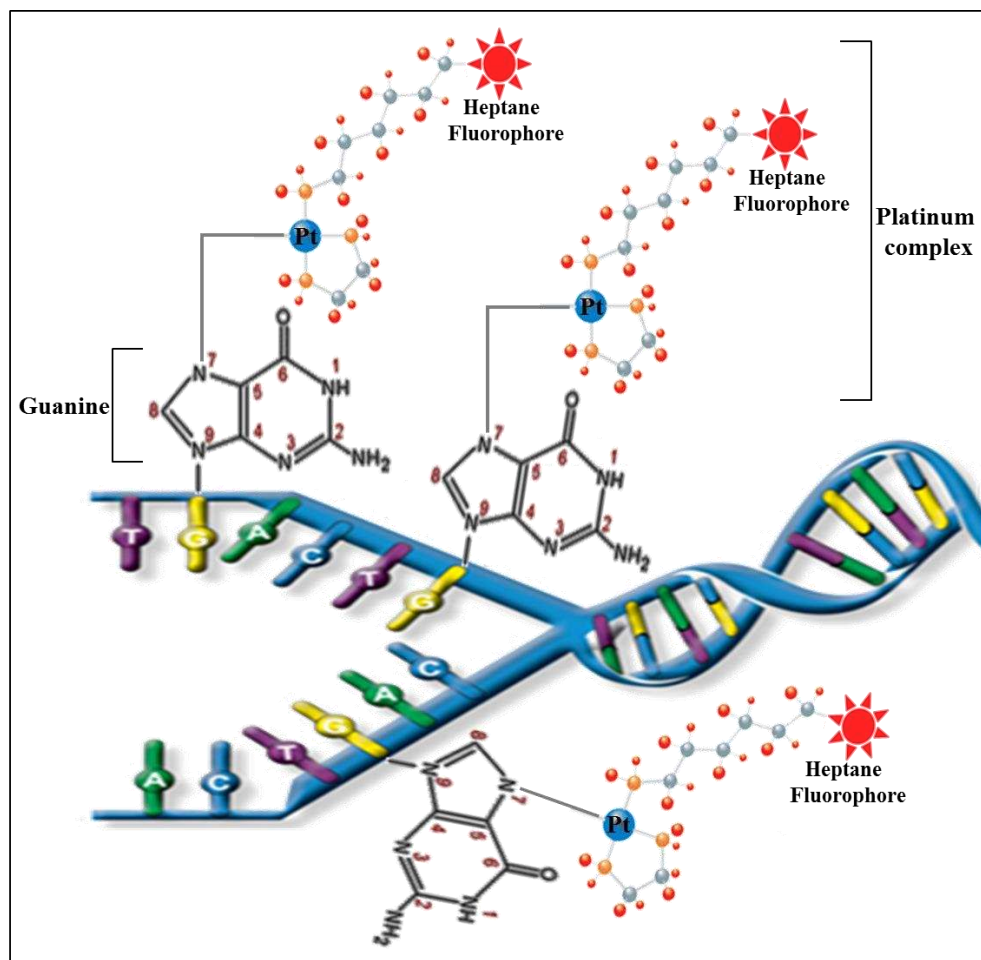


**Figure 3-2: Schematic drawing showing the working principle of the universal linkage system used for labelling nucleic acids.**

The amplified products were labelled by adding 2  $\mu\text{l}$  of the ULS dye/ $1\mu\text{g}$  of nucleic acid and 1/10 volume of 10X labelling solution. The final volume was adjusted with nuclease free water for a minimum final concentration of 50  $\text{ng}/\mu\text{l}$  of nucleic acids solution. The mixture was incubated for 30 minutes at 85  $^{\circ}\text{C}$  and then directly chilled on ice. The labelled materials were purified using the provided purification columns and centrifuged for 1 minute at 20800  $\text{xg}$ . Based on the Nanodrop readings, the degree of labelling (DOL) was determined.

The fragmented amplicons generated from the sonication step were labelled with dyomics 547 fluorescent dye while the amplified products sheared by DNase I were labelled with biotin dye. The different dyes would differentiate sample according to the fragmentation method used, and to use more samples in one experiment.

#### **3.3.4.4 Detection of the labelled amplicons using Southern blotting**

The labelled materials with biotin were subjected to southern blotting in order to detect their size and the labelling efficiency which may affect the microarray hybridization. Firstly, the amplified pTZ18R products were labelled with biotin dye as described in section 3.3.4.3 followed by running on 1% agarose gel as described in section 3.3.2.5.3. The gel was placed upside down onto a few well wetted layers of Whatman 3 MM filter paper supported by a small solid stage. A piece of nylon membrane (Amersham Hybond N) with similar dimensions to the agarose gel was put over the gel in order to transfer the separated bands of the labelled amplicons from the gel to the membrane. A few wetted sheets of Whatman 3 MM filter paper and a number of dry Quikblot papers (7-10) were assembled together and placed over the nylon membrane to provide an even surface for the best nucleic acids blotting and to prevent membrane flotation (figure 3-3).

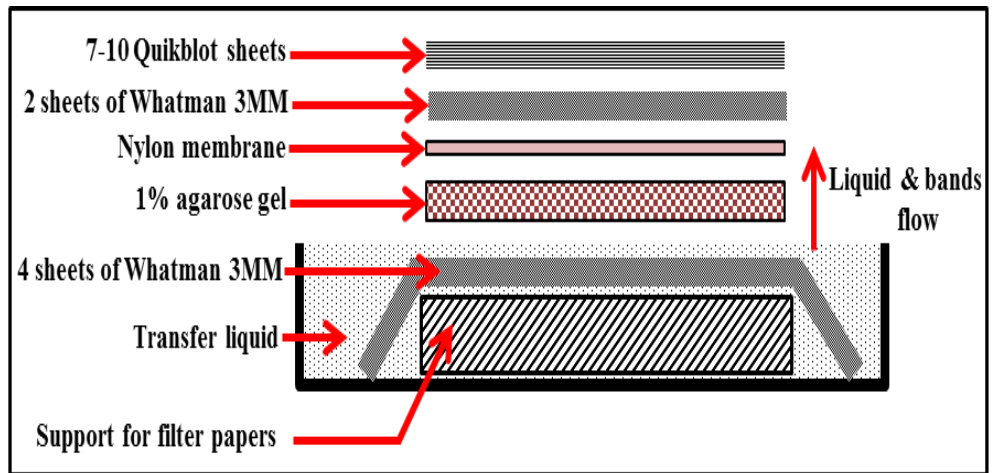


**Figure 3-3: Schematic drawing of the amplicons bands blotting.**

The blotting assembly was incubated overnight at room temperature in order to transfer the labelled bands from the gel to the membrane. The membrane was observed using a transilluminator in order to mark the ladder bands and then dipped in phosphate buffered saline (PBS) solution containing 0.02 % Tween 20 (PBS-Tween) and 5 % milk for one hour followed by 3 times washing with PBS-Tween for 5 minutes each. Finally, the membrane was covered with a layer of diluted Streptavidin (1:7000) in PBS-Tween solution for 30 minutes and scanned using an infrared scanner after washing with PBS-Tween solution as above.

### **3.3.5 Manufacturing experimental microarrays**

In order to test the efficiency of the MDA technique and to optimize the experimental conditions for manual hybridization using the designed printed chip, microarray templates were constructed using sets of experimental probes for enterovirus and pTZ18R plasmid.

#### **3.3.5.1 Generation of the N-hydroxysuccinimide (NHS)-activated-bovine serum albumin (BSA) coated slides**

##### **3.3.5.1.1 Slide cleaning**

Glass slides were marked using a diamond marker, and then incubated in a solution of 16.1% ammonia and 11.7% hydrogen peroxide in water for 20 minutes with gentle shaking. The slides were then washed 3 times using ultra-pure water with gentle shaking each time for 5 minutes and spun for 3 minutes at 1100 rpm using a slide centrifuge.

##### **3.3.5.1.2 Coating the slides with aminosilane**

The cleaned slides were coated with aminosilane using a solution of 2% of 3-aminopropyltriethoxysilane ethanol (APTS) and incubated for 30 minutes with shaking. The coated slides were washed 3 times with 100% ethanol and dried immediately using a slide centrifuge as above. Finally, the slides were baked in an oven at 130 °C for 45 minutes, cooled and stored at room temperature in a vacuum desiccator for further use.



### **3.3.5.1.3 Slide activation with N, N,-disuccinimidyl carbonate followed by coating with BSA**

Slides were activated in batches of 4 by soaking for 3 hours with shaking at room temperature in a solution of anhydrous N, N-dimethylformamide (DMF) containing 100 mM of each of N, N-disuccinimidyl carbonate and N, N-diisopropylethylamine, then rinsed in absolute ethanol. The slides were then incubated overnight in PBS, pH 7.5 containing 1% BSA. The slides were then washed twice with ultrapure water followed by 100% ethanol. The dried activated slides were stored under vacuum or directly used in the next step. As a final step for preparing slides for microarray printing, the activated slides were subjected to a repeat activating step as described above. The slides were ready for microarray printing directly after rinsing with an absolute ethanol for 4 times and drying using slide centrifuge, or can be stored in a vacuum desiccator for later printing.

### **3.3.5.2 Spotting the experimental enterovirus microarray**

Six 30-mer oligonucleotides specific for enterovirus (ENTC 1-6) shown in table (3-3), in addition to a single probe for HPRT (table 3-4) designed by a previous PhD student (Abdel-Hakeem, 2010), were provided at a concentration of 100  $\mu$ M by “Eurofins MWG Operon”, and used for constructing the experimental enterovirus microarray.

**Table 3-3: Sequences of the enterovirus probes used for printing the experimental enterovirus microarray.**

Adopted from (Abdel-Hakeem, 2010)

Probe ID	Target	Sequence (5'-3')
ENTC1	5' UTR	AGTCCTCCGGCCCCTGAATGCGGCTAATCC
ENTC2	5' UTR	AATCCTCCGGCCCCTGAATGCGGCTAATCC
ENTC3	5' UTR	TCTGTGGCGGAACCGACTACTTTGGGTGTC
ENTC4	5' UTR	TCCGTGGCGGAACCGACTACTTTGGGTGTC
ENTC5	5' UTR	TCTGCAGCGGAACCGACTACTTTGGGTGTC
ENTC6	5' UTR	GCGGAACCGACTACTTTGGGTGTCCGTGTT

**Table 3-4: Sequence of the HPRT probe used as internal positive control in the experimental microarrays.**

(Adopted from (Abdel-Hakeem, 2010)

Probe ID	Sequence (5'-3')	Position on gene
HPRT	AGAATGTCTTGATTGTGGAAGATATAATTG	550 - 579

Two  $\mu$ l of each probe was diluted in 3X saline sodium citrate (SSC) and 1.5 M betaine to a final working concentration of 20  $\mu$ M. Betaine was added to improve the binding efficiency and maintain the homogeneity of the oligonucleotides printed on the microarray slides. Each diluted probes was loaded sequentially in to a single well of the first column of a 384 well plate (16X24). The plate was located in the plate holder of the BioRobotics MicroGrid II 600 robot (Biogem) while the humidity inside the arrayer was adjusted to 70% in order to avoid evaporation of the printing buffer from both the source plate and the slide surface during the run.

The desired probes were fabricated on the NHS-coated BSA slides in a 24 (3x8) repeated grid layout using the robot split pin. Each grid consisted of 6 rows (one per each enterovirus probe) of 12 spots each plus 34 spots of the

HPRT probe printed in columns on both grid sides, the left one with an arrow head (figure 3-4).

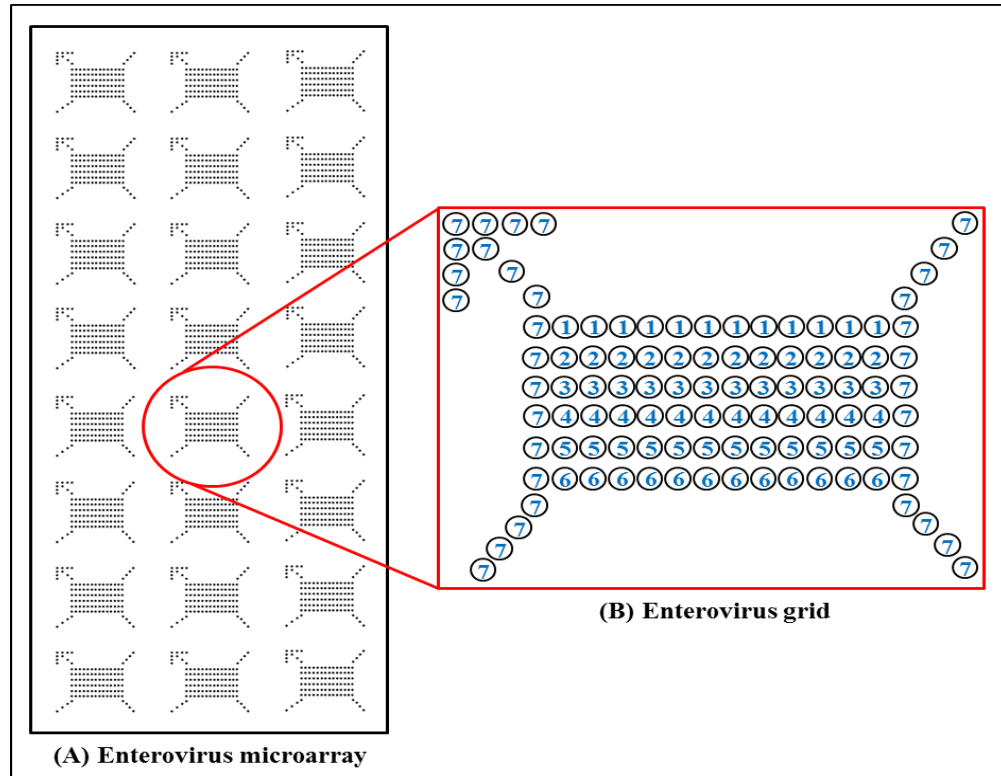


**Figure 3-4: Schematic drawing of the experimental enterovirus microarray.**

Figure (A) shows the printing layout of the 24 enterovirus grids on the microarray slide. Figure (B) represents a magnified diagram for one of the printed grids showing the spot locations represented in circles with a digit inside each one. Numbers from 1 to 6 refer to the enterovirus probes while number 7 refers to the HPRT probe.

The printing parameters such as spot numbers, their diameters, space between spots and the grid dimensions were defined using the Total Array System (TAS) application and saved in a comma-delimited format. Based on the comma delimited file, the GenePix array list (GAL) file was generated to be used later to determine the spot positions on the microarray slide during the scanning process.

### 3.3.5.3 Printing the experimental pTZ18R-enteroviral microarray

A new experimental microarray containing the six enteroviral probes ENTC 1-6, HPRT probe, and an additional set of twelve probes specific for pTZ18R plasmid was printed on NHS-coated BSA slides. Reverse complement software ([http://www.bioinformatics.org/sms/rev\\_comp.html](http://www.bioinformatics.org/sms/rev_comp.html)) was used to produce the second strand sequence of nucleotides (antisense) from the first strand sequence (sense) of the pTZ18R plasmid downloaded from the NCBI. Thus, at the end of this step two strands (sense and antisense) of the same size (2861 nucleotides) were available and used to generate specific probes for the pTZ18R plasmid using OligoArray software as described in chapter 2. From the few dozens of 30-mer probes generated by the probe design process for each strand of the plasmid, twelve specific probes (six per each strand) were selected for printing an experimental microarray (table 3-5). The position of the selected probes was distributed at the beginning, middle and the end of each sequence of the plasmid strands.

**Table 3-5: Characteristics of designed probes for printing the experimental pTZ18R-enteroviral microarray.**

	Probe ID	Sequence	Position 5' – 3'	Tm °C	GC %
Plasmid sense strand	Plas1	CGAATTCCCTATAGTGAGTCGTATTAATT	212-241	72.3	33
	Plas2	ATCCGCTCACAATTCCACACAACATACGAG	281-310	79.8	46
	Plas3	TAACTACGATACGGGAGGGCTTACCATCTG	1499-1528	79.6	50
	Plas4	CAGATTTATCAGCAATAAACCAGCCAGCCG	1574-1603	79.1	46
	Plas5	CTCCTTTTCGCTTTCTTCCCTTCCCTTTCTCG	2323-2352	79.8	50
	Plas6	ATGAGCGGATACATATTTGAATGTATTTAG	2492-2521	79.7	30
Plasmid anti-sense strand	Plas7	TCCAATTTAAAGAACGTGGACTCCAACGT	156-185	78.7	43
	Plas8	CGTAAAGCACTAAATCGGAACCCTAAAGGG	268-297	78.2	46
	Plas9	TATGGATGAACGAAATAGACAGATCGCTGA	1389-1418	76.8	40
	Plas10	CCAAGTTTACTCATATATACTTTAGATTGA	1458-1487	68.7	26
	Plas11	GTATTACCGCCTTTGAGTGAGCTGATACCG	2306-2335	79.4	50
	Plas12	GCGCAACGCAATTAATGTGAGTTAGCTCAC	2484-2513	79.6	46

The designed probes were synthesized and provided in a concentration of 100  $\mu\text{M}$  by “Eurofins MWG Operon”, then printed in 24 (3x8) repeated grids using the BioRobotics MicroGrid II 600 robot (Biogem) as described in section 3.3.5.2. The printing layout of the HPRT probes inside each grid was similar to that of the experimental enterovirus microarray while the probes of each of the enterovirus and pTZ18R were printed in rows of 6 spots in the middle area surrounded by the HPRT columns (figure 3-5).

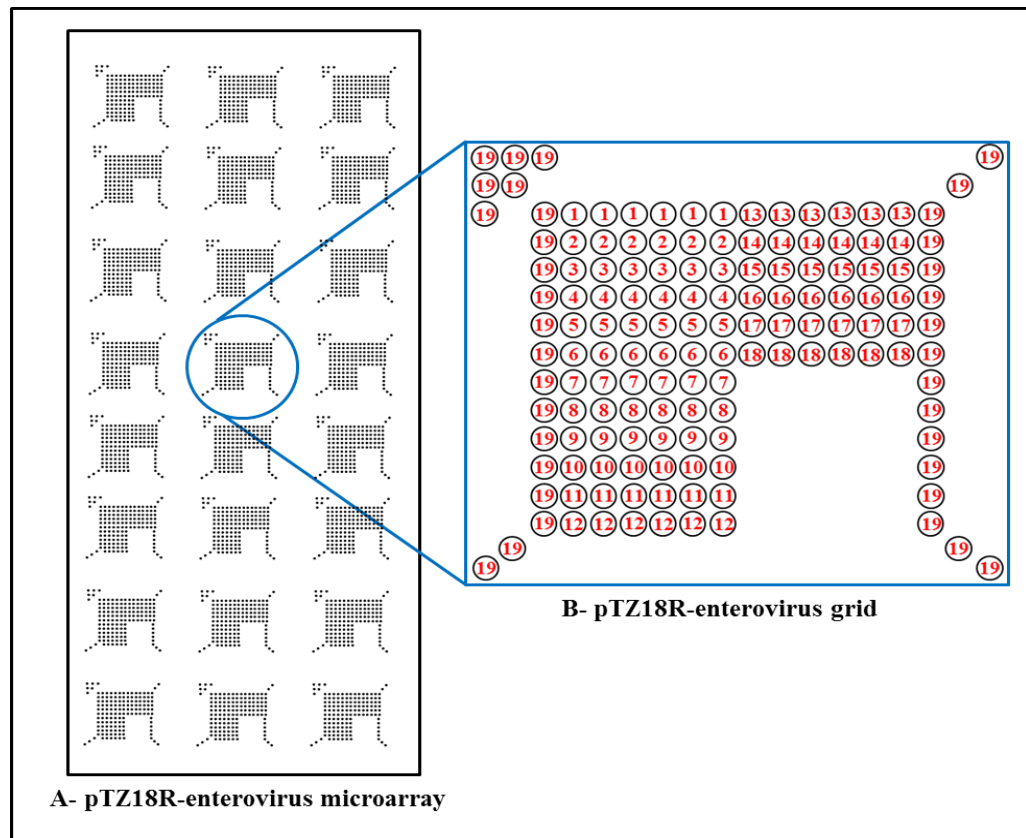


**Figure 3-5: Schematic drawing of the experimental pTZ18R-enterovirus microarray.**

Figure (A) shows the printing layout of the 24 pTZ18R-enterovirus grids on the microarray slide. Figure (B) represents a magnified diagram for one of the printed grids showing the spot locations represented in circles with a digit inside each one. Numbers from 1 to 12 refer to the pTZ18R plasmid probes, numbers from 13-18 represent the enterovirus probes while number 19 refer to the HPRT probe.

### **3.3.5.4 Post-printing slide processing**

The printed slides were subjected to post-printing processing steps included, incubation in 80% humidity for 10 minutes in order to maintain the precise shape of the spots. Then the slides were baked for 3 hours at 80 °C following a quick touch of the back slides to a hot plate at 120 °C.

## **3.3.6 Manual hybridization of the experimental microarrays**

### **3.3.6.1 Prehybridization samples preparation**

In order to inhibit any non-specific binding of the labelled oligonucleotides to the printed slides, slides were blocked by submersion in a blocking solution containing 1% BSA, 5X SSC and 0.2% SDS, with shaking for one hour directly before starting the hybridization process. The excess salts were removed by washing the slides with ultra-pure water twice followed by dipping them in absolute ethanol and drying immediately using the slide centrifuge.

Labelled nucleic acids as well as the internal positive control (HPRT) were precipitated using ethanol precipitation (as described in section 3.3.4.2), and resuspended in 60 µl hybridization buffer containing 2.4 M tetraethylammonium chloride (TEAC), 2% SDS, 2X SSC and 0.1 mg/ml lithium heparin.

### **3.3.6.2 Hybridization technique**

The blocked printed slide was placed in the metal hybridization cassette (ArrayIt Company) such that the slide surface containing the printed probes was oriented upside.

The cassette lid has a gasket on its inner surface which divides each slide surface into 24 (3X8) squares according to their printing layout, which enables separation of samples from each other when added to the slide surface (figure 3-6).

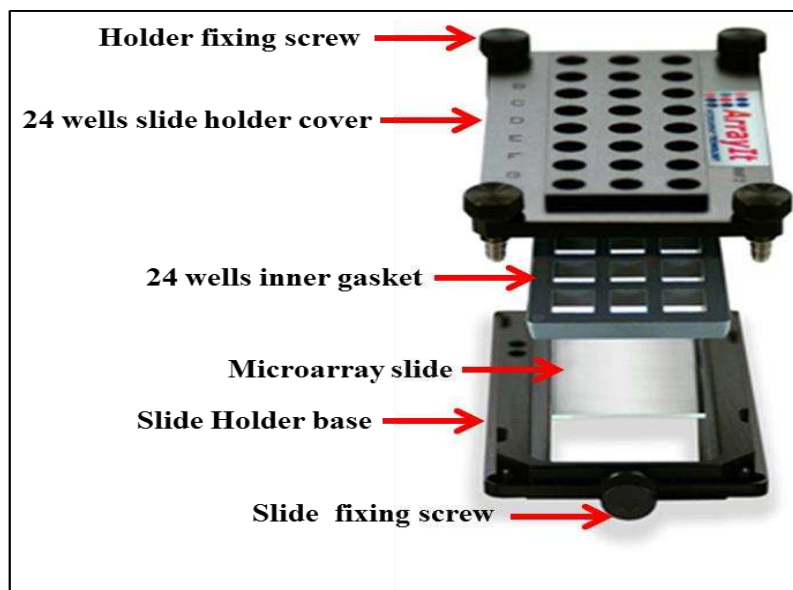


**Figure 3-6: Metal 24 wells hybridization cassette.**

The microarray slide is placed in the slide holder base and fixed by the in front screw. The slide is covered with the slide holder cover and fixed by the 4 upper screws. The inner gasket of the slide holder cover will divide the slide into 24 blocks.

One hundred  $\mu\text{l}$  of pre-warmed prehybridization buffer containing 0.1 mg/ml lithium heparin, 5X SSC and 0.2% SDS were loaded to each well of the hybridization cassette and sealed with a silicon mat to prevent evaporation. After 10 minutes of incubation at 40 °C with shaking, the prehybridization buffer was removed and the labelled amplicons suspended in the hybridization buffer were immediately loaded into a single well in an indexed way and sealed with same silicon mat.



The hybridization cassette was incubated at 40 °C for 8 hours or more (up to overnight) with shaking. Then, the hybridization cassette was washed 4 times with buffer A containing 2X SSC and 0.1% SDS, followed by two washes with buffer B containing 1X SSC and 0.1% SDS, and buffer C containing 0.1X SSC and 0.1% SDS for 3 minutes each. The final washing step was done once with buffer D containing 0.1% SSC only. Reducing the concentrations of the SSC during the post-hybridization washing process will increase the stringency of the washing buffer, lead to removal of the nucleic acids molecules attached loosely to the glass surface. This step helps in reducing the background noise which may affect detection of the generated hybridization signals during scanning the microarray slide.

For those hybridization experiments using biotin labelled amplicons, a further blocking step of 30 minutes in PBS solution containing 0.01% Tween 20 and 1% BSA was performed. In order to detect the signals generated from the hybridization between the biotin labelled nucleic acids and their complementary oligonucleotides, the arrays were incubated for 15 minutes in the same above PBS blocking solution containing (1:1000) streptavidin-peroxidase, and washed 3 times with tris buffered saline 0.01% tween (TBST) followed by one time with ultrapure water.

Two modifications were performed before starting hybridization using the experimental plasmid-enterovirus microarray. The first one was represented by skipping the purification step after MDA and moving directly to the fragmentation process as described in section 3.3.4.1.

Mixing each one of the fragmented amplicons with one-fifth volume of the HPRT amplicon and labelled together in one reaction with the same dye, was

the second modification. Thus, each sample had an internal positive control during the hybridization process.

### **3.3.6.3 Slide scanning**

A GenePix 4200AL autoloader scanner (Molecular Devices) was used to scan the slides after hybridization in order to detect the generated hybridization fluorescence signals. During the scanning process, an appropriate wavelength of laser light (635, 532, 488, or 594 nm) was used to excite the labelling fluorescence dye linked to the nucleic acids. The wavelength of the utilized laser light was selected according to the optimal wavelength used for the excitation of the fluorophores which was determined by the company.

The photo-multiplier tube (PMT) was calibrated for each array to determine the best emitted fluorescent signals of the hybridized viral nucleic acids. The laser power and the scan resolution were adjusted to 100% and 5- $\mu\text{m}/\text{pixel}$ , respectively. The GenePix Pro software was used to determine the fluorescent intensities of the foreground and the background of the microarray slide after hybridization process. The values of the background intensity were subtracted from the mean values of foreground intensity, and the resulted values were used for data analysis of the microarray hybridization experiment.

### **3.3.7 Quantification of the pTZ18R amplicons using microplate fluorescence assay**

For more accurate measurement of the amplified nucleic acid, SYBR Green I stain (Invitrogen) was used to quantify the amplified materials generated from MDA fluorescently with a microplate reader. One hundred microliters for six

different points of the DNA concentration standards ranging from 0-2 ng/ $\mu$ l were prepared from calf thymus DNA (Sigma) using double dilution technique in TE buffer (10 mM Tris/HCl, 1nM EDTA, pH 8.0) and loaded into the black 96-well microplate (8X12). An equivalent concentration of the purified amplicons were diluted in 100  $\mu$ l of TE buffer and loaded into another well of the same microplate. The final volume in each well of the DNA concentration standards and the amplified samples was adjusted to 200  $\mu$ l/well by adding an equal volume (100  $\mu$ l) of diluted SYBR Green I (1:1250) in TE buffer. After 10 minutes of incubation in the dark at room temperature, the luminescence optic filter attached to the fluorescence microplate reader (Fluostar Omega, BMG Labtech) was used to measure the emitted fluorescence in each well. The fluorescence values of the DNA concentration standards were plotted against the known DNA concentrations in order to generate a standard curve in order to provide the actual concentrations of the DNA presented in the amplified materials by entering their fluorescence readings into the standard curve equation. The resulted value was multiplied by 50 to find the initial concentration of the amplified nucleic acid.

### **3.3.8 Quantitative real time PCR (QPCR)**

The actual representation of the enteroviral nucleic acids in their amplified products was quantified using QPCR. Brilliant III Ultra-Fast SYBR Green QPCR Master Mix kit (Agilent Technologies, USA) was used for this purpose in combination with a set of universal primers designed by Dierssen et al 2008, for the detection of any type of human enteroviruses (Table 3-6).

**Table 3-6: The sequences of the universal enterovirus primes designed by Dierssen et al 2008 and their product size**

Primer ID	Sequence (5'→3')	Tm °C	Amplicon Size
Ent-1-FW	ACATGGTGTGAAGAGTCTATTGAGCT	60	141 bp
Ent-2-RV	CGACCTTGACCATCTTTGGA	60	

FW=Forward primer, RV= Reverse primer

A QPCR standard curve consisting of 6 points of 2 fold diluted concentrations of the enterovirus cDNA generated in section 3.3.2.3, starting with 6 ng/μl. Five microliters of each one of the diluted standard concentrations as well as the serially diluted amplicons generated from MDA process of the cDNA synthesized from RNA extracted from clinical sample known to be infected with enteroviruses, were added to the QPCR master mix consisting of 10 μl of 2X SYBR Green QPCR master mix, 600 nM of the reference dye and 200 μM of each one of the enterovirus primers mentioned in table 3. Nuclease free water was used in order to adjust the final volume of each QPCR reaction to 20 μl. The prepared QPCR samples were loaded in duplicate into the amplification microplate wells together with the no-template control sample (NTC: QPCR master mix containing 5 μl of nuclease free water instead of the target template) as an indicator for the assay quality as shown in figure 3-7.

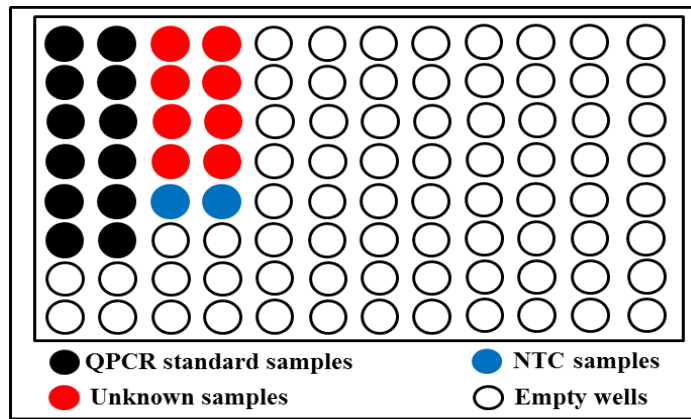


Figure 3-7: Loading of the standard, unknown and NTC samples into the QPCR microplate wells.

The microplate was sealed and placed in the Stratagene Mx 3000P machine, which was run according to the thermal profile shown in figure 3-8.

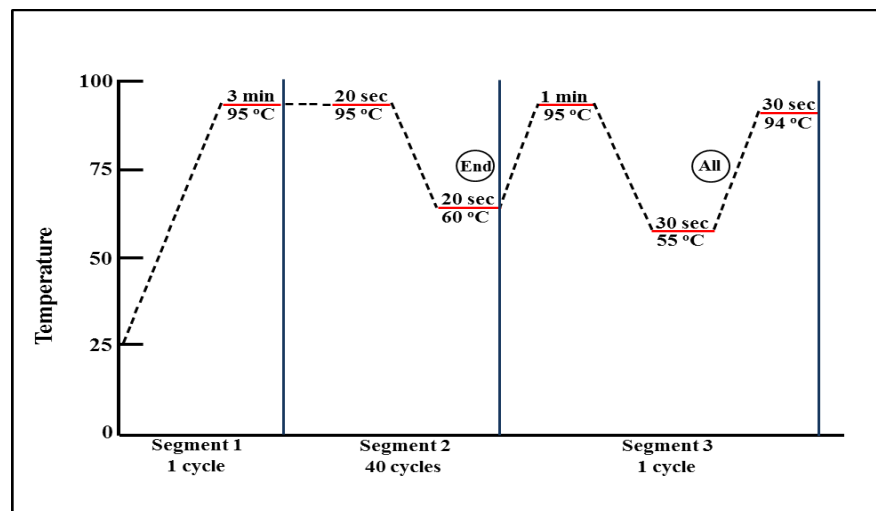
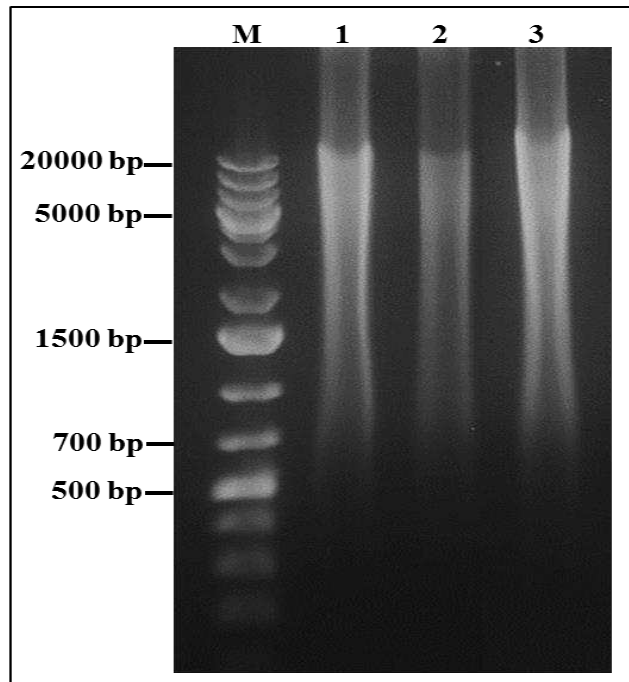


Figure 3-8: Thermal profile used in QPCR

## 3.4 Results

### 3.4.1 MDA results

Viral cDNA was synthesized from the RNA extract of the Human echovirus 30 transcript, using the random hexamers of the SuperScript III First-Strand Synthesis SuperMix kit. A second cDNA template was also generated from RNA extracted from an enterovirus infected stool sample using the Oligo dT primers of the  $\mu$ MACS one-step cDNA kit. MDA of the synthesized enteroviral cDNA using random primers of the REPLI-g UltraFast mini kit for 90 minutes, generated an average around 2 micrograms of nucleic acids measured by Nanodrop after purifying them using the purification columns of the Qiaquick PCR purification kit. Nanodrop readings also revealed that the absorbance ratio of the purified products generated from MDA process was (1.8-2) at both wavelengths 260/280 and 260/230 nanometre, signifying their purity. Visible smeared bands with a variable size ranging between 700 bp and 20 kb with some fragments which exceeded that size were revealed after running the purified MD amplified products on 1% agarose gel. A similar more bright smeared band with the same size range was observed with the negative control sample which contained nuclease free water instead of the cDNA template (figure 3-9).



**Figure 3-9: Agarose gel electrophoresis of the amplified enteroviral cDNA generated by MDA technique for 1.5 hour at 30 oC.**

Viral RNAs extracted from *H. echovirus-30* transcript (lane 1) and from a human stool sample (lane 2) known to contain an enterovirus were reverse transcribed into cDNA, amplified randomly using isothermal MDA at 30 °C for 90 minutes, purified using Qiaquick PCR purification columns and loaded into 1% agarose gel. Lane 3 of the gel was loaded with the materials generated from MDA of the negative control sample which contained nuclease free water rather than the viral cDNA. Smear bands which exceeded 20 kb were revealed after running the gel. M represents the 1 kb plus DNA ladder.

### 3.4.2 Amplicon fragmentation results

Different sizes of shorter segments between 200 bp and 1000 bp were generated from the fragmentation process of all three of the MD amplicons using 3 cycles of ultrasounds emitted from the Soniprep 150 MSE sonicator which were visualized as smeared bands when running them on 1% agarose gel after purifying them using ethanol precipitation (figure 3-10).

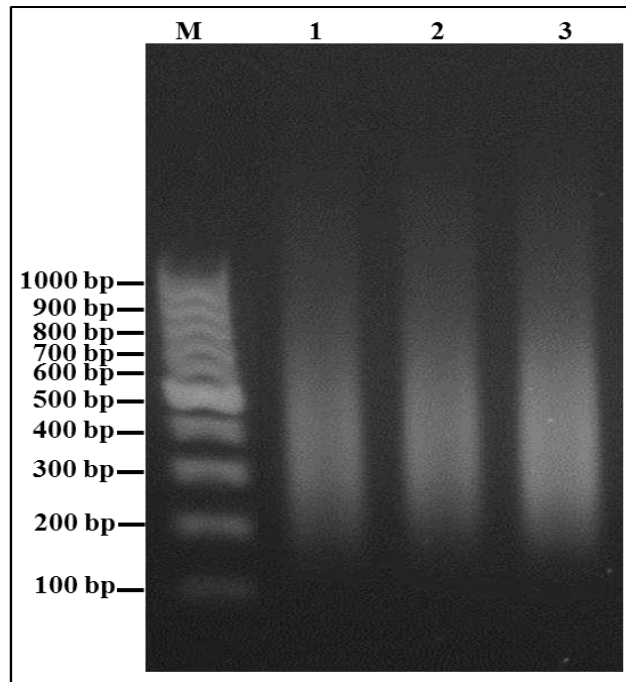


**Figure 3-10: Agarose gel electrophoresis of the fragmented enteroviral amplicons.**

The amplified products generated from MDA of the H. echovirus-30 (lane 1), human stool sample (lane 2) and negative control sample (lane 3) were sonicated for 3 cycles of 1 minute each, using amplitude 5 of the Soniprep 150 MSE sonicator, purified using ethanol precipitation and run in a 1% agarose gel which illustrated smeared bands of (200 – 1000) bp. M represents the 100 bp DNA ladder.

### 3.4.3 HPRT-PCR results

A PCR product of a part of the HPRT gene with the expected target size (160 bp) was generated from the extracted human DNA, using specific primers (table 3-1), in order to be used as an internal positive control through testing the experimental enterovirus microarray (figure 3-11).



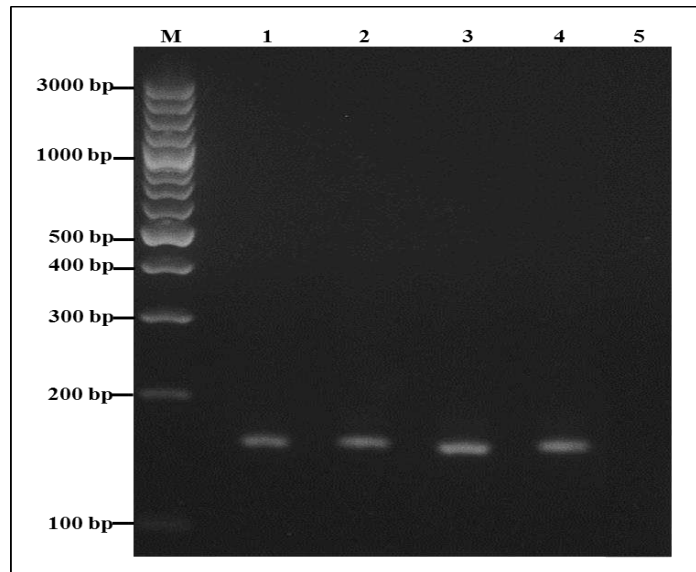


**Figure 3-11: Agarose gel electrophoresis of the HPRT PCR products.**

Part of the HPRT gene was amplified in quadruplicate from extracted human DNA using PCR. The amplified products were purified and loaded in lanes 1-4 of the 1% agarose gel which revealed single specific band with the expected size of 160 bp for each product. Lane 5 was loaded with the PCR negative control sample which contained nuclease free water instead of the human genome sample. M shows the 3000 bp DNA ladder.

#### **3.4.4 Labelling results**

The fragmented amplicons of the H. echovirus-30, the clinical sample of enterovirus, the MDA negative control and the PCR products of the HPRT were labelled with dyomics 547 fluorescent dye before starting the hybridization experiment. The efficiency of the labelling process was determined through calculating the DOL value (amounts of dye per 100 nucleotides) for each labelled sample using their nanodrop readings (figure 3-12) and the following equation recommended by the Kreatech Biotechnology Company:

$$\text{DOL (Labelling \%)} = 340 \times \text{pmol (dye)} / \text{ng (nucleic acids)} \times 1000 \times 100 \%$$

The resultant DOL of the labelled nucleic acids generated from the MDA was within the recommended value (<4.5%), also their absorbance ratio at 260/280 nanometre wavelength was >1.8 as displayed in the nanodrop results.

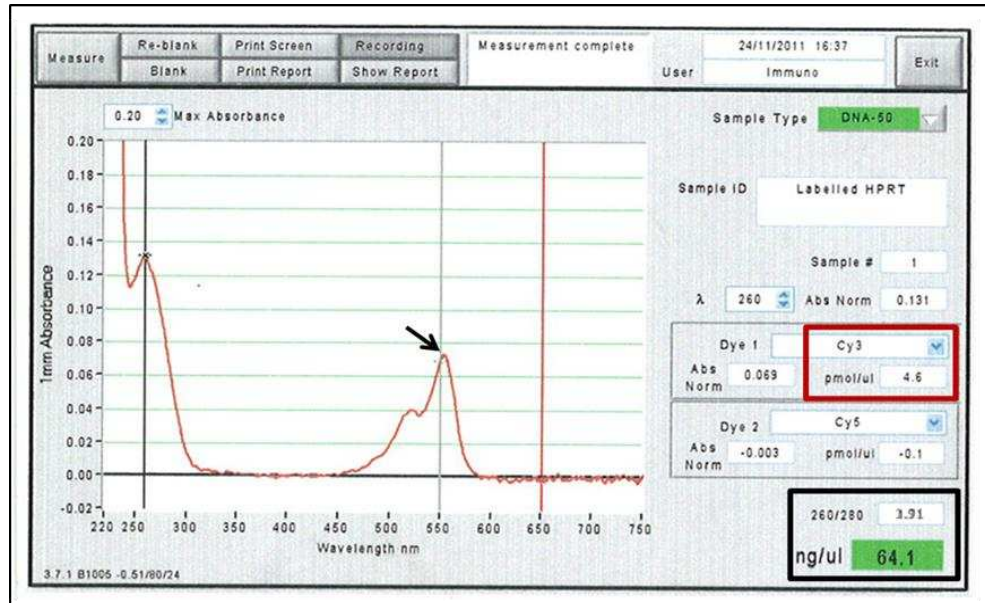


**Figure 3-12: Example of the nanodrop plots of the HPRT amplicon labelled with dyomics 547 fluorescent dye.**

The peak highlighted with the black arrow refers to the successful labelling process. The black rectangle displays the concentration of the labelled nucleic acids in ng/ $\mu$ l, and their purification ratio at 260/280 nanometre. The nanodrop also measured the fluorescent dye concentration in each microliter which was used for determining the labelling efficiency of the labelled nucleic acids. Similar labelling plots were generated for other enterovirus amplicons.

### **3.4.5 Hybridization results of the experimental enterovirus microarray**

The first trial of nucleic acid hybridization was done by loading the labelled amplified products derived from the H. echovirus-30, clinical enterovirus, HPRT and the negative control samples separately into the printed grids of the enterovirus microarray slide fixed in the hybridization cassette. Scanning the microarray slide at the end of the hybridization process using the GenePix scanner revealed clear hybridization signals generated only between the labelled amplicons of the HPRT and its complementary designed probe, displayed as red regular bright spots with an arrow shape on the left side and single column on the right side of the printed grid loaded with the HPRT amplicons. Neither the labelled amplified enterovirus samples nor the negative control loaded into the other three grids of the microarray showed any discernible signals for hybridization reaction with their relevant nor any other probes during the scan (figure 3-13).

Given the failure of the above MD amplicons to hybridize with microarray probes, the experiment was repeated (4 times) starting from the original viral RNA sample, proceeding through cDNA synthesis, MDA, sonication and labelling as describe above. In addition, a Human coxsackievirus-A16 RNA transcript (also provided by Professor Peter Simmonds) was also prepared by the same way and used in hybridization reaction. Each one of the new labelled amplicons was mixed with one-fifth volume of the labelled HPRT-PCR products. These further trials of hybridization also generated hybridization signals with the HPRT probes only.

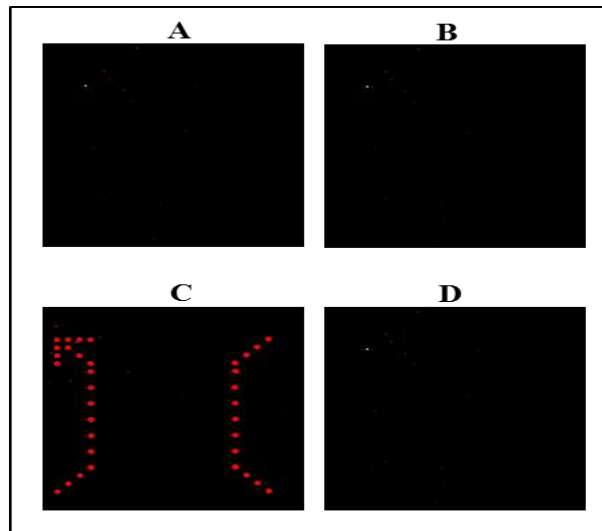


**Figure 3-13: Hybridization reaction results of the labelled amplified products with the experimental enterovirus microarray as seen on the GenePix laser scanner.**

Figures A, B and D represent scanned images of the three grids loaded with the labelled MD amplified materials of each of the H. echovirus-30, clinical enterovirus and the negative control, respectively, showing no signals with any of the printed probes. Figure C: The grid loaded with labelled HPRT amplicons shows fluorescent signals generated from hybridization reaction with the printed HPRT probes only, which appear as identical red spots arranged in the same shape of the HPRT printing layout.

### **3.4.6 Optimizing MDA/hybridization process using pTZ18R plasmid**

The low copy number or/and the short length of some of the viral RNA segments in both the viral positive controls and the clinical samples would be a challenge for the successful of their full length amplification using MDA technique. This challenge might be the reason for the failure of acquiring visible spots from the hybridization trials using the experimental enterovirus microarray.

Plasmids became the most ubiquitous instrument used in the molecular biology field which can provide a pattern of nucleic acids sequence with a high copy number due to their easy cultivation and manipulation. Therefore, it was decided to further develop the MDA/hybridization protocols using plasmid DNA, which could be produced in large copy number and hopefully act as a positive control instead of viral samples for optimizing the microarray hybridization reaction.

#### **3.4.6.1 Plasmid digestion results:**

The pTZ18R plasmid is circular dsDNA. Therefore, it was digested using SapI enzyme in order to generate a linear template suitable for WGA using MDA technique. SapI cut the circular plasmid at the recognition site (470-476 bp) and convert the plasmid into linear form (see figure 3-1). This step generated 0.6  $\mu$ g of linear DNA which was observed as a clear specific single band with the same length (2861 bp) of the circular plasmid when running on 1% agarose gel after purification (figure 3-14).

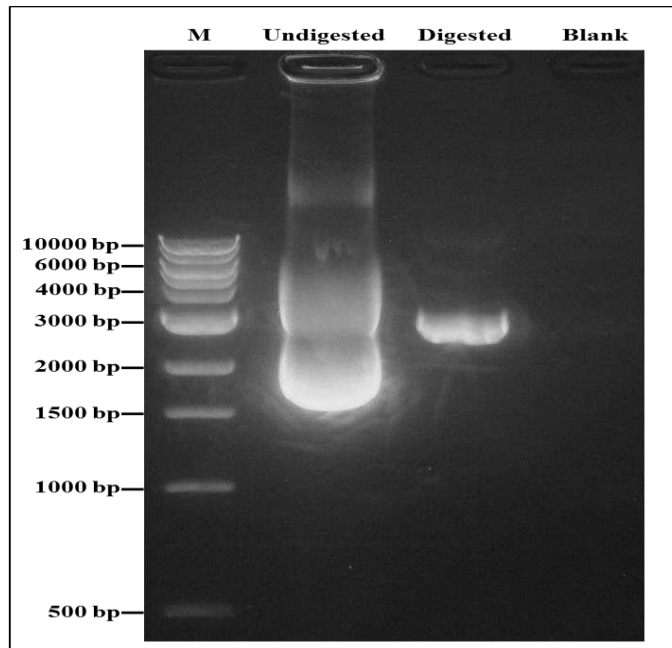


**Figure 3-14: Agarose gel electrophoresis of the digested pTZ18R plasmid.**

The 2861 nt circular pTZ18R plasmid was digested using SapI restriction enzyme which cut the circular plasmid at a specific recognition site and generated linear product of DNA with the same length as the undigested plasmid. The circular and the digested plasmid were loaded in lanes 1 and 2 of the 1% agarose gel which illustrated a smeared band in lane 1, and single band of 2681 bp for lane 2. Lane 3 was loaded with negative control sample which contained nuclease free water instead of the pTZ18R plasmid. M represents the 1 kb DNA ladder.

#### **3.4.6.2 Plasmid transcription results:**

Transcription of the digested pTZ18R plasmid started through binding of the T7 RNA polymerase to the T7 promoter site located upstream of the transcription initiation site near the 5' end (see figure 3-1). This process generated  $\approx 30$  micrograms of plasmid RNA. Nanodrop measurement of the transcribed RNA at both wavelengths 260/280 and 260/230 nanometre was 2.1, signifying an accepted purity.

Analysing the pTZ18R RNA generated from the transcription step, using Agilent 2100 Bioanalyzer revealed a single band with the expected size 2611 nt (figure 3-15-A). The electropherogram of the plasmid RNA also revealed the expected size of the transcribed RNA (figure 3-15-B).

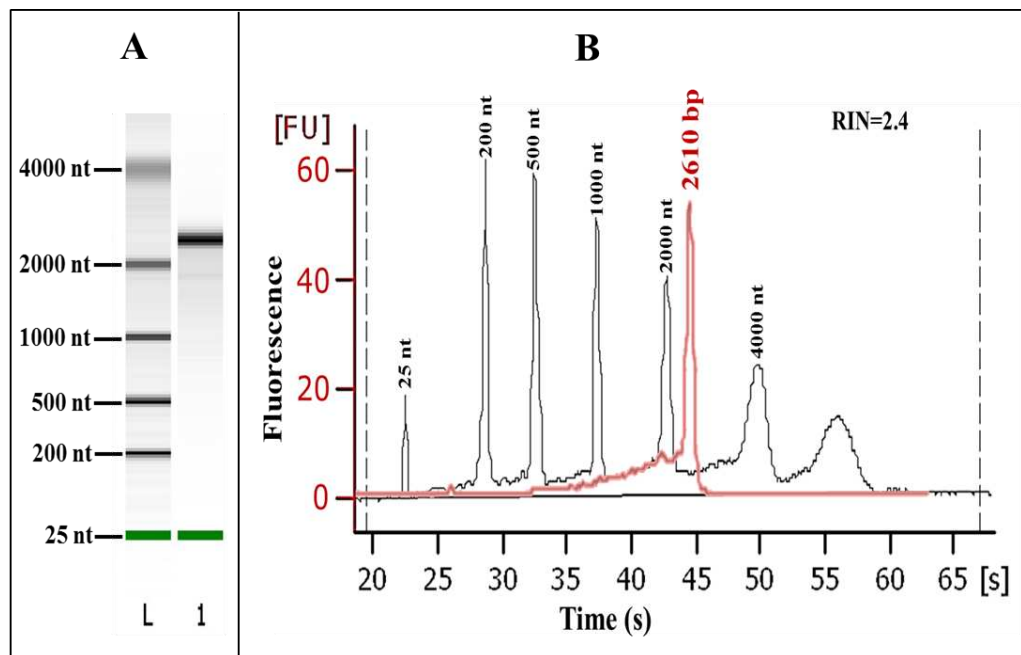


**Figure 3-15: Electropherogram generated from analysis of the plasmid RNA using Agilent 2100 Bioanalyzer showing the quality of the transcribed RNA.**

The electropherogram of the plasmid RNA (red colour) was aligned to the electropherogram of the Agilent RNA 6000 Nano marker (black colour) in order to elucidate the expected size of the transcribed RNA.

### 3.4.6.3 MDA results of the pTZ18R:

A different amplification kit (QuantiTect whole transcriptome kit) was used for MDA of the transcribed RNA of the pTZ18R plasmid and 2 other viral RNA templates extracted from the H. echovirus-30 transcript and an infected clinical sample with enteroviruses, respectively. Three sequential reactions were performed using this kit which started with reverse transcription of each one of the above RNA templates into first strand cDNA followed by ligating the generated fragments of each cDNA together and finished with MDA of the ligated cDNA templates. The generated MD amplicons were purified using Qiaquick PCR purification kit. According to the Nanodrop results, this process generated low concentration of amplicons for each of the above RNA templates. Agarose gel electrophoresis showed 3 faint smeared bands with variable length starting from 2000 bp to up to more than 20 kb while the negative control sample did not show any visible band (figure 3-16).



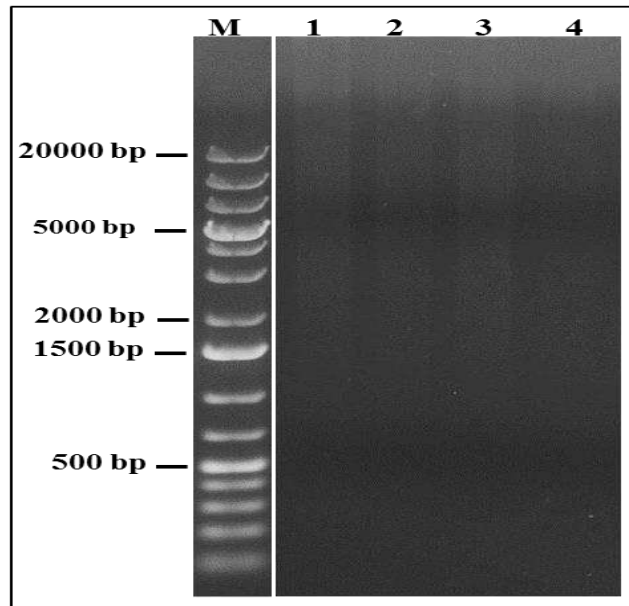


**Figure 3-16: Agarose gel electrophoresis of the amplified pTZ18R plasmid and enteroviral RNA using Whole transcriptome kit.**

The transcribed pTZ18R RNA (lane 1), enteroviral RNA extracted from the H. echovirus-30 transcript (lane 2) and human stool sample known to contain an enterovirus (lane 3) were reverse transcribed into cDNA for 30 minutes at 37 °C. The cDNA products were ligated together for 2 hours at 22 °C followed by MDA for 2 hours at 30 °C. The MD amplicons were purified using purification columns of the Qiaquick PCR purification kit. Only faint smeared bands exceeding 20 kb were seen after running the gel. Lane 4 of the gel was loaded with the materials generated from the MDA of the negative control sample contained nuclease free water rather than RNA template. M represents the 1 kb plus DNA ladder.

Running the amplified products generated in section 3.3.3.2 on 1 % Agarose gel without a purification step showed high concentrations of nucleic acids revealed as 3 bright smeared bands for each one of the amplified RNA templates, and for the negative control. The smeared bands were variable in size starting from 1500 bp and exceeding 20 kb with additional products which did not run through the gel due to their larger size (figure 3-17).

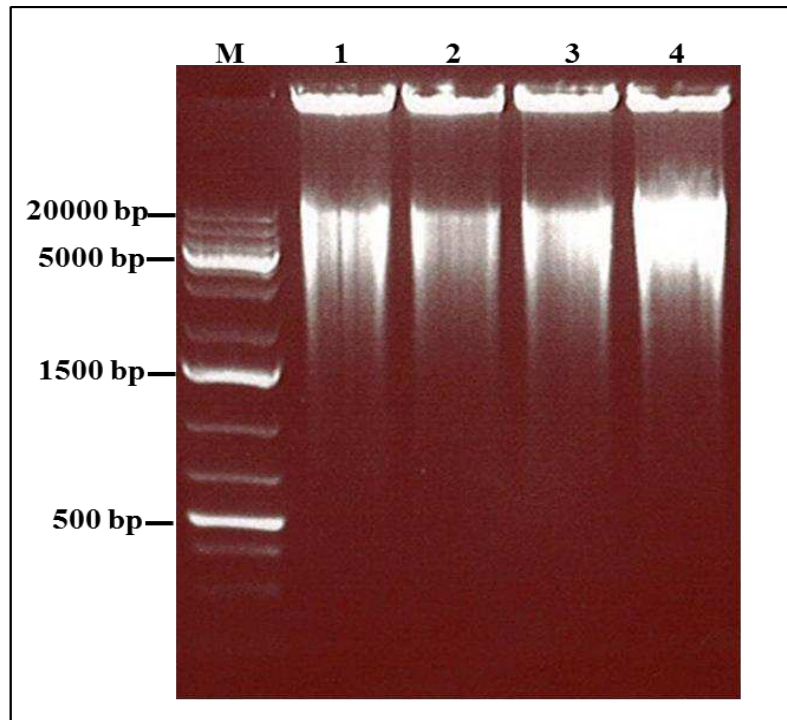


**Figure 3-17: Agarose gel electrophoresis of the unpurified amplicons generated from MDA of the pTZ18R plasmid and enteroviral RNA using Whole transcriptome kit.**

The amplified materials generated in section 3.3.3.2 were excluded from the purification step after MDA reaction and run directly on 1% agarose gel. The pTZ18R amplicons were loaded in lane 1 while viral amplified products of the H. echovirus-30 and clinical sample were loaded in lanes 2 and 3 of the gel, respectively. Lane 4 of the gel was loaded with the materials generated from the MDA of the negative control sample containing nuclease free water rather than RNA template. M represents the 1 kb plus DNA ladder.

This indicates that MDA of the ligated nucleic acid segments using QuantiTect whole transcriptome kit generated long strands of highly branched complicated amplicons which don't pass through the purification column with the elution solution. Therefore it was decided to skip purifying the amplicons generated from MDA technique, and to proceed directly to the sonication step.

#### **3.4.6.4 Hybridization results of the experimental plasmid- enteroviral microarray using the sonicated amplicons.**

The amplicons of the pTZ18R, H. echovirus-30, clinical stool sample and negative control generated from MDA using QuantiTect whole transcriptome kit, were fragmented directly using sonication techniques, and then purified using ethanol precipitation method. Each one of the above fragmented amplicons was mixed with one-fifth volume of the HPRT-PCR products, and then labelled with dyomics 547 fluorescent dye in order to be tested in hybridization reaction. Each labelled mixture was loaded into a single printed grid of the experimental plasmid-enterovirus microarray slide fixed in the hybridization cassette.

Uniform red spots with the same layout of the printed HPRT probes were revealed after scanning the experimental plasmid-enteroviral microarray slide at the end of the hybridization process. These spots reflect the specific hybridization reaction between the HPRT products and their complementary probes printed in the grids loaded with above labelled amplicons. No other discernible spots were seen with the other printed probes of both of the pTZ18R and the enteroviruses, indicating their hybridization failure (figure 3-18).

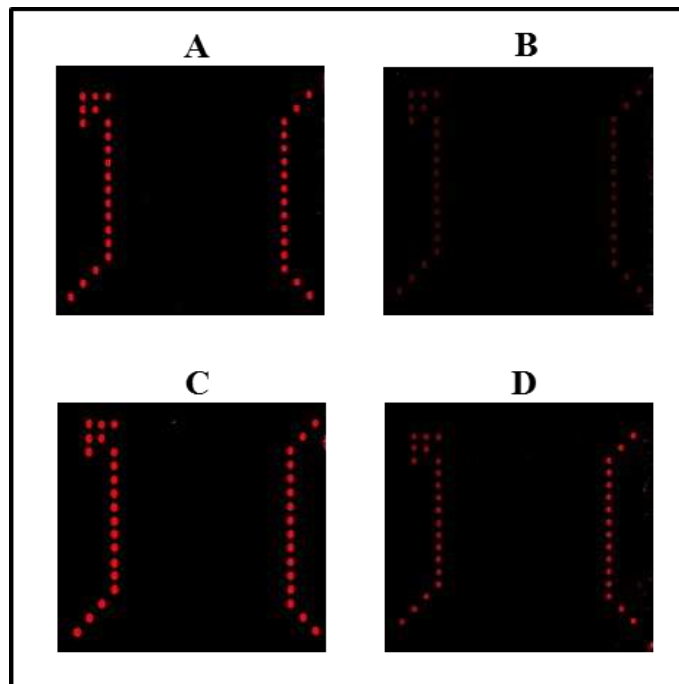


**Figure 3-18: Hybridization reaction results of the labelled amplified products with the experimental plasmid-enterovirus microarray as seen on the GenePix laser scanner.**

Figures A, B, C and D represent scanned images of the four grids loaded with the labelled amplified materials of each of the pTZ18R plasmid, H. echovirus-30, clinical enterovirus and the negative control sample, respectively. Each figure shows fluorescent red signals generated from hybridization of the HPRT products with their complementary printed probes. The other printed probes for both the pTZ18R and the enteroviruses did not show any specific hybridization signal against their related amplicons loaded into this microarray.

### 3.4.6.5 Fragmentation results using DNase I

One probable reason for the failure of the hybridization reaction in the previous experiments is the random fragmentation of the amplified materials caused by using the sonication technique which may leads to generate uneven lengths of nucleic acids fragments lacking part or all of the complementary sequence of the probes. Therefore, it was decided to fragment the MD amplicons using DNase I instead of sonication, and test the fragmented products in a hybridization reaction.

The amplified products of the pTZ18R generated from MDA using QuantiTect whole transcriptome kit were sheared directly using DNase I as another method for nucleic acid fragmentation. This process was performed through incubating 1 µg of the amplicons generated from MDA of the pTZ18R, with DNase I (0.0004 unit per reaction), at 37 °C for 10, 20, 30 or 40 minutes, in order to set the best conditions for the fragmentation. Running the products generated from the fragmentation reaction at the above selected times; revealed 4 smeared bands with variable length (figure 3-19). Forty minutes of incubation at 37 °C was the optimal time for shearing the vast majority of the pTZ18R amplified materials generated from MDA, which accumulated between 75-500 bp. The amplicons of each of the H. echovirus-30, clinical sample and negative control generated from MDA using QuantiTect whole transcriptome kit, were fragmented by DNase I using same above conditions.

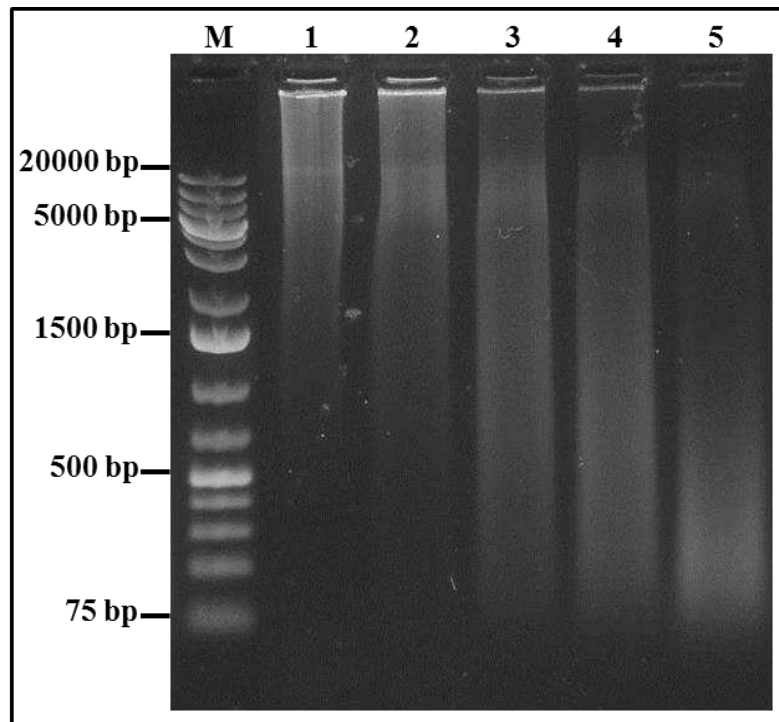


**Figure 3-19: Agarose gel electrophoresis of the pTZ18R products generated from the fragmentation process using DNase I at different times.**

One  $\mu\text{g}$  of the pTZ18R amplicons were treated with 0.0004 unit of DNase I and incubated at 37 °C for 10, 20, 30 and 40 minutes. The generated fragmented materials at the end of the above times were loaded in lanes 2-5, respectively. Lane 1 was loaded with the unfragmented pTZ18R amplicons for a comparison purpose. M represents the 1 kb plus DNA ladder.

#### **3.4.6.6 Blotting results of the biotin labelled amplicons:**

The amplified products of the pTZ18R, H. echovirus-30, clinical sample and negative control generated from MDA process using QuantiTect whole transcriptome kit were directly fragmented using DNase I. The fragmented amplicons were purified using ethanol precipitation and then labelled with the universal linkage system attached to a biotin molecule as a marker group through a non-enzymatic reaction called biotinylation. Biotinylation is a non-

fluorescent labelling process which its efficiency cannot be detected using nanodrop measurement process.

In order to evaluate the labelling efficiency with the biotin dye, the biotinylated amplicons were run on 1% agarose gel. Scanning the gel at this step using ultraviolet light, showed only the segments of the ladder which was used as a marker for the size of the labelled amplicons, with no other visible bands. After blotting the gel on a nylon membrane, the membrane was treated with streptavidin solution. Scanning the nylon membrane containing blot, using infrared scanner revealed 4 green smeared bands of biotinylated amplicons with variable size ranging from <500 bp up to 3000 bp referring to the Success of the labelling process (figure 3-20).

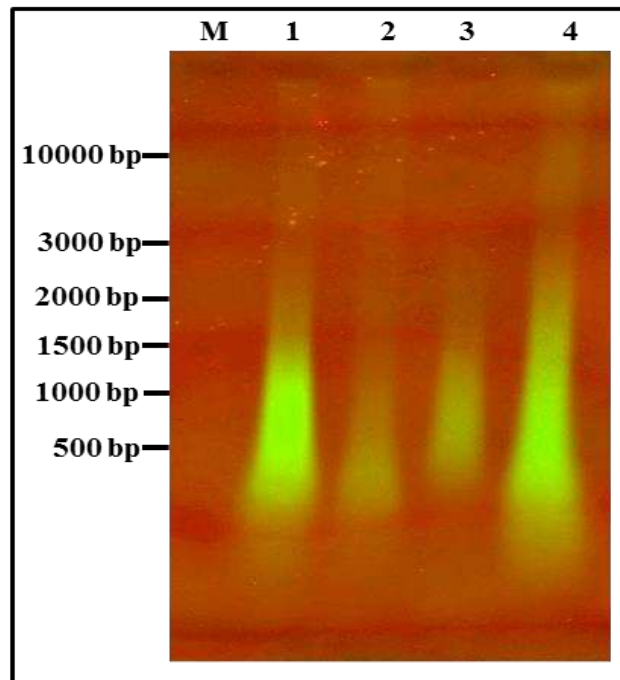


**Figure 3-20: Agarose gel electrophoresis of the biotinylated amplicons blotted on a nylon membrane as seen under infrared scanner.**

The amplicons generated from MDA of the RNA of each of pTZ18R (lane 1), H. echovirus-30 (lane 2), infected clinical sample with enteroviruses (lane 3) and negative control (lane 4) using QuantiTect whole transcriptome kit, were fragmented using DNase I and run on 1% agarose. The gel was then blotted on a nylon membrane followed by treating the membrane with streptavidin. The membrane containing the blot was then scanned using infrared scanner. M represents the 1 kb DNA ladder.



### **3.4.6.7 Hybridization results of the experimental plasmid-enteroviral microarray using the biotinylated amplicons.**

Due to the failure of the sonicated MD amplicons to hybridize with probes of the experimental plasmid-enteroviral microarray, another hybridization experiment was performed using the fragmented amplicons of the pTZ18R, H. echovirus-30, infected clinical sample with enteroviruses and negative control amplicons generated from DNase I reaction. The fragmented amplicons were purified using ethanol precipitation, mixed with one-fifth volume of the HPRT-PCR products and then labelled chemically with biotin using the ULS system. The biotinylated mixtures were loaded into a new experimental plasmid-enteroviral microarray slide to start hybridization reaction. The microarray slide was treated with the streptavidin-peroxidase diluted in PBS blocking solution (1:1000) at the end of the hybridization process and scanned using GenePix scanner after washing the slide with TBST. The outcome of this hybridization experiment was quite similar to the results of the previous hybridization trials generated from using the sonicated amplicons, as the hybridization signals were only generated with the HPRT probes which displayed as regular red spots arranged in the same printing layout of the HPRT probes (as presented previously in figure 3-18).

#### **3.4.6.8 Amplicon quantification using microplate fluorescence assay:**

A microplate fluorescence assay was used to determine the actual concentration of the nucleic acids represented in the pTZ18R, H. echovirus-30, clinical sample and negative control amplicons generated from MDA using QuantiTect whole transcriptome kit in section 3.3.3.2. A standard curve was created by linking the 7 known serially diluted concentrations of calf thymus DNA against their generated fluorescence values using an excitation/emission filter fixed to a fluorescent microplate reader. The fluorescence readings from the amplified material emissions were inputted into the standard curve equation in order to determine their concentrations (figure 3-21). The concentration of the materials generated from the negative control sample amplification was half the concentration of the pTZ18R amplicons, and double the amount of both of the H. echovirus-30 and the clinical enterovirus amplicons.

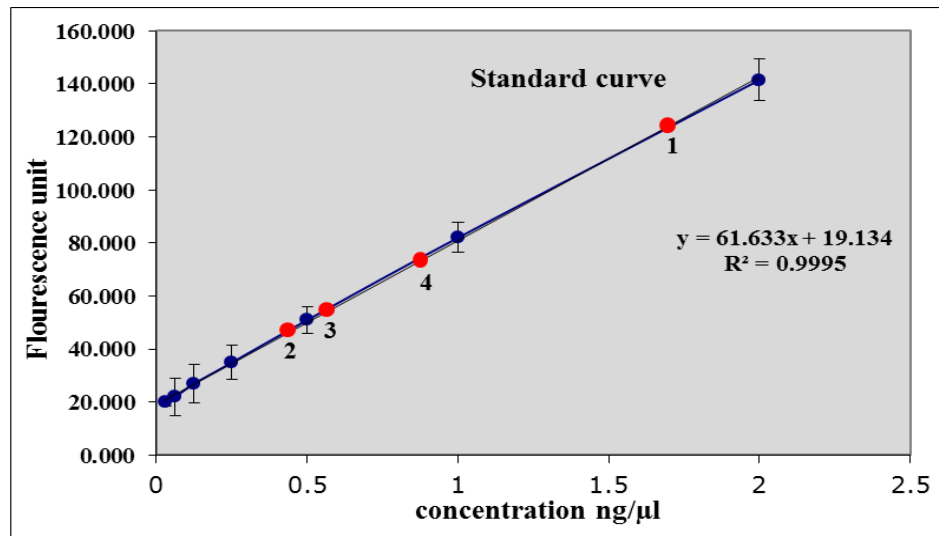


**Figure 3-21: Microplate fluorescence assay calibration results of the products generated from MDA.**

Double diluted concentrations ranging from 0-2 ng/μl (blue points) were prepared from calf thymus DNA, and used to generate a standard curve (blue linear line). The fluorescence emissions of the pTZ18R, H. echovirus-30, clinical sample and negative control products generated from MDA using QuantiTect whole transcriptome kit, were blotted on the standard curve as red spots numbered from 1-4, respectively, in order to determine their DNA concentrations.

### 3.4.7 Target amplification using GenomePlex complete WGA

#### kit:

Given the disappointing results of the experimental hybridization trials using MD amplicons it was decided to try a different approach for amplifying target nucleic acids. GenomePlex complete WGA kit was used to amplify cDNA derived from the pTZ18R, H.echvirus-30 and the clinical enterovirus samples through three successive reactions started with fragmenting the cDNA templates into shorter products with an average size 400 bp. During the second reaction, the generated small fragments will be converted into amplifiable

library molecules ending with universal priming sites in a process called library preparation. Finally, WGA-DNA polymerase will start extending the universal oligonucleotide primers (multiple primers) annealed to the resulted library molecules in 14 cycles of denaturation at 94 °C for 15 seconds followed by primers annealing and extension for 5 minutes at 65 °C using thermal cycler, which generated massive quantities of the amplified materials (figure 3-22).

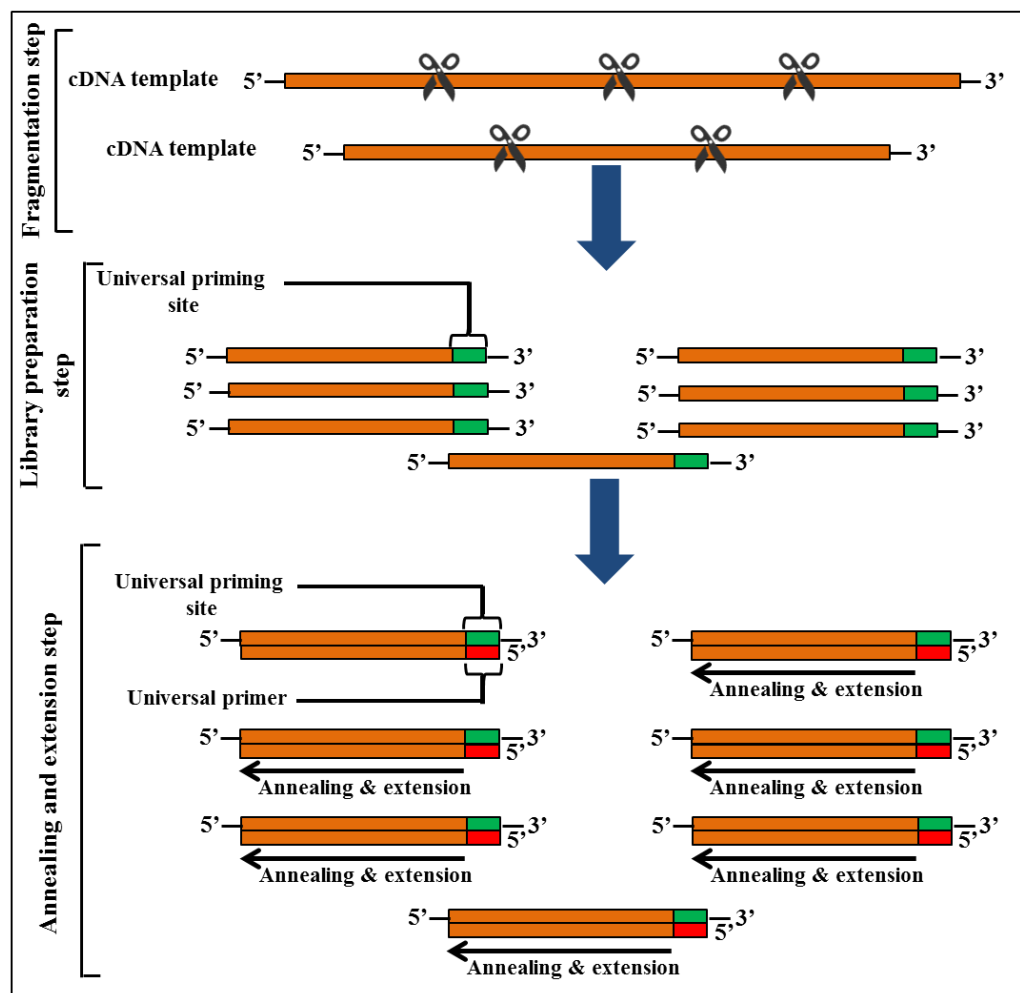
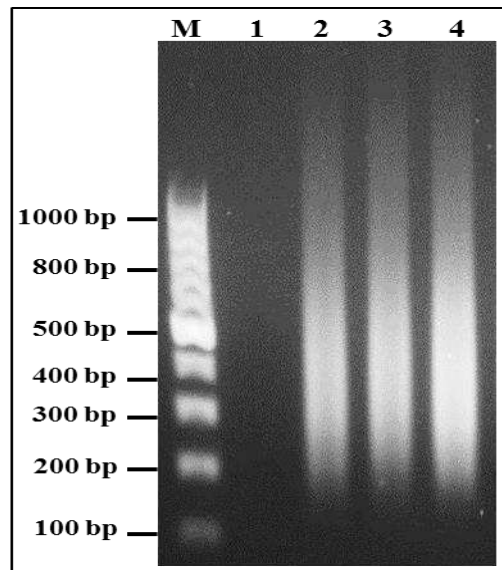


Figure 3-22: Schematic diagram showing the amplification steps of the target nucleic acids using GenomePlex complete WGA kit.

Nanodrop readings revealed that this technique generated 10 times more concentrations of amplicons (>20 µg) than the REPLI-g UltraFast mini kit and the QuantiTect whole transcriptome kit. The purity ratio of the amplified materials generated from the amplification process using GenomePlex complete WGA kit was equivalent to that of MD amplicons produced in sections 3.3.3.1 and 3.3.3.2. The size of the generated amplified materials ranged between 200-1000 bp as illustrated from the Agarose gel electrophoresis image which showed 3 bright smeared bands for each one of the above samples. No product was generated from the amplification process of the negative control sample as it did not show any visible band when it was run through the gel (figure 3-23).

Since the vast majority of the generated amplicons have an average size between 200-500 bp, they were excluded from the fragmentation step, purified using Qiaquick PCR purification kit, mixed with one-fifth volume of the HPRT-PCR products and labelled with the dyomics 547 fluorescent dye. Hybridization process of the pTZ18R, H.echvirus-30 and the clinical enterovirus labelled amplicons with the experimental plasmid-enteroviral microarray also generated hybridization signals with the HPRT probes only displayed as red spots while pTZ18R and enteroviral probes did not show any discernible hybridization signals (figure 3-18).



**Figure 3-23: Agarose gel electrophoresis of the amplified materials generated from amplification process using GenomePlex complete WGA kit.**

The cDNA template produced from the reverse transcription step of each of the pTZ18R, H. echovirus-30 and clinical enterovirus RNA was randomly fragmented into small PCR-amplifiable chunks of 100-1000 bp followed by PCR amplification using WGA DNA polymerase. The generated amplified materials of the negative control, H. echovirus-30, clinical enterovirus and pTZ18R were loaded in lanes 1-4 respectively. M represents the 1 kb plus DNA ladder.

### **3.4.8 Quantitative real time PCR (QPCR) results:**

The generation of the high molecular weight amplicons during MDA of the negative control sample is attributed to the polymerization of the random hexamers by Phi 29 DNA polymerase, according to the consultation of the amplification kits manufacturer. Primers polymerization may interfere with the MDA of the target nucleic acid and generate mixture of amplicon different from the original nucleic acid, and lead to hybridization failure. Therefore, it was decided to evaluate the efficiency of the MDA to generate specific amplicons representing the original target.

QPCR was used for this purpose through determining either the concentration or the copy number of a part of the enterovirus genome before and after MDA. Specific primers targeting a particular sequence (142 bp) of the enterovirus genome were used for this purpose. Therefore, the enterovirus amplicons generated from the MDA were re-amplified in parallel with 6 double diluted concentrations of the original enterovirus cDNA, following the PCR principles. The fluorescence emission generated from the excited nonspecific fluorescent dye (Sybrgreen) which binds to any dsDNA, was measured using a sensor fixed to the PCR machine. The fluorescence readings were analysed using the MxPro-Mx3005P software which calculates the concentration of the selected part of the enterovirus genome in both the cDNA template and the amplified materials generated from the MDA reaction.

The software generated a linear amplification curve between the 6 standard concentrations prepared from the enterovirus cDNA, and their threshold cycle (Ct) values. The software also plotted the Ct values generated from 2 of the serially diluted enterovirus MDA products on the QPCR standard curve which illustrated that the absolute concentration of the enterovirus nucleic acids presented in the MDA products was one twenty fifth the total concentration of these MDA products. Both of the efficiency factor and the R square ( $R^2$ ) values were within the recommended level indicating the satisfactory performance of the QPCR (figure 3-24).

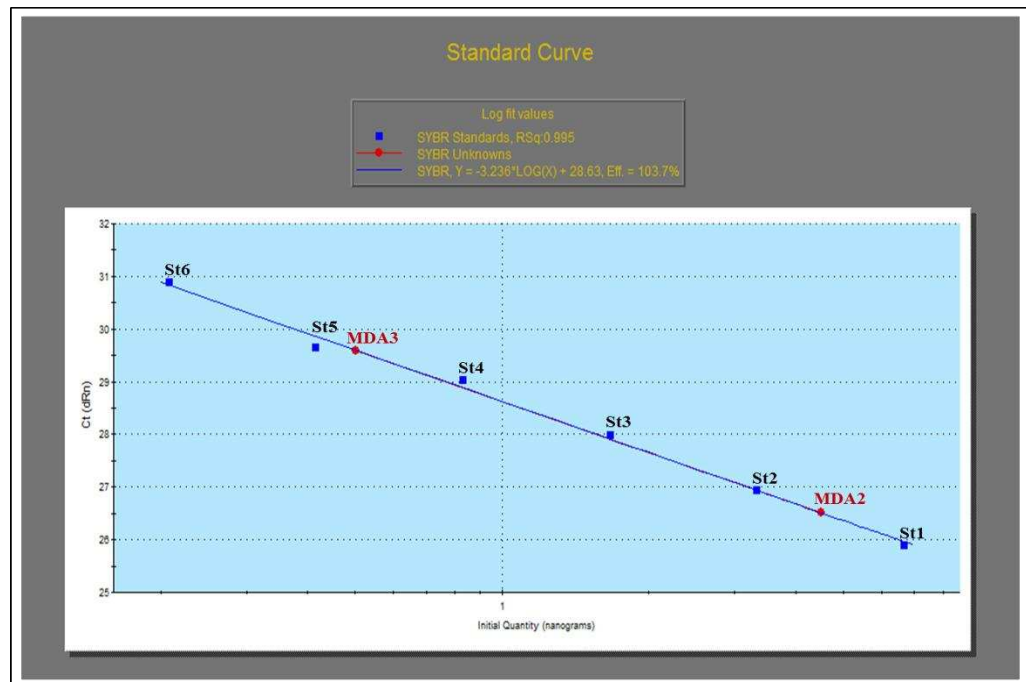


**Figure 3-24: Standard curve of the enterovirus QPCR used for determining the copy number of the enterovirus nucleic acids in their amplified materials generated from MDA.**

A QPCR standard curve was created from 6 double diluted standard concentrations (St1-St6) of the enterovirus cDNA starting from (6 ng/ $\mu$ l) using MxPro-Mx3005P software which linked each concentration versus its relevant Ct value. The resulted standard curve was used to quantify the enterovirus nucleic acids concentration in the serially diluted MDA products (MDA1-MDA4) starting from 1000 ng/ $\mu$ l. The enterovirus nucleic acids were only detected in the second and third dilutions (100 & 10 ng/ $\mu$ l) of the MDA products with a quantity representing one twenty fifth the quantity of the amplified materials generated from MDA process. The first and fourth dilutions of the enteroviruses nucleic acid were not quantified by the QPCR due to their very high and very low concentrations, respectively.



The QPCR amplification plots shows the logical inversely correlation between the standard concentrations (St1-St6) and their Ct values which increased with the diminution of these concentrations. The QPCR amplification plots of the enterovirus MDA products revealed that their Ct values were similar to the Ct value of the enterovirus cDNA template before MDA process which is opposite the expected (figure 3-25).

This QPCR experiment indicates that the enterovirus cDNA was not amplified during MDA, and the high molecular weight product generated from this process was resulted from the random hexamers polymerisation which can predominate on the MDA of the target enterovirus cDNA.

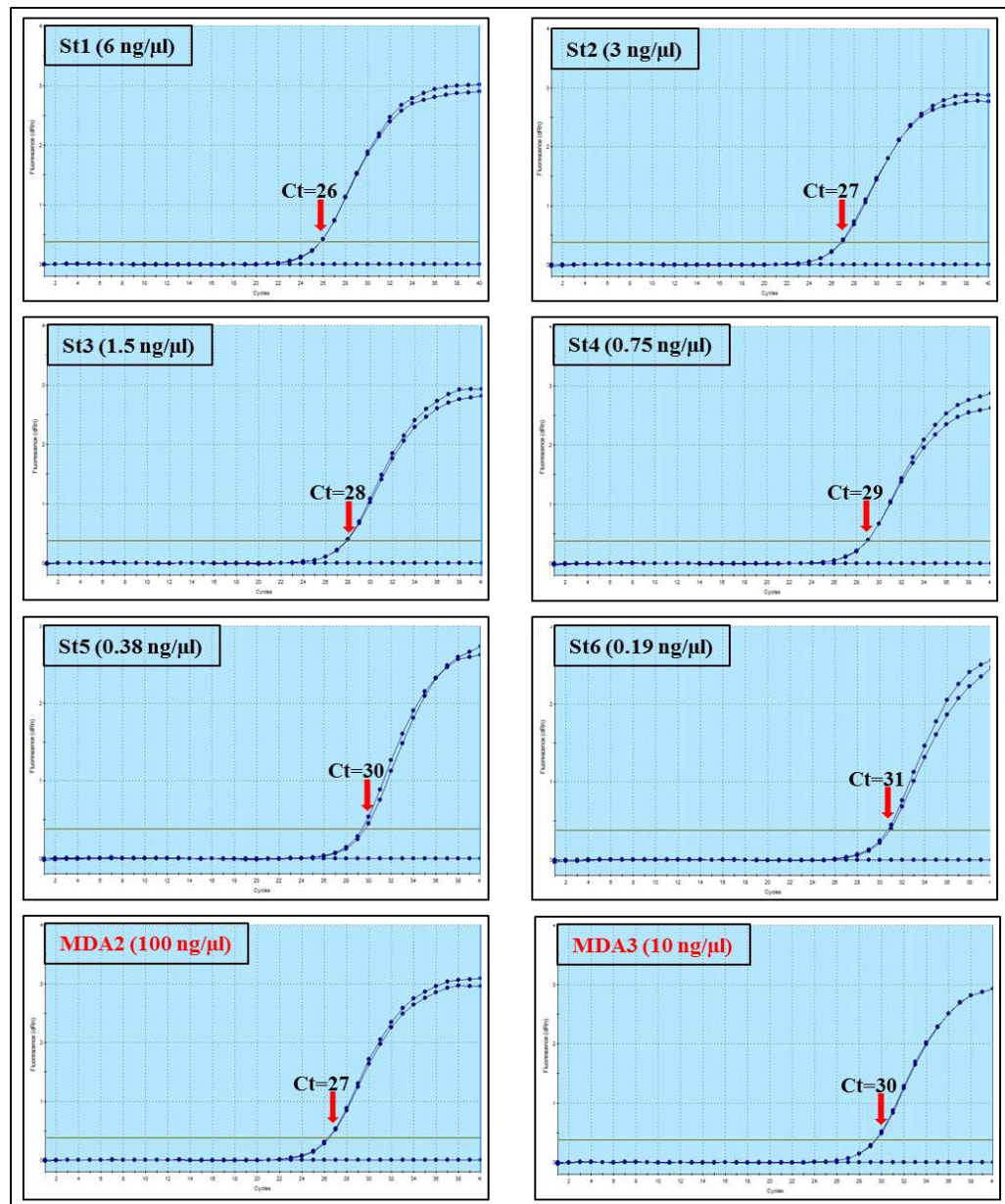


**Figure 3-25: Amplification plots of the enterovirus QPCR.**

The first 6 figures represent the amplification plots of the 2-fold standard concentrations (St1-St6) prepared from the enterovirus cDNA synthesized in section 3.3.2.3, showing an increasing in the amplification Ct value associated with decreasing the quantities of the enterovirus cDNA template required to start the QPCR. The last 2 figures in the bottom represent the amplification plots of only 2 serially diluted concentrations prepared from the enterovirus MDA products (MDA2, MDA3) which were detected by the QPCR, showing that their Ct values were similar to the Ct value of the unamplified enterovirus cDNA template.

### **3.5 Discussion:**

Nucleic acid microarray hybridization is a sequential multistep technique. Any defect in the preparation of the target samples during each step may affect the next step and lead to hybridization failure (Majtan et al., 2004, Kumar, 2009). It was necessary to evaluate the performance of sample preparation at the end of each step before starting the following one in order to avoid wasting time, efforts and costs, and to get reliable results. Therefore, an optimization process was done for all of the proposed steps required for sample preparation prior to use the main virochip designed in chapter 2, using experimental microarrays printed in the laboratory.

Manufacturing the viral nucleic acids microarray starts with the spotting of the viral oligonucleotides or probes which were designed particularly for the diagnosis of the target viruses which suspected to be the causative of the viral infections. Since the six enterovirus probes designed by Abdel-Hakeem, 2010 have the same length (30-mer) and GC ratio ( $\leq 50\%$ ) of the viral probes designed in chapter 2, they were selected for fabricating the experimental enterovirus microarray in order to be used for optimizing the microarray hybridization process of the virochip.

#### **3.5.1 Sample preparation:**

Microarray-based assays for the diagnosis of viral infections depend on the detection of viral nucleic acid in infected clinical samples (Hadidi et al., 2004, Liu et al., 2006, O'Connell et al., 2006, Guan et al., 2008, Yoo et al., 2009). Enteroviral RNA was extracted from a clinical sample known to be infected with enteroviruses in order to be used in addition to other two enterovirus RNA

transcripts (H.echo-30 and H. coxsackievirus-A16) for optimizing the hybridization process using the experimental enterovirus microarray. There are many obstacles preventing using RNA extracts directly for nucleic acid microarrays including their low concentration especially when using low biomass samples, and their susceptibility for degradation due to their fragile structure (single strand of nucleic acids, (Watson et al., 1998, Puskas et al., 2002, Wu et al., 2006).

Amplification of the nucleic acid has therefore now become a widespread method used to provide adequate amounts of nucleic acid required for different types of genetic analysis including microarray (Bowtell, 1999, Geiss et al., 2000, Hughes et al., 2001, Mori et al., 2002, Nygaard et al., 2003).

### **3.5.2 cDNA synthesis:**

The extracted viral RNA was reverse transcribed into cDNA in order to provide the required template for DNA polymerase to start the amplification process. Both of the Oligo dT and random primers were used to synthesize the cDNA template from the mRNA and the total RNA, respectively.

The fragile structure of extracted RNA makes it vulnerable for degradation and depletion during this process which may generate short fragments of cDNA (Wang, 2005). Reverse transcription reaction generates single strand of DNA complementary to the extracted RNA, which is also susceptible for degradation during any further step. The expected short lengths and the little quantities of the synthesized cDNA which is equivalent to the RNA template, led to exclude the cDNA products from the purification step in order to avoid its degradation and losing it (according to the personal communication with Invitrogen

technical services). For the above reasons, it was not possible to evaluate the quality or quantify the synthesized cDNA in the existence of the reaction components (primers, dNTPs, cations and the reverse transcriptase).

### **3.5.3 Amplification of the viral cDNA:**

Use of MDA for amplifying the nucleic acids is a debatable issue. Many studies described it as an optimal alternative technique to all conventional methods used for genetic profile analysis of different organisms as it can provide the required amounts of nucleic acids for many genome projects, from its tiny initial concentrations (Dean et al., 2001, Dean et al., 2002, Hosono et al., 2003, Luthra and Medeiros, 2004, Bergen et al., 2005, Monstein et al., 2005, Maragh et al., 2008). Therefore, MDA technique using DNA polymerase derived from *Bacillus subtilis* bacteriophage Phi 29, and the random primers, were selected for amplifying the viral genome in order to provide adequate amounts of desired viral nucleic acids for the microarray-hybridization experiment.

REPLI-g Ultrafast mini kit was used to amplify the enteroviral cDNA based on the MDA principle, which was efficient in generating high molecular weight amplicons for the target enterovirus nucleic acids. High molecular weight products were also generated from MDA of the negative control sample using the above kit, which displayed as a smeared band having the same size of the enteroviral amplicons on the agarose gel.

This high molecular weight product was generated in all trials of the MDA of the negative control sample prepared from different sources of nuclease free water, using different lots of the Repli-g amplification kit in different

laboratories which is attributed to the polymerization of the random hexamers during MDA of the negative control sample. The low numbers of the priming sites available in the tiny concentrations of the target template, which can be used for random primers annealing allows forming the primer dimers which can serve as a template for Phi 29 DNA polymerase and leads to a nonspecific amplification with high rate of bias causing hybridization failure (Uda et al., 2007, Abdel-Hakeem, 2010) .

Barber and his colleague (Barber and Foran, 2006) indicated that MDA of short fragments of nucleic acids using Phi 29 DNA polymerase will generate shorter forks of nucleic acids along these short fragments with less priming sites end with a complicated branched amplicon not representing the entire genome. Shoaib and his colleagues (Shoaib et al., 2008) suggested that ligation of the short fragments of nucleic acids will generate long linear template with lots of priming sites, which may generate more specific amplicons.

QuantiTect whole transcriptome kit was used as an alternative method for MDA of the desired viral genomes starting from their RNA which was reverse transcribed into cDNA followed by ligation of the generated cDNA segments in order to generate long linear template to provide more priming sites ready for annealing with the random hexamers to be amplified by Phi 29 DNA polymerase. High molecular weight products were generated from both of viral genomes and negative control samples.

Due to the high molecular weight (> 20 kb) of the complex MDA product generated from MDA using QuantiTect whole transcriptome kit, the vast majority of the amplicons were retained in the purification column and did not pass through the elution step. Therefore, these amplified materials were not

purified, but were fragmented directly in order to overcome this problem. Random ligation of the generated cDNA fragments prior to MDA may generate linear product with chunks of sequence different from the sequence of the original template, which may enhance the representational bias in the amplified materials (Ho-Pun-Cheung et al., 2009).

GenomePlex complete WGA kit was used as a third technique for amplifying viral genome based on fragmenting and converting viral nucleic acids into amplifiable molecules before starting amplifying them using WGA-DNA polymerase. This kit was efficient in generating amplicons with an average size of 500 bp ready for hybridization experiment without need for sonication step or endonuclease treatment.

#### **3.5.4 Fragmenting viral amplicons**

Adoption of the MDA principle for amplifying viral genomes using either REPLI-UltraFast mini kit or QuantiTect whole transcriptome kit generated high molecular weight products. These bulky amplicon molecules will either fail to hybridize to oligonucleotides on the solid surface due to spatial and steric limitations, or may generate noisy background that may conceal the weak signals of the specific hybridization (Shchepinov et al., 1997, Southern et al., 1999, Vora et al., 2004). Therefore, it was necessary to fragment the amplicons generated from MDA before going ahead with the hybridization experiment, which may facilitate their access to the target probes and enhance successful hybridization opportunities (Dai et al., 2002, Mehlmann et al., 2005).

### 3.5.5 Labelling viral amplicons

Labelling nucleic acids with detectable molecules is the most common way used for the detection of the successful microarray hybridization with their complementary printed oligonucleotides. Chemical labelling technique using Platinum based ULS was selected for this purpose due to its easy application within short time (40 minutes), low cost, no modification in the target structure, indefinite stability of the labelled materials and no interference or variation in the hybridization results (Akers et al., 1999, Hagedoorn et al., 2003, Majtan et al., 2004, Abdel-Hakeem, 2010).

### 3.5.6 Hybridizing viral amplicons:

All hybridization experiments revealed that HPRT-PCR products hybridized with its complementary probe and generated specific hybridization signals, while viral amplicons failed to hybridize with their target probes printed on the experimental microarrays. The probable reason for this failure could be attributed to the low concentration of the viral nucleic acids which allow polymerisation of the random primers by Phi 29 DNA polymerase during MDA of the viral genomes and generate high molecular weight of amplicons containing non-viral sequences. The ligation step which preceded MDA of the viral cDNA using QuantiTect whole transcriptome kit exacerbated this problem as it generated sequences of amplicons different from the original viral sequences. Amplifying viral genome using GenomePlex complete WGA kit was not improved due to the random fragmentation reaction that preceded their amplification (Singh et al., 2005, Jahn et al., 2008). Figure 3-26



summarises all the steps used for optimizing hybridization process using the experimental microarrays.



Figure 3-26: Schematic diagram showing the steps used for optimizing hybridization process using the experimental microarrays.

## **4 Application of the Polymerase Chain Reaction for testing the specificity of the designed viral microarray**

## 4.1 Introduction

The probes of the enteroviruses, (HMPV), (HRSV) and human influenza virus A printed on the microarray chip were designed in order to be used for diagnosing viral infections caused by these viruses through detecting their nucleic acids in clinical samples. These probes need to be tested in a hybridization reaction using positive control and clinical samples in order to explore their performance and determine the specificity and sensitivity of the probes which can hybridize to the related viral nucleic acids exist in these samples, and select the best performing probes for generating a diagnostic microarray chip. These probes were designed along the whole genomes of the selected RNA viruses in order to detect any part of the viral nucleic acids which may be existed in a clinical sample suspected to be infected with one or more of the above viruses. Therefore, amplifying the entire genomes of the desired viruses at this stage is necessary in order to provide nucleic acid templates with an adequate concentration able to hybridize with the complementary probes printed on the virochip. PCR has been widely utilized for in vitro unlimited amplification of nucleic acids which can generate millions copies of a target genome starting from a single copy (Hernandez-Rodriguez et al., 2011, Waters and Shapter, 2014). Many researchers have exploited the low detection limits of the PCR technique for the detection of viral nucleic acids in environmental and infected clinical samples, which leads to the diagnosis of the viral infections, identifies their causative agents and determines the appropriate treatment regimen (Clementi, 2000, Mackay, 2004). Kleinschmidt and his colleagues (Kleinschmidt-DeMasters et al., 2001) were able to diagnose viral nervous system infections when they detected human

herpesviruses in cerebrospinal fluid samples using the PCR method. Other researchers cited that two types of influenza viruses (A and B) were detected simultaneously in patients' samples who had symptoms of respiratory infections, using a PCR based method (van Elden et al., 2001). Therefore, PCR technique was adopted for amplifying the entire genomes of the pTZ18R plasmid, enteroviruses, HMPV, HRSV and human influenza virus A, after the failure of the hybridization experiments between the probes printed on the experimental microarrays and the amplified materials generated from MDA process in chapter 3.

## **4.2 Aims**

The aims of this chapter were: 1) Generate full length amplified DNA covering human enteroviruses, human influenza virus A, HMPV and HRSV in order to explore the efficiency of most of the probes designed using the microarray. 2) Hybridize the microarray to full length viral sequences in order to describe the performance characteristics of the designed probes especially their sensitivity and specificity.

## **4.3 Materials and methods**

### **4.3.1 Samples**

Several nucleic acids samples were used for completing optimizing the microarray hybridization conditions and validating the performance of the microarray chip containing viral probes designed in chapter 2. These samples included:

- 1- Enteroviral RNA including i) RNA transcripts consisted of  $10^6$  copies/ $\mu$ l for each of the Human echovirus 7 and Human coxsackievirus A-21 which were provided kindly by Professor Peter Simmonds, Centre of Infectious Diseases, University of Edinburgh, Summerhall, Edinburgh, UK, ii) an extracted RNA from a clinical stool sample infected with enteroviruses which was provided by the clinical Virology laboratory, QMC, Nottingham, UK.
- 2- RNA extracts for each of i) HMPV, ii) HRSV, iii) human influenza virus A, which were extracted from clinical samples (nasopharyngeal aspirate) and provided by clinical Virology laboratory, QMC, Nottingham, UK.
- 3- pTZ18R plasmid RNA generated from its transcription reaction in section 3.3.2.5.5.
- 4- HPRT product generated from PCR amplification of the human DNA extracted from the human peripheral blood in section 3.3.2.6.1.
- 5- Varicella zoster virus (VZV) DNA extracted from live attenuated vaccine for this virus (GlaxoSmithKline, UK) using QIAamp DNA mini extraction kit as described in section 3.3.2.6.1.

## **4.3.2 Amplification of the samples nucleic acids using PCR technique**

### **4.3.2.1 Designing specific primers**

PCR amplification reaction requires the use of specific primers for the desired template to be amplified. Primer 3 software version 0.4.0 (<http://bioinfo.ut.ee/primer3-0.4.0/>) was used for designing the required primers for PCR amplification of the entire genome of the pTZ18R,

enteroviruses, HMPV and HRSV in addition to the entire HA and NA genetic segments of the human influenza virus A, and part of the VZV genome. Primer picking conditions of the software were set as follow: primer size was 15-28 bases, primer T<sub>m</sub> was 50 °C to 61 °C and primer GC% was 20-50 %. Loading the sequence of the pTZ18R plasmid into the Primer 3 software generated one set of primers (forward and reverse) for amplifying the whole genome (2686 bp) of the pTZ18R. Similarly, one set of primers targeting part of the VZV genome (5514 bp) was generated after loading the sequence of that part into the software (table 4-1).

Designing one pair of primers for each viral group capable of amplifying the whole genome of all subtypes within each viral group is almost impossible. Therefore, it was decided to design several sets of primers for each group of the selected RNA viruses through several repeated trials, covering their whole genomes.

#### **4.3.2.1.1 Human enterovirus primers design**

Due to the high genetic diversity among the 87 serotypes of the human enterovirus, several trials of primer design were implemented in order to generate the required primers for amplifying their entire genomes, by loading different sequences of them as a template into the Primer 3 software. In the first trial, the sequence of the Human coxsackievirus A-2 was loaded into the Primer 3 software. Aligning the sequences of the primers generated from this trial to the sequences of the enterovirus serotypes revealed that the Ent-FW1 primer showed high degree of homology with the most serotypes (89 %) except Human coxsackievirus A-5 and 11, Human coxsackievirus B-4, Human

echovirus 12 and 18-19 and Human enterovirus 81, and 90 which they showed 1 base mismatch with the above primer sequence, which is acceptable as long as it's not at the 3' end of the primer (Thweatt et al., 1990, Kolmodin and Birch, 2002). Alignment results also showed that the Ent-FW1 primer has several noncomplementarities at its 3' end with the Human echovirus 30 and therefore another forward primer (Ent-FW2) was designed specifically for this enterovirus serotype.

The sequence of the Ent-FW1 primer was used as a conserved forward primer during designing the reverse primers which were designed specifically for each enterovirus subtype by loading the sequences of the Human coxsackievirus A-2, Human coxsackievirus A-9, Human coxsackievirus A-11, and human enterovirus 70 as representative templates for the human enterovirus A, B, C and D, respectively into the software. Accordingly, the alignment results showed that the reverse primers Ent-RV1, 3, 4 and 6 generated from further primer design trials, were conserved with most serotypes of the human enterovirus A, B, C and D, respectively, therefore they were selected for amplifying their entire genomes. The alignment results also revealed that the Ent-RV1 primers and the Ent-RV4 primer showed many nucleotide mismatches especially at their 3' end with some of the human enterovirus A and C serotypes, respectively, therefore the reverse primers Ent-RV2 and 5 were designed for amplifying the above mismatched serotypes, respectively (table 4-1).

#### 4.3.2.1.2 HMPV primers design

One of the HMPV sequences was used as a template for designing the required primers for amplifying the entire genome of the HMPV. In order to simplify the process of the primers design and the subsequent PCR amplification step, the template sequence of the HMPV was separated into three smaller segments (Seg-1, 2 and 3); each segment was loaded separately into the Primer 3 software. This primer design process generated one set of primers for each segment of the HMPV. Alignment results of the generated primers sequences with the sequences of the HMPV strains revealed that the reverse primer of the second segment (HMPV-RV2) showed one base mismatch, and the forward primer of the third segment (HMPV-FW3) showed two base mismatches with some of the HMPV strains, while other primers were conserved in most strains. Use of the degenerate nucleotides at the mismatch positions of the above primers can make them conserved in all of the HMPV strains through providing several unique sequences of each primer differ at the mismatch positions only such that each primer sequence contains one of the four possible nucleotides (A, T, G or C) at each mismatch position (Linhart and Shamir, 2002). Accordingly, one degenerate nucleotides symbolized by R (which represents either A or G) was used at the mismatch position of the primer HMPV-RV2, while two degenerate nucleotides symbolized by R and Y (which represents either C or T) were used at the two mismatch positions of the primer HMPV-FW3 (see table 4-1).



#### **4.3.2.1.3 HRSV primers design**

The same primer design process of the HMPV was used for designing the required primers for amplifying the entire genome of the HRSV through selecting one of the HRSV sequences as a template and chopping it into three parts which were loaded separately into the Primer 3 software. One set of primers for each part of the HRSV genome was generated after running the software. The sequences of the generated primers were aligned with the sequences of the HRSV strains and the results revealed that the forward primer HRSV-FW1, and the reverse primers HRSV-RV1 and HRSV-RV2 were conserved in all sequences, while the forward primer HRSV-FW2 and the reverse primer HRSV-RV3 showed two base mismatches with only two of the HRSV strains (HRSV-strain B1 and HRSV-cp52). Two degenerate nucleotides symbolized by W (which represents either A or T), and R were used at the mismatch positions of the HRSV-FW2 primer, while other two degenerate nucleotides represented by R were used at the mismatch positions of the HRSV-RV3 primer in order to provide the required sequences of them for amplifying all the strains belong to the HRSV. The alignment results also showed that the HRSV-FW3 primer has four noncomplementarities with the above two strains (see table 4-1).

#### **4.3.2.1.4 Human influenza virus A primers design**

One set of specific primers for each of the HA and NA genomic segments belong to H1N1 and H3N2; the most common subtypes of human influenza virus A, was generated after loading one of each segment sequences as a template into the Primer 3 software. Alignment results of the generated primers

sequences with the sequences of the HA and NA segments of the viral strains belong to the above viral subtypes revealed 100 % homology with most strains. However, the alignment results also showed variable degree of noncomplementarity with some viral strains (see table 4-1).

All primers generated from Primer 3 software for amplifying all the above samples were synthesized and provided as a lyophilized form by Eurofins MWG Operon, resuspended in nuclease free water at a concentration of 100  $\mu$ M and stored at -80 °C.

Table 4-1: Characteristics of the primers used for PCR amplification of the viral groups.

	Primer ID	Sequence (5'→3')	T <sub>m</sub> °C	GC%	Amplicon size	
<b>pTZ18R</b>	Plas-FW	AAGGCGATTAAGTTGGGTAAC	55.9	42.9	2686 bp	
	Plas-RV	ATCGGCAAAATCCCTTATAAAT	52.8	31.8		
<b>VZV</b>	VZV-FW	AACCTCCAAAAGCATCAATAAC	54.7	36.4	5514 bp	
	VZV-RV	AGTTCAACCCTTATCAAACCTCG	56.5	40.9		
<b>Enterovirus</b>	Ent-FW1	ACTACTTTGGGTGTCCGTGTTT	58.4	45.5	≈ 6.9 kb	
	Ent-FW2	ACTACTTTGGGTGTTTTTCCTT	54.7	36.4		
	Ent-RV1	TTATAACAAATTTACCCCCACCA	57.9	47.6		
	Ent-RV2	ATCTTTGGTGACTTTGTCAAGC	55.3	34.8		
	Ent-RV3	ATGCGGAGAATTTACCCCTAC	56.5	40.9		
	Ent-RV4	AATCCAATTCGACTGAGGTAGG	58.4	45.5		
	Ent-RV5	AAGCCAATTCGGGTGAGGTA	57.3	50		
	Ent-RV6	CCCAATTAACCAAAATTTACCT	52.8	31.8		
<b>Human metapneumo virus</b>	<b>Seg-1</b>	HMPV-FW1	AAAATGTCTCTTCAAGGGATTCA	55.3	34.8	≈ 4.1 kb
		HMPV-RV1	GTGCTGACTTTGCATGGGTA	57.3	50	
	<b>Seg-2</b>	HMPV-FW2	CTAAGCAAAGTTGAGGGTGAAC	58.4	45.5	≈ 4.2 kb
		HMPV-RV2	GCTTTTCATTTAATACCATCTCA	55	31.3	
	<b>Seg-3</b>	HMPV-FW3	CCRGAAACYTTAACAAAGTATGGTGA	60.1	38.5	≈ 3.3 kb
		HMPV-RV3	CCTGCTCCTTCTCCAATAAAG	57.9	47.6	

		Primer ID	Sequence (5'→3')	Tm °C	GC%	Amplicon size
Human respiratory syncytial virus	Seg-1	HRSV-FW1	GGGGCAAATAAGAATTTGATAAG	55.3	34.8	≈ 3.2 kb
		HRSV-RV1	TTGTTACAGTATGTTTCCATATTT	54.2	29.2	
	Seg-2	HRSV-FW2	CAGC <b>W</b> GCTGTTCA <b>R</b> TACAATG	55.9	42.9	≈ 5.8 kb
		HRSV-RV2	TGTATTAACCATGATGGAGGATG	57.1	39.1	
	Seg-3	HRSV-FW3	CTTGACATGGAAAGATATTAGCC	57.1	39.1	≈ 5.3 kb
		HRSV-RV3	GGCAT <b>R</b> ATGAAATTTTT <b>R</b> GTT	52	33.3	
Flu-A	HA	(H1N1) FW	CAATTCAACAGACACTGTAGACACA	59.7	40	≈ 1.5 kb
		(H1N1) RV	ATCTGGTAAATCCTTGTTGATTCC	57.6	37.5	
		(H3N2) FW	TCCCGGAAATGACAACAG	52.2	46.3	≈ 1.6 kb
		(H3N2) RV	TGCAAATGTTGCACCTAAT	50.2	36.8	
	NA	(H1N1) FW	CCATTGGTTCGGTCTGTATG	57.3	50	≈ 1.3 kb
		(H1N1) RV	AAGACCAACCCACAGTGTC	57.3	50	
		(H3N2) FW	CCTTATGTGTCATGCGATCC	57.3	50	≈ 1 kb
		(H3N2) RV	ATGTACCTGAGGTGCCACAA	57.3	50	

Abbreviation; FW: Forward, RV: Reverse, HMPV: Human metapneumovirus, RSV: Respiratory syncytial virus, HA: Hemagglutinin, NA: Neuraminidase, R: A or G, Y: C or T, W: A or T.

### 4.3.2.2 Long range cDNA synthesis

Maxima H Minus First Strand cDNA Synthesis kit (provided by Thermo Scientific) was used for efficient synthesis of the full length cDNA templates (up to 20 kb) from the selected viral RNAs as well as pTZ18R plasmid RNA. Oligo-dT primers were used to synthesize cDNA strand from the enterovirus RNA containing poly-A tail at its 3' end, while random hexamer primers were used to generate cDNA from total RNA of each of the of the pTZ18R, human influenza virus A, HMPV and HRSV RNAs.

According to the manufacturer's guideline, 10  $\mu$ l of the viral RNA were mixed with 1  $\mu$ l of either oligo-dT or random hexamer primers (100  $\mu$ M), and 1  $\mu$ l of dNTP mix (10 mM). The reaction volume was adjusted to 15  $\mu$ l by adding 3  $\mu$ l of nuclease free water. The reaction mixture was incubated at 65 °C for 5 minutes in thermal cycler and chilled immediately on ice for 1 minute and spun briefly. Generation of the viral cDNA was initiated by adding 4  $\mu$ l of 5X RT buffer and 1  $\mu$ l of Maxima H Enzyme mix containing the reverse transcriptase. The reaction mixture was incubated in thermal cycler at 50 °C for 30 minutes, preceded by 10 minutes at 25 °C when using random hexamers. The reaction was terminated by heating the mixture for 5 minutes at 85 °C. The generated cDNA was stored at -80 °C for further use.

### 4.3.2.3 Long-range PCR amplification

LongAmp Hot Start Taq DNA polymerase kit (New England, Biolabs) was used for PCR amplification of the viral nucleic acids. This enzyme is able to generate long PCR products (up to 30 kb) in one reaction.

According to the manufacturer's protocol, 2  $\mu$ l of each of the desired nucleic acid templates (pTZ18R cDNA generated in section 3.3.2.5.5, viral cDNAs generated in section 4.3.2.2 and VZV DNA extracted from live attenuated vaccine for VZV) were added to 23  $\mu$ l of reaction mixture containing 1X PCR LongAmp Taq Reaction Buffer, 300  $\mu$ M of each dNTP, 0.4  $\mu$ M of each primer and 2.5 units of LongAmp Hot Start Taq DNA polymerase. The PCR reaction was incubated in a thermal cycler (Techne TC-3000) with the following thermal profile: 30 seconds of initial denaturation at 94 °C followed by 40 cycles composed of denaturation for 30 seconds at 94 °C, primer annealing for 60 seconds at the  $T_m$  temperature specific for each set of primers (clarified in table 4-1) and primer extension at 65 °C for 50 seconds/ kb, with a final extension step for 10 minutes at 65 °C.

PCR amplicons were purified using Qiaquick PCR purification kit as described in section 3.3.2.5.2 followed by measuring their concentration and purity using the NanoDrop ND 1000 as described in section 3.3.2.5.4 and finally run on a 1% agarose gel as described in section 3.3.2.5.3 in order to detect their expected size.

### **4.3.3 Fragmenting and Labelling the PCR products**

The purified amplicons generated from PCR amplification of samples under study in this chapter were fragmented by sonication using the same conditions described in section 3.3.4.1.1 followed by ethanol precipitation as described in section 3.3.4.2. Finally, the clean fragmented amplicons were mixed with one-fifth volume of the HPRT-PCR product and labelled with dyomics 547 and 495 fluorescent dyes as described in section 3.3.4.3. The DOL was calculated using

the Nanodrop results in order to determine the efficiency of the nucleic acid labelling process.

#### **4.3.4 Manual hybridization experiments**

A hybridization trial was performed using an experimental microarray in order to optimize the hybridization process and evaluate the efficiency of the PCR amplification process and validate the appropriateness of the generated amplicons for hybridization before starting any hybridization experiments using the virochip microarray designed in chapter 2. One of the NHS-coated BSA slides prepared in section 3.3.5.1 was used for fabricating a new experimental microarray in order to be used for testing some of the amplicons generated from long-range PCR including enterovirus, pTZ18R and VZV in a hybridization experiment. Accordingly, two dozen of probes specific for VZV and herpes simplex virus type 1 (HSV1), and eight probes for HSV2 designed by Abdel-Hakim, 2010 (table-4-2), in addition to HPRT, enterovirus and pTZ18R probes described in tables 3-3, 3-4 and 3-5 were used for printing the experimental microarray (HHVs-pTZ18R-enterovirus microarray) following the same printing protocol described in section 3.3.5.2. Each probe was printed in duplicate according to the printing layout illustrated in figure 4-1. Then the labelled amplicons of the enterovirus, pTZ18R and VZV generated from long-range PCR amplification process were tested in a hybridization experiment using the experimental HHVs-pTZ18R-enterovirus microarray following the hybridization technique described in section 3.3.6.2.

**Table 4-2: Sequences of the HHVs probes used for printing the experimental microarray.**

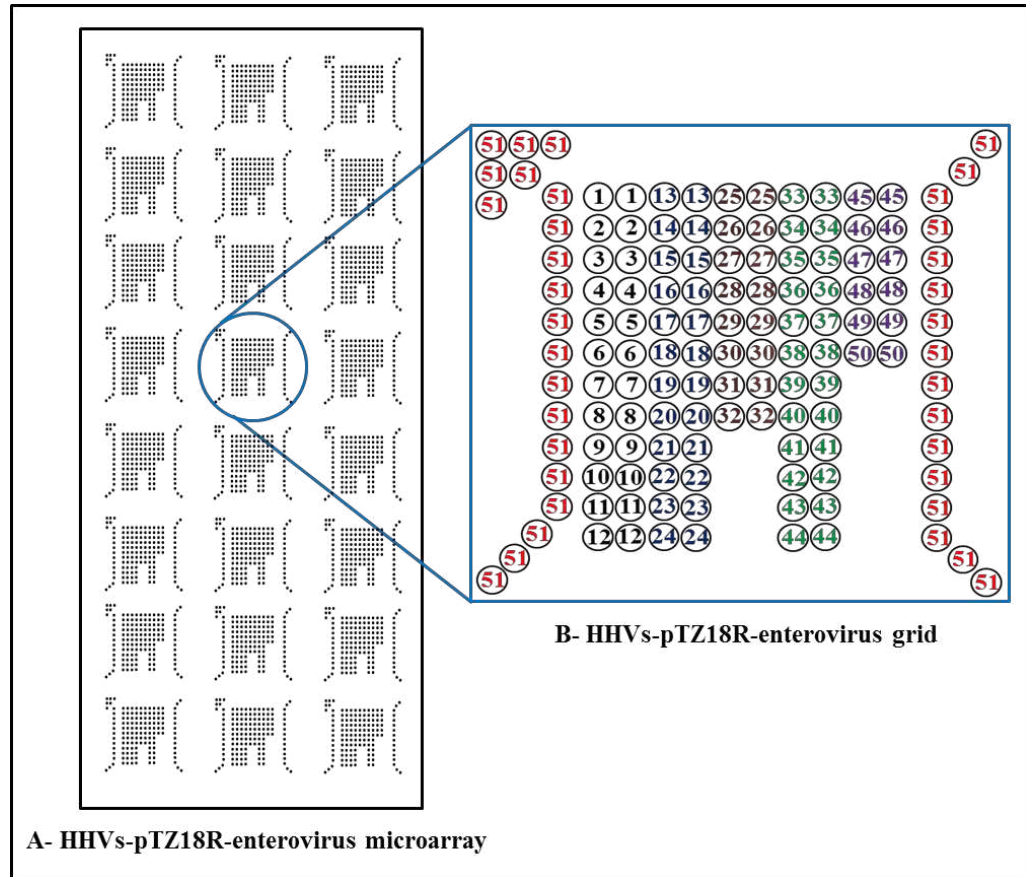
Adopted from (Abdel-Hakeem, 2010)

	Probe ID	Sequence (5'-3')	Position on gene
HSV1	HSV1-5	GAAATTACCTTCCTCTTCGGACTCGATATC	24958-24987
	HSV1-7	AATCCCATAAACATACGACACACAGGCATA	34978-35007
	HSV1-12	TACCGCAGAATCTGGTTTGCCATGTAGTAC	59350-59379
	HSV1-13	GATTATAACCGACAAGATCAAGCTCTCGAG	64391-64420
	HSV1-18	TTTGAGCAGAAGGACATTCTCCACTACTAC	90251-90280
	HSV1-21	TGTTGGTGCTTTATTGTCTGGGTACGGAAG	105458-105487
	HSV1-22b	AGAGTCCCTTCTGGTTTCTTAGCAAATTCG	109729-109758
	HSV1-22a	CAATCACAAACATCATCCTGGATCTCGACA	110914-110943
	HSV1-24	AAAGTTGTTCTAAAGCGAGGATACGGAGG	119871-119900
	HSV1-25	CCCATTAATGAGTTTCTAATTACCATACCG	124779-124808
	HSV1-27	GTTGGTATATTACAGGCCCGTGTCCGATTT	134934-134963
	HSV1-28	CTTCTCGGTGTTTGTGTTGTATCGTGCTTG	141275-141304
HSV2	HSV2-2	AGACGGAATATTTCTTCGCTATCACTGCCC	9630 – 9652
	HSV2-5	CATTTCTGTCTTTATTCGCTATCAGAGAGT	24803 – 24832
	HSV2-6	AACAAACCTAGGATCTTGTGTA CTACGCC	28761 – 28790
	HSV2-12	TACCTCAAGATCTGGTTGGCCATGTAGTAC	59744 – 59773
	HSV2-17	AACAGGCCCTTTAAACATTTGCGTATGCAC	84871 – 84900
	HSV2-20	GGTAAGCGTCGCGTTAATTATATACTGGGC	100559 – 100588
	HSV2-21	AATAACGATCTCGAGAGGCCAATGAGACGT	105790 – 105810
	HSV2-23	TATGCTAATCGACCTAGGATTGGACCTGTC	114610 – 114640



	Probe ID	Sequence (5'-3')	Position on gene
<b>VZV</b>	VZV-1	TTGTA AATACATACCATATACAAACCATGC	4870 – 4899
	VZV-2	ATATGTTTGTAGGTTAAGGGAACATCGATA	9985 – 10014
	VZV-7	AAATTTAAACCAACTGTAGACGTGCCGGAT	35203 – 35232
	VZV-9	GATGGTTGACTGTTTCATCATCGGAACATCG	45334 – 45363
	VZV-10	AAGTAATAACGGTACCAAGCGGTCGTGTTG	50196 – 50225
	VZV-12	ATCTGATTTGCAAACATATCGGCGTCGTCT	60344 – 60373
	VZV-15	GTTCTACCGAAATGACACAGGATCCGTGTG	75557 – 75586
	VZV-16	GTTGTTGTAGCCACAATTTACATCACGCGC	80586 – 80615
	VZV-17	AATAGACCTACAATGGCAAATCTACGGGAC	85607 – 85636
	VZV-19	CTTGTCCATCGGTATATCCAAAGTCACCGG	95718 – 95747
	VZV-20	TATGGATCTTGACCAATAATTACAACGCGA	100776 – 100805
	VZV-23	CAGAGCATCCGTCTTGCGATACGATGATTT	115896 – 115925

HHVs: Human herpesviruses



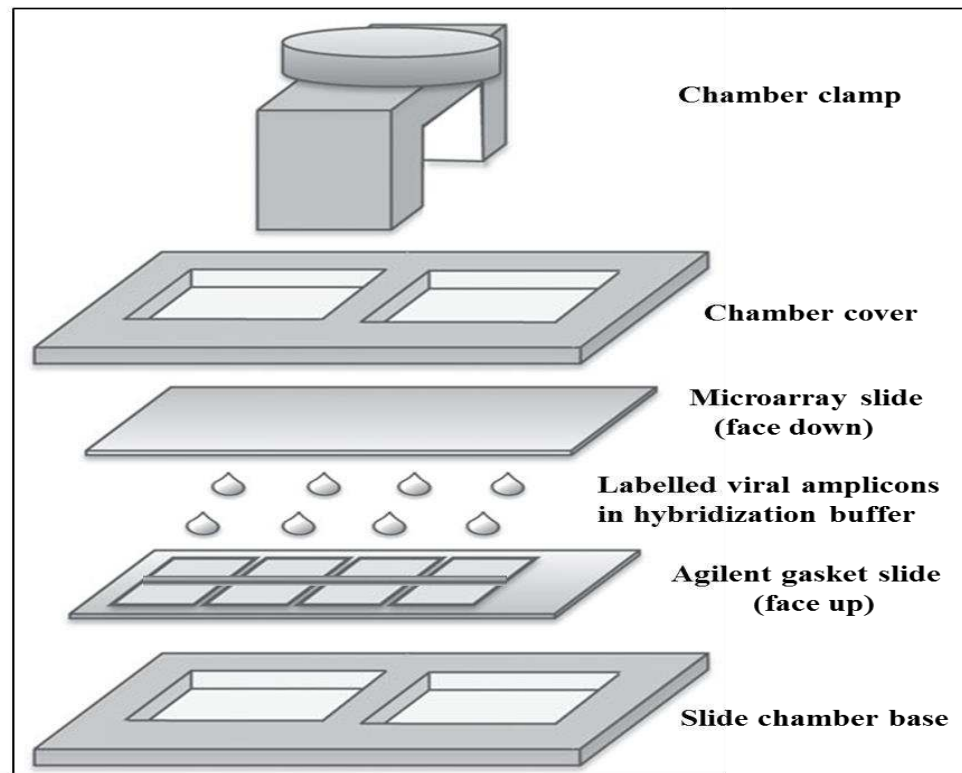
**Figure 4-1: Schematic drawing of the experimental HHVs-pTZ18R-enterovirus microarray.**

Figure (A) shows the printing layout of the 24 HHVs-pTZ18R-enterovirus grids on the microarray slide that was used during optimization steps. Figure (B) represents a magnified diagram for one of the printed grids showing the spot locations represented in circles with a digit inside each one. Numbers from 1 to 12 refer to the VZV probes, 13-24 represent HSV1 probes, 25-32 refer to HSV2 probes, 33-44 represent the pTZ18R plasmid probes, 45-50 represent the enterovirus probes while number 51 refers to the HPRT probe.

#### 4.3.4.1 Hybridization experiment using virochip

An Agilent Microarray Hybridization Chamber Kit (Agilent Technologies) was used for holding the virochip containing the specific probes designed for the selected RNA viruses in chapter 2, during the hybridization process. An Agilent gasket slide enclosing 8 chambers (2x4) matching the format of the virochip grids was used in order to separate the grids and prevent samples

intermixing during the hybridization reaction. Therefore, and according to the hybridization chamber user guide, the prehybridization buffer as well as the labelled viral amplicons suspended in the hybridization buffer, were loaded into the Agilent gasket slide surface fixed in the slide chamber base, rather than the microarray slide. After that, the microarray slide surface containing the printed viral probes was carefully lowered on the top of the Agilent gasket slide surface. The chamber cover was placed onto the chamber base holding both the microarray and the Agilent gasket slides, and fixed using the clamp assembly located in the centre of the chamber cover (figure 4-2). The hybridization reaction was performed following the same hybridization technique described in section 3.3.6.2.



**Figure 4-2: Agilent Microarray Hybridization Chamber Kit used for holding the virochip during hybridization with the labelled viral amplicons.**

Adopted from (Berger and Bulyk, 2009).

## 4.4 Results

### 4.4.1.1 Long-range PCR amplification results

Long-range PCR amplification of the selected viral RNAs was preceded by reverse transcribing them into cDNA templates using Maxima H Minus First Strand cDNA synthesis kit. Poly-A tail RNA extracts including these derived from Human echovirus 7, Human coxsackievirus A-21 and a clinical sample known to contain an enterovirus were reverse transcribed into cDNA using Oligo-dT primers. First strand cDNA was also synthesised from three RNAs of each of HMPV, HRSV and human influenza virus A (two for H1N1 and one for H3N2) extracted from clinical samples containing these viruses, in addition to the pTZ18R plasmid using random primers.

The cDNA templates generated from reverse transcription reaction of the human enteroviruses, HMPV, HRSV, H1N1, H3N2 and pTZ18R plasmid RNAs in section 4.3.2.2, in addition to the VZV DNA extracted from a VZV vaccine were amplified using LongAmp Hot Start Taq DNA polymerase kit following the PCR principles. The Qiaquick PCR purification kit was used for purifying the amplicons generated from long-range PCR amplification reaction of the above viral and plasmid nucleic acids. The PCR products generated from Long-range PCR amplification reaction of the pTZ18R genome and part of the VZV genome using their specific designed primers were revealed as a clear single bands for each one with the expected target size (2610 and 5514 bp, respectively) after running them on 1% agarose gel as shown in figure 4-3.

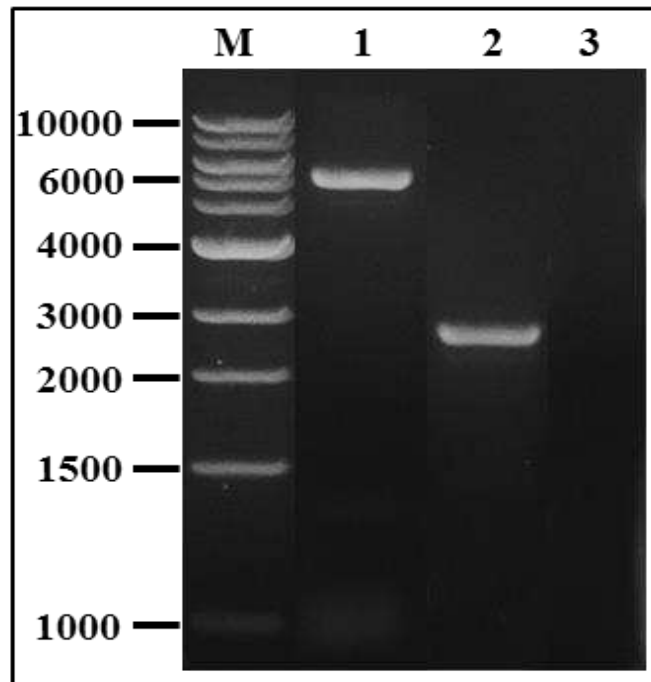


**Figure 4-3: Agarose gel electrophoresis of the pTZ18R cDNA and VZV DNA generated from Long-range PCR amplification reaction.**

pTZ18R plasmid RNA was reverse transcribed into cDNA and then amplified in parallel with the VZV DNA extracted from a VZV vaccine using PCR. Lane 1 was loaded with PCR amplicon of the VZV while PCR amplicon of the pTZ18R plasmid was loaded into lane 2. PCR negative control sample containing nuclease free water was loaded into lane 3. M refers to 1 kb ladder.

Long-range PCR amplification reaction of the Human echovirus 7 and Human coxsackievirus A-21 cDNA using Ent-FW1 as a forward primer, and Ent-RV1 and Ent-RV4 as a reverse primer for each one, respectively, generated approximately 9  $\mu\text{g}$  of nucleic acids. Agarose gel electrophoresis of the generated amplicons revealed single bright bands of the expected size ( $\approx 7$  kb) for the entire genome of each of the above mentioned enterovirus serotypes. The gel also showed some less bright bands related to shorter fragments of the amplified enteroviral cDNA (figure 4-4).

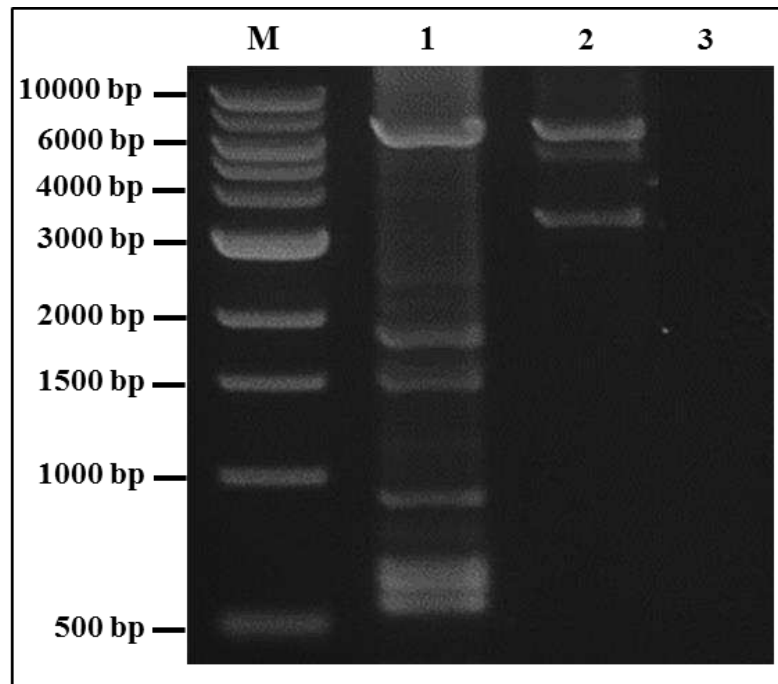


**Figure 4-4: Agarose gel electrophoresis of Long-range PCR amplification of enteroviral cDNA.**

Ent-FW1 and Ent-RV1, and Ent-FW1 and Ent-RV4 primers were tested for amplifying the whole genome of Human echovirus 7 and Human coxsackievirus A-21, respectively, using their cDNA preparations in Long-range PCR amplification reaction. Lane 1 was loaded with PCR amplicon of Human echovirus 7 while PCR amplicon of Human coxsackievirus A-21 was loaded into lane 2. PCR negative control sample containing nuclease free water instead of enteroviral cDNA template was loaded into lane 3. M refers to 1 kb ladder.

As the enterovirus serotype isolated from the clinical sample was not known, all enterovirus primers were loaded together into one PCR reaction for amplifying the cDNA generated from this sample. A temperature gradient was used for optimizing the primer annealing temperature during the above PCR reaction. Running the amplified products generated from the temperature gradient step revealed that 56 °C was the optimal temperature for annealing the

relevant enterovirus primers to their complementary nucleic acid sequences available in the clinical enterovirus cDNA template, as shown in figure 4-5.

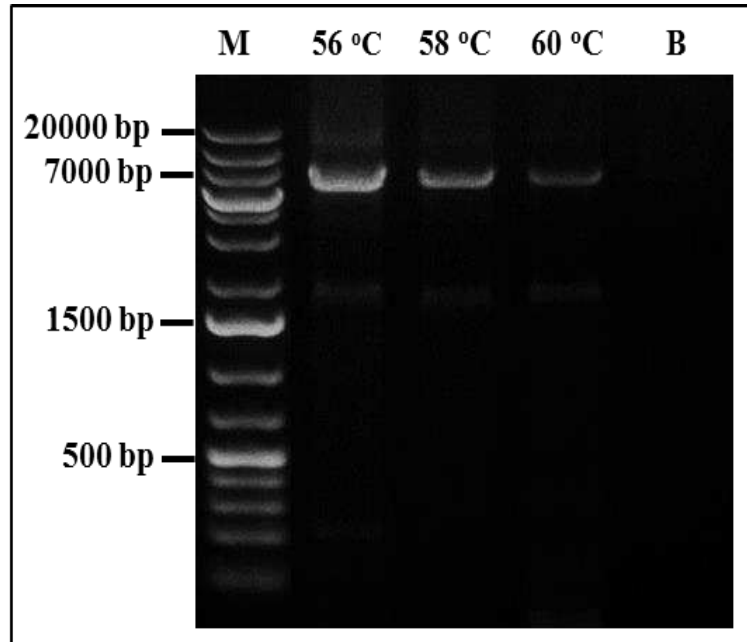


**Figure 4-5: Agarose gel electrophoresis of the clinical enterovirus amplicons generated from Long-range PCR reaction using temperature gradient.**

Enterovirus RNA extracted from a clinical sample was reverse transcribed into cDNA and then amplified using PCR. Three different temperatures (56 °C, 58 °C and 60 °C) were used. M represents the 1 kb plus ladder while B refers to the gel well loaded with the negative control sample containing nuclease free water instead of enteroviral cDNA template.

Amplifying the three segments of each of HMPV or HRSV genomes using their specific three sets of primers described in table 4-1, together in one Long-range PCR amplification reaction was failed. Therefore, three Long-range PCR amplification reactions were performed; each reaction was dedicated for amplifying part of the viral genome using one set of the related primers.

Three PCR products with a concentration ranging from 5-9  $\mu$ g, were generated from long-range PCR amplification process of each of the HPMV and HRSV cDNAs derived from clinical samples. A bright main band with the expected size was observed after running each PCR product of HMPV or HRSV on 1% agarose gel (figures 4-6 and 4-7).

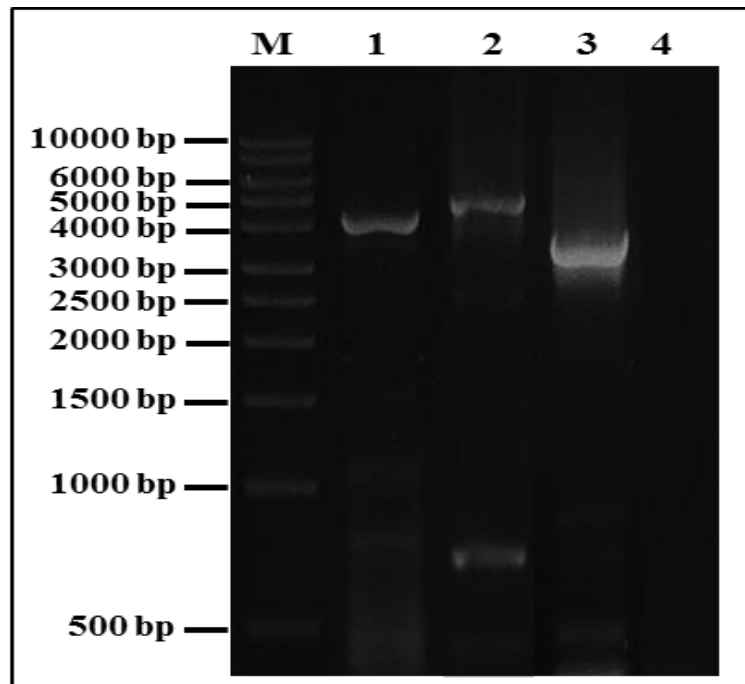


**Figure 4-6: Agarose gel electrophoresis of HMPV amplicons generated from Long-range PCR amplification process.**

Three different sets of specific primers were designed and used in Long-range PCR amplification reactions, for amplifying the entire genome of HMPV. Each set of primers was used for amplifying part (1/3) of the entire viral genome using cDNA template generated from a reverse transcription reaction of HMPV RNA isolated from a known positive clinical sample. PCR product of first segment of the above viral genome was loaded in lane 1 (expected size is 4.1 kb), middle segment in lane 2 (expected size is 4.2 kb) and last segment in Lane 3 (expected size is 3.3 kb). Lane 4 was loaded with PCR negative control. M represents 1 kb DNA ladder.



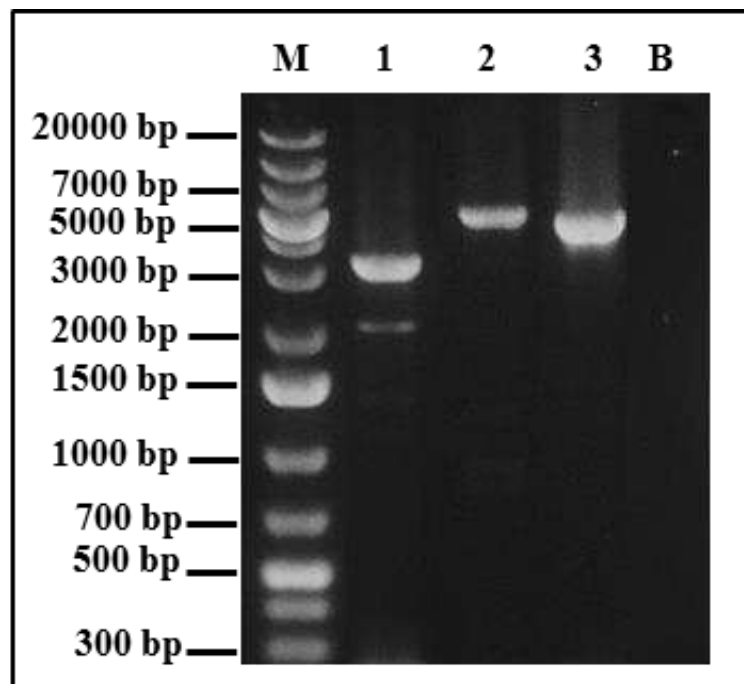


**Figure 4-7: Agarose gel electrophoresis of HRSV amplicons generated from Long-range PCR amplification process.**

Three different sets of specific primers were designed and used in Long-range PCR amplification reactions, for amplifying the entire genome of HRSV. Each set of primers was used for amplifying part (1/3) of the entire viral genome using cDNA template generated from a reverse transcription reaction of HRSV RNA isolated from a known positive clinical sample. PCR product of first segment of the above viral genome was loaded in lane 1 (expected size is 3.2 kb), middle segment in lane 2 (expected size is 5.8 kb) and last segment in Lane 3 (expected size is 5.3 kb). Lane 4 was loaded with PCR negative control. M represents 1 kb plus DNA ladder.

The total size of the three amplified segments generated from long-range PCR amplification process of HMPV and HRSV was  $\approx$  11.6 kb and 14.3 kb, respectively, which represent most of their entire genomes ( $\approx$  90 %). The rest of the HMPV and HRSV genomes (1.7 kb and 0.9 kb, respectively) were not targeted by the designed primers due to their high sequence diversity among the HMPV and HRSV strains, therefore they were not amplified (figure 4-8).

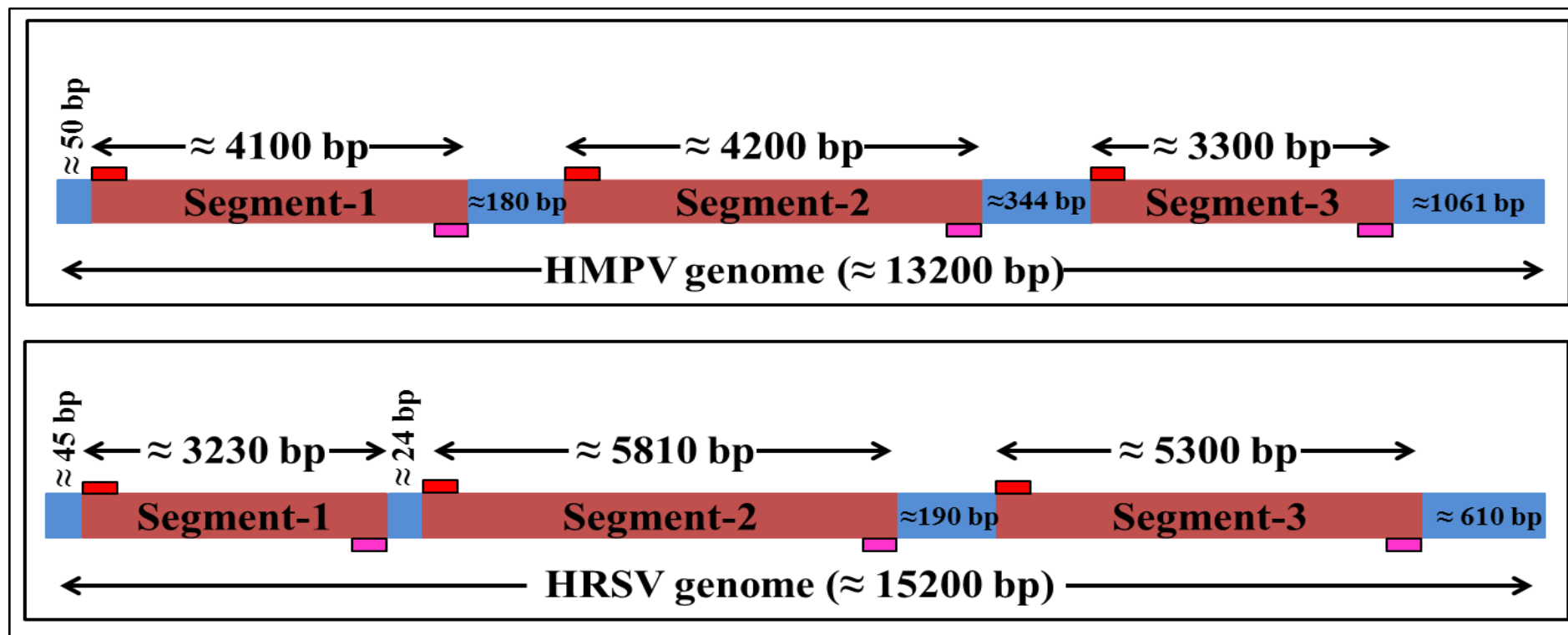


**Figure 4-8:** Schematic diagram shows the size and position of the amplified and the unamplified parts of the HMPV and HRSV genomes generated from long-range PCR amplification process.

Three segments (1, 2 and 3 shown as brown bars) of each of the HMPV and HRSV genomes were amplified using three sets of primers. The red bars above the amplified segments refer to the forward primers and the pink bars below the amplified segments refer to the reverse primers, used for amplifying the genome segments. The blue bars represent the unamplified sequences of the above genomes.

HA and NA genomic segments of H1N1 and H3N2 subtypes of human influenza A virus were amplified individually in four different PCR reactions using their respective specific set of primers (table 4-1), in order to avoid the difficulties that accompanied their amplification process when using all primers sets in one PCR reaction. PCR amplification process generated abundant quantities of amplified materials representing most length of the above genomic segments for each H1N1 and H3N2 subtypes. The amplified materials of each segment appeared as a single bright band having the expected amplicon size as mentioned in table 4-1, after running on an agarose gel (figure 4-9).

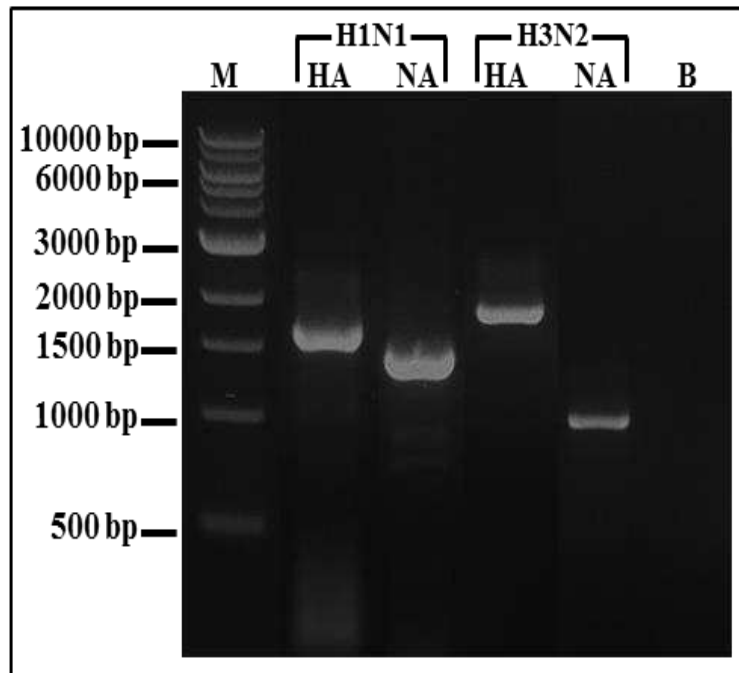


**Figure 4-9: Agarose gel electrophoresis of the products of HA and NA genomic segments of H1N1 and H3N2 subtypes generated from Long-range PCR amplification process.**

Four different sets of specific primers were designed and used in Long-range PCR amplification reaction, for amplifying two genomic segments (HA and NA) of two subtypes (H1N1 and H3N2) of human influenza virus A. Each set of primers was used for amplifying most of the desired segment using cDNA template generated from reverse transcription reaction of human influenza virus A RNA isolated from known positive clinical sample.

The size of the amplified products generated from long-range PCR amplification process of the HA and NA of the H1N1 subtype was  $\approx 1.5$  kb and 1.3 kb, respectively, which represent 90 % of the full length of the above segments. In contrast, the size of the same segments of the H3N2 subtype was  $\approx 1.6$  kb and 1 kb, respectively, which represent 96 % of the full length of the HA segment and 71 % of the NA segment. The rest sequence of each segment was not amplified as it was not targeted by the designed primers due to the genetic diversity among the strains of each subtype (figure 4-10).

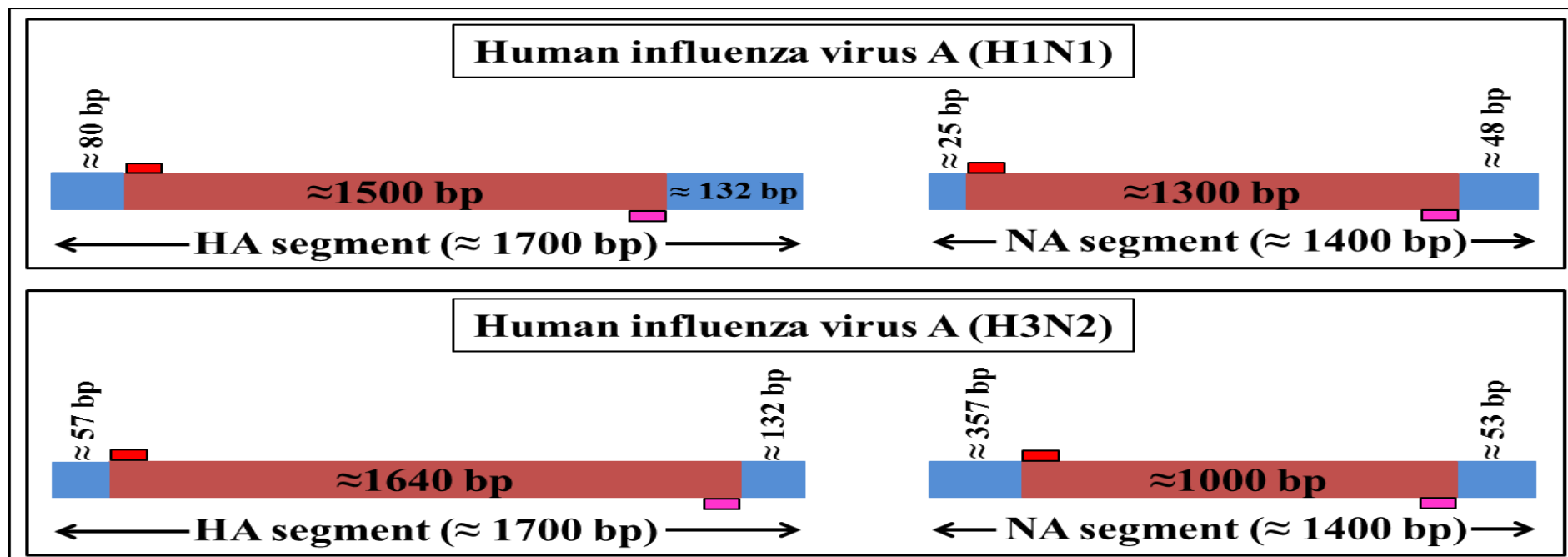


Figure 4-10: Schematic diagram shows the size of the amplified and unamplified products generated from long-range PCR amplification process of the HA and NA segments of the H1N1 and H3N2 subtypes of the human influenza virus A.

The brown bars represent the amplified parts of the HA and NA segments generated from long-range PCR amplification process. The red bars above the amplified segments refer to the forward primers and the pink bars below the amplified segments refer to the reverse primers, used for amplifying the above segments. The blue bars represent the unamplified sequences.

#### **4.4.2 Experimental hybridization results of the VZV, pTZ18R and enterovirus long-PCR products**

The amplicons of the clinical enterovirus, pTZ18R and VZV generated from Long-range PCR amplification process using LongAmp Hot Start Taq DNA polymerase kit in section 4.3.3.2, were applied into a hybridization reaction with the experimental HHVs-pTZ18R-enterovirus microarray in order to test their behaviour after fragmenting them; the step which was omitted from the hybridization experiment of the enterovirus QPCR products. The amplicons were purified using Qiaquick PCR purification kit, sonicated using Soniprep 150 MSE sonicator and precipitated using ethanol precipitation. Each one of the above fragmented amplicons were mixed with one-fifth volume of the HPRT-PCR product and then labelled with the dyomics 547 fluorescent dye using ULS system. Each labelled mixture was loaded separately into a single printed grid of the experimental HHVs-pTZ18R-enterovirus microarray slide fixed in the hybridization cassette in order to start their hybridization reaction. Scanning the HHVs-pTZ18R-enterovirus microarray slide at the end of hybridization process revealed hybridization signals generated between the above labelled amplicons and their complementary probes displayed as clear red bright spots. Since all the probes used for fabricating the above microarray were printed in duplicate, two hybridization signals were generated for each probe hybridized to its complementary target amplicon. Therefore, VZV amplicon generated four hybridization signals as it hybridized with only the first two probes (VZV-1 and VZV-2) of the twelve VZV probes described in table 4-2 (figure 4-11-A). However, the pTZ18R amplicon generated 24 hybridization signals as it hybridized with all of the twelve probes described in

table 3-5 (figure 4-11-B). In contrast the enterovirus amplicons generated eight hybridization signals as they hybridized with the last four probes (ENTC3-4) of the six enteroviral probes described in table 3-3 (figure 4-11-C). As each one of the above amplicons was mixed with one-fifth volume of the HPRT-PCR product, their grids showed 36 fluorescent hybridization signals generated from hybridization of the HPRT product with its complementary probe printed on the HHVs-pTZ18R-enterovirus microarray.

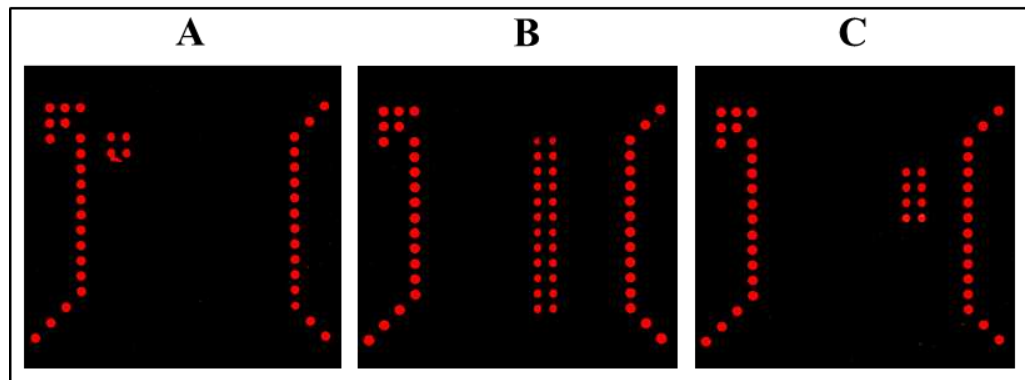


**Figure 4-11: Hybridization reaction results of the labelled VZV, pTZ18R and enterovirus amplicons generated from Long-range PCR amplification process with the experimental HHVs-pTZ18R-enterovirus microarray as seen on the GenePix laser scanner.**

Figures A, B and C represent scanned images of the three grids loaded with the labelled fragmented products generated from Long-range PCR amplification process of each of the VZV, pTZ18R and clinical enterovirus, respectively, showing the fluorescent hybridization signals generated with their complementary printed probes. Each figure also shows fluorescent red signals generated from hybridization of the HPRT products with their complementary printed probes.

### 4.4.3 Hybridization results using virochip

Having optimized all the steps and conditions used for preparing the pTZ18R plasmid, VZV and enteroviral nucleic acids starting from their extraction and reverse transcription steps, passing through their amplification and fragmentation methods, and ending with their labelling reaction down to the hybridization reaction which led to successful hybridization between them and their complementary probe, it was decided to apply the amplicons of the selected RNA viruses generated from the Long-range PCR amplification process in a hybridization process with the virochip containing the viral probes designed in chapter 2, in order to test its performance. Since the viral amplicons generated from the MDA process in chapter 3 had not been used in a hybridization reaction with the virochip, it was decided to use a MD amplicon for only one sample of each of the selected RNA viral groups, in parallel with the viral amplicons generated from Long-range PCR amplification for testing the virochip and studying the performance of the probes on the chip.

Three different RNA extracts for each of the HMPV, HRSV and human influenza virus A, and one enterovirus RNA extracted from clinical samples, in addition to the echovirus 7 and coxsackievirus A-21 transcripts were reverse transcribed into cDNA using Maxima H Minus First Strand cDNA synthesis kit. The generated viral cDNAs were amplified using LongAmp Hot Start Taq DNA polymerase kit following the PCR principles, and then purified using Qiaquick PCR purification kit. At the same time, one cDNA of each of the above viral groups was amplified using REPLI-g UltraFast mini kit following MDA principle. Thus, twelve viral amplicons were generated from Long-range PCR, and four amplicons were generated from MDA process (table 4-3).



**Table 4-3: Shows the amplification methods and fluorescent dyes used for amplifying and labelling the viral samples used for validating the designed viral probes.**

<b>Amplification method</b>	<b>Viral sample</b>	<b>Labelling dye</b>
<b>Long-range PCR</b>	Echovirus 7	Dyomics 547
	Coxsackievirus A-21	Dyomics 495
	Clinical enterovirus	Dyomics 547
	HMPV-1	Dyomics 547
	HMPV-2	Dyomics 547
	HMPV-3	Dyomics 495
	HRSV-1	Dyomics 547
	HRSV-2	Dyomics 495
	HRSV-3	Dyomics 495
	H1N1-1	Dyomics 547
	H1N1-2	Dyomics 495
H3N2	Dyomics 495	
<b>MDA</b>	Clinical enterovirus	Dyomics 547
	HMPV-1	Dyomics 547
	HRSV-1	Dyomics 495
	H1N1-1	Dyomics 495

All of the purified products generated from Long-range PCR, and the amplicons generated by MDA were sonicated using a Soniprep 150 MSE sonicator. Then the sonicated viral amplicons were ethanol precipitated and each was mixed with one-fifth volume of the HPRT-PCR product. Then, the viral amplicon-HPRT mixtures were labelled with dyomics 547 and dyomics 495 fluorescent dye (table 4-3). The labelled amplicons were ethanol precipitated and resuspended in the prehybridization buffer, then each two of the above amplicon mixtures labelled with the two different dyes were loaded together into one of the eight chambers of the Agilent gasket slide surface fixed in the slide chamber base (figure 4-12). This process enabled using three

different PCR products and one MD amplicon for each group of the selected RNA viruses for validating the behaviour of the virochip probes.

<p><b>1</b></p> <p>● Echovirus 7 (PCR product)</p> <p>● HRSV-2 (PCR product)</p>	<p><b>2</b></p> <p>● HMPV-1 (PCR product)</p> <p>● H1N1-2 (PCR product)</p>	<p><b>3</b></p> <p>● HRSV-1 (PCR product)</p> <p>● Cox. A-21 (PCR product)</p>	<p><b>4</b></p> <p>● HMPV-2 (PCR product)</p> <p>● HRSV-3 (PCR product)</p>	Barcode
<p><b>5</b></p> <p>● Clinical enterovirus (PCR product)</p> <p>● HMPV-3 (PCR product)</p>	<p><b>6</b></p> <p>● H1N1-1 (PCR product)</p> <p>● H3N2 (PCR product)</p>	<p><b>7</b></p> <p>● Clinical enterovirus MDA product</p> <p>● HRSV-1 MDA product</p>	<p><b>8</b></p> <p>● HMPV-1 MDA product</p> <p>● H1N1-1 MDA product</p>	

**Figure 4-12: Schematic diagram shows the loading sequence of the labelled amplicons into the chambers of the Agilent gasket slide.**

The amplicons of the enteroviruses, HMPV, HRSV and human influenza virus A generated from Long-range PCR amplification reaction and MDA process were mixed with one-fifth volume of HPRT-PCR product and labelled with the dyes 547 (red colour) and 495 (green colour) fluorescent dyes. Then two amplicons labelled with each of the above two dyes were loaded into one of the Agilent gasket chambers.

The surface of the microarray slide containing viral probes was lowered down on the Agilent gasket containing the labelled viral amplicon samples to start the hybridization process. The hybridization signals were displayed as regular spots during scanning of the microarray slide using the appropriate filter of GenePix 4200AL autoloader scanner for each fluorescent dye used. Hybridization signals, whose fluorescent intensities exceeded the mean of the negative control by more than two times standard deviation, were considered as positive signals, and those positive signals showing high fluorescent intensities were adopted for evaluating the sensitivity and specificity of the designed viral probes.

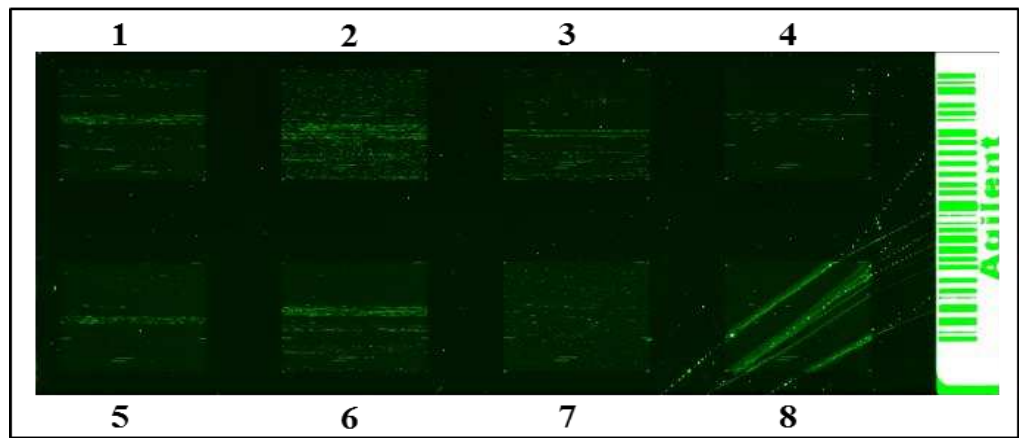


**Figure 4-13:** Scanned image of the virochip after hybridization reactions with the labelled amplicons of the enteroviruses, HMPV, HRSV and human influenza virus A, showing the fluorescent hybridization signals generated with their complementary printed probes.

#### **4.4.4 Description of the virochip**

The designed virochip consists of eight repeated grids; each grid contained several thousands of probes designed specifically for each of the human enterovirus, HMPV, HRSV and human influenza virus A, B and C using OligoArray and Agilent technologies eArray software, in addition to the HHVs probes designed by a previous PhD student (Abdel-Hakeem, 2010) table 4-4.

**Table 4-4: Shows the number of the probes designed for each species or subtype of the selected RNA viruses, using OligoArray and Agilent eArray software**

Family	Genus	Species	Subtype	Probe No.	
				OligoArray	Agilent eArray
Picornaviridae	Enterovirus	Human enterovirus-A	-----	703	142
		Human enterovirus-B		1081	439
		Human enterovirus-C		858	126
		Human enterovirus-D		310	30
		Human rhinovirus A and B		108	170
Paramyxoviridae	Pneumovirus	Human respiratory syncytial virus		649	42
	Metapneumovirus	Human metapneumovirus		473	66
Orthomyxoviridae	Influenzavirus A	Influenza A virus	HA-H1N1	63	302
			HA-H1N2	61	21
			HA-H2N2	66	25
			HA-H3N2	61	165
			HA-H7N7	93	20
			NA-H1N1	52	375
			NA-H1N2	57	11
			NA-H2N2	57	22
			NA-H3N2	57	212
NA-H7N7	62	10			

Family	Genus	Species	Subtype	Probe No.	
				OligoArray	Agilent eArray
Orthomyxoviridae	Influenzavirus A	Influenza A virus	MP-H1N1	28	143
			MP-H1N2	26	7
			MP-H2N2	27	19
			MP-H3N2	26	97
			MP-H7N7	42	15
	Influenzavirus B	Influenza B virus	HA	57	77
			NA	50	123
			MP	31	61
	Influenzavirus C	Influenza C virus	HEF	71	22
MP			44	12	
Herpesviridae	Simplexvirus	Human herpesvirus 1	-----	12	-----
		Human herpesvirus 2		9	-----
	Varicellovirus	Human herpesvirus 3		12	-----
	Lymphocryptovirus	Human herpesvirus 4		11	-----
	Cytomegalovirus	Human herpesvirus 5		12	-----
	Roseolovirus	Human herpesvirus 6		17	-----
		Human herpesvirus 7		7	-----
Total				5293	2754
				8047	

#### **4.4.4.1 Hybridization results of the human enterovirus amplicons**

The amplicons of the echovirus 7 and coxsackievirus A-21 transcripts, and clinical enterovirus generated by long-range PCR amplification reaction and MDA process were sonicated and labelled with dyes 547 and 495 fluorescent dyes (table 4-3). The labelled enterovirus amplicons were loaded into hybridization reactions with the probes designed for the selected RNA virus groups using four different grids of the virochip.

##### **4.4.4.1.1 Sensitivity of the human enterovirus probes designed using OligoArray software**

Echovirus 7 and coxsackievirus A-21 belong to human enterovirus B and C, respectively. Analysing the positive signals generated from the hybridization reactions of the human enterovirus amplicons revealed that 50 probes out of 1081 of the OligoArray probes designed specifically for human enterovirus B, and one probe out of 858 of the OligoArray probes designed specifically for human enterovirus C generated positive specific hybridization signals of high intensities with the amplicons of the echovirus 7 and coxsackievirus A-21, respectively (see table 4-4). On the other hand, several of the OligoArray probes designed specifically for of the human enterovirus A (5' UTR) showed cross hybridization with the echovirus 7 amplicon (figure 4-14).

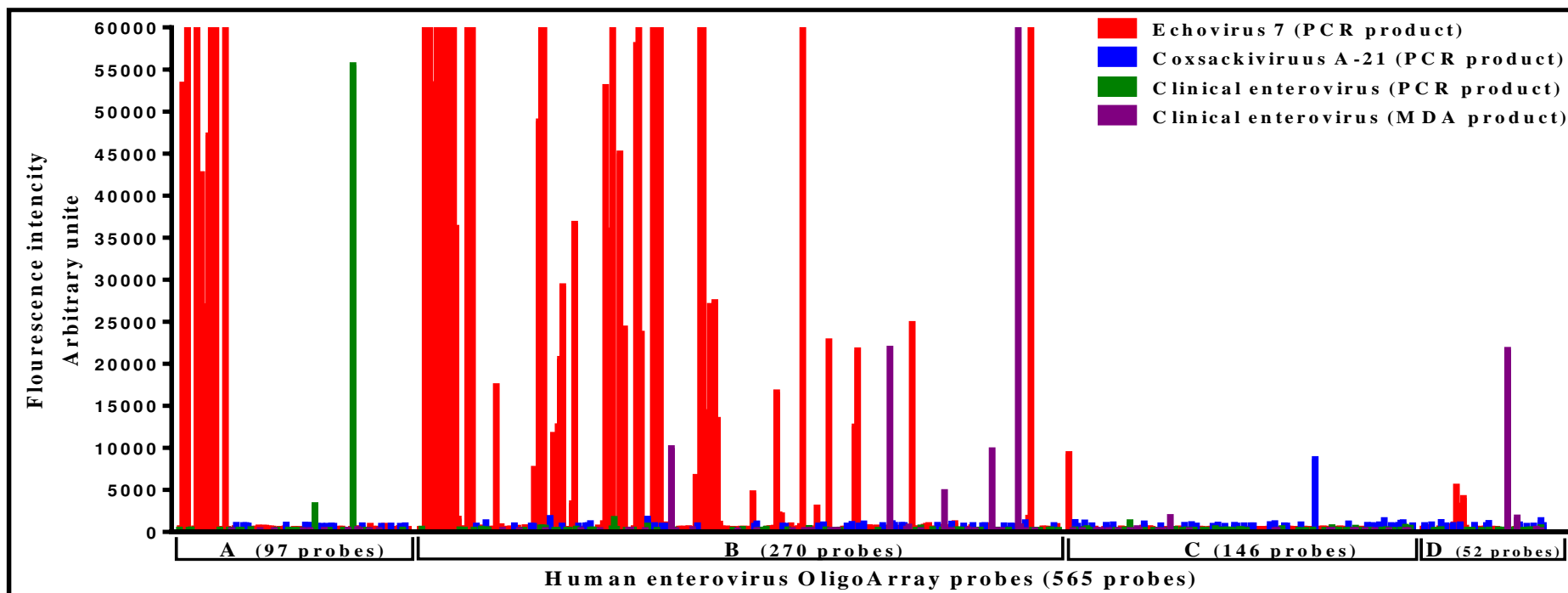


**Figure 4-14: Signals generated from the hybridization reactions of four of the human enterovirus amplicons with the probes designed specifically for the human enteroviruses using OligoArray software.**

RNA extracts of the echovirus 7, coxsackievirus A-21 and clinical enterovirus were reverse transcribed into cDNA and amplified using long-range PCR amplification. The cDNA of the clinical enterovirus was also amplified using MDA. The generated amplicons were sonicated, labelled and loaded into hybridization reactions with the designed probes of the selected RNA viruses and HHVs. The red, blue, green and purple columns represent the positive hybridization signals generated from the human enterovirus OligoArray probes after hybridization to the PCR products of the echovirus 7, coxsackievirus A-21 and clinical enterovirus, and the MD amplicon of the clinical enterovirus, respectively.

For the amplicons of the clinical enterovirus, they showed different behaviour during their hybridization reactions with the human enterovirus OligoArray probes as only one of the human enterovirus A OligoArray probes generated a positive hybridization signal of high fluorescent intensity with the amplicon generated by long-range PCR, while five of the human enterovirus B and one of the human enterovirus D OligoArray probes showed high fluorescent intensities from the hybridization reaction with the MD amplicon of the clinical enterovirus (figure 4-14). The outcome of the hybridization reactions with clinical enterovirus amplicons revealed that this enterovirus can be identified as one of the human enterovirus B strains since the positive hybridization signals generated from the human enterovirus B OligoArray probes were more than the positive signals generated from other human enterovirus OligoArray probes. The possible explanation for the hybridization results of the coxsackievirus A-21 is that the PCR product of this virus was either contaminated with another amplicon of other viruses during the preparation steps (sonication, labelling and ethanol precipitation) or replaced with an amplicon of the other viruses, which will be illustrated later.



#### **4.4.4.1.2 Sensitivity of the human enterovirus probes designed using Agilent eArray software**

Analysing the positive signals generated from the hybridization reactions of the human enterovirus amplicons revealed that 30 probes out of 439 of the Agilent eArray probes designed specifically for the human enterovirus B generated positive specific signals of high fluorescent intensities with the echovirus 7 PCR amplicon (See table 4-4). On the other hand, several other Agilent eArray probes designed specifically for the human enterovirus A, C and D (CDS) showed cross hybridization with the above enterovirus amplicon. The fluorescent intensities of the positive signals generated from the hybridization reactions of the human enterovirus Agilent eArray probes with the amplicons of the coxsackievirus A-21 and clinical enterovirus were very low (figure 4-15).

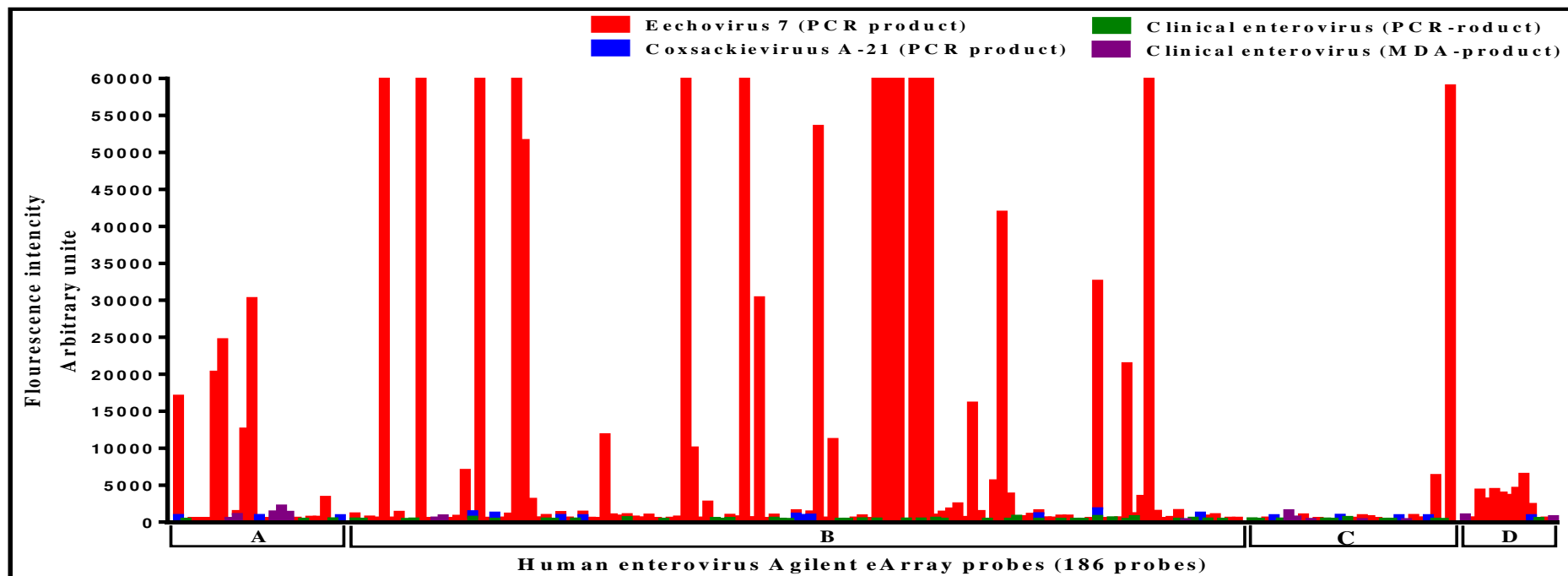


**Figure 4-15: Signals generated from the hybridization reactions of four of the enterovirus amplicons with the probes designed specifically for the human enteroviruses using Agilent eArray software.**

RNA extracts of the echovirus 7, coxsackievirus A-21 and clinical enterovirus were reverse transcribed into cDNA and amplified using long-range PCR. The cDNA of the clinical enterovirus was also amplified by MDA. The generated amplicons were sonicated, labelled and loaded into hybridization reactions with the designed probes of the selected RNA viruses and HHVs. The red, blue, green and purple columns represent the positive hybridization signals generated from the human enterovirus Agilent eArray probes after hybridization to the PCR products of the echovirus 7, coxsackievirus A-21 and clinical enterovirus, and the MD amplicon of the clinical enterovirus, respectively.

Those human enterovirus OligoArray and Agilent eArray probes showing higher fluorescent intensities with the above human enterovirus amplicons are listed in table 4-5. Tracking the position of these probes revealed that they are targeting different genes of the human enterovirus genome as shown in table 4-5. The table shows that the OligoArray probe EB3-0013 and the Agilent eArray probe AGV-0376 had the same sequence and generated a positive hybridization signal of high fluorescent intensity with echovirus 7 amplicon.

**Table 4-5: Characteristics of the human enterovirus OligoArray and Agilent eArray probes which showed higher fluorescent intensities with the amplicons of the echovirus 7, coxsackievirus A-21, clinical enterovirus, and cross hybridization with the amplicons of the HMPV, HRSV and human influenza virus A, during their hybridization reactions.**

Sample	Probe ID	Probe Sequence	Position	Cross hybridization			
				HMPV	HRSV	Flu-A	
Echovirus 7 (PCR product)	OligoArray probes	EA5-0013	AAATTGTTACCATATAGCTATTGGATTGGC	5' UTR	√	√	√
		EA5-0030	TTGTTACCATATAGCTATTGGATTGGCCAT	5' UTR	-	-	-
		EA5-0032	AATTGAGAGATTGTTACCATATAGCTATTG	5' UTR	-	-	-
		EA5-0038	CTATTGGATTGGCCATCCGGTGACAAACAG	5' UTR	-	-	-
		EA5-0039	CTGGCTGCTTATGGTGACAATTGAGAGATT	5' UTR	√	√	√
		EA5-0050	TGTTACCATATAGCTATTGGATTGGCCATC	5' UTR	√	√	√
		EA5-0064	ATATAGCTATTGGATTGGCCATCCGGTGAA	5' UTR	√	-	√
		EA5-0094	ATATAGCTATTGGATTGGCCATCCGGTGAC	5' UTR	√	√	√
		EA3-0002	TGACAAAGTCACCAAAGATTAATTACCCTA	3' UTR	-	√	-
		EB5-0018	AATTGAGAGATTGTTACCATATAGCTATTG	5' UTR	-	-	√
		EB5-0021	TTGTTACCATATAGCTATTGGATTGGCCAT	5' UTR	√	√	√
		EB5-0023	TTGGCTGCTTATGGTGACAATTGAGAGATT	5' UTR	√	√	√
		EBC-0040	CCTGAAAGAGTCACTAGTGGGTCAAGACTC	VP1	-	-	-
		EBC-0134	ATACAGTTCAAGTCCAAATGCCGTATTGAG	VP1	√	√	√
		EBC-0248	CGGTGGCTCAAACAGAAAGTGTCACAATAT	VP1	-	√	√
		EBC-0132	CAATGGATGGCTTAAGAAGTTCCTGAGAT	VP1-2A	-	-	√
		EBC-0133	GCCGTATTGAGCCTGTATGTTTGCTCCTAC	2A	-	√	-
		EBC-0254	GATGACAAACGCCTGCAAGGGTATGGAATG	2A	-	-	-
		EBC-0257	AAGTCCAAATGCCGTATTGAACCTGTATGT	2A	-	-	-
EBC-0258	CATACAGTTCAAGTCCAAATGCCGTATTGA	2A	-	√	√		

Sample	Probe ID	Probe Sequence	Position	Cross hybridization			
				HMPV	HRSV	Flu-A	
Echovirus 7 (PCR product)	OligoArray probes	EBC-0529	TTCAAGTCCAAATGCCGTATTGAACCTGTA	2A	-	-	-
		EBC-0655	AGCAACTACATACAGTTCAAGTCCAAATGC	2A	-	-	-
		EBC-0656	AAGTCCAAATGCCGTATTGAACCTGTATGT	2A	-	-	-
		EBC-0942	TTCAAGTCCAAATGCCGTATTGAACCTGTA	2A	√	-	√
		EBC-0154	AAGTCACAGATTACGGCTTCCTAAACCTGG	2C	-	-	-
		EBC-0160	GACCAACCATCCTGATGAATGACCAGGAAG	2C	-	-	-
		EBC-0161	GAAGTTCAGAGACATCAGAGGCTTCTTAGC	2C	-	-	-
		EBC-0375	GAAGTTCAGAGACATCAGAGGCTTCTTGGC	2C	-	-	√
		EBC-0376	AAACCGGAATGAGAAGTTCAGAGACATCAG	2C	-	√	√
		EBC-0764	GGAGTGTTGCCCGGTCAATTTCAAGAAATG	2C	-	-	-
		EBC-0169	TCAAAGGAAGCAGGGTTCCCAATCATCAAC	3A	-	-	-
		EBC-0280	CAGGACAATTGGCCACCCTAGATATCAGCA	3C	-	-	√
		EBC-0283	CACCCTAGATATCAGCACTGAACCAATGAA	3C	-	-	-
		EBC-0291	GTTGACCATTATGCAGGACAATTGGCCACC	3C	-	-	√
		EBC-0377	GATGGTCATCTCATAGCCTTTGATTACTCT	3C	-	-	-
		EBC-0386	AGTGATGTTGGATGGTCATCTCATAGCCTT	3C	-	-	-
		EBC-0387	TCATAGCCTTTGATTACTCTGGGTATGATG	3C	-	-	-
		EBC-0480	TATGGCTTGAACCTGCCAATGGTGACTTAT	3C	-	-	-
		EBC-0199	CTTAGTGCACCCTGTTATGCCCATGAAAGA	3D	-	-	-
		EBC-0300	CACGAGTATGAGGAGTTCATCCGTAAGATC	3D	-	√	√
		EBC-0302	AAGGGAATTGACTTGGACCAGTTCAGGATG	3D	-	-	-
		EBC-0308	ACTTGGACCAGTTCAGGATGATTGCATATG	3D	-	-	√
		EBC-0310	CATATGGTGACGATGTGATTGCGTCATACC	3D	-	-	√
EBC-0312	AGGATGATTGCATATGGTGACGATGTGATT	3D	-	-	√		

Sample	Probe ID	Probe Sequence	Position	Cross hybridization			
				HMPV	HRSV	Flu-A	
Echovirus 7 (PCR product)	OligoArray probes	EBC-0379	GGATACACGCACAAGGAGACAAATTACATT	3D	-	-	-
		EBC-0597	GACCAATTCAGGATGATTGCATATGGTGAT	3D	-	-	-
		EB3-0004	GCACTAACCGAACTAGATAACGGTGCAGTA	3' UTR	√	√	√
		EB3-0005	TTGAAATTGGCTTAACCCTACTGCACTAAC	3' UTR	√	√	√
		EB3-0006	TAACCCTACTGCACTAACCGAACTAGATAA	3' UTR	√	√	√
		EB3-0009	AACCCTACTGCGCTAACCGAACTAGATAAC	3' UTR	-	-	-
		EB3-0010	TAAATTGGCTTAACCCTACTGCGCTAACCG	3' UTR	√	-	√
		EB3-0012	TTGATATAATTTGAATTGGCTTAACCCTAC	3' UTR	√	-	√
		EB3-0013	TTGAATTGGCTTAACCCTACTGCACTAAC	3' UTR	√	√	√
		EB3-0014	CCCTACTGCACTAACCGAACTAGATAACGG	3' UTR	√	√	√
		EB3-0016	TTGAAATAATTTGAATTGGCTTAACCCTAC	3' UTR	√	-	√
		EB3-0017	CCCTACTGTACTAACCGAACTAGATAACGG	3' UTR	-	-	-
		EB3-0018	ATTGGCTTAACCCTACTGTACTAACCGAAC	3' UTR	√	-	√
		EB3-0019	ATTTGAATTGGCTTAACCCTACTGCATTAA	3' UTR	√	-	√
	EB3-0020	CAATTTGAAATAATTTGAATTGGCTTAACC	3' UTR	-	-	-	
	Agilent eArray probes	AGV-0205	TGATTGCATATGGTGACGATGTGATTGCGT	3D	-	-	√
		AGV-0220	CCTTTCTAAAGAGGTATTTTAGAGCAGATG	3D	-	-	√
		AGV-0256	CTCTCATGCTAAAAGTGTATAAGGGAATTG	3D	-	-	√
		AGV-0343	AATATGAGGAGTTCATCCGCAAGATCAGGA	3D	√	√	√
		AGV-0448	TGTATAAGGGAATTGACCTGGACCAGTTCA	3D	-	-	-
AGV-0449		TGCATATGGTGACGATGTGATTGCGTCATA	3D	-	-	-	
AGV-0451		TGGACCAATGTCACATTTCTAAAGAGGTAT	3D	-	-	-	
AGV-0452		TTTAGAGCAGATGAGCAATATCCCTTCCTG	3D	-	-	√	
AGV-0454	GGAAGTGGTTGGACTCTTTTAAATTAGAG	3D	√	-	-		

Sample	Probe ID	Probe Sequence	Position	Cross hybridization			
				HMPV	HRSV	Flu-A	
Echovirus 7 (PCR product)	Agilent eArray probes	AGV-0455	AACTAGATAACGGCGCAGTAGGGGTAAATT	3' UTR	-	-	√
		AGV-0462	ATTGGCTTAACCTTACTGCACTAACCGAAC	3' UTR	-	-	√
		AGV-0529	TTGGCTTAACCCTACTGTACTAACCGAACT	3D	-	-	√
		AGV-0607	AATTGGCTTAACCCTACTGCACTAACCGAA	3D	-	√	-
		AGV-2711	TAGTAACCCTACCTCAGTCGAATTGGATTG	3D-3'UTR	-	-	√
		AGV-0243	TTTGAATTGGCTTAACCCTACTGCGCTAAC	3D-3'UTR	-	-	√
		AGV-0261	AATTGGCTTAACCCTACTGCACTTACCGAA	3D-3'UTR	-	-	√
		AGV-0376	TTGAATTGGCTTAACCCTACTGCACTAACCC	3D-3'UTR	-	√	-
		AGV-0424	TGAATTGGCTTAACCCTACTGTACTAACCG	3D	-	-	√
Coxsackievirus A-21(PCR product)	OligoArray probes	ECC-0507	ACTCACTTACCGACTCAAATTCATGAGACC	3D	-	√	-
Clinical enterovirus (PCR product)		EAC-0483	ACAAAATAGCAAGATGCAAGTGCAAAACTGG	VP1	√	√	-
Clinical enterovirus (MDA)		EBC-0722	CAGGTAGCAGTGAGAGCCAACAATTCAAGC	VP2	√	√	√
		EBC-0327	ATGACCTAATCACAGTAACTGCCACACTAG	VP1	√	-	-
		EBC-0874	ATACATCATTTACAAGTTGTTTGCAGGCTT	2C	√	-	-
		EBC-0802	TAACACACACGTGGATGAGTACATGCAAGA	3B	√	√	√
		EBC-0914	CCAAGATCATGTGCGATCCTTGTGCCTATT	3D	√	-	√
		EDC-0152	TACCAGACTAATGTACTTCTAGCAGCTGGC	VP1	-	√	-

Abbreviations; EA: human enterovirus A probes, EB: human enterovirus B probes, EC: human enterovirus C probes, ED: human enterovirus D probes,

AGV: Agilent eArray probes, √: hybridization signal, -: no hybridization.

#### 4.4.4.1.3 Specificity of the human enterovirus probes

Many of the human enterovirus OligoArray and Agilent eArray probes shown in table 4-5 showed cross hybridization with the amplicons of the HMPV, HRSV, H1N1 and H3N2 revealed as nonspecific signals of various fluorescent intensities (figures 4-16 to 4-18).

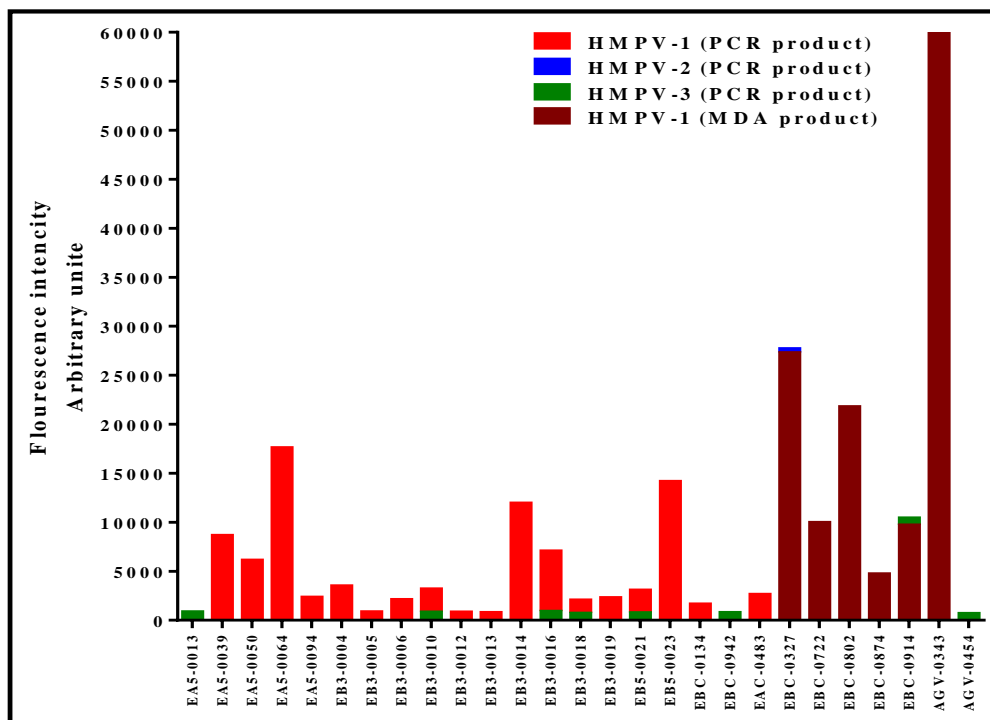


Figure 4-16: Signals of cross hybridization generated between the human enterovirus probes and the HMPV amplicons.



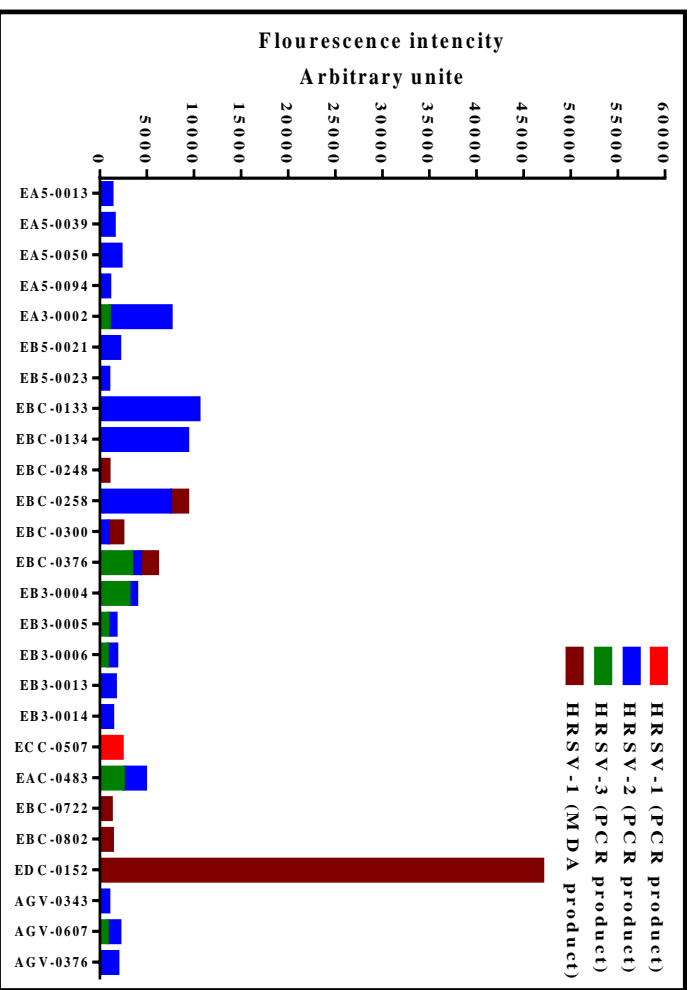


Figure 4-17: Signals of cross hybridization generated between the human enterovirus probes and the HRSV amplicons.

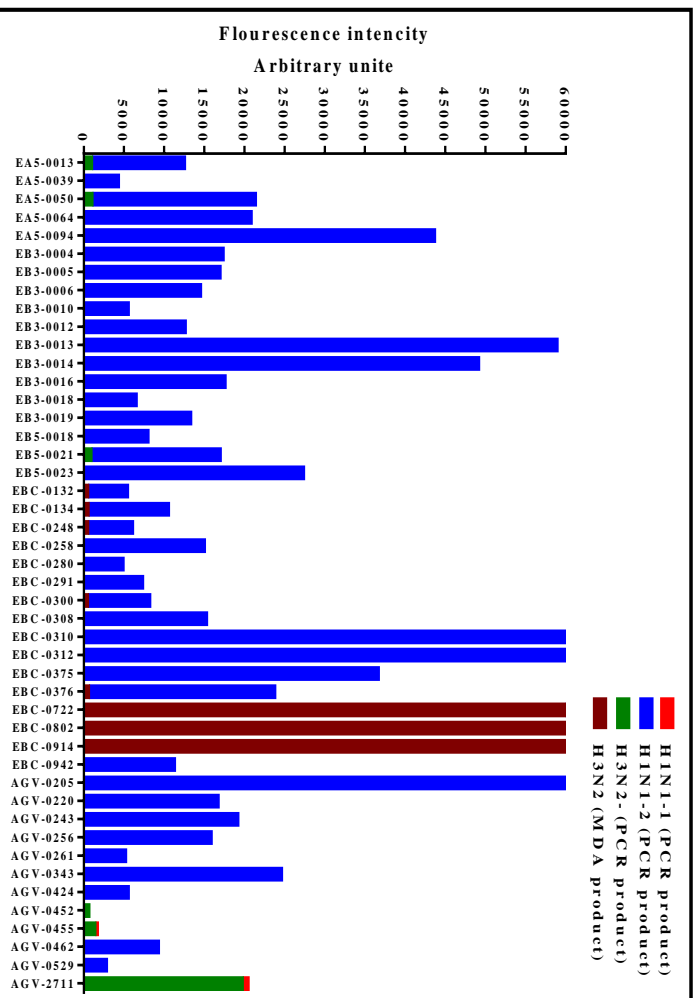


Figure 4-18: Signals of cross hybridization generated between the human enterovirus probes and the amplicons of the H1N1 and H3N2.

#### **4.4.4.2 Hybridization results of the HMPV amplicons**

RNA extracts of three HMPV clinical samples (HMPV-1, 2 and 3) were reverse transcribed into cDNA and then amplified using long-range PCR. The cDNA of HMPV-1 was also amplified by MDA. The amplicons were fragmented by sonication. The fragmented PCR amplicons of the HMPV-1 and 2 in addition to the MDA of the HMPV-1 were labelled with dyomics 547 fluorescent dye, while the fragmented PCR amplicon of the HMPV-3 was labelled with dyomics 495 fluorescent dye (see table 4-3). The labelled HMPV amplicons were loaded into hybridization reactions with the probes designed for the selected RNA virus groups using four different grids of the virochip. None of the HMPV probes designed using Agilent eArray software generated positive hybridization signals during the hybridization reactions of the HMPV amplicons. This might be due to the use of whole viral genome sequences of the HMPV rather than using their consensus sequence during the probe design stage.

##### **4.4.4.2.1 Sensitivity of the HMPV probes designed using OligoArray software**

Hybridization reactions of the HMPV amplicons showed that 347 probes out of 473 of the OligoArray probes designed specifically for the HMPV generated positive specific hybridization signals (see table 4-4). Analysing these positive hybridization signals revealed that more than 120 of these positive HMPV OligoArray probes showed high fluorescent intensities with the HMPV-2 amplicon generated by long-range PCR (figure 4-19). For the HMPV-1, all the positive signals generated from the HMPV OligoArray probes showed low

fluorescent intensities when the hybridization reaction was carried out with the HMPV-1 amplicon generated by long-range PCR. This might be due to the extensive processing of the samples which might affect the resultant hybridization signals. In contrast, the hybridization reactions of the HMPV-1 and HMPV-3 amplicons generated by MDA and long-range PCR, respectively, revealed positive signals of various fluorescent intensities generated from several of the HMPV OligoArray probes which most of them showed positive hybridization signals with the amplicon of the HMPV-2 (figure 4-19).

Those HMPV OligoArray probes showing higher fluorescent intensities with the HMPV amplicons are listed in table 4-6. Tracking the position of these probes revealed that they are targeting different genes of the HMPV genome as shown in table 4-6.

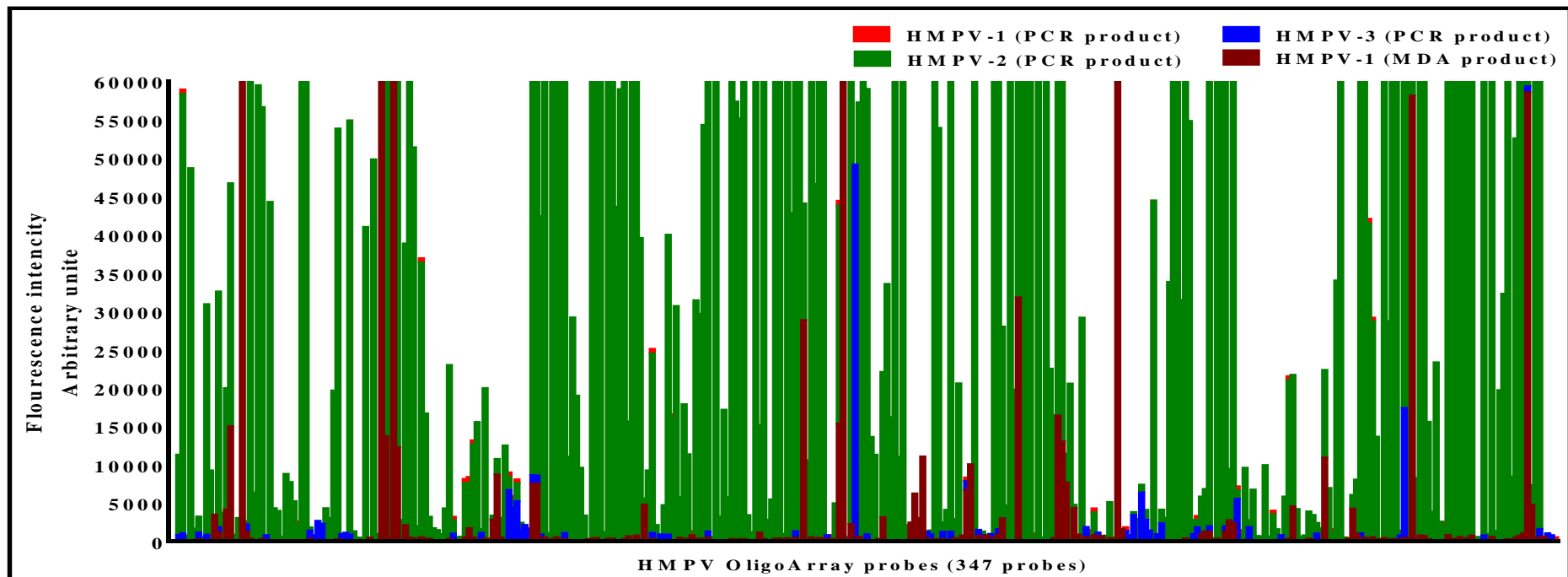


**Figure 4-19: Signals generated from the hybridization reactions of four of the HMPV amplicons with the probes designed specifically for the HMPV using OligoArray software.**

RNA extracts of three HMPV clinical samples (HMPV1-3) were reverse transcribed into cDNA and amplified using long-range PCR. The cDNA of the HMPV-1 was also amplified using MDA. The generated amplicons were sonicated, labelled and loaded into hybridization reactions with the designed probes of the selected RNA viruses and HHVs. The red, green, blue and brown columns represent the positive hybridization signals generated from the HMPV OligoArray probes after hybridization to the PCR products of the HMPV-1, 2 and 3, and the MD amplicon of the HMPV-1, respectively.

**Table 4-6: Characteristics of the HMPV OligoArray probes which showed higher fluorescent intensities with the HMPV amplicons, and cross hybridization with the amplicons of the human enteroviruses, HRSV and human influenza virus A, during their hybridization reactions.**

Probe ID	Probe sequence	Position	Cross hybridization		
			H. enteroviruses	HRSV	Flu-A
HMPV-0003	GAGAGAGTACAGCAGATTCTAAGAACTCA	N	√	√	-
HMPV-0006	ATTCTAAGAACTCAGGCAGTGAAGTTCAA	N	-	-	-
HMPV-0011	TACAAATATGCTGCAGAAATAGGAATACAA	N	-	-	-
HMPV-0014	GACACCCTCATCATTGCAACAAGAAATAAC	N	-	-	-
HMPV-0017	TCTCTTCAAGGGATTACCTGAGTGATCTA	N	-	-	-
HMPV-0022	GAGGCTGCAGAACACTTCTTAAATGTGAGT	N	-	-	√
HMPV-0024	TATCGAGGGAGAGTGCCAAACACAGAACTA	N	-	√	-
HMPV-0026	CAACTTTGCTAGTGTGTTCTCGGCAATGC	N	-	√	-
HMPV-0027	GCTGGACTGTTATCATTAGCCAATTGTCCC	N	-	√	-
HMPV-0225	GTTTGTTTCATTGAGTATGGCAAAGCATTAG	N	√	√	√
HMPV-0226	TAGGATGGACATACCAAAGATTGCTAGATC	N	√	√	-
HMPV-0227	AATCTTATTATGTGTAGGTGCCTTAATATT	N	√	√	-
HMPV-0228	CAGTCAGAAGAGCTAACCGTGTGCTAAGTG	N	√	√	-
HMPV-0229	TTAGAGACCACAGTCAGAAGAGCTAACCGT	N	-	√	-
HMPV-0237	TGTTAATATATTCATGCAAGCTTATGGAGC	N	-	-	-
HMPV-0239	CTTCTACAGGCAGCAAAGCAGAAAGTTTAT	N	-	√	-
HMPV-0241	TATTACAGAAGTTTGTTTCATTGAGTATGGC	N	√	√	-
HMPV-0029	GGCTATTAAGAACACTCAACATTGCAACAG	P	-	-	-
HMPV-0039	TCATCATTAAGCATTGAGGCCAGACTAGAA	P	-	√	-
HMPV-0040	GAAGATGCAGAATCCTCAATCTTAACCTTT	P	-	√	-

Probe ID	Probe sequence	Position	Cross hybridization		
			H. enteroviruses	HRSV	Flu-A
HMPV-0253	GAAGATGACATTTACCAGTTAATTATGTAG	P	-	√	-
HMPV-0256	AATGATGGAAGAGGAAATGAATCAACGGTC	P	√	√	√
HMPV-0053	AGAACTAGGAGCATATGTCCAGGCTGAAAG	M	√	√	-
HMPV-0057	TATGCAAGACTTGGAGCCATCAAGGAACAA	M	-	-	-
HMPV-0252	GTTACCTGCAAGCCTAACAAATATGGTTTCC	M	√	√	-
HMPV-0263	ACACAGCAGCTGTTCAAGTTGATCTAGTAG	M	-	√	√
HMPV-0272	TAAGCAGTGAAGCAGACCAAGCTCTAACAC	M	√	√	-
HMPV-0273	ATCAAAGAGAGTGAATCAGCCACTGTTGAA	M	√	√	√
HMPV-0276	ACAATACCAGCATTTATCAAATCAGTTTCA	M	-	√	-
HMPV-0278	GAATCAGCCACTGTTGAAGCTGCAATAAGC	M	√	√	√
HMPV-0050	GCTAATAACACCTCAACACGGTCTTAAAGA	F	-	√	-
HMPV-0060	ATCATGTAGCACTATAACTGAGGGATATCT	F	-	-	-
HMPV-0062	GTGTTATAGATACGCCTTGCTGGATAGTAA	F	√	√	√
HMPV-0063	GTGCAGCTGCCAATCTTTGGTGTATAGAT	F	√	√	-
HMPV-0064	TAATTTACATGGTGCAGCTGCCAATCTTTG	F	-	√	-
HMPV-0067	AATTACCCATGCAAAGTCAGCACAGGAAGA	F	√	√	√
HMPV-0068	ATCTACTACAAATTACCCATGCAAAGTCAG	F	√	√	√
HMPV-0070	AAGGAGTGCAACATCAACATATCTACTACA	F	-	-	-
HMPV-0071	ATCAATGTTGCTGAGCAATCAAAGGAGTGC	F	√	√	√
HMPV-0072	CTATGCTTGCCTCCTAAGAGAAGACCAAGG	F	-	√	-
HMPV-0279	AGTGAAGTTACAGCAATTAAGAATGCCCTC	F	√	√	-
HMPV-0280	ACGGCTTGAGAGTGAAGTTACAGCAATTA	F	√	√	-
HMPV-0281	ACTTAATGACAGATGCTGAACTAGCCAGAG	F	√	√	-
HMPV-0283	TTGTTCTAGGAGCAATAGCACTCGGTGTTG	F	√	√	-

Probe ID	Probe sequence	Position	Cross hybridization		
			H. enteroviruses	HRSV	Flu-A
HMPV-0285	ATGCTGAACTAGCCAGAGCTGTTTCAAACA	F	-	√	-
HMPV-0288	AACAGAAGGTTTCTAAATGTTGTGCGGCAA	F	√	√	√
HMPV-0289	CAGTCAATTCAACAGAAGGTTTCTAAATGT	F	-	-	-
HMPV-0318	TATCAGCTAAGCAAAGTTGAGGGTGAACAG	F	√	√	√
HMPV-0076	ATTGATGATAACCAAAGCATAACAAAGGCT	M2	-	-	-
HMPV-0337	AGTGGAGAACATTCGAGCAATAGACATGCT	G	-	-	-
HMPV-0114	GTAAACATGCAACATGAAATAATGAAGAAT	L	√	√	√
HMPV-0115	AGTAGAACCAGTAAACATGCAACATGAAAT	L	-	√	√
HMPV-0116	ATTACAAGGTAGTAGAACCAGTAAACATGC	L	-	-	-
HMPV-0117	AAATAACAATGGATCCTCTTAATGAATCCA	L	√	√	-
HMPV-0119	TCCAAGAGACAAATAACAATGGATCCTCTT	L	-	√	-
HMPV-0120	GAGAATCCTGTTATTGAGCATGTTAGACTC	L	√	√	√
HMPV-0121	TCCTCTTAATGAATCCACTGTTAATGTCTA	L	-	√	-
HMPV-0123	AAATAATGAAGAATGTACACAGTTGTGAGC	L	-	√	-
HMPV-0131	GAGAATGCTGCAGAATTATACTATATATTC	L	√	√	√
HMPV-0132	TGAAGTTGTA CTTAAATTATTAGGAGATAC	L	√	√	-
HMPV-0133	TGATTATCCAATGTATGAAGTTGTA CTTAA	L	√	√	-
HMPV-0135	CTCAATTCAGTACTAGATTTAGAAATACTT	L	√	√	-
HMPV-0136	TCTTAGGATTACTGAACATGCTCAATTCAG	L	-	√	-
HMPV-0137	TGAGTGAAATTCTTAGGATTACTGAACATG	L	-	-	-
HMPV-0138	GGTTTTATTATGAGTGAAATTCTTAGGATT	L	-	√	-
HMPV-0139	GTTGGAGAGCTTGACAGA ACTAAGAGGAGC	L	-	√	-
HMPV-0141	ACTGAACATGCTCAATTCAGTACTAGATTT	L	-	√	√
HMPV-0142	AGAGTTCGAAGGTTTTATTATGAGTGAAAT	L	√	√	√

Probe ID	Probe sequence	Position	Cross hybridization		
			H. enteroviruses	HRSV	Flu-A
HMPV-0143	CACCCAATGGTAGATGAGAGAGATGCAATG	L	-	-	-
HMPV-0154	AACTTATACATGCATGAATCAAAGCAACAT	L	-	-	-
HMPV-0157	CTGGCTGTATAACTTATACATGCATGAATC	L	-	-	-
HMPV-0167	AATGACATCTTTATTAACGGTGACAACCA	L	-	-	-
HMPV-0169	AGAACCTAGGATTATTATCTAGAATATTGT	L	-	√	-
HMPV-0170	TGACAGAACTACAAGAGGTCAAAGAGGTCC	L	√	√	-
HMPV-0173	GGAGTAACATCTCCTAGCATCACTACATGT	L	-	√	√
HMPV-0178	GTCAGTAGTTGTTGATAGTATAGAAATTCC	L	√	√	-
HMPV-0179	CTAGAATATTGTCAGTAGTTGTTGATAGTA	L	-	√	-
HMPV-0180	ATGATGTTGGAGAACCTAGGATTATTATCT	L	-	√	√
HMPV-0181	GGAAATAGTTGGAGTAACATCTCCTAGCAT	L	-	√	-
HMPV-0184	CTAGTTCTCATTTGAAAGGGATAATTATTG	L	-	√	-
HMPV-0186	AGCTGTATCTATGATGTTGGAGAACCTAGG	L	-	√	-
HMPV-0189	ATCTGCTATTAATGGTGAAGATATTGACAG	L	-	√	√
HMPV-0190	TACAGAGAACATCTGCTATTAATGGTGAAG	L	-	√	-
HMPV-0192	AATCTTATTGAGTCTTTATCAGCAGCATT	L	-	√	-
HMPV-0193	CCATGGAAATAATCTTATTGAGTCTTTATC	L	-	-	-
HMPV-0194	GATGAAGATATAATAGATGAATCAATAGAC	L	-	√	-
HMPV-0195	TCTTTATCAGCAGCATTAGCATGTCATTGG	L	-	√	-
HMPV-0199	GGTGTGGGATATTAACAGAACAATGCATAG	L	-	√	-
HMPV-0200	GCATGTCATTGGTGTGGGATATTAACAGAA	L	-	-	-
HMPV-0201	ACTTCTGATCAACATATCTTCAGTCCTGAC	L	-	√	-
HMPV-0202	AGATAAGATAACTTCTGATCAACATATCTT	L	√	√	-
HMPV-0220	GTTCTGTACTTTATTGGAGAAGGAGCAGGA	L	√	√	√



Probe ID	Probe sequence	Position	Cross hybridization		
			H. enteroviruses	HRSV	Flu-A
HMPV-0342	TCATCATATGGATGTATAGTCAAGAGCAAC	L	-	-	-
HMPV-0343	TAGAATTTATACCTAGTTGGGTAAGCAATT	L	-	√	-
HMPV-0344	AAATTAAATATGATATGTGATTGGCTGCAG	L	-	√	√
HMPV-0346	GTGAGCTTCTTCACATACAACCAACTGTTA	L	-	-	-
HMPV-0348	GTAATCTGCAAGGTATGTAACTAATAAAT	L	√	√	√
HMPV-0349	GGGTTTAGAAGTAATCTGCAAGGTATGTTA	L	-	√	-
HMPV-0354	AACCAACTGTTAACATGGAAAGATGTGATG	L	√	√	√
HMPV-0356	GGAAGTAATAAGAAGTGGTTCAATCTTATG	L	√	√	√
HMPV-0357	GGTAAGCAATTGGTTTAGTAATTGGTACAA	L	-	√	-
HMPV-0358	GAGCTTGCTGCAATACAATTTGAACAAGAG	L	√	√	-
HMPV-0361	CCAATCTTGAGATGGTATTAATGATAAAG	L	√	√	√
HMPV-0398	GTAGTAGATCTATGGATGAACATACCAATG	L	-	-	-
HMPV-0400	GGAGGAGATCCAGTAGTCTTCTATAGATCT	L	√	√	-
HMPV-0405	ATGAGAGATCCTCAGGCTGTTGGATCAGAA	L	√	√	√
HMPV-0406	GACAACACTAATGAGAGATCCTCAGGCTGT	L	-	√	-
HMPV-0407	GTGCTACACTGACAACACTAATGAGAGATC	L	-	-	-
HMPV-0412	CACCAGTGTTTCAAGGGAAATTC AATTATA	L	√	√	-
HMPV-0414	TAGCATAATGAGTGTAGTAGAACAATTAAC	L	-	√	-
HMPV-0415	CAATTAATCAAGCACTAAGTGAGAGATTTG	L	√	√	√
HMPV-0419	TGTAGTAGAACAATTA ACTGGTAGAAGCCC	L	√	√	√
HMPV-0420	GCTGTGGAATTAGCATAATGAGTGTAGTAG	L	√	√	-
HMPV-0421	TAAGTGAGAGATTTGGGAATGAAGATATTA	L	√	√	√
HMPV-0423	GACCTATGGAATTC CAGCATCAGTCCAG	L	√	√	-
HMPV-0424	TGTCAGTAGTAGACCTATGGAATTC CAGC	L	√	√	√

Probe ID	Probe sequence	Position	Cross hybridization		
			H. enteroviruses	HRSV	Flu-A
HMPV-0432	AGTTCCAGCTTATAGAACAACAAATTACCA	L	√	√	√
HMPV-0433	TCCCAGCATCAGTTCCAGCTTATAGAACAA	L	√	√	-
HMPV-0434	GATATAACTTTGTCTTTAGTTCTACTGGAT	L	√	√	-
HMPV-0435	GCATGTTAATAGATATAACTTTGTCTTTAG	L	√	√	-
HMPV-0436	AGCTAACAAGAAATTACATGATACTATTGC	L	√	√	-
HMPV-0437	TTATGCTAAAGGGAAGCTAACAAGAAATTA	L	√	√	-
HMPV-0438	CAAGTTCAAATTATGCTAAAGGGAAGCTAA	L	√	√	-
HMPV-0443	GCTGAAGGTGATTTGGTTGAGATCAAATCA	L	√	√	-
HMPV-0445	GATTGTCAATGCTGAAGGTGATTTGGTTGA	L	√	√	√
HMPV-0449	TCTCACACGATTAATTAGAAAGAAGTTGAT	L	-	-	-
HMPV-0450	ATTGCCATGGCAGCATGTTAATAGATATAA	L	√	√	-
HMPV-0452	AAGTTGATGTGTGATAATGCACTTTTAACT	L	-	√	-
HMPV-0453	AATTAGAAAGAAGTTGATGTGTGATAATGC	L	√	√	-
HMPV-0454	TGGCACATGCTCTCACACGATTAATTAGAA	L	√	√	-
HMPV-0455	AAGTACCTTGGATTGTCAATGCTGAAGGTG	L	√	√	√
HMPV-0457	TAGGGTTTAAGAAGCTGGTTTATAGAGCAGT	L	√	√	-
HMPV-0458	GTAGGTTATATAGGGTTTAAGAAGCTGGTTT	L	√	√	-

Abbreviations; √: hybridization signal, -: no hybridization.

#### 4.4.4.2.2 Specificity of the HMPV probes

Many of the HMPV OligoArray probes shown in table 4-6 showed cross hybridization with the amplicons of the human enterovirus, HRSV, H1N1 and H3N2 revealed as nonspecific signals of various fluorescent intensities (figures 4-20 to 4-22).

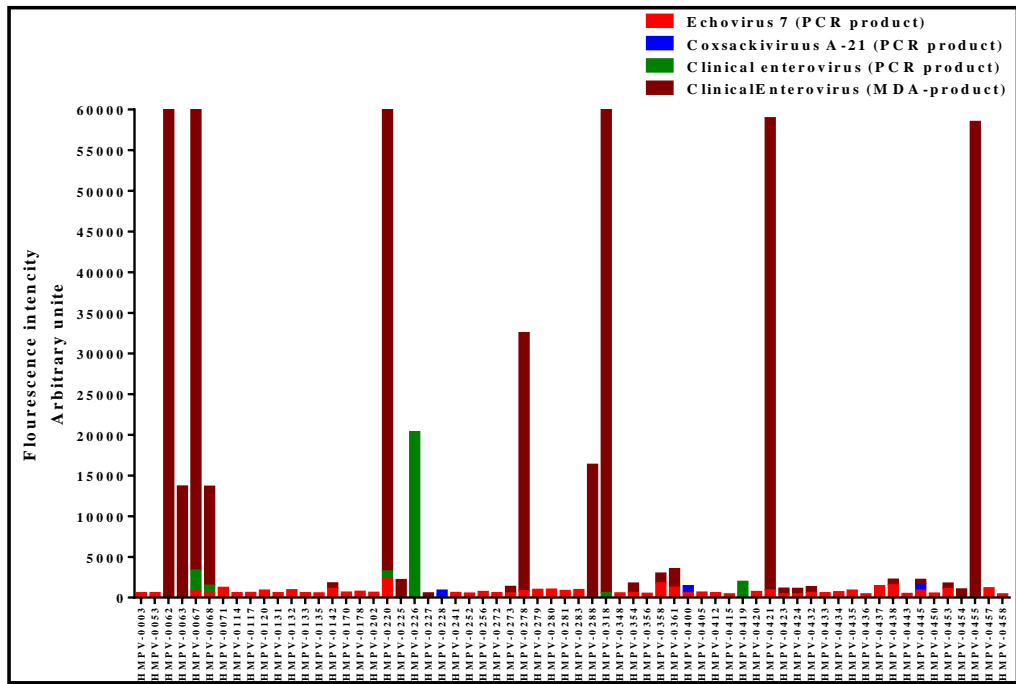


Figure 4-20: Signals of cross hybridization generated between the HMPV probes and the human enterovirus amplicons.

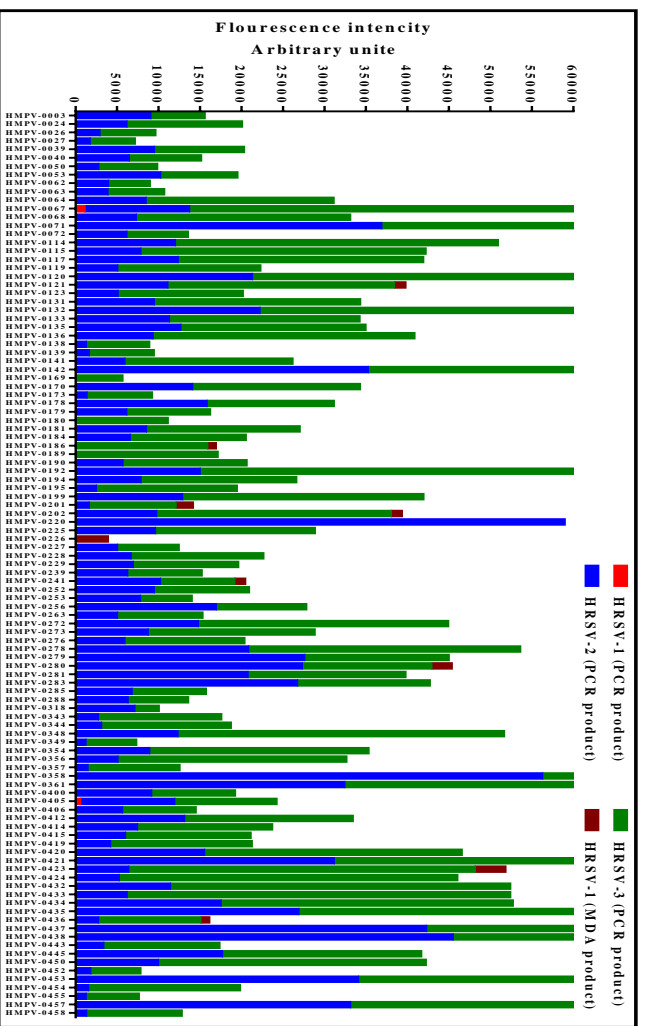


Figure 4-21: Signals of cross hybridization generated between the HMPV probes and the HRSV amplicons.

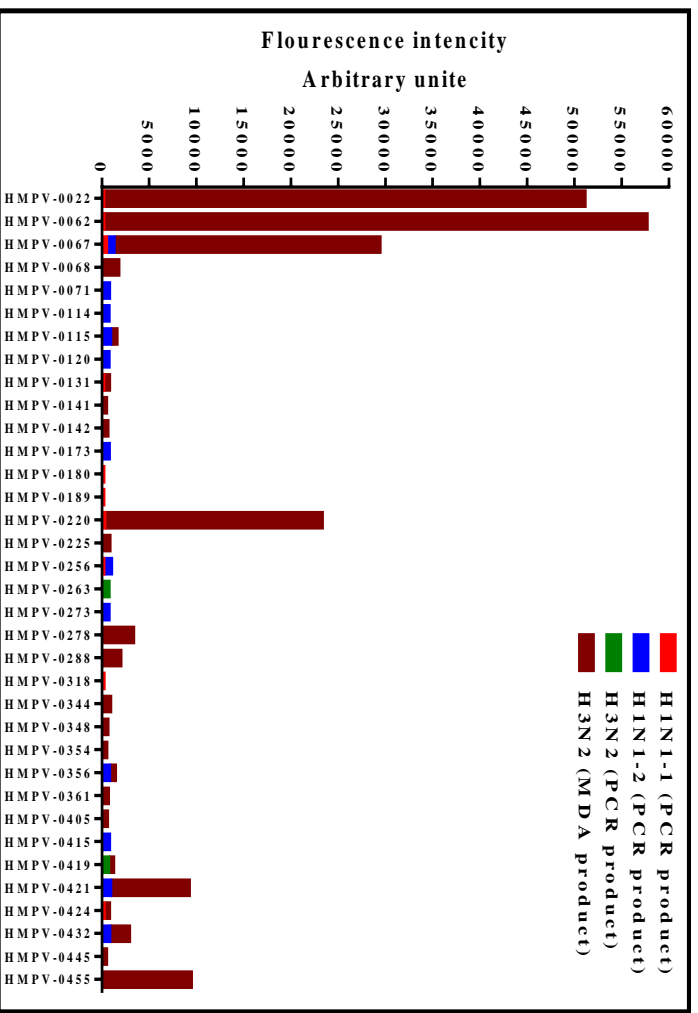


Figure 4-22: Signals of cross hybridization generated between the HMPV probes and the amplicons of the HIN1 and H3N2.

#### **4.4.4.3 Hybridization results of the HRSV amplicons**

RNA extracts of three HRSV clinical samples (HRSV-1, 2 and 3) were reverse transcribed into cDNA and then amplified using long-range PCR. The cDNA of the HRSV-1 was also amplified by MDA. The generated HRSV amplicons were fragmented by sonication. The fragmented PCR amplicon of the HRSV-1 was labelled with dyomics 547 fluorescent dye, while the fragmented PCR amplicons of the HRSV-2 and HRSV-3 in addition to the fragmented MD amplicon of the HRSV-1 were labelled with dyomics 495 fluorescent dye (see table 4-3). The labelled HRSV amplicons were loaded into hybridization reactions with the probes designed for the selected RNA virus groups using four different grids of the virochip.

##### **4.4.4.3.1 Sensitivity of the HRSV probes designed using OligoArray software**

Hybridization reactions of the HRSV amplicons showed that 498 probes out of 649 of the OligoArray probes designed specifically for the HRSV generated positive specific hybridization signals (see table 4-4). Analysing these positive hybridization signals revealed that more than 200 of these positive HRSV OligoArray probes showed high fluorescent intensities with the HRSV-1 amplicon generated by long-range PCR (figure 4-23). For the HRSV-2, all the positive signals generated from the HRSV OligoArray probes showed low fluorescent intensities when the hybridization reaction was carried out with the HRSV-2 amplicon generated by long-range PCR. In contrast, the hybridization reactions of the HRSV-1 and HRSV-3 amplicons generated by MDA and long-range PCR, respectively, revealed positive signals of various fluorescent

intensities generated from several of the HRSV OligoArray probes which most of them showed positive hybridization signals with the amplicon of the HRSV-1 (figure 4-23).

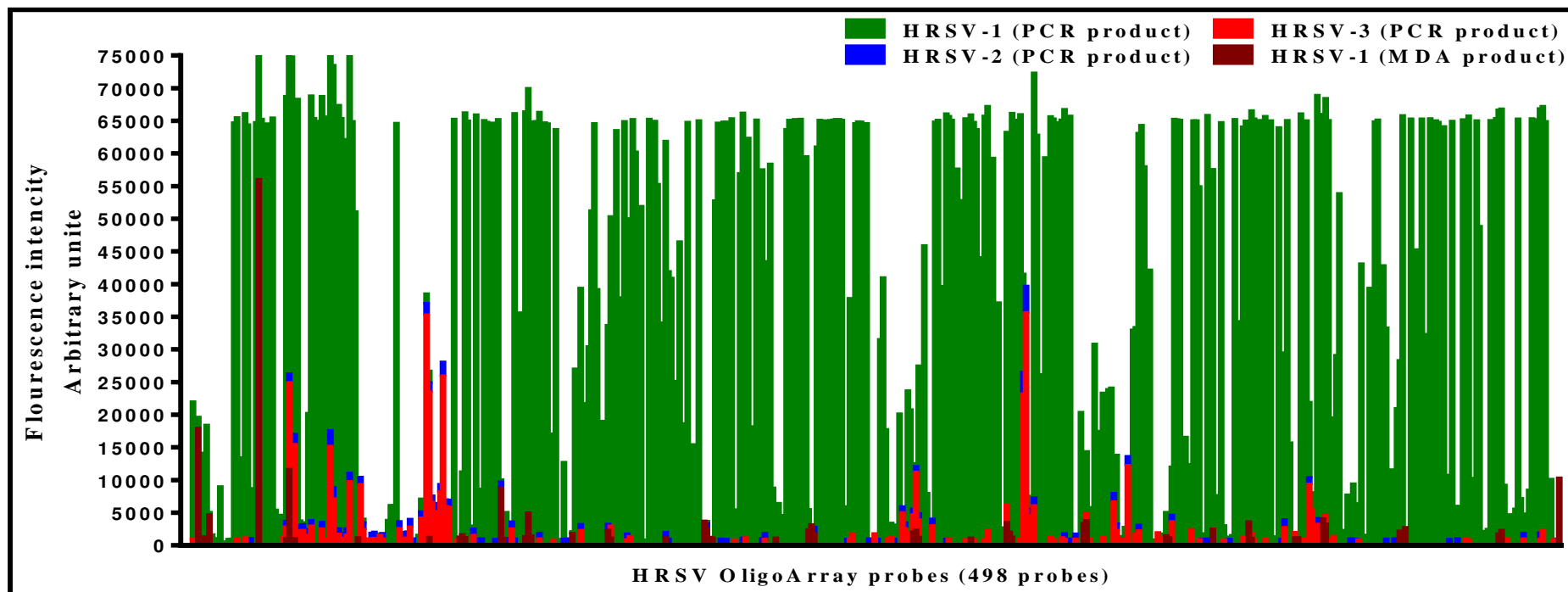


**Figure 4-23: Signals generated from the hybridization reactions of four of the HRSV amplicons with the probes designed specifically for the HRSV using OligoArray software.**

RNA extracts of three HRSV clinical samples (HRSV1-3) were reverse transcribed into cDNA and amplified using long-range PCR. The cDNA of the HRSV-1 was also amplified by MDA. The generated amplicons were sonicated, labelled and loaded into hybridization reactions with the designed probes of the selected RNA viruses and HHVs. The green, blue, red and brown columns represent the positive hybridization signals generated from the HRSV OligoArray probes after hybridization to the PCR products of the HRSV-1, 2 and 3, and the MD amplicon of the HRSV-1, respectively.

#### 4.4.4.3.2 Sensitivity of the HRSV probes designed using Agilent eArray software

Analysing the positive signals generated from the hybridization reactions of the HRSV amplicons revealed that only 14 probes out of 42 of the Agilent eArray probes designed specifically for the HRSV generated positive specific signals when the hybridization reaction was carried out with the HRSV-1 amplicon generated by long-range PCR; eight of them showed high fluorescent intensities. None of the HRSV Agilent eArray probes generated positive hybridization signals during the hybridization reactions of other HRSV amplicons (figure 4-24).

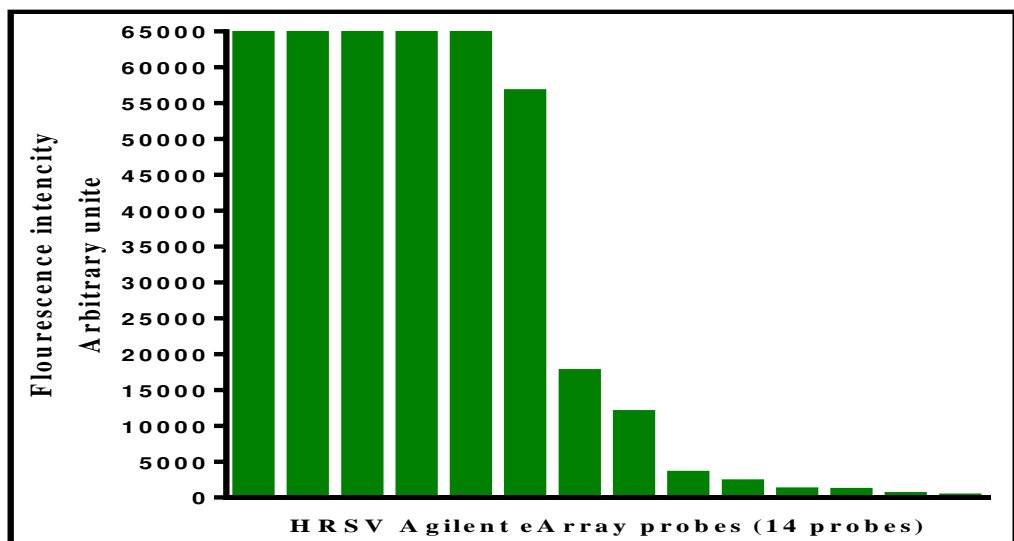


**Figure 4-24: Signals generated from the hybridization reactions of the HRSV-1 amplicon with the probes designed specifically for the HRSV using Agilent eArray software.**

RNA extract of the HRSV clinical sample (HRSV-1) were reverse transcribed into cDNA and amplified using long-range PCR. The generated amplicon was sonicated, labelled and loaded into hybridization reaction with the designed probes of the selected RNA viruses and HHVs. The green columns represent the positive hybridization signals generated from the HRSV Agilent eArray probes after hybridization to the PCR products of the HRSV-1.



Those HRSV OligoArray and Agilent eArray probes showing higher fluorescent intensities with the HRSV amplicons are listed in table 4-7. Tracking the position of these probes revealed that they are targeting different genes of the HRSV genome as shown in table 4-7. The table shows that the OligoArray probe HRSV-0300 and the Agilent eArray probe AGV-2736 had the same sequence and generated a positive hybridization signal of high fluorescent intensity with PCR product of the HRSV-1.

**Table 4-7: Characteristics of the HRSV OligoArray and Agilent eArray probes which showed higher fluorescent intensities with the HRSV amplicons, and cross hybridization with the amplicons of the human enteroviruses, HMPV and human influenza virus A, during their hybridization reactions.**

Probe ID	Probe sequence	Position	Cross hybridization			
			H. enteroviruses	HMPV	Flu-A	
OligoArray probes	HRSV-0330	CAACTAGCAAATCAATGTCACTAACACCAT	NS1	-	-	-
	HRSV-0314	TATTTATCAATCATGATGGGTTCTTAGAAT	NS2	-	-	-
	HRSV-0315	CCTATGCCAATATTTATCAATCATGATGGG	NS2	-	-	-
	HRSV-0020	TGTTATTAATCACAGAAGATGCTAATCATA	N	√	-	-
	HRSV-0021	AGTTATGTGGCATGTTATTAATCACAGAAG	N	√	√	√
	HRSV-0024	GAATGATACTCAACAAAGATCAACTTCT	N	√	√	-
	HRSV-0025	AAGTCAAGTTGAATGATACTCAACAAAG	N	√	√	-
	HRSV-0030	ATTCCTGGGTTAATAGGTATGTTATATGC	N	√	√	√
	HRSV-0031	CTAATCATAAATTCCTGGGTTAATAGGTA	N	√	√	-
	HRSV-0032	ACAGAAGATGCTAATCATAAATTCCTGGG	N	√	√	√
	HRSV-0034	TACTCCTAATTATGATGTGCAGAAACACAT	N	√	√	-
	HRSV-0038	GCTCTTAGCAAAGTCAAGTTGAATGATACA	N	√	√	√
	HRSV-0335	CTTCTACCAGAGGTGGCAGTAGAGTTGAAG	N	√	√	-
	HRSV-0336	TATAGACAATCTTCTACCAGAGGTGGCAG	N	√	√	√
	HRSV-0340	CCTGATTGTGGGATGATAATATTATGTATA	N	-	-	-
	HRSV-0341	AATTCAAATCAACATTGAGATAGAATCTAG	N	√	-	√

Probe ID	Probe sequence	Position	Cross hybridization			
			H. enteroviruses	HMPV	Flu-A	
OligoArray probes	HRSV-0342	TAACAACACTGAAATTCAAATCAACATTGAGA	N	√	-	√
	HRSV-0343	TTGGCAAGCTTAACAACACTGAAATTCAAATC	N	√	-	-
	HRSV-0345	ATGTAACAACACATCGTCAAGACATTAATG	N	-	-	-
	HRSV-0346	AGCAGTGATTAGGAGAGCTAATAATGTCCT	N	-	-	-
	HRSV-0348	GCAGCATTAGTAATAACCAAATTAGCAGCA	N	√	-	√
	HRSV-0349	ATTATGTATAGCAGCATTAGTAATAACCAA	N	-	-	-
	HRSV-0350	GGATGATAATATTATGTATAGCAGCATTAG	N	√	√	√
	HRSV-0351	GCATGACTCTCCTGATTGTGGGATGATAAT	N	√	√	√
	HRSV-0352	CAGAATACAGGCATGACTCTCCTGATTGTG	N	√	√	√
	HRSV-0354	TGAAATTTGAAGTGTTAACATTGGCAAGCT	N	-	-	-
	HRSV-0356	ACTAGAGGCTATCAAACATCAGCTTAATCC	N	√	√	√
	HRSV-0357	CAGCAGAAGAACTAGAGGCTATCAAACATC	N	√	√	√
	HRSV-0361	TCTTTGACTCAATTCCTCACTTCTCCAGT	N	-	-	-
	HRSV-0364	TTAGACTTGACAGCAGAAGAACTAGAGGCT	N	-	-	-
	HRSV-0367	GAGTACAGAGGTACACCAAGGAATCAAGAT	N	-	-	-
	HRSV-0369	AGCAGGATTCTACCATATATTGAACAACCC	N	√	√	√
	HRSV-0370	TGGGTGGAGAAGCAGGATTCTACCATATAT	N	√	√	√
	HRSV-0373	GCAGAAATGGAACAAGTTGTGGAGGTTTAT	N	√	√	√
	HRSV-0044	ACGATAATATAACAGCAAGATTAGATAGGA	P	-	√	√
	HRSV-0045	GAAGAAATAAATGATCAGACAAACGATAAT	P	√	√	√

Probe ID	Probe sequence	Position	Cross hybridization			
			H. enteroviruses	HMPV	Flu-A	
OligoArray probes	HRSV-0046	CTAAACTATACAAAGAAACCATAGAAACAT	P	√	√	√
	HRSV-0048	AGTAAGTTTCAAAGAAGACCCTACACCAAG	P	√	√	√
	HRSV-0053	AGAAAGCCCTATAACATCAAATTCAACCAT	P	-	√	√
	HRSV-0054	TATCATATCTGTCAACTCAATAGATATAGA	P	√	-	-
	HRSV-0055	ACTAGGAATGCTTCACACATTAGTAGTTGC	P	-	-	-
	HRSV-0056	TAAGTGAAATACTAGGAATGCTTCACACAT	P	√	√	√
	HRSV-0057	GATCAGACAAACGATAATATAACAGCAAGA	P	√	√	√
	HRSV-0059	GAAGAATCTAGCTATTCATATGAAGAAATA	P	-	-	√
	HRSV-0060	CATAGAAACATTTGATAACAATGAAGAAGA	P	√	√	√
	HRSV-0061	AAGTAACCAAAGAAAGCCCTATAACATCAA	P	√	√	√
	HRSV-0062	ATAGATATAGAAGTAACCAAAGAAAGCCCT	P	√	√	√
	HRSV-0063	GGCAAATTCACATCACCCAAAGATCCCAAG	P	√	√	√
	HRSV-0064	ATCAATAAAGGGCAAATTCACATCACCCAA	P	√	√	√
	HRSV-0065	AATTCCTAGAATCAATAAAGGGCAAATTCA	P	√	√	√
	HRSV-0067	TGCAAACAACAGAGCTACCAAATTCCTAGA	P	-	-	-
	HRSV-0068	ATGGAGAAGATGCAAACAACAGAGCTACCA	P	√	√	√
	HRSV-0069	CCTGAATTCATGGAGAAGATGCAAACAAC	P	√	√	√
	HRSV-0070	TACTGCAGGGAACAAGCCCAATTATCAAAG	P	-	-	-
	HRSV-0113	AAATCCAGAACACACAAGTCAAAGGAAAC	P	-	√	-
	HRSV-0375	AACACACAACACCAACAGAAGACCAACAAA	P	-	√	-

Probe ID	Probe sequence	Position	Cross hybridization			
			H. enteroviruses	HMPV	Flu-A	
OligoArray probes	HRSV-0378	CAAACAAACCAACTCAACCATCCAACCAAA	P	√	√	-
	HRSV-0382	ATCACTTGAAGATTTCTGATTAGTTACCAA	P	-	-	-
	HRSV-0385	TGACAGATTAGAAGCTATGGCAAGACTCAG	P	-	-	-
	HRSV-0387	AGAACTGAAGCATTAAATGACCAATGACAGA	P	√	√	√
	HRSV-0388	CCTACATCTGCTCGGGATGGTATAAGAGAT	P	√	√	√
	HRSV-0389	ACAATGATCTATCACTTGAAGATTTCTGAT	P	√	√	√
	HRSV-0390	AATGATAGTGACAATGATCTATCACTTGAA	P	√	-	√
	HRSV-0391	GTTGGAAGGGAATGATAGTGACAATGATCT	P	√	√	√
	HRSV-0392	AGATGAAGTGTCTCTCAATCCAACATCAGA	P	√	√	√
	HRSV-0393	CCATGGTTGGTTTAAGAGAAGAAATGATAG	P	√	√	√
	HRSV-0394	GTATAAGAGATGCCATGGTTGGTTTAAGAG	P	-	√	√
	HRSV-0096	ACACAGCTGCTGTTCAATACAATGTCCTAG	M	√	-	-
	HRSV-0414	CAGCTACACGATTTGCAATCAAACCCATGG	M	-	-	-
	HRSV-0431	ACTAACAACCTGCAATCATAACAAGATGCAAC	G	-	-	-
	HRSV-0432	ACAAAGTCACACTAACAACCTGCAATCATAC	G	-	-	-
	HRSV-0433	TCGGCAAACCACAAAGTCACACTAACAACCT	G	-	-	-
	HRSV-0434	TATTCATAGCCTCGGCAAACCACAAAGTCA	G	-	√	-
	HRSV-0435	TAATTGCAGCCATCATATTCATAGCCTCGG	G	-	√	-
	HRSV-0439	GTTAAATCTTAAATCTATAGCACAAATCAC	G	-	-	-
	HRSV-0123	AGCATATCAAACATTGAAACTGTGATAGAG	F	√	-	√

Probe ID	Probe sequence	Position	Cross hybridization			
			H. enteroviruses	HMPV	Flu-A	
OligoArray probes	HRSV-0127	CAAATAGTTAGACAGCAAAGTTACTCTATC	F	√	-	√
	HRSV-0128	CAACAATGTTCAAATAGTTAGACAGCAAAG	F	√	-	-
	HRSV-0131	GCAAAGCTGCAGCATATCAAACATTGAAAC	F	√	-	√
	HRSV-0135	GCTCTACTATCCACAAACAAGGCTGTAGTC	F	√	-	-
	HRSV-0136	ATCAATGATATGCCTATAACAAATGATCAG	F	√	-	-
	HRSV-0139	AATTTAGTGTTAATGCAGGTGTAACACTACAC	F	-	-	-
	HRSV-0145	CTGAGTGGTATAAATAATATTGCATTTAGT	F	-	-	√
	HRSV-0148	CTGGTAAATCCACCACAAATATCATGATAA	F	-	-	-
	HRSV-0157	AATGTAAATGCTGGTAAATCCACCACAAAT	F	√	-	-
	HRSV-0160	GAATTTGATGCATCAATATCTCAAGTCAAT	F	-	-	-
	HRSV-0450	GGCTATCTTAGTGCTCTAAGAACTGGTTGG	F	√	-	√
	HRSV-0451	AGTTAGCAAAGGCTATCTTAGTGCTCTAAG	F	√	-	√
	HRSV-0452	CATGCAGTGCAGTTAGCAAAGGCTATCTTA	F	√	-	√
	HRSV-0461	TATCACATCTCTAGGAGCCATTGTGTCATG	F	√	-	-
	HRSV-0462	TAAGCAGCTCCGTTATCACATCTCTAGGAG	F	√	-	-
	HRSV-0463	AGTAAATCTCTGCAACATTGACATATTCAA	F	-	-	-
	HRSV-0467	CCCACAAGCTGAAACATGTAAAGTTCAATC	F	√	-	-
	HRSV-0470	CACAATGAACAGTTTAAACATTACCAAGTGA	F	-	-	-
	HRSV-0473	GAGGATGGTACTGTGACAATGCAGGATCAG	M2	√	√	√
	HRSV-0481	ATGTTAAACAGAATACTTAAGTCTATGGAT	M2	-	-	√

Probe ID	Probe sequence	Position	Cross hybridization			
			H. enteroviruses	HMPV	Flu-A	
OligoArray probes	HRSV-0482	ATCCTTGCAAATTTGAAATTCGAGGTCATT	M2	-	-	-
	HRSV-0485	AATATAACTAAACAATCAGCATGTGTTGCC	M2	√	√	√
	HRSV-0486	AGTTGGAGTGCTAGAGAGTTATATAGGATC	M2	√	-	-
	HRSV-0487	CTCTTGGTGTAGTTGGAGTGCTAGAGAGTT	M2	-	-	-
	HRSV-0488	AGAGTTGGACAGAACAGAAGAGTATGCTCT	M2	√	-	√
	HRSV-0489	AATAAGTGGAGCTGCAGAGTTGGACAGAAC	M2	√	√	√
	HRSV-0490	AGGTCATTGCTTGAATGGTAAGAGGTGTCA	M2	√	-	-
	HRSV-0491	TTGAAATTCGAGGTCATTGCTTGAATGGTA	M2	-	√	√
	HRSV-0494	GGACCTCTCAAGACTTGATTGATGCAATTC	M2	√	-	√
	HRSV-0495	GAAATCCATTGGACCTCTCAAGACTTGATT	M2	√	√	√
	HRSV-0496	AACATTCAATGAAATCCATTGGACCTCTCA	M2	√	-	√
	HRSV-0504	AATGATACTACCTGACAAATATCCTTGTAG	M2	√	-	√
	HRSV-0507	ACTGTCATATCATATATTGAAAGCAACAGG	M2	√	-	√
	HRSV-0165	AGTGATGTCAAAGTCTATGCTATATTGAAT	L	√	-	√
	HRSV-0166	TATAGAAATAAGTGATGTCAAAGTCTATGC	L	√	-	-
	HRSV-0167	ACAAGAGTATGACCTCGTCAGAACAGATTG	L	-	-	-
	HRSV-0168	CCTTAATATCTAAGTATCATAAAGGTGAAA	L	√	-	-
	HRSV-0169	ATAACACAGTCCTTAATATCTAAGTATCAT	L	√	-	-
	HRSV-0170	GAAACTAAATATAACACAGTCCTTAATATC	L	√	-	√
	HRSV-0172	GGAAGTTACATATTCAATGGTCCTTATCTC	L	√	-	√

Probe ID	Probe sequence	Position	Cross hybridization			
			H. enteroviruses	HMPV	Flu-A	
OligoArray probes	HRSV-0173	TAATGCTTTAGGAAGTTACATATTCAATGG	L	√	-	√
	HRSV-0177	CAGTCATTACTTATGACATACAAGAGTATG	L	-	-	-
	HRSV-0196	ACCCAATGGTAGATGAAAGACAAGCCATGG	L	-	-	-
	HRSV-0199	TACATTTAACTATTCCTCATGTCACAATAA	L	-	-	-
	HRSV-0200	ATTTGTAGTGATGTACTGGATGAACTGCAT	L	-	-	-
	HRSV-0201	GTGCTCTATCATCACAGATCTCAGCAAATT	L	-	-	-
	HRSV-0202	ACATTAGTAAGTGCTCTATCATCACAGATC	L	-	-	-
	HRSV-0206	AATGTTCAAGCAAGTTCAAATATTAGCAGA	L	-	-	-
	HRSV-0207	TTGACAGGCAAAGAAAGAGAACTCAGTGTA	L	-	-	-
	HRSV-0208	GTCACAATAATATGCACATATAGGCATGCA	L	-	-	-
	HRSV-0209	CTGGATGAACTGCATGGTGTACAATCTCTA	L	-	-	√
	HRSV-0211	AAGCATTTTCGATATGAAACATCATGTATTT	L	-	-	-
	HRSV-0212	CTCAGCAAATTCAATCAAGCATTTTCGATAT	L	-	-	√
	HRSV-0213	GAATAAGTAACAAATCAAATCGTTACAATG	L	-	-	-
	HRSV-0214	TTGAAAGCAGGAATAAGTAACAAATCAAAT	L	-	-	-
	HRSV-0215	TGCAACCAGGAATGTTTCAGACAAGTTCAA	L	-	-	√
	HRSV-0216	TGTGGTATCATTGACAGGCAAAGAAAGAGA	L	-	-	-
	HRSV-0220	ATGTTTGCAATGCAACCAGGAATGTTTCAGA	L	-	-	-
	HRSV-0223	AAGTTCTTAACATGCATAATCACGTTTGAC	L	√	-	√
	HRSV-0224	GATAGATTGAATAAGTTCTTAACATGCATA	L	√	-	√



Probe ID	Probe sequence	Position	Cross hybridization			
			H. enteroviruses	HMPV	Flu-A	
OligoArray probes	HRSV-0225	TCTGTCAGATGATAGATTGAATAAGTTCTT	L	√	-	√
	HRSV-0226	AACTTCAAGATCTGTCAGATGATAGATTGA	L	-	-	-
	HRSV-0227	G TTCATACTTAGTTATTATACAAACCATGA	L	-	-	-
	HRSV-0229	GAGGCTATAGTTCACTCTGTGTTCCATACTT	L	-	-	-
	HRSV-0230	TATCGAAGTTTCTATAGAAGAAGCTCCTGAC	L	-	-	-
	HRSV-0231	CAACTTGTTATATCGAAGTTTCTATAGAAG	L	-	-	-
	HRSV-0236	GGTGAAAGTCTATTATGCAGTTTAATATTT	L	-	-	-
	HRSV-0240	GTGGTGATCCCAACTTGTTATATCGAAGTT	L	√	-	√
	HRSV-0244	ATACTAGCCCTATTAATCGCATATTAACAG	L	-	-	-
	HRSV-0250	CTAGTGGCATAATTATAGAGAAATATAATG	L	-	-	-
	HRSV-0251	TATCACTTTGATACTAGCCCTATTAATCGC	L	√	-	√
	HRSV-0253	GTAGTAGACCATGTGAATCCCTGCATCAA	L	√	-	√
	HRSV-0254	CTTACAGTCAGTAGTAGACCATGTGAATTC	L	√	-	√
	HRSV-0258	GGGTGTATGCATCTATAGATAACAAGGATG	L	-	-	√
	HRSV-0261	AGCACTATAGCTAGTGGCATAATTATAGAG	L	-	-	-
	HRSV-0262	ATATAACAACAAGCACTATAGCTAGTGGCAT	L	-	-	-
	HRSV-0264	AACAACAAATTATCACTTTGATACTAGCCC	L	-	-	-
	HRSV-0267	CATCTATTAACATAACATATAAGGATTGCT	L	-	-	√
	HRSV-0269	CTCAGATAATACTCATCTATTAACATAACA	L	-	-	-
	HRSV-0270	ATAGATCTTGTTAGAATGGGATTGATAAAT	L	-	-	-

Probe ID	Probe sequence	Position	Cross hybridization			
			H. enteroviruses	HMPV	Flu-A	
OligoArray probes	HRSV-0273	TAAACGTCTTAATGTAGCAGAATTCACAGT	L	-	-	-
	HRSV-0279	CCAACACATATGAAAGCAATATTA ACTTAT	L	-	-	-
	HRSV-0280	AGATTATCATCCAACACATATGAAAGCAAT	L	√	-	√
	HRSV-0281	TTGTTAACATAGATTATCATCCAACACATA	L	-	-	-
	HRSV-0282	TGCCCTTGGGTTGTTAACATAGATTATCAT	L	√	-	√
	HRSV-0284	AGTAGTTATTGGAAGTCTATGTCTAAGGTA	L	-	-	√
	HRSV-0285	ATTAATAGACAGTAGTTATTGGAAGTCTAT	L	-	-	-
	HRSV-0286	GTGTATTGGAATTAATAGACAGTAGTTATT	L	-	-	-
	HRSV-0291	TACAATGGACATATCAACATTGATTATGGT	L	-	-	√
	HRSV-0292	ATATTTACAGAAGTCTGAAAGATTGCAATG	L	√	√	√
	HRSV-0294	GGAATTTATTATTGCGTACAGTAGTGGAAC	L	√	√	√
	HRSV-0295	GCTGAATTGCCTGTAACAGTCAACTGGAGT	L	√	√	√
	HRSV-0296	AGTCTGAAAGATTGCAATGATCATAGTTTA	L	√	√	√
	HRSV-0297	GATCTGAAGTTTACTTAGTCCTTACAATAG	L	-	-	√
	HRSV-0298	AAGTTAAAGGGATCTGAAGTTTACTTAGTC	L	√	-	√
	HRSV-0299	CTTAGGCAGTAAGTTAAAGGGATCTGAAGT	L	√	-	-
	HRSV-0300	CTTATGTATGCTTAGGCAGTAAGTTAAAGG	L	√	-	-
	HRSV-0303	GGAGCAAGCATGTAAGAAAGTGCAAGTACT	L	-	-	-
	HRSV-0305	TACATATAAAGTTTGCTGAACCTATCAGTC	L	√	-	√
	HRSV-0306	TGGTCTTATTTACATATAAAGTTTGCTGAA	L	√	-	√

Probe ID	Probe sequence	Position	Cross hybridization			
			H. enteroviruses	HMPV	Flu-A	
OligoArray probes	HRSV-0307	CAACAACATTCATTGGTCTTATTTACATAT	L	-	-	√
	HRSV-0308	CTACAGATGCAACCAACAACATTCATTGGT	L	√	-	√
	HRSV-0309	TTTGACCATTCCTGCTACAGATGCAACCAA	L	√	-	√
	HRSV-0516	AAAGATAATCAATCTCATCTTAAAGCAGAC	L	√	-	√
	HRSV-0520	TGGACAAGATGAAGACAACACTCAGTTATTAC	L	-	-	-
	HRSV-0524	GACATGGAAAGATATTAGCCTTAGTAGATT	L	√	√	√
	HRSV-0525	ATCAATTCCTTGACATGGAAAGATATTAGCC	L	√	√	√
	HRSV-0528	GCAACATCCTCCATCATGGTTAATACATTG	L	√	√	√
	HRSV-0529	ATGTGTTCAATGCAACATCCTCCATCATGG	L	√	-	√
	HRSV-0534	TGTTGGAACCTTACAGAAAGAGATTTGATTG	L	-	-	-
	HRSV-0550	TCAAAGTGAGTCTAGAATCTATAGGTAGTT	L	-	-	-
	HRSV-0553	GTATATTACCCAGCTAGTATAAAGAAAGTC	L	-	-	-
	HRSV-0555	GTCAGACTCATGGAAGGTCAAACCTCATGCT	L	√	-	√
	HRSV-0556	TAAGTAAACCAGTCAGACTCATGGAAGGTC	L	-	-	√
	HRSV-0557	GCTTTAATTAATGGTGACAATCAATCAATA	L	-	-	-
	HRSV-0558	CTCAATTACTGCTTTAATTAATGGTGACAA	L	-	-	-
	HRSV-0559	AAGGGAAATTCTCAATTACTGCTTTAATTA	L	-	-	-
	HRSV-0565	GTATAAAGAAAGTCCTAAGAGTGGGACCGT	L	√	-	√
	HRSV-0571	TCAAACCTCATGCTCAAGCAGATTATTTGCT	L	-	-	√
	HRSV-0573	ATATCTCTCAAAGGGAAATTCTCAATTACT	L	-	-	-

Probe ID	Probe sequence	Position	Cross hybridization			
			H. enteroviruses	HMPV	Flu-A	
OligoArray probes	HRSV-0576	CTAAGAGTGGGACCGTGGATAAACACTATA	L	-	-	-
	HRSV-0577	TATAGATATCATATGGGTGGTATCGAAGGG	L	-	-	-
	HRSV-0580	AGTTGGTGTTACATCACCCAGTATCATGTA	L	-	-	-
	HRSV-0581	TATCCAATATAGTTGGTGTACATCACCCA	L	-	-	-
	HRSV-0583	AGATATTGATAGAGCCACTGAGATGATGAG	L	√	-	√
	HRSV-0584	TAGACTTAACAGATATTGATAGAGCCACTG	L	-	-	√
	HRSV-0587	TCTTGGTCTTTATCCAATATAGTTGGTGT	L	-	-	-
	HRSV-0590	GGGCTAAGAGTTGTTTATGAAAGTTTACCC	L	√	-	√
	HRSV-0595	ATTCACAGGTGATGTTGATATTCACAAGTT	L	√	-	√
	HRSV-0597	ACTAATGTATGTCCTAACAGAATTATTCTC	L	-	-	-
	HRSV-0598	GTAGTAGAACAATTTACTAATGTATGTCCT	L	-	-	√
	HRSV-0601	TGTATAAGCTTTGGCCTTAGCTTAATGTCA	L	√	-	√
	HRSV-0602	GGGATATATAACTGATCATATGTTTATTAA	L	-	-	-
	HRSV-0606	AAGTACTAATTTAGCTGGACATTGGATTCT	L	√	-	√
	HRSV-0607	GACTCAATATGTGGAATTATTCTTAAGTAA	L	-	-	√
	HRSV-0608	AACCTCCCATATTCACAGGTGATGTTGATA	L	√	-	√
	HRSV-0609	CATTTGATGAAACCTCCCATATTCACAGGT	L	√	-	√
	HRSV-0610	TAATGAGATACATTTGATGAAACCTCCCAT	L	√	-	√
	HRSV-0620	ATAAGAAGCTTATTAAATCGTCTACAATGA	L	√	-	√
	HRSV-0626	GCTTCCTTGGCATCATATTAATAGATTCAA	L	√	-	-

Probe ID		Probe sequence	Position	Cross hybridization		
				H. enteroviruses	HMPV	Flu-A
OligoArray probes	HRSV-0627	CACATCACTTTATTGCATGCTTCCTTGGCA	L	√	√	√
	HRSV-0628	TGCACAATAGCACATCACTTTATTGCATGC	L	√	-	√
	HRSV-0629	GCCAAATCTAACCAACTTTACTACTACT	L	√	-	√
	HRSV-0630	AGGTAATACAGCCAAATCTAACCAACTTTA	L	√	-	√
	HRSV-0631	TAGATCATTCAGGTAATACAGCCAAATCTA	L	√	-	√
Agilent eArray probes	AGV-2729	ATGTATGCTTAGGCAGTAAGTTAAAGGGAT	L	√	-	-
	AGV-2736	CTTATGTATGCTTAGGCAGTAAGTTAAAGG	L	√	-	-
	AGV-2745	CTATCAGTCTTTTTGTCTGTGATGCTGAAT	L	√	-	√
	AGV-2748	ATGTATGCTTAGGCAGTAAGTTAAAGGGGT	L	-	-	-
	AGV-2749	CTGAAGTTTACTTAGTCCTTACAATAGGTC	L	√	-	-
	AGV-2750	CTGCAAATGTGTTCCAGTATTTAATGTAG	L	√	-	-

Abbreviations; AGV: Agilent eArray probes, √: hybridization signal, -: no hybridization.

**4.4.4.3.3 Specificity of the HRSV probes**

Many of the HRSV OligoArray and Agilent eArray probes shown in table 4-7 showed cross hybridization with the amplicons of the human enterovirus HMPV, H1N1 and H3N2 revealed as nonspecific signals of various fluorescent intensities (figures 4-25 to 4-27).

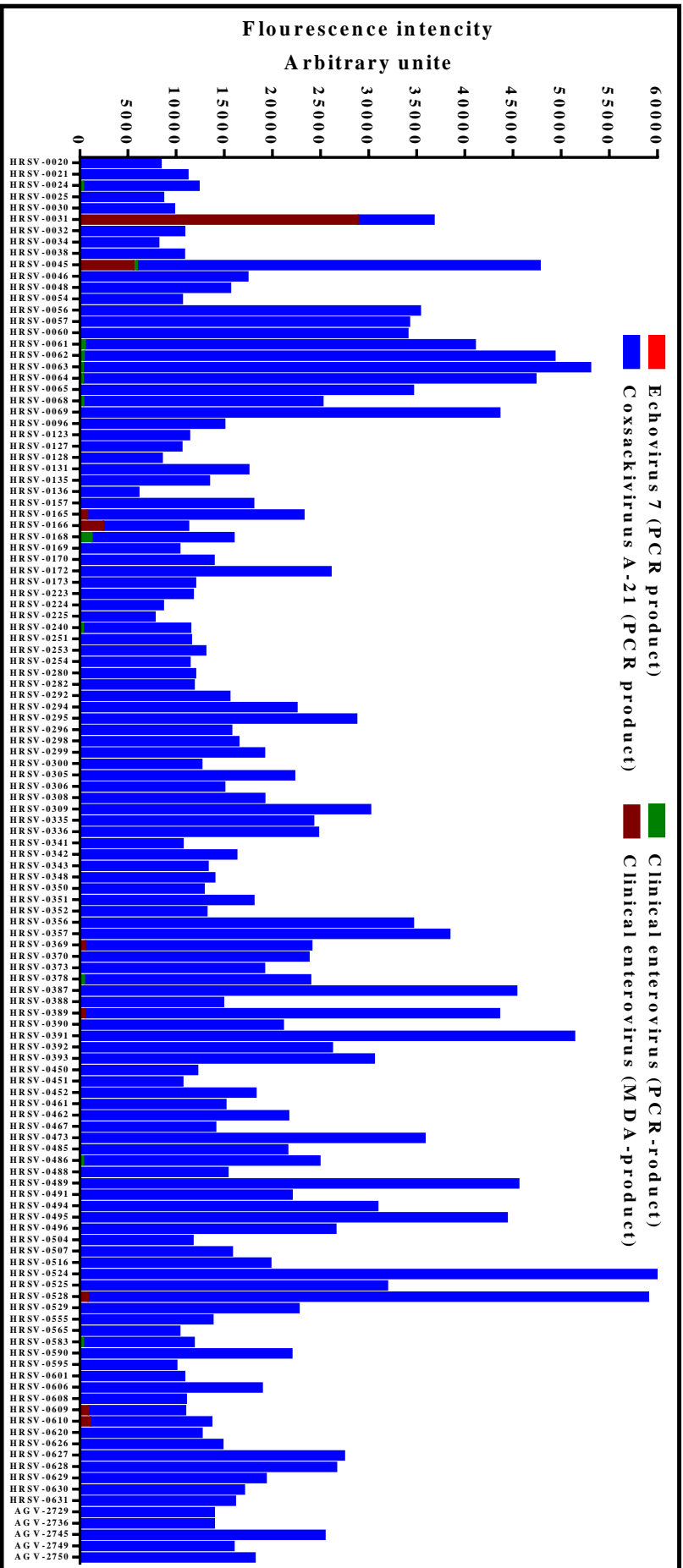


Figure 4-25: Signals of cross hybridization generated between the HRSV probes and the human enterovirus amplicons.

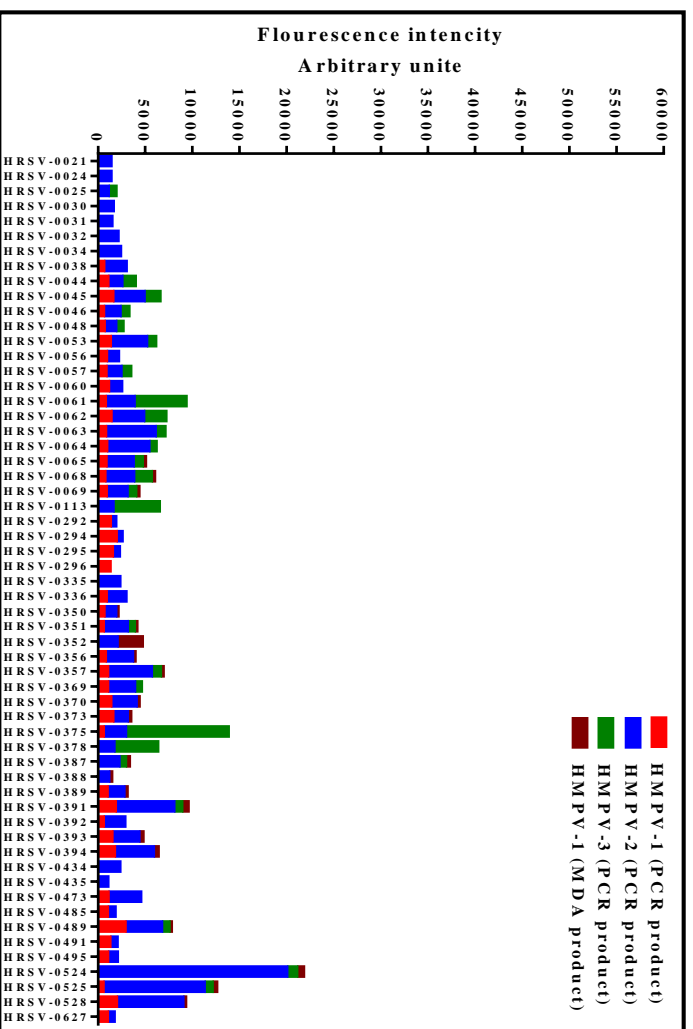


Figure 4-26: Signals of cross hybridization generated between the HRSV probes and the HMPV amplicons.



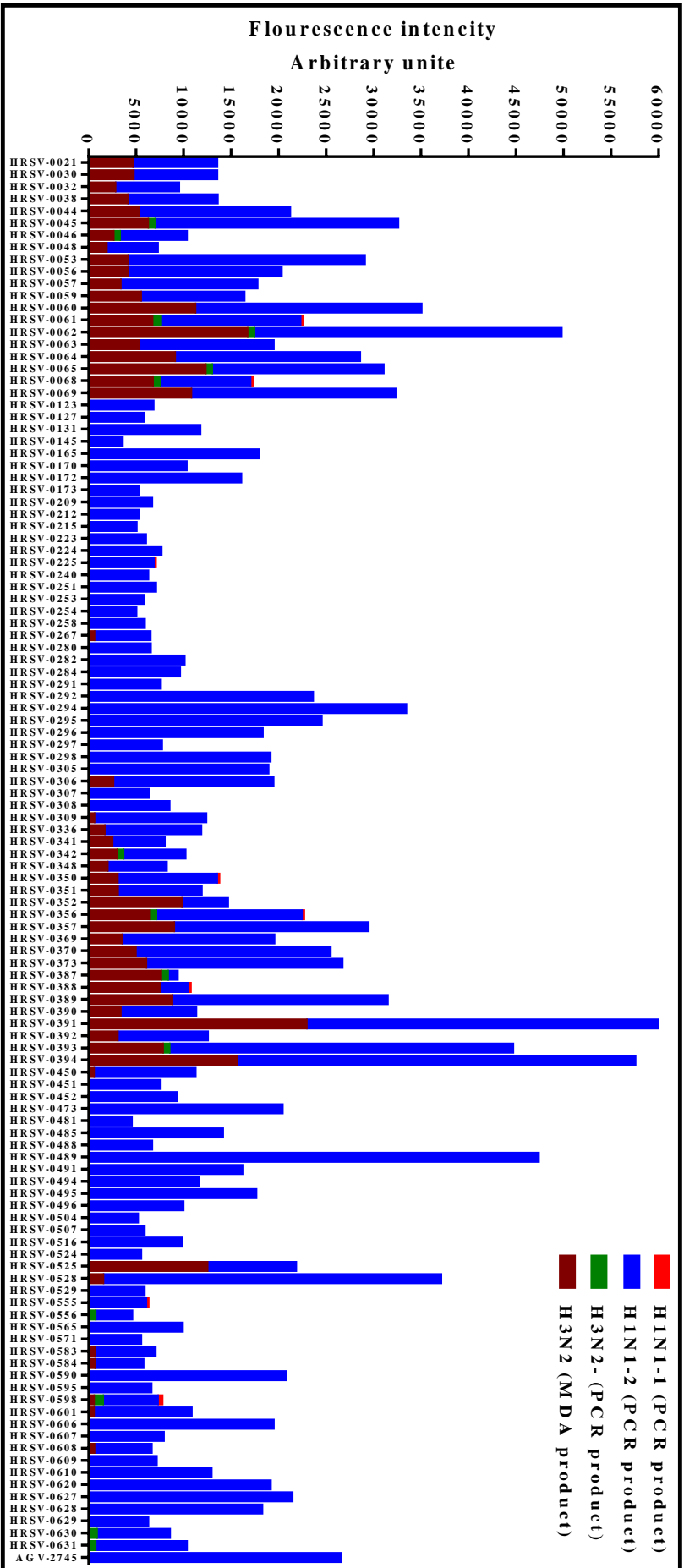


Figure 4-27: Signals of cross hybridization generated between the HRSV probes and the amplicons of the H1N1 and H3N2.

#### **4.4.4.4 Hybridization results of the human influenza virus A amplicons**

RNA extracts of three clinical samples infected with human influenza virus A (H1N1-1, H1N1-2 and H3N2) were reverse transcribed into cDNA and then amplified using long-range PCR. The cDNA of the H3N2 was also amplified by MDA. The generated amplicons were fragmented by sonication. The fragmented PCR amplicon of the H1N1-1 was labelled with dyomics 547 fluorescent dye, while the fragmented PCR amplicons of the H1N1-2 and H3N2 in addition to the fragmented MD amplicon of the H3N2 were labelled with dyomics 495 fluorescent dye (see table 4-3). The labelled amplicons were loaded into hybridization reactions with the probes designed for the selected RNA virus groups using four different grids of the virochip.

##### **4.4.4.4.1 Sensitivity of the human influenza virus A probes designed using OligoArray software**

Analysing the positive signals generated from the hybridization reactions of the human influenza virus A amplicons revealed that the vast majority of the OligoArray probes designed specifically for the HA and NA genomic segments of the H1N1 generated positive specific signals of high fluorescent intensities with the HA and NA PCR products of the H1N1 (see table 4-4) . Most of these H1N1 OligoArray probes showed signals of cross hybridization with the HA and NA PCR products of the H3N2. In contrast, all the positive hybridization signals generated from the OligoArray probes designed specifically for the HA genomic segment of the H3N2 showed very low fluorescent intensities with all

amplicons of the H1N1-1, H1N1-2 and H3N2. Many of the OligoArray probes designed specifically for the NA genomic segment of the H3N2 generated positive specific hybridization signals with their target H3N2 amplicons, and also showed cross hybridization signals with the H1N1-1 and H1N1-2 amplicons. All other OligoArray probes designed specifically for other subtypes of the human influenza virus A, and human influenza B and C did not generate any positive hybridization signals with the amplicons of the H1N1 and H3N2 (figure 4-28).

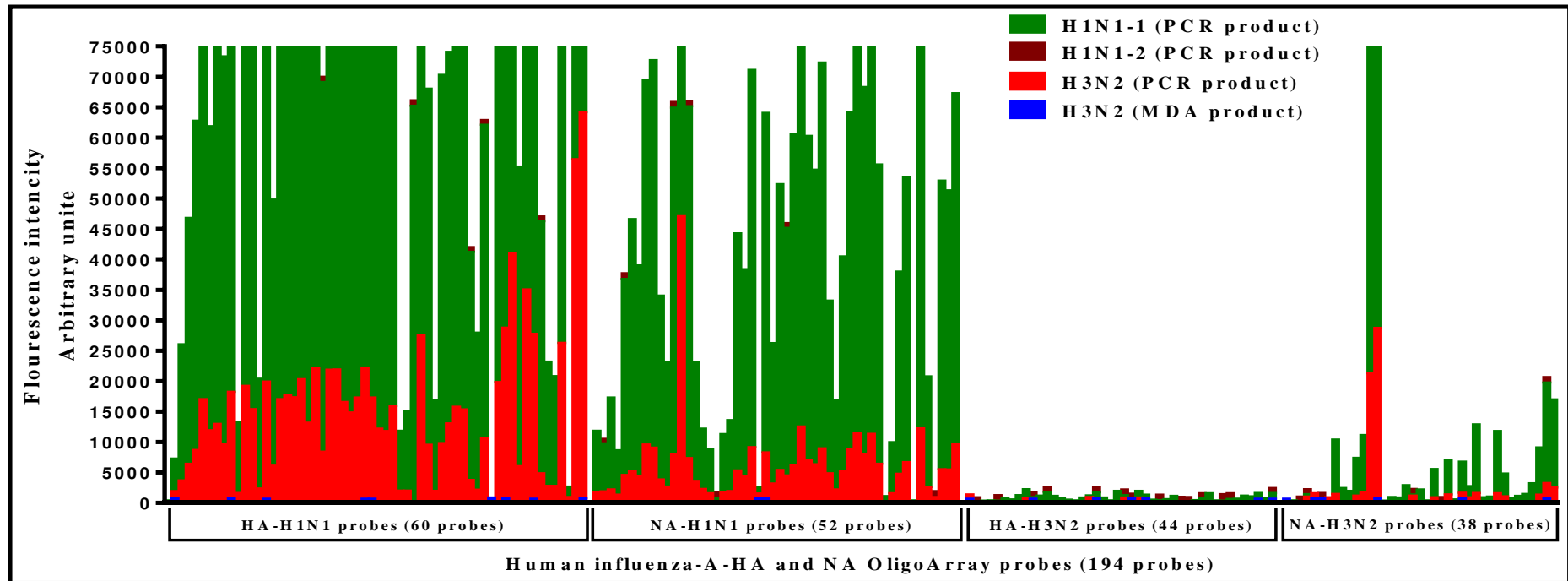


**Figure 4-28: Signals generated from the hybridization reactions of four of the human influenza virus A amplicons with the probes designed specifically for the HA and NA genomic segments of the H1N1 and H3N2 using OligoArray software.**

RNA extracts of two H1N1 (H1N1-1 and 2) and one H3N2 clinical samples were reverse transcribed into cDNA and amplified using long-range PCR. The cDNA of the H3N2 was also amplified by MDA. The generated amplicons were sonicated, labelled and loaded into hybridization reactions with the designed probes of the selected RNA viruses and HHVs. The green, brown, red and blue columns represent the positive hybridization signals generated from the human influenza virus A OligoArray probes after hybridization to the PCR products of the H1N1-1, H1N1-2 and H3N2, and the MD amplicon of the H3N2, respectively.

#### **4.4.4.2 Sensitivity of the human influenza virus A probes designed using Agilent eArray software**

Analysing the positive signals generated from the hybridization reactions of the human influenza virus A amplicons revealed that 126 probes out of 302 of the Agilent eArray probes designed specifically for the HA genomic segment, and 170 probes out of 375 of the Agilent eArray probes designed specifically for NA genomic segment of H1N1 generated positive specific signals of high fluorescent intensities with the HA and NA PCR products of the H1N1 (see table 4-4). Most of these H1N1 Agilent eArray probes showed signals of cross hybridization with the HA and NA PCR products of the H3N2. In contrast, all the positive hybridization signals generated from the Agilent eArray probes designed specifically for the HA genomic segment of the H3N2 showed very low fluorescent intensities with all amplicons of the H1N1-1, H1N1-2 and H3N2. Many of the Agilent eArray probes designed specifically for the NA genomic segment of the H3N2 generated positive specific hybridization signals of various fluorescent intensities with their target H3N2 amplicons, and also showed cross hybridization signals with the H1N1-1 and H1N1-2 amplicons. All other Agilent eArray probes designed specifically for other subtypes of the human influenza virus A, B and C did not generate any positive hybridization signals with the amplicons of the H1N1 and H3N2 (figure 4-29).

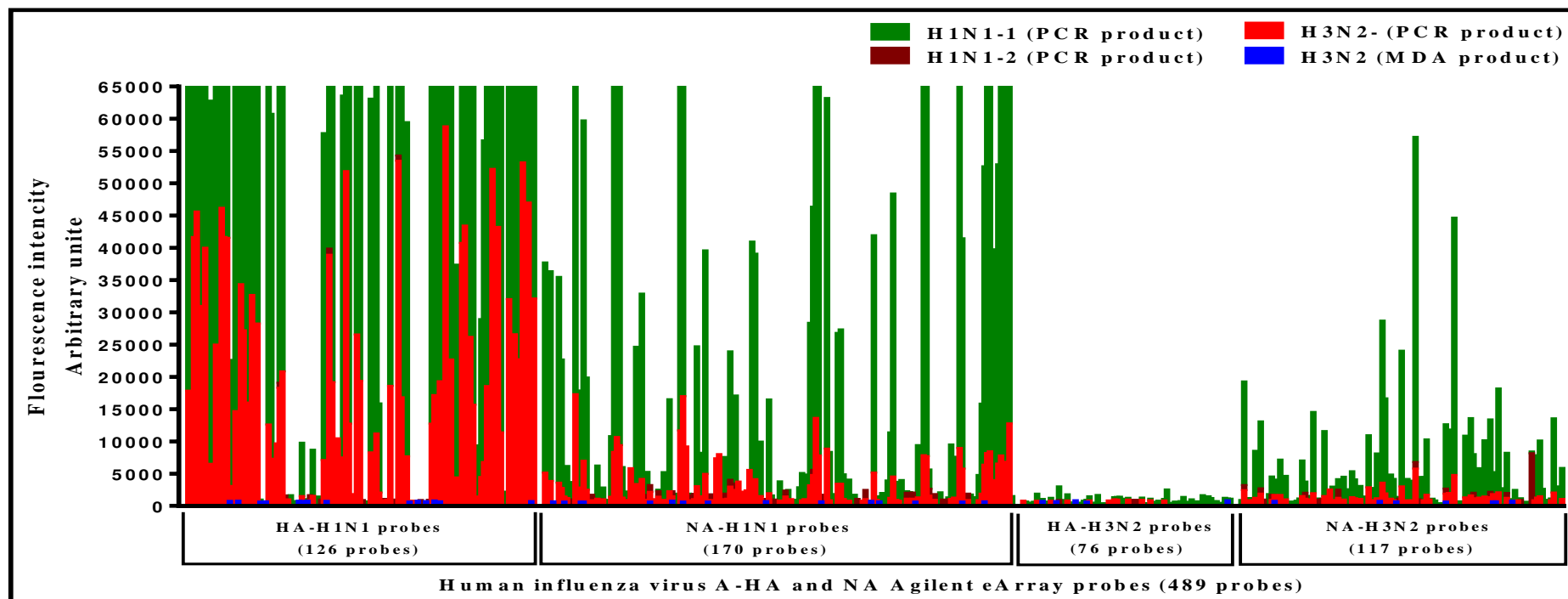


**Figure 4-29: Signals generated from the hybridization reactions of four of the human influenza virus A amplicons with the probes designed specifically for the HA and NA genomic segments of the H1N1 and H3N2 using Agilent eArray software.**

RNA extracts of two H1N1 (H1N1-1 and 2) and one H3N2 clinical samples were reverse transcribed into cDNA and amplified using long-range PCR. The cDNA of the H3N2 was also amplified by MDA. The generated amplicons were sonicated, labelled and loaded into hybridization reactions with the designed probes of the selected RNA viruses and HHVs. The green, brown, red and blue columns represent the positive hybridization signals generated from the human influenza virus A Agilent eArray probes after hybridization to the PCR products of the H1N1-1, H1N1-2 and H3N2, and the MD amplicon of the H3N2, respectively.

Those OligoArray and Agilent eArray probes designed for the HA and NA genomic segments of the human influenza virus A which showed higher fluorescent intensities with the H1N1 and H3N2 amplicons are listed in table 4-8. The table shows that the OligoArray probe INF-A-H1N1-HA-0063 and the Agilent eArray probe AGV-1007 had the same sequence and generated a positive hybridization signal of high fluorescent intensity with PCR product of the HA genomic segment of the H1N1-1.

**Table 4-8: Characteristics of the OligoArray and Agilent eArray probes of the HA and NA genomic segments of the human influenza virus A which showed higher fluorescent intensities with the H1N1 and H3N2 amplicons, and cross hybridization with the amplicons of the human enteroviruses, HMPV and HRSV, during their hybridization reactions.**

	Probe ID	Sequence	Cross hybridization		
			H. enteroviruses	HMPV	HRSV
OligoArray probes	INF-A-H1N1-HA-0005	CATACCCAAAGCTCAGCAAATCCTACATTA	-	√	-
	INF-A-H1N1-HA-0006	ATCATGACTCGAACAAAGGTGTAACGGCAG	√	-	-
	INF-A-H1N1-HA-0007	GTTCATGGCCCAATCATGACTCGAACAAAG	-	-	-
	INF-A-H1N1-HA-0008	CATCTAGTTCAGACAATGGAACGTGTTACC	-	-	-
	INF-A-H1N1-HA-0009	ATTGTGGAAACATCTAGTTCAGACAATGGA	-	-	-
	INF-A-H1N1-HA-0010	TCTGTTAACCTTCTAGAAGACAAGCATAAC	-	-	-
	INF-A-H1N1-HA-0012	TTCTAGAAGACAAGCATAACGGGAAACTAT	-	-	-
	INF-A-H1N1-HA-0014	TAAATGTAACATTGCTGGCTGGATCCTGGG	-	-	-
	INF-A-H1N1-HA-0015	AAGCATAACGGGAAACTATGCAAACCTAAGA	-	√	√
	INF-A-H1N1-HA-0017	TGCATTTGGGTAAATGTAACATTGCTGGCT	-	√	-
	INF-A-H1N1-HA-0018	AGTAACACACTCTGTAAACCTTCTAGAAGA	-	-	-
	INF-A-H1N1-HA-0019	AGTGTTCATCATTTGAAAGGTTTGAGATATT	-	-	-
	INF-A-H1N1-HA-0020	AATTGAGCTCAGTGTTCATCATTTGAAAGGT	-	-	-
	INF-A-H1N1-HA-0021	AGACAATGGAACGTGTTACCCAGGAGATTT	-	-	-
	INF-A-H1N1-HA-0022	ATTATGAGGAGCTAAGAGAGCAATTGAGCT	-	-	-
	INF-A-H1N1-HA-0023	ATTTCAGAATATACATCCGATCACAATTGG	√	√	-
	INF-A-H1N1-HA-0024	CCAGCCTCCCATTTTCAGAATATACATCCGA	-	-	-
	INF-A-H1N1-HA-0025	ATTGCAATACAACCTTGTTCAGACACCCAAGG	-	-	√
	INF-A-H1N1-HA-0026	CCAGTCCACGATTGCAATACAACCTTGTTCAG	-	-	-



	Probe ID	Sequence	Cross hybridization		
			H. enteroviruses	HMPV	HRSV
OligoArray probes	INF-A-H1N1-HA-0027	TTCAGATACACCAGTCCACGATTGCAATAC	√	-	-
	INF-A-H1N1-HA-0028	GTATTATCATTTTCAGATACACCAGTCCACG	√	-	-
	INF-A-H1N1-HA-0029	GCTGGATCTGGTATTATCATTTTCAGATACA	-	-	-
	INF-A-H1N1-HA-0030	GGAAAGAAATGCTGGATCTGGTATTATCAT	-	-	-
	INF-A-H1N1-HA-0031	CATTCGCAATGGAAAGAAATGCTGGATCTG	-	-	-
	INF-A-H1N1-HA-0032	CCGAGATATGCATTCGCAATGGAAAGAAAT	-	-	-
	INF-A-H1N1-HA-0033	TCTAGTGGTACCGAGATATGCATTCGCAAT	-	-	-
	INF-A-H1N1-HA-0034	CAACTGGAAATCTAGTGGTACCGAGATATG	√	-	-
	INF-A-H1N1-HA-0035	ACATTCGAAGCAACTGGAAATCTAGTGGTA	√	-	-
	INF-A-H1N1-HA-0038	GAAGTTCAAGCCGGAAATAGCAATAAGACC	√	√	√
	INF-A-H1N1-HA-0039	GATACAGCAAGAAGTTCAAGCCGGAAATAG	√	√	√
	INF-A-H1N1-HA-0040	CAACAAAGTCTCTATCAGAATGCAGATGCA	-	-	-
	INF-A-H1N1-HA-0043	GTCCCGTCTATTCAATCTAGAGGCCTATTT	√	-	√
	INF-A-H1N1-HA-0044	ATTGAGGAATGTCCCGTCTATTCAATCTAG	-	-	-
	INF-A-H1N1-HA-0045	GCTATAAACACCAGCCTCCCATTTTCAGAAT	√	√	-
	INF-A-H1N1-HA-0046	GAGGGATCAAGAAGGGAGAATGAACTATTA	√	√	√
	INF-A-H1N1-HA-0047	CCGGAAATAGCAATAAGACCCAAAGTGAGG	-	-	-
	INF-A-H1N1-HA-0049	ATGGTCCTACATTGTGGAAACATCTAGTTC	-	-	-
	INF-A-H1N1-HA-0051	ACAGGGATGGTAGATGGATGGTACGGTTAT	-	-	-
	INF-A-H1N1-HA-0052	AAAGAACTTTGGACTACCACGATTCAAATG	-	√	-
INF-A-H1N1-HA-0053	CTGGACATTTGGACTTACAATGCCGAACTG	-	-	-	
INF-A-H1N1-HA-0054	CGAGATTACTAACAAGTAAATTCTGTTAT	-	-	-	

	Probe ID	Sequence	Cross hybridization		
			H. enteroviruses	HMPV	HRSV
OligoArray probes	INF-A-H1N1-HA-0055	TGATGGTTTCCTGGACATTTGGACTTACAA	-	-	-
	INF-A-H1N1-HA-0056	GGACTACCACGATTCAAATGTGAAGAACTT	-	-	-
	INF-A-H1N1-HA-0057	CAGCAGTAGGTAAAGAGTTCAACCACCTGG	-	-	-
	INF-A-H1N1-HA-0060	ACTTACAATGCCGAAGTGTGGTTCTATTG	-	-	-
	INF-A-H1N1-HA-0062	AAATGCGATAACACGTGCATGGAAAGTGTC	-	-	-
	INF-A-H1N1-HA-0063	TAAAGCTGGAATCAACAAGGATTTACCAGA	√	√	-
H1N1-HA-Agilent eArray probes	AGV-0946	GGCTGCTTTGAATTTTACCATAAATGCGAT	-	-	-
	AGV-0954	TTGAAACGGCTGCTTTGAATTTTACCACA	√	-	-
	AGV-0955	AATGCGATAACACGTGCATGGAAAGTGTC	√	-	-
	AGV-0957	ATGGTTTCCTGGACATTTGGACTTACAATG	√	-	-
	AGV-0958	CCGAAGTGTGGTTCTATTGGAAAATGAAA	-	-	-
	AGV-0960	GGCTGCTTTGAATTTTACCACAAATGCAAT	-	-	-
	AGV-0961	CTGTTGGTTCTATTGGAAAACGAAAGAACT	-	-	-
	AGV-0969	TGAATTTTACCACAAGTGCATAACACGTG	-	-	-
	AGV-0972	TCAACAAGGATTTACCAGATTTTGGCGATT	√	-	-
	AGV-0974	GGCTGCTTTGAATTTTATCACAAATGCGAT	-	-	-
	AGV-0976	CCAAGGAAATTGGAAACGGCTGCTTTGAAT	-	-	-
	AGV-0977	TTTACCACAAATGCGATAACACGTGCATGG	-	-	-
	AGV-0978	AAAGTGTCAAAAATGGGACTTATGACTACC	-	-	-
	AGV-0981	CCAGCTAAAAACAATGCCAAGGAAATTGG	√	√	-
	AGV-0982	GACTATCCAAAATACTCAGAGGAAGCAAAA	-	√	√
AGV-0985	TTTCCTGGACATTTGGACTTACAATGCCGA	-	-	-	

	Probe ID	Sequence	Cross hybridization		
			H. enteroviruses	HMPV	HRSV
H1N1-HA-Agilent eArray probes	AGV-0986	GCTGTTGGTTCTATTGGAAAATGAAAGAAC	-	-	-
	AGV-0991	GGACTATCACGATTCAAATGTGAAGAACTT	-	-	-
	AGV-0992	TGGTTTCTGGACATTTGGACTTATAATGC	-	-	-
	AGV-0998	TTCCTGGACATTTGGACTTACAATGCCGAA	-	-	-
	AGV-0999	CTGTTGGTTCTGTTGGAAAATGAAAGAACT	-	-	-
	AGV-1007	CAATGCCAAGGAAATTGGAAATGGCTGCTT	-	-	-
	AGV-1077	CCAAAATACTCAGAGGAAGCAAAATTGAAC	-	-	√
	AGV-1078	GCCGAACTGTTGGTTTTATTGGAAAATGAA	-	-	-
	AGV-1095	GAGTTCAACCACCTGGAAAAAAGAATAGAG	√	√	√
	AGV-1096	GACATTTGGACTTACAATGCCGAAGTGTG	-	-	-
	AGV-1396	CAGTTAAAAACAATGCCAAGGAAGTGGGA	-	-	-
	AGV-1397	GACTACCCAAAATACTCAGAAGAAGCAAAA	-	-	-
	AGV-1419	AGAACAATGCCAAGGAAATTGGAAACGGCT	-	√	√
	AGV-1436	GGCTGCTTTGAATTTTACCACAAATGTGAT	-	-	-
	AGV-1524	GCCGAATTGTTGGTTCTATTGGAAAATGAA	-	-	-
	AGV-1554	TGCATGGAAAGTGTCAAAAATGGGACTTAT	-	-	-
	AGV-1555	GATTACCCAAAATACTCAGAGGAAGCAAAA	-	-	√
	AGV-1579	CAATGCCAAGGAAATTGGAAACGGATGCTT	√	-	√
	AGV-1581	TCAACAAGGATTTACCAGATCTTGGCGATC	√	-	-
	AGV-1663	CCGAAATACTCAGAGGAAGCAAAATTAAC	-	-	-
AGV-1664	ATGGCTTCTGGACATTTGGACTTACAATG	-	-	-	
AGV-1665	GGACTACCACGATTCAAATGTGAAGAATTT	-	-	-	

	Probe ID	Sequence	Cross hybridization		
			H. enteroviruses	HMPV	HRSV
H1N1-HA-Agilent eArray probes	AGV-1710	GCATGGAAAGTGTCAAAAATGGAACCTTATG	√	-	-
	AGV-1811	TAAAGCTGGAATCAACAAGGATTTACCAGA	√	-	-
	AGV-1812	CAATGCTAAGGAAATTGGAAACGGCTGCTT	-	-	-
	AGV-1814	GGACTACCATGATTCAAATGTGAAGAACTT	-	-	-
	AGV-1815	CCAGAATACTCAGAGGAAGCAAAATTAAC	-	-	-
	AGV-1963	CATGGAAAGTGTCAAAAACGGGACTTATGA	-	-	-
	AGV-2000	GCATGAAAAGTGTCAAAAATGGGACTTATG	-	-	-
	AGV-2020	CGTGCATGGAAAGTGTAAAAAATGGGACTT	√	-	-
	AGV-2026	GAATCAACAAGGATTTACCAGATTTTGGCG	√	-	-
	AGV-2028	GCTGAACTGTTGGTTCTATTGGAAAATGAA	-	-	-
	AGV-2102	GCATGGAAAGTGTAAAAAATGGGACTTATG	-	-	-
	AGV-2104	TGAATTTTACCACAAATGCGACAACACGTG	-	-	-
	AGV-2229	CCAGTTAAAAACAATGCCAAGGAAATTGG	√	-	-
	AGV-2230	GCTGCTTTGAATTTTACCACAAATGCGATA	-	-	-
	AGV-2265	CAATGCCAAGGAAATTAGAAACGGCTGCTT	-	-	-
	AGV-2266	TCAACAAGGATTTACCAGATTCTGGCGATC	-	-	-
	AGV-2268	CCAGTTAAAAACAATGCCAAGGAAGTTGG	√	-	-
	AGV-2301	TGGTTTCTTGGACATTTGGACTTACAATGC	-	-	-
	AGV-2320	AACTTTGGACTACCACGATTCAAATGTGAA	-	-	-
	AGV-2321	GAACTTGTATGAAAAGGTAAGAAGCCAGTT	-	-	-
AGV-2322	AATGCCAAGGAAATTGGAAACGGCTGCTTT	-	-	-	
AGV-2323	TTTTACCACAAATGCGATAACACGTGCATG	-	-	-	

	Probe ID	Sequence	Cross hybridization		
			H. enteroviruses	HMPV	HRSV
H1N1-HA-Agilent eArray probes	AGV-2324	GAAAGTGTCAAAAATGGGACTTATGACTAC	-	-	-
	AGV-2325	CCCAAATACTCAGAGGAAGCAAAATTAAC	-	-	√
	AGV-2331	GATGGTTTCCTGGACATTTGGACTTACAAT	√	-	-
	AGV-2352	TGGTTTCCTGGACATTTGGACTTACAATGC	-	-	-
	AGV-2353	CGAACTGTTGGTTCTATTGGAAAATGAAAG	-	-	-
	AGV-2354	GACTACCACGATTCAAATGTGAAGAACTTA	-	-	-
	AGV-2355	AAACAATGCCAAGGAAATTGGAAACGGCTG	-	√	√
	AGV-2356	TGAATTTTACCACAAATGCGATAACACGTG	-	-	-
	AGV-2357	CATGGAAAGTGTCAAAAATGGGACTTATGA	-	-	-
	AGV-2358	CTACCCAAAATACTCAGAGGAAGCAAAATT	-	-	-
	AGV-2359	TCAACAAGGATTTACCAGATTTTGGCGATC	√	-	-
OligoArray probes	INF-A-H1N1-NA-0005	AAGAGTTGGAGAAACAATATATTGAGAACA	-	-	-
	INF-A-H1N1-NA-0006	AGACACTATCAAGAGTTGGAGAAACAATAT	-	-	√
	INF-A-H1N1-NA-0007	GCATAATAACAGACACTATCAAGAGTTGGA	-	-	-
	INF-A-H1N1-NA-0008	CATATCGAACCCCTAATGAGCTGTCCTATTG	√	-	-
	INF-A-H1N1-NA-0009	TGGACAGTCAGTGGTTTCCGTGAAATTAGC	√	-	-
	INF-A-H1N1-NA-0012	AAGACAGGAGCCCATATCGAACCCCTAATGA	√	√	√
	INF-A-H1N1-NA-0013	TAATAACCATTGGTTCGGTCTGTATGACAA	√	-	-
	INF-A-H1N1-NA-0014	CATTCCAATGGAACCATTAAGACAGGAGC	√	-	-
	INF-A-H1N1-NA-0021	CCTATTGGTGAAGTTCCTCTCCATAACAAC	-	-	-
	INF-A-H1N1-NA-0022	CAATTCCTCTCTGCCCCTGTTAGTGGATG	-	-	-
	INF-A-H1N1-NA-0023	CTTGTCATGATGGCATCAATTGGCTAACAA	-	-	-

	Probe ID	Sequence	Cross hybridization		
			H. enteroviruses	HMPV	HRSV
OligoArray probes	INF-A-H1N1-NA-0025	CTTGCTAAATGACAAACATTCCAATGGAAC	√	-	-
	INF-A-H1N1-NA-0027	AGATATCGTAGGAATAAATGAGTGGTCAGG	-	-	-
	INF-A-H1N1-NA-0028	GGGACAGACAATAACTTCTCAATAAAGCAA	-	√	-
	INF-A-H1N1-NA-0029	TCCAGTATCGTCTAATGGAGCAAATGGAGT	-	-	-
	INF-A-H1N1-NA-0030	CAGGCAGTTGTGGTCCAGTATCGTCTAATG	-	-	-
	INF-A-H1N1-NA-0031	GATTCTAGTGAAATCACATGTGTGTGCAGG	-	-	-
	INF-A-H1N1-NA-0032	CTGTTATCCTGATTCTAGTGAAATCACATG	-	-	-
	INF-A-H1N1-NA-0033	GAAAGATAGTCAAATCAGTCGAAATGAATG	-	-	-
	INF-A-H1N1-NA-0036	CATTCAAATACGGCAATGGTGTGGATAG	-	-	-
	INF-A-H1N1-NA-0037	CCAAGTGATGGACAGGCCTCATACAAGATC	-	-	-
	INF-A-H1N1-NA-0038	GAACTAATCAGAGGGCGACCCAAAGAGAAC	√	√	√
	INF-A-H1N1-NA-0039	CAGAATAACAGGGCTGGATTGTATAAGAC	-	√	-
	INF-A-H1N1-NA-0040	TCTGAATGTGCATGTGTAAATGGTTCTTGC	-	-	-
	INF-A-H1N1-NA-0041	AGGAATGCTCCTGTTATCCTGATTCTAGTG	√	-	-
	INF-A-H1N1-NA-0044	CTGTTAGTGGATGGGCTATATACAGTAAAG	-	-	-
	INF-A-H1N1-NA-0045	CTAACAATTGGAATTTCTGGCCCAGACAAT	-	-	-
	INF-A-H1N1-NA-0047	AATGAGCTGTCCTATTGGTGAAGTTCCTC	-	-	-
	INF-A-H1N1-NA-0050	GGAATAAATGAGTGGTCAGGATATAGCGGG	-	-	-
	INF-A-H1N1-NA-0051	TATAAGACCTTGCTTCTGGGTTGAACTAAT	-	-	-
	INF-A-H1N1-NA-0052	GGCTGGATTGTATAAGACCTTGCTTCTGGG	-	-	-
	INF-A-H3N2-NA-0022	TTATGTGTCATGCGATCCTGACAAGTGTTA	-	-	-
	INF-A-H3N2-NA-0023	CAAGAGAACCTTATGTGTCATGCGATCCTG	-	-	-

	Probe ID	Sequence	Cross hybridization		
			H. enteroviruses	HMPV	HRSV
H1N1-NA-Agilent eArray probes	AGV-0947	TCAAATACGGCAATGGTGTGGATAGGGA			
	AGV-0949	GGATTTTCATTCAAATACGGCAATGGAGTT			
	AGV-0968	GGGTTTTCATTCAAATACGGCAATGGTGT			
	AGV-0995	ATATGCAGTGGGATTTTCGGAGACAATCCA	-	-	-
	AGV-1005	AAGACCTTGCTTCTGGGTGAACTAATCAG	-	-	-
	AGV-1081	GATATCGTAGGAATAAATGAGTGGTCAGGA	-	-	-
	AGV-1082	TATAGCGGGAGTTTTGTTCAGCATCCAGAA	-	-	-
	AGV-1083	AACAGGGCTGGATTGTATAAGACCTTGCTT	-	-	-
	AGV-1437	ATCCTTTTGTGGTGTAAACAGTGACACTGT	√	-	-
	AGV-1438	AGCATATCCTTTTGTGGTGTAAACAGTGAC	-	-	-
	AGV-1472	GTATCGTCTAATGGAGCAAATGGAGTGAAA	-	-	-
	AGV-1585	TGGATTGTATAAGACCTTGCTTCTGGGTTG	-	-	-
	AGV-1586	AATTAATCAGAGGGCGACCCAAAGAGAACA	-	-	-
	AGV-1757	GGGACAGACAATAACTTCTCAATAAAGCAA	-	-	-
	AGV-1758	TAATGATAAGACAGGCAGTTGTGGTCCAGT	-	-	√
	AGV-1759	ATCGTCTAATGGAGCAAATGGAGTAAAAGG	-	-	-
	AGV-1804	TCCAGAACTAACAGGGCTGGATTGTATAAG	-	-	-
	AGV-1979	TTTCGGAGACAATCCACGCCCTAATGATAA	-	-	-
	AGV-2033	ATGGTCAGGATATAGCGGGAGTTTTGTTC	-	-	-
	AGV-2235	TTTTGTTCAGCATCCAGAACTAACAGGGCT	-	-	-
AGV-2236	TTGTATAAGACCTTGCTTCTGGGTGAACT	-	-	-	
AGV-2269	CGTCTAATGGAGCAAATGGAGTAAAAGGAT	-	-	-	

	Probe ID	Sequence	Cross hybridization		
			H. enteroviruses	HMPV	HRSV
H1N1-NA-Agilent eArray probes	AGV-2270	ATTCAAATACGGCAATGGTGTGTTGGATAGG	-	-	-
	AGV-2327	CGTAGGAATAAATGAGTGGTCAGGATATAG	-	-	-
	AGV-2342	GTATCGTCTAATGGAGCAAATGGAGTAAAA	-	-	-
	AGV-2343	GGATTTTCATTCAAATACGGCAATGGTGTGTT	-	-	-
	AGV-2344	TGGATAGGGAGAACTAAAAGCATTAGTTCA	-	-	-
	AGV-2346	GGACAGACAATAACTTCTCAATAAAGCAAG	-	-	-
	AGV-2347	TAGGAATAAATGAGTGGTCAGGATATAGCG	-	-	-
	AGV-2348	CATCCAGAACTAACAGGGCTGGATTGTATA	-	-	-
	AGV-2349	AGACCTTGCTTCTGGGTTGAACTAATCAGA	-	-	-
	AGV-2350	TTTGTGGTGTAAACAGTGACACTGTGGGTT	-	-	-
H3N2-NA-Agilent eArray probes	AGV-1644	AGGACTTGTTGGAGACACCCAGAAAAAA	-	-	-
	AGV-1645	GAGGTGATAGGTCCGGTTATTCTGGTATTT	-	-	-
	AGV-1825	TTGTGTTTTGTGGCACCTCAGGTACATATG	-	-	-
	AGV-1878	AACAGTATTGTTGTGTTTTGTGGCACCTCC	√	-	√
	AGV-1990	ACAGTATTGTTGTGTTTTGTGGCACCTCAG	-	-	-
	AGV-2129	CCAAATTGCAGATAAATAGGCAAGTCATAG	-	-	-



#### 4.4.4.3 Specificity of the human influenza virus A probes

Many of the OligoArray probes and Agilent eArray probes targeting the HA and NA genomic segments of the H1N1 shown in table 4-6 showed cross hybridization with the amplicons of the human enterovirus, HMPV and HRSV revealed as weak nonspecific signals for most of them (figures 4-30 to 4-32).

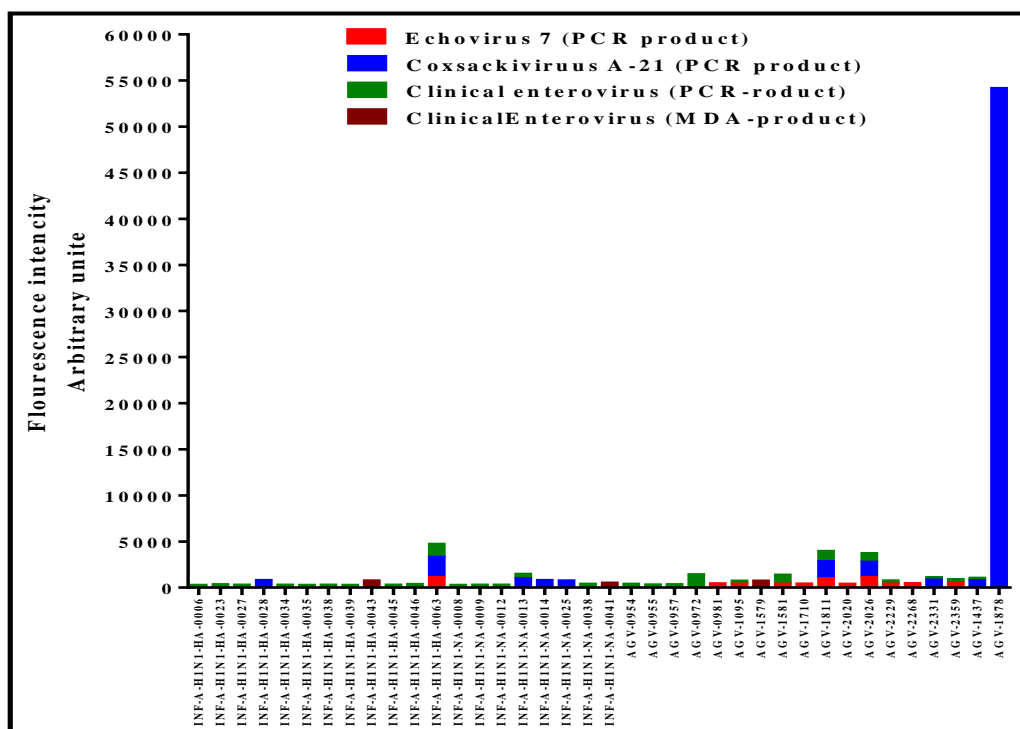


Figure 4-30: Signals of cross hybridization generated between the H1N1 and H3N2 probes, and the human enterovirus amplicons.

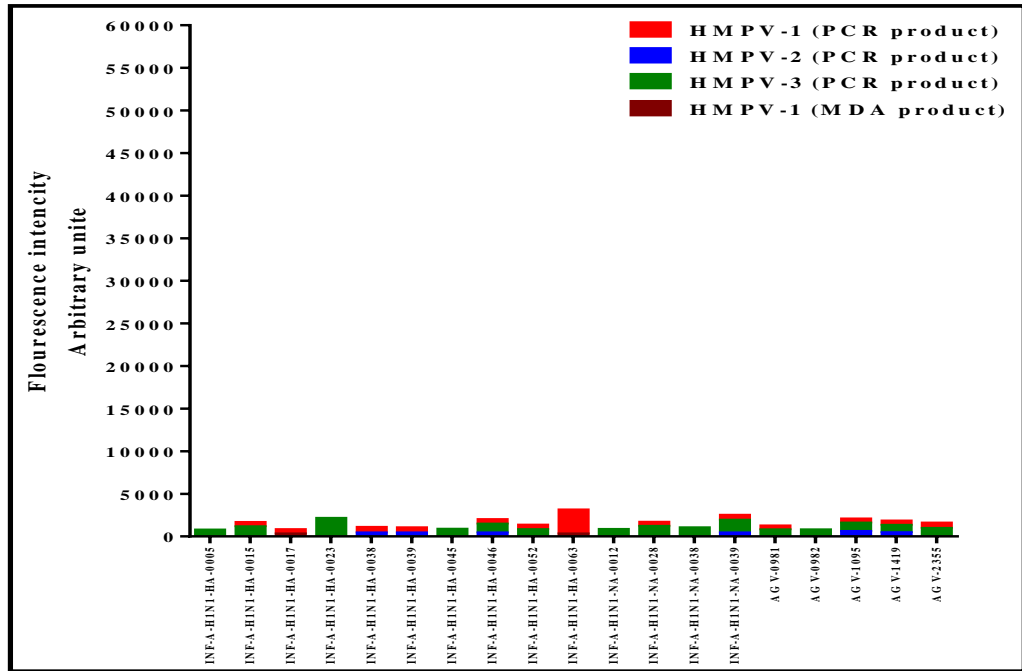


Figure 4-31: Signals of cross hybridization generated between the H1N1 and H3N2 probes, and the HMPV amplicons.

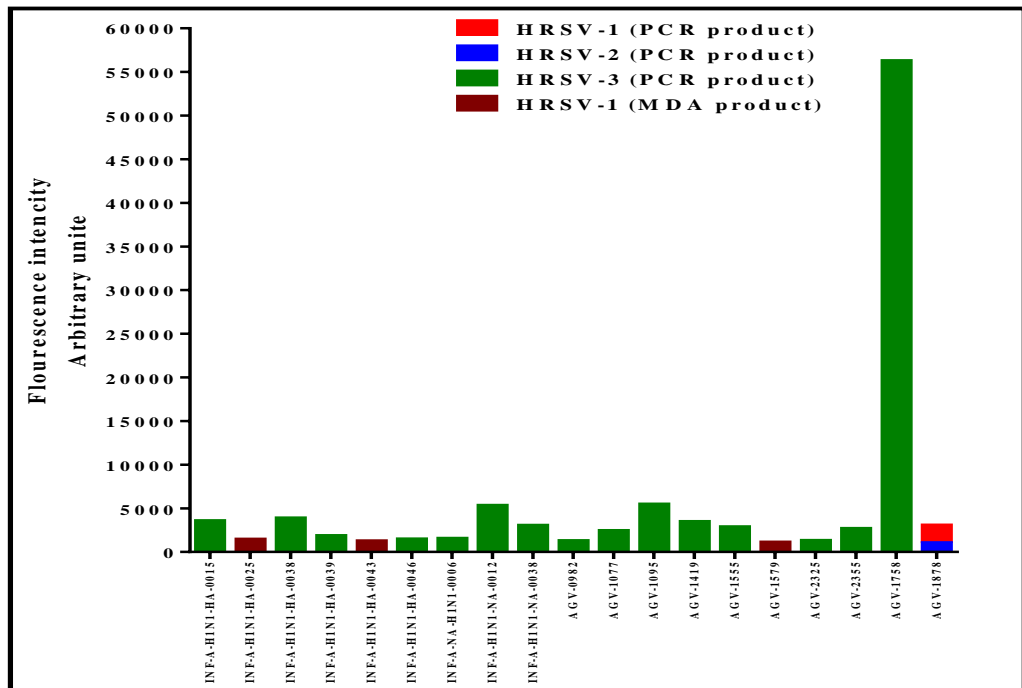


Figure 4-32: Signals of cross hybridization generated between the H1N1 and H3N2 probes, and the HRSV amplicons.

## 4.5 Discussion

In spite of the widespread usage of the nucleic acid microarray technology in different aspects of researches over the past twenty years, many researchers believe that it is still in its infancy as it needs more efforts in order to determine the specific detection limit for each microarray assay (Trevino et al., 2007, Wei et al., 2012). The limited quantities of viral RNA which can be acquired from infected clinical samples, often mixed with human genomic nucleic acids, can limit the application of the nucleic acids microarray for the diagnosis of the viral infections (Puskas et al., 2002). Since the detection limit of this viral microarray assay is still undetermined, the nucleic acids of the selected RNA viruses were amplified in order to provide adequate quantities for the hybridization reaction. In order to evaluate the performance of the OligoArray and Agilent eArray probes which were designed along the whole viral genomes, it was necessary to amplify the full genome length of the echovirus 7, coxsackievirus A-21, clinical enterovirus, HMPV, HRSV, H1N1 and H3N2 in order to provide complementary sequences of the viral nucleic acid for each one of the designed probes. Long-range PCR amplification reaction was used in parallel with the MDA process for amplifying the whole genome of the above viruses as there was a concern that the amplified viral products generated from the MDA may fail to hybridize to the designed viral probes as described in the previous chapter. Amplification efficiency of the full length viral genomes is mainly affected by the integrity of the cDNA generated from the reverse transcription reaction of the viral RNA (Wang, 2005). Therefore, Maxima H Minus First Strand cDNA Synthesis kit was used for generating full length cDNA of the selected RNA viruses from their RNA extracts especially

HMPV and HRSV, whose RNA length exceeds the reverse transcription limit (12 kb) of the SuperScript III First-Strand Synthesis SuperMix kit used in section 3.3.2.3.

The specific single bands with the expected size generated from long-range PCR of the selected viral genomes as visualized by gel electrophoresis in figures 4-3 to 4-9 indicates the success of the amplification process. Moreover, the negative control samples did not show any band on the gel indicating the specificity of the amplification process.

Fragmentation of the viral amplicons was performed in order to enhance the hybridization sensitivity through minimizing the background fluorescent noise which could be generated from the non-specific binding of large-sized sequences of the viral amplicons to the slide surface after labelling with the fluorescent dyes (Liu et al., 2007).

Hybridization reactions of the above viral amplicons revealed that many of the probes designed specifically for the selected RNA viruses showed high specificity as they were hybridized to the nucleic acid of their target viruses while many other probes were nonspecific and showed cross hybridization with the nucleic acid of other non-target viruses. Some of the unexpected results generated from the virochip hybridization reaction, especially those signals generated from the different amplicons of the same viral type (HMPV, HRSV or Influenza virus A), and the cross hybridization between the HRSV probes and the amplicons of the coxsackievirus A-21 and H1N1, could be related to unobserved accidental technical mistakes during the preparation of the viral nucleic acids for this complex experiment, such as the probable loss of the viral amplicon pellet during the precipitation step following the fragmentation

and/or labelling processes in spite of the precautions and the meticulous care used. On the other hand, most of those cross reacting HMPV OligoArray probes generated signals of high fluorescent intensities with the HRSV amplicons due to the nucleotides sequence homology in approximately 50% of the HMPV and HRSV genomes.

Apart from the hybridization results of the HMPV amplicons which did not show any positive hybridization signal with the HMPV Agilent eArray probes the hybridization results of other viral amplicons especially HRSV and H1N1 revealed that the Agilent eArray probes showed better specificity to their target viral amplicons than OligoArray probes as most of the Agilent eArray positive probes showed no or weak signals of cross hybridization with other non-target viral amplicons. The specificity of the Agilent eArray probes is attributed to their designing process which was based on loading the original sequences of the human enterovirus, HMPV, HRSV and human influenza virus into the Agilent eArray software, while the OligoArray probes were designed by loading the consensus sequences of the above viruses which contained degenerate nucleotides into the OligoArray software. This means that the Agilent eArray probes were better more specific for their target nucleic acids of the above viruses than the OligoArray probes.

Hegde et al (2000) indicated that both sensitivity and specificity of the nucleic acid microarray hybridization may be affected by many factors including probe characteristics such as their length, GC content and melting temperature, hybridization conditions such as hybridization temperature and period, washing stringency and signal detection. Wei and his group (2012) however, found that the probe melting temperature and GC content, and hybridization period had no

effect on the nucleic acid hybridization reaction efficiency. The potential formation of secondary structure in some long fragments of the viral amplicons which may prevent the probes from accessing their specific targets and/or sequence repetition of some probes along the target viral genomes may explain the discrepancy of the hybridization results of each of the HMPV, HRSV and H1N1 PCR amplicons (Peplies et al., 2003, Ratushna et al., 2005, Liu et al., 2007, Mueckstein et al., 2010). Wei et al (2012) demonstrated that each nucleic acid target may have three different regions: the first one is completely complementary and exposed to the probe sequence and generates strong hybridization signals; the second region is partially complementary and/or exposed to the probe sequence and generates weak hybridization signals, while the third region is inaccessible and the probe is incapable to hybridize with it resulting in no signals of hybridization.

Non-specific cross hybridization is a common problem in nucleic acid microarray hybridization which is attributed to the potential similarity among the target nucleic acids sequences (Kane et al., 2000, Evertsz et al., 2001, Barrett and Kawasaki, 2003, Trevino et al., 2007). The nucleotide mismatches between the sequences of some probes and the target nucleic acid is considered as another reason for variability of the hybridization results (Fotin et al., 1998, Southern et al., 1999). Urakawa and his group (Urakawa et al., 2003) reported that the stability of the nucleic acid duplexes generated from hybridization reactions can be affected by the number, position and type (A, T, G or C) of the nucleotide mismatches. Those probes showing nucleotide mismatches at their central part would hybridize more strongly to their target nucleic acids than other probes showing nucleotide mismatches at their edges (Shchepinov et al.,

1997, Hughes et al., 2001, Zhang et al., 2007). The fluorescent intensities of the signals generated from the hybridization reaction reflect the matching ratio between the probes and their targets, but it is not a rule, as many of the probes showing nucleotide mismatches generated hybridization signals of higher fluorescent intensities than those signals generated from hybridization with perfect-matching probes (Naef and Magnasco, 2003, Wei et al., 2012).

## **5 General Discussion**



Viruses cause different types of human infectious diseases accompanied by various clinical symptoms, which assist the diagnosis of these infections. However, the similarities among the symptoms of some of viral diseases in addition to those asymptomatic infections make their clinical diagnosis difficult without proper laboratory investigations (Collier and Oxford, 2000). The global migration during the past few years has continuously raised the emergence and re-emergence of several viral infections in both developed and developing countries, which represent 44% of the total infectious diseases (Tyler, 2009). The vast majority of these emerged and/or re-emerged viral infections are caused by RNA viruses due to the high error rate of their polymerases responsible for their genomes replication leading to generate new strains of these viruses (Nichol et al., 2000). Proper management of viral infections helps in preventing many of their serious complications, such as poliomyelitis caused by polioviruses, and reducing the cost of unnecessary hospitalization (Ramers et al., 2000).

It is tempting to identify next generation sequencing (NGS) as an alternative method for the microarray assay. However, it is important to keep in mind that the NGS method requires relatively higher concentration of viral nucleic acid than the microarray assay (Marston et al., 2013). The advantages of the NGS method lie in the ability to discover new viral strains and viral SNPs. On the other hand, the microarray assay can facilitate the fast and specific diagnosis of viral infections from relatively low concentrations of viral nucleic acids available in clinical samples. Thus, as far as the current project results show, the microarray assay seem to provide a more clinically reliable method for detection and diagnosis of viral infections.

## 5.1 Conclusion

Nucleic acid microarray is being used for early and accurate diagnosis of viral infections through detection of viral nucleic acid in a clinical sample. The tiny amount of viral nucleic acid presented in some clinical samples such as CSF, limits the application of nucleic acid microarray for this purpose. MDA has been used in order to overcome this problem through amplifying the whole genome of the target viruses. In spite of the efficiency of MDA in generating micrograms of high molecular weight of the entire viral genome within less than two hours, this process has the following drawbacks:

- a) Samples with very low concentrations (<10 ng) and or short fragments of viral nucleic acids, resulted in nonspecific amplification with high rate of bias.
- b) Amplifying the contaminated nucleic acid especially those of human origin.

PCR can be used as an alternative method for specific amplification of the whole viral genome through designing many sets of specific primers some of them containing 1-2 of degenerate nucleotides, targeting conserved sequences along the entire genome of each one of the selected viral groups. This method was so efficient in amplifying approximately 90% of the entire genome of each of the human enteroviruses, human respiratory syncytial viruses, human metapneumoviruses and influenza viruses, which facilitated investigating the performance of hundreds of probes designed specifically for each of these viruses.

## 5.2 Limitations of the study

Single stranded viral RNA is a fragile structure, highly susceptible for degradation, provides a major obstacle to whole genome amplification. The scarce concentrations of the viral nucleic acids existing in the positive control and clinical samples (few picograms) used for validating the assay was another challenge to viral nucleic acid amplification. The unavailability of the CSF samples infected with human enteroviruses prevented validating the assay against cases with CNS viral infections.

## 5.3 Future work

Many of the probes designed specifically for the selected RNA viruses generated hybridization signals of high fluorescent intensity which is very promising, while many other probes did not generate any signal of hybridization with their target viral nucleic acid such as enterovirus probe, or showed signals of cross hybridization with other non-target nucleic acid. Therefore, it is recommended to re-print the probes designed specifically for each of the selected viral groups on a separate grid or slide, and then revalidating their performance using single sample per each grid which have not been done due to time limitation. It is also recommended to validate the performance of the probes designed specifically for human rhinoviruses using samples containing these viruses. Using CSF samples infected with human enteroviruses in order to validate the designed enterovirus probes against cases of CNS viral infections. It is important to build a library of control positive samples of viral genomes with preferably a concentration of more than 10 ng/ $\mu$ l. This library would help validating the hybridization process in order to

select the most appropriate probes designed specifically for each viral group. Finally, it is very important to define the sensitivity of the designed probes using diluted concentrations on viral nucleic acids. This would help to select the cut off point for viral genome concentration used, and thus minimize the reagents, efforts, time and cost of the experiment.

It might be worth trying to validate the microarray assay with other methods used in the diagnosis of viral infections in clinical samples such as conventional PCR and QPCR.

## 6 REFERENCES

- ABDEL-HAKEEM, M. A. 2010. Development of DNA Microarray System for The Diagnosis of Virus Infections of The Central Nervous System. PhD, The University of Nottingham.
- AGOL, V. I. 2006. Molecular mechanisms of poliovirus variation and evolution. *Curr Top Microbiol Immunol*, 299, 211-59.
- ALBRECHT, V., CHEVALLIER, A., MAGNONE, V., BARBRY, P., VANDENBOS, F., BONGAIN, A., LEFEBVRE, J. C. & GIORDANENGO, V. 2006. Easy and fast detection and genotyping of high-risk human papillomavirus by dedicated DNA microarrays. *J Virol Methods*, 137, 236-44.
- ALERS, J. C., ROCHAT, J., KRIJTENBURG, P. J., VAN DEKKEN, H., RAAP, A. K. & ROSENBERG, C. 1999. Universal linkage system: an improved method for labeling archival DNA for comparative genomic hybridization. *Genes Chromosomes Cancer*, 25, 301-5.
- ANDERSEN, P. 1998. Pathogenesis of lower respiratory tract infections due to Chlamydia, Mycoplasma, Legionella and viruses. *Thorax*, 53, 302-7.
- BAEK, T. J., PARK, P. Y., HAN, K. N., KWON, H. T. & SEONG, G. H. 2008. Development of a photodiode array biochip using a bipolar semiconductor and its application to detection of human papilloma virus. *Anal Bioanal Chem*, 390, 1373-8.
- BANERJEE, S., BHARAJ, P., SULLENDER, W., KABRA, S. K. & BROOR, S. 2007. Human metapneumovirus infections among children with acute respiratory infections seen in a large referral hospital in India. *J Clin Virol*, 38, 70-2.
- BARBER, A. L. & FORAN, D. R. 2006. The utility of whole genome amplification for typing compromised forensic samples. *J Forensic Sci*, 51, 1344-9.
- BARRETT, J. C. & KAWASAKI, E. S. 2003. Microarrays: the use of oligonucleotides and cDNA for the analysis of gene expression. *Drug Discov Today*, 8, 134-41.
- BARRY, J. M. 2004. The site of origin of the 1918 influenza pandemic and its public health implications. *J Transl Med*, 2, 3.
- BERGEN, A. W., HAQUE, K. A., QI, Y., BEERMAN, M. B., GARCIA-CLOSAS, M., ROTHMAN, N. & CHANOCK, S. J. 2005. Comparison of yield and genotyping performance of multiple displacement amplification and OmniPlex whole genome amplified DNA generated from multiple DNA sources. *Hum Mutat*, 26, 262-70.
- BERGER, M. F. & BULYK, M. L. 2009. Universal protein-binding microarrays for the comprehensive characterization of the DNA-binding specificities of transcription factors. *Nat Protoc*, 4, 393-411.
- BERTINO, J. S. 2002. Cost burden of viral respiratory infections: issues for formulary decision makers. *Am J Med*, 112 Suppl 6A, 42S-49S.
- BHARAJ, P., SULLENDER, W. M., KABRA, S. K., MANI, K., CHERIAN, J., TYAGI, V., CHAHAR, H. S., KAUSHIK, S., DAR, L. & BROOR, S. 2009. Respiratory viral infections detected by multiplex PCR among pediatric

- patients with lower respiratory tract infections seen at an urban hospital in Delhi from 2005 to 2007. *Virology*, 6, 89.
- BIACCHESI, S., SKIADOPOULOS, M. H., BOIVIN, G., HANSON, C. T., MURPHY, B. R., COLLINS, P. L. & BUCHHOLZ, U. J. 2003. Genetic diversity between human metapneumovirus subgroups. *Virology*, 315, 1-9.
- BIG, C., REINECK, L. A. & ARONOFF, D. M. 2009. Viral infections of the central nervous system: a case-based review. *Clin Med Res*, 7, 142-6.
- BINGA, E. K., LASKEN, R. S. & NEUFELD, J. D. 2008. Something from (almost) nothing: the impact of multiple displacement amplification on microbial ecology. *ISME J*, 2, 233-41.
- BORISKIN, Y. S., RICE, P. S., STABLER, R. A., HINDS, J., AL-GHUSEIN, H., VASS, K. & BUTCHER, P. D. 2004. DNA microarrays for virus detection in cases of central nervous system infection. *J Clin Microbiol*, 42, 5811-8.
- BOROS, A., PANKOVICS, P., SIMMONDS, P. & REUTER, G. 2011. Novel positive-sense, single-stranded RNA (+ssRNA) virus with di-cistronic genome from intestinal content of freshwater carp (*Cyprinus carpio*). *PLoS One*, 6, e29145.
- BOWTELL, D. D. 1999. Options available--from start to finish--for obtaining expression data by microarray. *Nat Genet*, 21, 25-32.
- BROWN, P. O. & BOTSTEIN, D. 1999. Exploring the new world of the genome with DNA microarrays. *Nat Genet*, 21, 33-7.
- CALL, D. 2001a. DNA microarrays--their mode of action and possible applications in molecular diagnostics. *Veterinary Sciences Tomorrow*
- CALL, D. J. 2001b. DNA microarrays - their mode of action and possible applications in molecular diagnosis. *Veterinary Sciences Tomorrow*, 1-9.
- CALL, D. R., CHANDLER, D. P. & BROCKMAN, F. 2001. Fabrication of DNA microarrays using unmodified oligonucleotide probes. *Biotechniques*, 30, 368-72, 374, 376 passim.
- CARTER, J. B. & SAUNDERS, V. A. 2007. *Virology Principles and Applications*, Chichester, John Wiley & Sons Ltd.
- CASAS, I., POZO, F., TRALLERO, G., ECHEVARRIA, J. M. & TENORIO, A. 1999. Viral diagnosis of neurological infection by RT multiplex PCR: a search for entero- and herpesviruses in a prospective study. *J Med Virol*, 57, 145-51.
- CASSADY, K. & WHITLEY, R. 2004. Pathogenesis and Pathophysiology of Viral Infections of the Central Nervous System. In: SCHELD, W., MARRA, C. & WHITLEY, R. (eds.) *Infections of the Central Nervous System*. 4th ed. London: Wolter Kluwer Health.
- CHADWICK, D. R. 2005. Viral meningitis. *Br Med Bull*, 75-76, 1-14.
- CHARLTON, B., CROSSLEY, B. & HIETALA, S. 2009. Conventional and future diagnostics for avian influenza. *Comp Immunol Microbiol Infect Dis*, 32, 341-50.

- CHIU, C. Y., URISMAN, A., GREENHOW, T. L., ROUSKIN, S., YAGI, S., SCHNURR, D., WRIGHT, C., DREW, W. L., WANG, D., WEINTRUB, P. S., DERISI, J. L. & GANEM, D. 2008. Utility of DNA microarrays for detection of viruses in acute respiratory tract infections in children. *J Pediatr*, 153, 76-83.
- CHIU, S. K., HSU, M., KU, W. C., TU, C. Y., TSENG, Y. T., LAU, W. K., YAN, R. Y., MA, J. T. & TZENG, C. M. 2003. Synergistic effects of epoxy- and amine-silanes on microarray DNA immobilization and hybridization. *Biochem J*, 374, 625-32.
- CHONMAITREE, T., BALDWIN, C. D. & LUCIA, H. L. 1989. Role of the virology laboratory in diagnosis and management of patients with central nervous system disease. *Clin Microbiol Rev*, 2, 1-14.
- CHUNG, J. Y., HAN, T. H., KIM, S. W., KIM, C. K. & HWANG, E. S. 2007. Detection of viruses identified recently in children with acute wheezing. *J Med Virol*, 79, 1238-43.
- CLEMENTI, M. 2000. Quantitative molecular analysis of virus expression and replication. *J Clin Microbiol*, 38, 2030-6.
- COLLIER, L. & OXFORD, J. 2000. *Human Virology*, Oxford, Oxford University Press.
- COLLINS, P. L. & KARRON, R. A. 2013. Respiratory Syncytial virus and Metapneumovirus. In: KNIPE, D. & HOWLEY, P. (eds.) *Fields Virology*. 6th ed. London: Walters Kluwer Health / Lippincott Williams & Wilkins.
- CONDIT, R. 2013. Principles of Virology. In: KNIPE, D. & HOWLEY, P. (eds.) *Fields Virology*. 6th ed. London: Walters Kluwer Health / Lippincott Williams & Wilkins.
- CORNISH-BOWDEN, A. 1985. Nomenclature for incompletely specified bases in nucleic acid sequences: recommendations 1984. *Nucleic Acids Res*, 13.
- DAI, H., MEYER, M., STEPANIANTS, S., ZIMAN, M. & STOUGHTON, R. 2002. Use of hybridization kinetics for differentiating specific from non-specific binding to oligonucleotide microarrays. *Nucleic Acids Res*, 30.
- DAWSON, E. D., MOORE, C. L., SMAGALA, J. A., DANKBAR, D. M., MEHLMANN, M., TOWNSEND, M. B., SMITH, C. B., COX, N. J., KUCHTA, R. D. & ROWLEN, K. L. 2006. MChip: a tool for influenza surveillance. *Anal Chem*, 78, 7610-5.
- DE MURO, M. A. 2005. Probe Design, Production, and Applications. In: WALKER, J. M. & RAPLEY, R. (eds.) *Medical Biomethods Handbook*. 5 ed. New Jersey: Humana Press.
- DEAN, F. B., HOSONO, S., FANG, L., WU, X., FARUQI, A. F., BRAY-WARD, P., SUN, Z., ZONG, Q., DU, Y., DU, J., DRISCOLL, M., SONG, W., KINGSMORE, S. F., EGHOLM, M. & LASKEN, R. S. 2002. Comprehensive human genome amplification using multiple displacement amplification. *Proc Natl Acad Sci U S A*, 99, 5261-6.



- DEAN, F. B., NELSON, J. R., GIESLER, T. L. & LASKEN, R. S. 2001. Rapid amplification of plasmid and phage DNA using Phi 29 DNA polymerase and multiply-primed rolling circle amplification. *Genome Res*, 11, 1095-9.
- DEBIASI, R. L. & TYLER, K. L. 2004. Molecular methods for diagnosis of viral encephalitis. *Clin Microbiol Rev*, 17, 903-25, table of contents.
- DIAZ-HORTA, O., SARMIENTO, L., BAJ, A., CABRERA-RODE, E. & TONIOLO, A. 2011. Echovirus Epidemics, Autoimmunity, and Type 1 Diabetes. In: WAGNER, D. (ed.) *Type 1 Diabetes - Pathogenesis, Genetics and Immunotherapy*. Croatia: INTECH.
- DUGGAN, D. J., BITTNER, M., CHEN, Y., MELTZER, P. & TRENT, J. M. 1999. Expression profiling using cDNA microarrays. *Nat Genet*, 21, 10-4.
- DWYER, D. E., SMITH, D. W., CATTON, M. G. & BARR, I. G. 2006. Laboratory diagnosis of human seasonal and pandemic influenza virus infection. *Med J Aust*, 185, S48-53.
- EHRENREICH, A. 2006. DNA microarray technology for the microbiologist: an overview. *Appl Microbiol Biotechnol*, 73, 255-73.
- EKINS, R. P. 1989. Multi-analyte immunoassay. *J Pharm Biomed Anal*, 7, 155-68.
- ELNIFRO, E. M., ASHSHI, A. M., COOPER, R. J. & KLAPPER, P. E. 2000. Multiplex PCR: optimization and application in diagnostic virology. *Clin Microbiol Rev*, 13, 559-70.
- ESPY, M. J., UHL, J. R., SLOAN, L. M., BUCKWALTER, S. P., JONES, M. F., VETTER, E. A., YAO, J. D., WENGENACK, N. L., ROSENBLATT, J. E., COCKERILL, F. R., 3RD & SMITH, T. F. 2006. Real-time PCR in clinical microbiology: applications for routine laboratory testing. *Clin Microbiol Rev*, 19, 165-256.
- EUSCHER, E., DAVIS, J., HOLZMAN, I. & NUOVO, G. J. 2001. Coxsackie virus infection of the placenta associated with neurodevelopmental delays in the newborn. *Obstet Gynecol*, 98, 1019-26.
- EVERTSZ, E. M., AU-YOUNG, J., RUVOLO, M. V., LIM, A. C. & REYNOLDS, M. A. 2001. Hybridization cross-reactivity within homologous gene families on glass cDNA microarrays. *Biotechniques*, 31, 1182, 1184, 1186 passim.
- FLINT, S., ENQUIST, L., RACANNIELLO, V. & SKALKA, A. 2009. *Principles of Virology*, Washington, American Society for Microbiology.
- FORTINA, P., CHENG, J., KRICKA, L. J., WATERS, L. C., JACOBSON, S. C., WILDING, P. & RAMSEY, J. M. 2001. DOP-PCR amplification of whole genomic DNA and microchip-based capillary electrophoresis. *Methods Mol Biol*, 163, 211-9.
- FOTIN, A. V., DROBYSHEV, A. L., PROUDNIKOV, D. Y., PEROV, A. N. & MIRZABEKOV, A. D. 1998. Parallel thermodynamic analysis of duplexes on oligodeoxyribonucleotide microchips. *Nucleic Acids Res*, 26, 1515-21.

- FOUCHIER, R. A., RIMMELZWAAN, G. F., KUIKEN, T. & OSTERHAUS, A. D. 2005. Newer respiratory virus infections: human metapneumovirus, avian influenza virus, and human coronaviruses. *Curr Opin Infect Dis*, 18, 141-6.
- FRESHNEY, R. 2000. *Culture of animal cells*, New York, Wiley-Liss.
- FUJII, Y., GOTO, H., WATANABE, T., YOSHIDA, T. & KAWAOKA, Y. 2003. Selective incorporation of influenza virus RNA segments into virions. *Proc Natl Acad Sci U S A*, 100, 2002-7.
- GARBINO, J., GERBASE, M. W., WUNDERLI, W., KOLAROVA, L., NICOD, L. P., ROCHAT, T. & KAISER, L. 2004. Respiratory viruses and severe lower respiratory tract complications in hospitalized patients. *Chest*, 125, 1033-9.
- GARMAN, E. & LAVER, G. 2004. Controlling influenza by inhibiting the virus's neuraminidase. *Curr Drug Targets*, 5, 119-36.
- GARMAN, E. & LAVER, G. 2005. The Structure, Function, and Inhibition of Influenza Virus Neuraminidase. In: FISCHER, W. (ed.) *Viral Membrane Proteins: Structure, Function, and Drug Design*. New York: Kluwer Academic / Plenum Publishers.
- GEISS, G. K., BUMGARNER, R. E., AN, M. C., AGY, M. B., VAN 'T WOUT, A. B., HAMMERSMARK, E., CARTER, V. S., UPCHURCH, D., MULLINS, J. I. & KATZE, M. G. 2000. Large-scale monitoring of host cell gene expression during HIV-1 infection using cDNA microarrays. *Virology*, 266, 8-16.
- GERHOLD, D. L., JENSEN, R. V. & GULLANS, S. R. 2002. Better therapeutics through microarrays. *Nat Genet*, 32 Suppl, 547-51.
- GERN, J. E. & PALMENBERG, A. C. 2013. Rhinoviruses. In: KNIPE, D. & HOWLEY, P. (eds.) *Fields Virology*. 6th ed. London: Walters Kluwer Health / Lippincott Williams & Wilkins.
- GILLIM-ROSS, L. & SUBBARAO, K. 2006. Emerging respiratory viruses: challenges and vaccine strategies. *Clin Microbiol Rev*, 19, 614-36.
- GLEZEN, W. P., TABER, L. H., FRANK, A. L. & KASEL, J. A. 1986. Risk of primary infection and reinfection with respiratory syncytial virus. *Am J Dis Child*, 140, 543-6.
- GOLDSMITH, C. S. & MILLER, S. E. 2009. Modern uses of electron microscopy for detection of viruses. *Clin Microbiol Rev*, 22, 552-63.
- GRANDIEN, M. 1996. Viral diagnosis by antigen detection techniques. *Clin Diagn Virol*, 5, 81-90.
- GUAN, J., CHAN, M., MA, B., GRENIER, C., WILKIE, D. C., PASICK, J., BROOKS, B. W. & SPENCER, J. L. 2008. Development of methods for detection and quantification of avian influenza and Newcastle disease viruses in compost by real-time reverse transcription polymerase chain reaction and virus isolation. *Poult Sci*, 87, 838-43.
- GUERRERO-PLATA, A. 2013. Dendritic cells in human Pneumovirus and Metapneumovirus infections. *Viruses*, 5, 1553-70.

- HADIDI, A., CZOSNEK, H. & BARBA, M. 2004. DNA microarrays and their Potential Applications for the Detection of Plant Viruses, Viroids, and Phytoplasmas. *Plant Pathology*, 86, 97-104.
- HAGEDOORN, R., JOSEPH, R., KASANMOENTALIB, S., EILERS, P., KILLIAN, J. & RAAP, A. K. 2003. Chemical RNA labeling without 3' end bias using fluorescent cis-platin compounds. *Biotechniques*, 34, 974-6, 978, 980.
- HALL, C. B., WEINBERG, G. A., IWANE, M. K., BLUMKIN, A. K., EDWARDS, K. M., STAAT, M. A., AUINGER, P., GRIFFIN, M. R., POEHLING, K. A., ERDMAN, D., GRIJALVA, C. G., ZHU, Y. & SZILAGYI, P. 2009. The burden of respiratory syncytial virus infection in young children. *N Engl J Med*, 360, 588-98.
- HAZELTON, P. R. & GELDERBLOM, H. R. 2003. Electron microscopy for rapid diagnosis of infectious agents in emergent situations. *Emerg Infect Dis*, 9, 294-303.
- HEGDE, P., QI, R., ABERNATHY, K., GAY, C., DHARAP, S., GASPARD, R., HUGHES, J. E., SNESRUD, E., LEE, N. & QUACKENBUSH, J. 2000. A concise guide to cDNA microarray analysis. *Biotechniques*, 29, 548-50, 552-4, 556 passim.
- HEIKKINEN, T., OSTERBACK, R., PELTOLA, V., JARTTI, T. & VAINIONPAA, R. 2008. Human metapneumovirus infections in children. *Emerg Infect Dis*, 14, 101-6.
- HEISE, M. & VIRGIN, H. 2013. Pathogenesis of Viral Infection. In: KNIPE, D. & HOWLEY, P. (eds.) *Fields Virology*. 6th ed. London Walters Kluwer Health / Lippincott Williams & Wilkins.
- HELLER, M. J. 2002. DNA microarray technology: devices, systems, and applications. *Annu Rev Biomed Eng*, 4, 129-53.
- HELLER, R. A., SCHENA, M., CHAI, A., SHALON, D., BEDILION, T., GILMORE, J., WOOLLEY, D. E. & DAVIS, R. W. 1997. Discovery and analysis of inflammatory disease-related genes using cDNA microarrays. *Proc Natl Acad Sci U S A*, 94, 2150-5.
- HERNANDEZ-RODRIGUEZ, P., DIAZ, C. A., DALMAU, E. A. & QUINTERO, G. M. 2011. A comparison between polymerase chain reaction (PCR) and traditional techniques for the diagnosis of leptospirosis in bovines. *J Microbiol Methods*, 84, 1-7.
- HO-PUN-CHEUNG, A., BASCOUL-MOLLEVI, C., ASSENAT, E., BOISSIERE-MICHOT, F., BIBEAU, F., CELLIER, D., YCHOU, M. & LOPEZ-CRAPEZ, E. 2009. Reverse transcription-quantitative polymerase chain reaction: description of a RIN-based algorithm for accurate data normalization. *BMC Mol Biol*, 10, 31.
- HOSONO, S., FARUQI, A. F., DEAN, F. B., DU, Y., SUN, Z., WU, X., DU, J., KINGSMORE, S. F., EGHOLM, M. & LASKEN, R. S. 2003. Unbiased whole-genome amplification directly from clinical samples. *Genome Res*, 13, 954-64.

- HOWBROOK, D. N., VAN DER VALK, A. M., O'SHAUGHNESSY, M. C., SARKER, D. K., BAKER, S. C. & LLOYD, A. W. 2003. Developments in microarray technologies. *Drug Discov Today*, 8, 642-51.
- HSIUNG, G. D. 1984. Diagnostic virology: from animals to automation. *Yale J Biol Med*, 57, 727-33.
- [HTTP://WWW.ICTVONLINE.ORG/INDEX.ASP](http://www.ictvonline.org/index.asp). 2009. Virus Taxonomy [Online]. International Committee on Taxonomy of Viruses [Accessed 10 April 2010].
- HUANG, Y., TANG, H., DUFFY, S., HONG, Y., NORMAN, S., GHOSH, M., HE, J., BOSE, M., HENRICKSON, K. J., FAN, J., KRAFT, A. J., WEISBURG, W. G. & MATHER, E. L. 2009. Multiplex assay for simultaneously typing and subtyping influenza viruses by use of an electronic microarray. *J Clin Microbiol*, 47, 390-6.
- HUGHES, T. R., MAO, M., JONES, A. R., BURCHARD, J., MARTON, M. J., SHANNON, K. W., LEFKOWITZ, S. M., ZIMAN, M., SCHELTER, J. M., MEYER, M. R., KOBAYASHI, S., DAVIS, C., DAI, H., HE, Y. D., STEPHANIANTS, S. B., CAVET, G., WALKER, W. L., WEST, A., COFFEY, E., SHOEMAKER, D. D., STOUGHTON, R., BLANCHARD, A. P., FRIEND, S. H. & LINSLEY, P. S. 2001. Expression profiling using microarrays fabricated by an ink-jet oligonucleotide synthesizer. *Nat Biotechnol*, 19, 342-7.
- HYOTY, H. & TAYLOR, K. W. 2002. The role of viruses in human diabetes. *Diabetologia*, 45, 1353-61.
- IRANI, D. N. 2008. Aseptic meningitis and viral myelitis. *Neurol Clin*, 26, 635-55, vii-viii.
- JAFRI, H. S., WU, X., MAKARI, D. & HENRICKSON, K. J. 2013. Distribution of respiratory syncytial virus subtypes A and B among infants presenting to the emergency department with lower respiratory tract infection or apnea. *Pediatr Infect Dis J*, 32, 335-40.
- JAHN, C. E., CHARKOWSKI, A. O. & WILLIS, D. K. 2008. Evaluation of isolation methods and RNA integrity for bacterial RNA quantitation. *J Microbiol Methods*, 75, 318-24.
- JAYAPAL, M. & MELENDEZ, A. J. 2006. DNA microarray technology for target identification and validation. *Clin Exp Pharmacol Physiol*, 33, 496-503.
- JENSEN, C. & JOHNSON, F. B. 1994. Comparison of various transport media for viability maintenance of herpes simplex virus, respiratory syncytial virus, and adenovirus. *Diagn Microbiol Infect Dis*, 19, 137-42.
- JOHNSON, N. P. & MUELLER, J. 2002. Updating the accounts: global mortality of the 1918-1920 "Spanish" influenza pandemic. *Bull Hist Med*, 76, 105-15.
- JOHNSTON, S. L., PATTEMORE, P. K., SANDERSON, G., SMITH, S., LAMPE, F., JOSEPHS, L., SYMINGTON, P., O'TOOLE, S., MYINT, S. H., TYRRELL, D. A. & ET AL. 1995. Community study of role of viral

- infections in exacerbations of asthma in 9-11 year old children. *BMJ*, 310, 1225-9.
- KAHN, J. S. 2006. Epidemiology of human metapneumovirus. *Clin Microbiol Rev*, 19, 546-57.
- KANE, M. D., JATKOE, T. A., STUMPF, C. R., LU, J., THOMAS, J. D. & MADORE, S. J. 2000. Assessment of the sensitivity and specificity of oligonucleotide (50mer) microarrays. *Nucleic Acids Res*, 28, 4552-7.
- KANNANGAI, R., ABRAHAM, A. M., SANKAR, S. & SRIDHARAN, G. 2010. Nanotechnology tools for single-virus particle detection. *Indian J Med Microbiol*, 28, 95-9.
- KASLOW, R. & EVANS, A. 1997. Epidemiologic Concepts and Methods. In: EVANS, A. & KASLOW, R. (eds.) *Viral Infections of Humans: Epidemiology and Control*. 4th ed. New York: Plenum Publishing Corporation.
- KELLER, G. H., HUANG, D. P. & MANAK, M. M. 1989. Labeling of DNA probes with a photoactivatable hapten. *Anal Biochem*, 177, 392-5.
- KESSLER, N., FERRARIS, O., PALMER, K., MARSH, W. & STEEL, A. 2004. Use of the DNA flow-thru chip, a three-dimensional biochip, for typing and subtyping of influenza viruses. *J Clin Microbiol*, 42, 2173-85.
- KHAN, S., CHATURVEDI, S., GOEL, N., BAWA, S., DRABU, S. 2010. Review: DNA Microarray Technology and Drug Development. *Conservation & Society*, 1, 1-5.
- KHODAKOV, D. A., ZAKHAROVA, N. V., GRYADUNOV, D. A., FILATOV, F. P., ZASEDATELEV, A. S. & MIKHAILOVICH, V. M. 2008. An oligonucleotide microarray for multiplex real-time PCR identification of HIV-1, HBV, and HCV. *Biotechniques*, 44, 241-6, 248.
- KITTLER, R., STONEKING, M. & KAYSER, M. 2002. A whole genome amplification method to generate long fragments from low quantities of genomic DNA. *Anal Biochem*, 300, 237-44.
- KLAASSEN, C. H., PRINSEN, C. F., DE VALK, H. A., HORREVORTS, A. M., JEUNINK, M. A. & THUNNISSEN, F. B. 2004. DNA microarray format for detection and subtyping of human papillomavirus. *J Clin Microbiol*, 42, 2152-60.
- KLEINSCHMIDT-DEMASTERS, B. K., DEBIASI, R. L. & TYLER, K. L. 2001. Polymerase chain reaction as a diagnostic adjunct in herpesvirus infections of the nervous system. *Brain Pathol*, 11, 452-64.
- KNIGHT, J. 2001. When the chips are down. *Nature*, 410, 860-1.
- KOLMODIN, L. A. & BIRCH, D. E. 2002. Polymerase chain reaction. Basic principles and routine practice. *Methods Mol Biol*, 192, 3-18.
- KONONEN, J., BUBENDORF, L., KALLIONIEMI, A., BARLUND, M., SCHRAML, P., LEIGHTON, S., TORHORST, J., MIHATSCH, M. J.,

- SAUTER, G. & KALLIONIEMI, O. P. 1998. Tissue microarrays for high-throughput molecular profiling of tumor specimens. *Nat Med*, 4, 844-7.
- KORTEWEG, C. & GU, J. 2008. Pathology, molecular biology, and pathogenesis of avian influenza A (H5N1) infection in humans. *Am J Pathol*, 172, 1155-70.
- KOSKINIEMI, M., PIIPARINEN, H., RANTALAIHO, T., ERANKO, P., FARKKILA, M., RAIHA, K., SALONEN, E. M., UKKONEN, P. & VAHERI, A. 2002. Acute central nervous system complications in varicella zoster virus infections. *J Clin Virol*, 25, 293-301.
- KSIAZEK, T. G., ERDMAN, D., GOLDSMITH, C. S., ZAKI, S. R., PERET, T., EMERY, S., TONG, S., URBANI, C., COMER, J. A., LIM, W., ROLLIN, P. E., DOWELL, S. F., LING, A. E., HUMPHREY, C. D., SHIEH, W. J., GUARNER, J., PADDOCK, C. D., ROTA, P., FIELDS, B., DERISI, J., YANG, J. Y., COX, N., HUGHES, J. M., LEDUC, J. W., BELLINI, W. J. & ANDERSON, L. J. 2003. A novel coronavirus associated with severe acute respiratory syndrome. *N Engl J Med*, 348, 1953-66.
- KUIKEN, T., FOUCHIER, R., RIMMELZWAAN, G. & OSTERHAUS, A. 2003. Emerging viral infections in a rapidly changing world. *Curr Opin Biotechnol*, 14, 641-6.
- KUMAR, R. 2009. The Widely Used Diagnostics "DNA Microarray"-A Review. *American Journal of Infectious Diseases*, 5.
- LAGE, J. M., LEAMON, J. H., PEJOVIC, T., HAMANN, S., LACEY, M., DILLON, D., SEGRAVES, R., VOSSBRINCK, B., GONZALEZ, A., PINKEL, D., ALBERTSON, D. G., COSTA, J. & LIZARDI, P. M. 2003. Whole genome analysis of genetic alterations in small DNA samples using hyperbranched strand displacement amplification and array-CGH. *Genome Res*, 13, 294-307.
- LAMSON, D., RENWICK, N., KAPOOR, V., LIU, Z., PALACIOS, G., JU, J., DEAN, A., ST GEORGE, K., BRIESE, T. & LIPKIN, W. I. 2006. MassTag polymerase-chain-reaction detection of respiratory pathogens, including a new rhinovirus genotype, that caused influenza-like illness in New York State during 2004-2005. *J Infect Dis*, 194, 1398-402.
- LANDER, E. S. 1999. Array of hope. *Nat Genet*, 21, 3-4.
- LEDFORD, R. M., PATEL, N. R., DEMENCZUK, T. M., WATANYAR, A., HERBERTZ, T., COLLETT, M. S. & PEVEAR, D. C. 2004. VP1 sequencing of all human rhinovirus serotypes: insights into genus phylogeny and susceptibility to antiviral capsid-binding compounds. *J Virol*, 78, 3663-74.
- LELAND, D. S. & GINOCCHIO, C. C. 2007. Role of cell culture for virus detection in the age of technology. *Clin Microbiol Rev*, 20, 49-78.
- LI, X., GU, W., MOHAN, S. & BAYLINK, D. J. 2002. DNA microarrays: their use and misuse. *Microcirculation*, 9, 13-22.
- LINDE, A., KLAPPER, P. E., MONTEYNE, P., ECHEVARRIA, J. M., CINQUE, P., ROZENBERG, F., VESTERGAARD, B. F., CIARDI, M., LEBON, P. & CLEATOR, G. M. 1997. Specific diagnostic methods for herpesvirus infections of the central nervous system: a consensus review by the European

- Union Concerted Action on Virus Meningitis and Encephalitis. *Clin Diagn Virol*, 8, 83-104.
- LINHART, C. & SHAMIR, R. 2002. The degenerate primer design problem *Bioinformatics* 18, S172-S180.
- LIU, H. H., CAO, X., YANG, Y., LIU, M. G. & WANG, Y. F. 2006. Array-based nano-amplification technique was applied in detection of hepatitis E virus. *J Biochem Mol Biol*, 39, 247-52.
- LIU, W. T., GUO, H. & WU, J. H. 2007. Effects of target length on the hybridization efficiency and specificity of rRNA-based oligonucleotide microarrays. *Appl Environ Microbiol*, 73, 73-82.
- LODES, M. J., SUCIU, D., WILMOTH, J. L., ROSS, M., MUNRO, S., DIX, K., BERNARDS, K., STOVER, A. G., QUINTANA, M., IIHOSHI, N., LYON, W. J., DANLEY, D. L. & MCSHEA, A. 2007. Identification of upper respiratory tract pathogens using electrochemical detection on an oligonucleotide microarray. *PLoS One*, 2, e924.
- LOPEZ-CAMPOS, G., COIRAS, M., SANCHEZ-MERINO, J. P., LOPEZ-HUERTAS, M. R., SPITERI, I., MARTIN-SANCHEZ, F. & PEREZ-BRENA, P. 2007. Oligonucleotide microarray design for detection and serotyping of human respiratory adenoviruses by using a virtual amplicon retrieval software. *J Virol Methods*, 145, 127-36.
- LOVMAR, L. & SYVANEN, A. C. 2006. Multiple displacement amplification to create a long-lasting source of DNA for genetic studies. *Hum Mutat*, 27, 603-14.
- LU, H. Z., BLOCH, K. C. & TANG, Y. W. 2002. Molecular Techniques in the Diagnosis of Central Nervous System Infections. *Curr Infect Dis Rep*, 4, 339-350.
- LUTHRA, R. & MEDEIROS, L. J. 2004. Isothermal multiple displacement amplification: a highly reliable approach for generating unlimited high molecular weight genomic DNA from clinical specimens. *J Mol Diagn*, 6, 236-42.
- MACKAY, I. M. 2004. Real-time PCR in the microbiology laboratory. *Clin Microbiol Infect*, 10, 190-212.
- MACKIE, P. L. 2003. The classification of viruses infecting the respiratory tract. *Paediatr Respir Rev*, 4, 84-90.
- MAHONY, J. B. 2008. Detection of Respiratory Viruses by Molecular Methods. *Clinical Microbiology Reviews.*, 21, 32.
- MAJTAN, T., BUKOVSKA, G. & TIMKO, J. 2004. DNA microarrays--techniques and applications in microbial systems. *Folia Microbiol (Praha)*, 49, 635-64.
- MALANOSKI, A. P., LIN, B., WANG, Z., SCHNUR, J. M. & STENGER, D. A. 2006. Automated identification of multiple micro-organisms from resequencing DNA microarrays. *Nucleic Acids Res*, 34, 5300-11.

- MANJARREZ-ZAVALA, M., ROSETE-OLVERA, D., GUTIÉRREZ-GONZÁLEZ, L., OCADIZ-DELGADO, R. & CABELLO-GUTIÉRREZ, C. 2013. Pathogenesis of Viral Respiratory Infection. In: MAHBOUB, B. & VATS, M. (eds.) Respiratory Disease and Infection - A New Insight. London: InTech.
- MARAGH, S., JAKUPCIAK, J. P., WAGNER, P. D., ROM, W. N., SIDRANSKY, D., SRIVASTAVA, S. & O'CONNELL, C. D. 2008. Multiple strand displacement amplification of mitochondrial DNA from clinical samples. *BMC Med Genet*, 9, 7.
- MARSTON, D. A., MCELHINNEY, L. M., ELLIS, R. J., HORTON, D. L., WISE, E. L., LEECH, S. L., DAVID, D., DE LAMBALLERIE, X. & FOOKS, A. R. 2013. Next generation sequencing of viral RNA genomes. *BMC Genomics*, 14, 444.
- MASKOS, U. & SOUTHERN, E. M. 1992. Oligonucleotide hybridizations on glass supports: a novel linker for oligonucleotide synthesis and hybridization properties of oligonucleotides synthesised in situ. *Nucleic Acids Res*, 20, 1679-84.
- MAUGHAN, N. J., LEWIS, F. A. & SMITH, V. 2001. An introduction to arrays. *J Pathol*, 195, 3-6.
- MEHLMANN, M., TOWNSEND, M. B., STEARS, R. L., KUCHTA, R. D. & ROWLEN, K. L. 2005. Optimization of fragmentation conditions for microarray analysis of viral RNA. *Anal Biochem*, 347, 316-23.
- MELNICK, J. L. & PHILLIPS, C. A. 1970. Enteroviruses: vaccines, epidemiology, diagnosis, classification. *CRC Crit Rev Clin Lab Sci*, 1, 87-118.
- MICHOS, A. G., SYRIOPOULOU, V. P., HADJICHRISTODOULOU, C., DAIKOS, G. L., LAGONA, E., DOURIDAS, P., MOSTROU, G. & THEODORIDOU, M. 2007. Aseptic meningitis in children: analysis of 506 cases. *PLoS One*, 2, e674.
- MIKHAILOVICH, V., GRYADUNOV, D., KOLCHINSKY, A., MAKAROV, A. A. & ZASEDATELEV, A. 2008. DNA microarrays in the clinic: infectious diseases. *Bioessays*, 30, 673-82.
- MILLER, M. B. & TANG, Y. W. 2009. Basic concepts of microarrays and potential applications in clinical microbiology. *Clin Microbiol Rev*, 22, 611-33.
- MIZUTANI, T., ENDOH, D., OKAMOTO, M., SHIRATO, K., SHIMIZU, H., ARITA, M., FUKUSHI, S., SAJO, M., SAKAI, K., LIM, C. K., ITO, M., NEROME, R., TAKASAKI, T., ISHII, K., SUZUKI, T., KURANE, I., MORIKAWA, S. & NISHIMURA, H. 2007. Rapid genome sequencing of RNA viruses. *Emerg Infect Dis*, 13, 322-4.
- MONSTEIN, H. J., OLSSON, C., NILSSON, I., GRAHN, N., BENONI, C. & AHRNE, S. 2005. Multiple displacement amplification of DNA from human colon and rectum biopsies: bacterial profiling and identification of *Helicobacter pylori*-DNA by means of 16S rDNA-based TTGE and pyrosequencing analysis. *J Microbiol Methods*, 63, 239-47.



- MORENS, D. M. & FAUCI, A. S. 2007. The 1918 influenza pandemic: insights for the 21st century. *J Infect Dis*, 195, 1018-28.
- MORI, M., MIMORI, K., YOSHIKAWA, Y., SHIBUTA, K., UTSUNOMIYA, T., SADANAGA, N., TANAKA, F., MATSUYAMA, A., INOUE, H. & SUGIMACHI, K. 2002. Analysis of the gene-expression profile regarding the progression of human gastric carcinoma. *Surgery*, 131, S39-47.
- MORSHED, M. G., LEE, M. K., JORGENSEN, D. & ISAAC-RENTON, J. L. 2007. Molecular methods used in clinical laboratory: prospects and pitfalls. *FEMS Immunol Med Microbiol*, 49, 184-91.
- MUECKSTEIN, U., LEPARC, G. G., POSEKANY, A., HOFACKER, I. & KREIL, D. P. 2010. Hybridization thermodynamics of NimbleGen microarrays. *BMC Bioinformatics*, 11, 35.
- MUIR, P., KAMMERER, U., KORN, K., MULDER, M. N., POYRY, T., WEISSBRICH, B., KANDOLF, R., CLEATOR, G. M. & VAN LOON, A. M. 1998. Molecular typing of enteroviruses: current status and future requirements. The European Union Concerted Action on Virus Meningitis and Encephalitis. *Clin Microbiol Rev*, 11, 202-27.
- MULLIS, K. B. 1990. The unusual origin of the polymerase chain reaction. *Sci Am*, 262, 56-61, 64-5.
- MURRAY, P. R., ROSENTHAL, K. S. & PFALLER, M. A. 2009. *Medical Microbiology*, Philadelphia, Mosby Elsevier.
- NAEF, F. & MAGNASCO, M. O. 2003. Solving the riddle of the bright mismatches: labeling and effective binding in oligonucleotide arrays. *Phys Rev E Stat Nonlin Soft Matter Phys*, 68, 011906.
- NAGLER, F. P. & RAKE, G. 1948. The Use of the Electron Microscope in Diagnosis of Variola, Vaccinia, and Varicella. *J Bacteriol*, 55, 45-51.
- NAKASHIMA, N. & ISHIBASHI, J. 2010. Identification of the 3C-protease-mediated 2A/2B and 2B/2C cleavage sites in the nonstructural polyprotein precursor of a Dicistrovirus lacking the NPGP motif. *Arch Virol*, 155, 1477-82.
- NICHOL, S. T., ARIKAWA, J. & KAWAOKA, Y. 2000. Emerging viral diseases. *Proc Natl Acad Sci U S A*, 97, 12411-2.
- NIESTERS, H. G. 2002. Clinical virology in real time. *J Clin Virol*, 25 Suppl 3, S3-12.
- NISSEN, M. D. & SLOOTS, T. P. 2002. Rapid diagnosis in pediatric infectious diseases: the past, the present and the future. *Pediatr Infect Dis J*, 21, 605-12; discussion 613-4.
- NOKES, D. J., OKIRO, E. A., NGAMA, M., WHITE, L. J., OCHOLA, R., SCOTT, P. D., CANE, P. A. & MEDLEY, G. F. 2004. Respiratory syncytial virus epidemiology in a birth cohort from Kilifi district, Kenya: infection during the first year of life. *J Infect Dis*, 190, 1828-32.
- NORDBERG, E. K. 2005. YODA: selecting signature oligonucleotides. *Bioinformatics*, 21, 1365-70.

- NORDSTROM, H., FALK, K. I., LINDEGREN, G., MOUZAVI-JAZI, M., WALDEN, A., ELGH, F., NILSSON, P. & LUNDKVIST, A. 2005. DNA microarray technique for detection and identification of seven flaviviruses pathogenic for man. *J Med Virol*, 77, 528-40.
- NYGAARD, V., LOLAND, A., HOLDEN, M., LANGAAS, M., RUE, H., LIU, F., MYKLEBOST, O., FODSTAD, O., HOVIG, E. & SMITH-SORENSEN, B. 2003. Effects of mRNA amplification on gene expression ratios in cDNA experiments estimated by analysis of variance. *BMC Genomics*, 4, 11.
- O'CONNELL, K. P., BUCHER, J. R., ANDERSON, P. E., CAO, C. J., KHAN, A. S., GOSTOMSKI, M. V. & VALDES, J. J. 2006. Real-time fluorogenic reverse transcription-PCR assays for detection of bacteriophage MS2. *Appl Environ Microbiol*, 72, 478-83.
- OBERSTE, M. S., MAHER, K., KILPATRICK, D. R. & PALLANSCH, M. A. 1999. Molecular evolution of the human enteroviruses: correlation of serotype with VP1 sequence and application to picornavirus classification. *J Virol*, 73, 1941-8.
- OBERSTE, M. S., PENARANDA, S., MAHER, K. & PALLANSCH, M. A. 2004. Complete genome sequences of all members of the species Human enterovirus A. *J Gen Virol*, 85, 1597-607.
- OHUMA, E. O., OKIRO, E. A., OCHOLA, R., SANDE, C. J., CANE, P. A., MEDLEY, G. F., BOTTOMLEY, C. & NOKES, D. J. 2012. The natural history of respiratory syncytial virus in a birth cohort: the influence of age and previous infection on reinfection and disease. *Am J Epidemiol*, 176, 794-802.
- OSTERHAUS, A. D. 2008. New respiratory viruses of humans. *Pediatr Infect Dis J*, 27, S71-4.
- PALESE, P. & SHAW, M. 2013. Orthomyxoviridae In: KNIFE, D. & HOWLEY, P. (eds.) *Fields Virology*. 6th ed. London: Walters Kluwer Health / Lippincott Williams & Wilkins.
- PAPENBURG, J., HAMELIN, M. E., OUHOUMMANE, N., CARBONNEAU, J., OUAKKI, M., RAYMOND, F., ROBITAILLE, L., CORBEIL, J., CAQUETTE, G., FRENETTE, L., DE SERRES, G. & BOIVIN, G. 2012. Comparison of risk factors for human metapneumovirus and respiratory syncytial virus disease severity in young children. *J Infect Dis*, 206, 178-89.
- PARIJA, S. C. 2009. Orthomyxoviruses. *Textbook of Microbiology & Immunology Haryana: Elsevier*.
- PEIRIS, J. S. & MADELEY, C. R. 2009. Respiratory Viruses. In: COOK, G. C. & ZUMLA, A. I. (eds.) *Manson's Tropical Diseases*. 22nd ed. Edinburgh: Saunders Elsevier.
- PEPLIES, J., GLOCKNER, F. O. & AMANN, R. 2003. Optimization strategies for DNA microarray-based detection of bacteria with 16S rRNA-targeting oligonucleotide probes. *Appl Environ Microbiol*, 69, 1397-407.
- PEYTAVI, R., RAYMOND, F. R., GAGNE, D., PICARD, F. J., JIA, G., ZOVAL, J., MADOU, M., BOISSINOT, K., BOISSINOT, M., BISSONNETTE, L.,

- OUELLETTE, M. & BERGERON, M. G. 2005. Microfluidic device for rapid (<15 min) automated microarray hybridization. *Clin Chem*, 51, 1836-44.
- POGGIO, G. P., RODRIGUEZ, C., CISTERNA, D., FREIRE, M. C. & CELLO, J. 2000. Nested PCR for rapid detection of mumps virus in cerebrospinal fluid from patients with neurological diseases. *J Clin Microbiol*, 38, 274-8.
- POKORN, M. 2003. Pathogenesis and Classification of Central Nervous System Infection. *The Journal of the International Federation of Clinical Chemistry and Laboratory Medicine*, 15, 1-4.
- PORTER, A. G., SMITH, J. C. & EMTAGE, J. S. 1980. Nucleotide sequence of influenza virus RNA segment 8 indicates that coding regions for NS1 and NS2 proteins overlap. *Proc Natl Acad Sci U S A*, 77, 5074-8.
- PUSKAS, L. G., ZVARA, A., HACKLER, L., JR. & VAN HUMMELEN, P. 2002. RNA amplification results in reproducible microarray data with slight ratio bias. *Biotechniques*, 32, 1330-4, 1336, 1338, 1340.
- QUAN, P. L., PALACIOS, G., JABADO, O. J., CONLAN, S., HIRSCHBERG, D. L., POZO, F., JACK, P. J., CISTERNA, D., RENWICK, N., HUI, J., DRYSDALE, A., AMOS-RITCHIE, R., BAUMEISTER, E., SAVY, V., LAGER, K. M., RICHT, J. A., BOYLE, D. B., GARCIA-SASTRE, A., CASAS, I., PEREZ-BRENA, P., BRIESE, T. & LIPKIN, W. I. 2007. Detection of respiratory viruses and subtype identification of influenza A viruses by GreeneChipResp oligonucleotide microarray. *J Clin Microbiol*, 45, 2359-64.
- RABENAU, H. F., KESSLER, H. H., KORTENBUSCH, M., STEINHORST, A., RAGGAM, R. B. & BERGER, A. 2007. Verification and validation of diagnostic laboratory tests in clinical virology. *J Clin Virol*, 40, 93-8.
- RACANIELLO, V. 2013. Picornaviridae: The Viruses and Their Replication. In: KNIPE, D. & HOWLEY, P. (eds.) *Fields Virology*. 6th ed. London: Walters Kluwer Health / Lippincott Williams & Wilkins.
- RAMERS, C., BILLMAN, G., HARTIN, M., HO, S. & SAWYER, M. H. 2000. Impact of a diagnostic cerebrospinal fluid enterovirus polymerase chain reaction test on patient management. *JAMA*, 283, 2680-5.
- RATUSHNA, V. G., WELLER, J. W. & GIBAS, C. J. 2005. Secondary structure in the target as a confounding factor in synthetic oligomer microarray design. *BMC Genomics*, 6, 31.
- REDINGTON, J. J. & TYLER, K. L. 2002. Viral infections of the nervous system, 2002: update on diagnosis and treatment. *Arch Neurol*, 59, 712-8.
- RHOADES, R. E., TABOR-GODWIN, J. M., TSUENG, G. & FEUER, R. 2011. Enterovirus infections of the central nervous system. *Virology*, 411, 288-305.
- RICKMAN, D. S., BOBEK, M. P., MISEK, D. E., KUICK, R., BLAIVAS, M., KURNIT, D. M., TAYLOR, J. & HANASH, S. M. 2001. Distinctive molecular profiles of high-grade and low-grade gliomas based on oligonucleotide microarray analysis. *Cancer Res*, 61, 6885-91.

- RUBINS, J. B. 2003. Alveolar macrophages: wielding the double-edged sword of inflammation. *Am J Respir Crit Care Med*, 167, 103-4.
- RUSSELL, R. 2003. Designing microarray oligonucleotide probes. *Brief Bioinform*, 4, 361-7.
- SACHSE, K., HOTZEL, H., SLICKERS, P., ELLINGER, T. & EHRLICH, R. 2005. DNA microarray-based detection and identification of *Chlamydia* and *Chlamydomonas* spp. *Mol Cell Probes*, 19, 41-50.
- SATO, K., TANABE, T. & OHYA, M. 2010. How to Classify Influenza A Viruses and Understand Their Severity. *Open Systems & Information Dynamics*, 17.
- SCHEINA, M., SHALON, D., DAVIS, R. W. & BROWN, P. O. 1995. Quantitative monitoring of gene expression patterns with a complementary DNA microarray. *Science*, 270, 467-70.
- SENGUPTA, S., ONODERA, K., LAI, A. & MELCHER, U. 2003. Molecular detection and identification of influenza viruses by oligonucleotide microarray hybridization. *J Clin Microbiol*, 41, 4542-50.
- SEVERGNINI, M., CREMONESI, P., CONSOLANDI, C., BELLIS, G., CASTIGLIONI, B. 2011. Advances in DNA Microarray Technology for the Detection of Foodborn Pathogens. *Food Bioprocess Technol*, 4, 936-953.
- SHCHEPINOV, M. S., CASE-GREEN, S. C. & SOUTHERN, E. M. 1997. Steric factors influencing hybridisation of nucleic acids to oligonucleotide arrays. *Nucleic Acids Res*, 25, 1155-61.
- SHIEH, B. & LI, C. 2004. Multi-faceted, multi-versatile microarray: simultaneous detection of many viruses and their expression profiles. *Retrovirology*, 1, 11.
- SHOAIB, M., BACONNAIS, S., MECHOLD, U., LE CAM, E., LIPINSKI, M. & OGRYZKO, V. 2008. Multiple displacement amplification for complex mixtures of DNA fragments. *BMC Genomics*, 9, 415.
- SIMMONDS, P. 2006. Recombination and selection in the evolution of picornaviruses and other Mammalian positive-stranded RNA viruses. *J Virol*, 80, 11124-40.
- SINGH, R., MAGANTI, R. J., JABBA, S. V., WANG, M., DENG, G., HEATH, J. D., KURN, N. & WANGEMANN, P. 2005. Microarray-based comparison of three amplification methods for nanogram amounts of total RNA. *Am J Physiol Cell Physiol*, 288, C1179-89.
- SOUTHERN, E., MIR, K. & SHCHEPINOV, M. 1999. Molecular interactions on microarrays. *Nat Genet*, 21, 5-9.
- SPITS, C., LE CAIGNEC, C., DE RYCKE, M., VAN HAUTE, L., VAN STEIRTEGHEM, A., LIEBAERS, I. & SERMON, K. 2006. Whole-genome multiple displacement amplification from single cells. *Nat Protoc*, 1, 1965-70.
- STEARNS, R. L., GETTS, R. C. & GULLANS, S. R. 2000. A novel, sensitive detection system for high-density microarrays using dendrimer technology. *Physiol Genomics*, 3, 93-9.

- STEINHAEUER, D. A. & SKEHEL, J. J. 2002. Genetics of influenza viruses. *Annu Rev Genet*, 36, 305-32.
- STORCH, G. A. 2000. Diagnostic virology. *Clin Infect Dis*, 31, 739-51.
- SUNDARAM, C., SHANKAR, S. K., THONG, W. K. & PARDO-VILLAMIZAR, C. A. 2011. Pathology and diagnosis of central nervous system infections. *Patholog Res Int*, 2011, 878263.
- TANG, Y. W., PROCOP, G. W. & PERSING, D. H. 1997. Molecular diagnostics of infectious diseases. *Clin Chem*, 43, 2021-38.
- TAUBENBERGER, J. K. & MORENS, D. M. 2008. The pathology of influenza virus infections. *Annu Rev Pathol*, 3, 499-522.
- TEBRUEGGE, M. & CURTIS, N. 2009. Enterovirus infections in neonates. *Semin Fetal Neonatal Med*, 14, 222-7.
- THOMPSON, W. W., SHAY, D. K., WEINTRAUB, E., BRAMMER, L., COX, N., ANDERSON, L. J. & FUKUDA, K. 2003. Mortality associated with influenza and respiratory syncytial virus in the United States. *JAMA*, 289, 179-86.
- THWEATT, R., GOLDSTEIN, S. & SHMOOKLER REIS, R. J. 1990. A universal primer mixture for sequence determination at the 3' ends of cDNAs. *Anal Biochem*, 190, 314-6.
- TODT, S. & BLOHM, D. H. 2009. Immobilization chemistries. *Methods Mol Biol*, 529, 81-100.
- TREVINO, V., FALCIANI, F. & BARRERA-SALDANA, H. A. 2007. DNA microarrays: a powerful genomic tool for biomedical and clinical research. *Mol Med*, 13, 527-41.
- TSAI, H. P., KUO, P. H., LIU, C. C. & WANG, J. R. 2001. Respiratory viral infections among pediatric inpatients and outpatients in Taiwan from 1997 to 1999. *J Clin Microbiol*, 39, 111-8.
- TYLER, K. L. 2009. Emerging viral infections of the central nervous system: part 1. *Arch Neurol*, 66, 939-48.
- UDA, A., TANABAYASHI, K., FUJITA, O., HOTTA, A., YAMAMOTO, Y. & YAMADA, A. 2007. Comparison of whole genome amplification methods for detecting pathogenic bacterial genomic DNA using microarray. *Jpn J Infect Dis*, 60, 355-61.
- URAKAWA, H., EL FANTROUSSI, S., SMIDT, H., SMOOT, J. C., TRIBOU, E. H., KELLY, J. J., NOBLE, P. A. & STAHL, D. A. 2003. Optimization of single-base-pair mismatch discrimination in oligonucleotide microarrays. *Appl Environ Microbiol*, 69, 2848-56.
- VAN DEN HOOGEN, B. G., DE JONG, J. C., GROEN, J., KUIKEN, T., DE GROOT, R., FOUCHIER, R. A. & OSTERHAUS, A. D. 2001. A newly discovered human pneumovirus isolated from young children with respiratory tract disease. *Nat Med*, 7, 719-24.

- VAN DEN HOOGEN, B. G., HERFST, S., SPRONG, L., CANE, P. A., FORLEONETO, E., DE SWART, R. L., OSTERHAUS, A. D. & FOUCHIER, R. A. 2004. Antigenic and genetic variability of human metapneumoviruses. *Emerg Infect Dis*, 10, 658-66.
- VAN ELDEN, L. J., NIJHUIS, M., SCHIPPER, P., SCHUURMAN, R. & VAN LOON, A. M. 2001. Simultaneous detection of influenza viruses A and B using real-time quantitative PCR. *J Clin Microbiol*, 39, 196-200.
- VAN ROOYEN, C. E. & SCOTT, G. D. 1948. Smallpox diagnosis with special reference to electron microscopy. *Can J Public Health*, 39, 467-77.
- VORA, G. J., MEADOR, C. E., STENGER, D. A. & ANDREADIS, J. D. 2004. Nucleic acid amplification strategies for DNA microarray-based pathogen detection. *Appl Environ Microbiol*, 70, 3047-54.
- WAGNER, E. K. & HEWLETT, M. J. 2008. *Basic Virology*, London, Blackwell Science.
- WANG, D., COSCOY, L., ZYLBERBERG, M., AVILA, P. C., BOUSHEY, H. A., GANEM, D. & DERISI, J. L. 2002. Microarray-based detection and genotyping of viral pathogens. *Proc Natl Acad Sci U S A*, 99, 15687-92.
- WANG, D., URISMAN, A., LIU, Y. T., SPRINGER, M., KSIAZEK, T. G., ERDMAN, D. D., MARDIS, E. R., HICKENBOTHAM, M., MAGRINI, V., ELDRED, J., LATREILLE, J. P., WILSON, R. K., GANEM, D. & DERISI, J. L. 2003. Viral discovery and sequence recovery using DNA microarrays. *PLoS Biol*, 1, E2.
- WANG, D. G., FAN, J. B., SIAO, C. J., BERNO, A., YOUNG, P., SAPOLSKY, R., GHANDOUR, G., PERKINS, N., WINCHESTER, E., SPENCER, J., KRUGLYAK, L., STEIN, L., HSIE, L., TOPALOGLOU, T., HUBBELL, E., ROBINSON, E., MITTMANN, M., MORRIS, M. S., SHEN, N., KILBURN, D., RIOUX, J., NUSBAUM, C., ROZEN, S., HUDSON, T. J., LIPSHUTZ, R., CHEE, M. & LANDER, E. S. 1998. Large-scale identification, mapping, and genotyping of single-nucleotide polymorphisms in the human genome. *Science*, 280, 1077-82.
- WANG, E. 2005. RNA amplification for successful gene profiling analysis. *J Transl Med*, 3, 28.
- WANG, J., VAN NOSTRAND, J. D., WU, L., HE, Z., LI, G. & ZHOU, J. 2011. Microarray-based evaluation of whole-community genome DNA amplification methods. *Appl Environ Microbiol*, 77, 4241-5.
- WANG, Z., MALANOSKI, A. P., LIN, B., KIDD, C., LONG, N. C., BLANEY, K. M., THACH, D. C., TIBBETTS, C. & STENGER, D. A. 2008. Resequencing microarray probe design for typing genetically diverse viruses: human rhinoviruses and enteroviruses. *BMC Genomics*, 9, 577.
- WATERS, D. L. & SHAPTER, F. M. 2014. The polymerase chain reaction (PCR): general methods. *Methods Mol Biol*, 1099, 65-75.

- WATSON, A., MAZUMDER, A., STEWART, M. & BALASUBRAMANIAN, S. 1998. Technology for microarray analysis of gene expression. *Curr Opin Biotechnol*, 9, 609-14.
- WEBSTER, R. G., BEAN, W. J., GORMAN, O. T., CHAMBERS, T. M. & KAWAOKA, Y. 1992. Evolution and ecology of influenza A viruses. *Microbiol Rev*, 56, 152-79.
- WEI, T., PEARSON, M. N., ARMSTRONG, K., BLOHM, D. & LIU, J. 2012. Analysis of crucial factors resulting in microarray hybridization failure. *Mol Biosyst*, 8, 1325-38.
- WHITE, D. O. & FENNER, F. J. 1994. *Orthomyxoviridae. Medical virology*. 4th ed. San Diego: Academic Press.
- WILLEY, J., SHERWOOD, L. & WOOLVERTON, C. 2008. Prescott, Harley, and Klein's Microbiology, London, McGraw-Hill Higher Education.
- WILSON, W. J., STROUT, C. L., DESANTIS, T. Z., STILWELL, J. L., CARRANO, A. V. & ANDERSEN, G. L. 2002. Sequence-specific identification of 18 pathogenic microorganisms using microarray technology. *Mol Cell Probes*, 16, 119-27.
- WRIGHT, P., NEUMANN, G. & KAWAOKA, Y. 2013. Orthomyxoviruses. In: KNIPE, D. & HOWLEY, P. (eds.) *Fields Virology*. 6th ed. London: Walters Kluwer Health / Lippincott Williams & Wilkins.
- WU, L., LIU, X., SCHADT, C. W. & ZHOU, J. 2006. Microarray-based analysis of subnanogram quantities of microbial community DNAs by using whole-community genome amplification. *Appl Environ Microbiol*, 72, 4931-41.
- YOLKEN, R. H., COUTLEE, F. & VISCIDI, R. P. 1989. New prospects for the diagnosis of viral infections. *Yale J Biol Med*, 62, 131-9.
- YOO, S. M., CHOI, J. H., LEE, S. Y. & YOO, N. C. 2009. Applications of DNA microarray in disease diagnostics. *J Microbiol Biotechnol*, 19, 635-46.
- ZAJAC, A., SONG, D., QIAN, W. & ZHUKOV, T. 2007. Protein microarrays and quantum dot probes for early cancer detection. *Colloids Surf B Biointerfaces*, 58, 309-14.
- ZAMMATTEO, N., JEANMART, L., HAMELS, S., COURTOIS, S., LOUETTE, P., HEVESI, L. & REMACLE, J. 2000. Comparison between different strategies of covalent attachment of DNA to glass surfaces to build DNA microarrays. *Anal Biochem*, 280, 143-50.
- ZHANG, L., WU, C., CARTA, R. & ZHAO, H. 2007. Free energy of DNA duplex formation on short oligonucleotide microarrays. *Nucleic Acids Res*, 35, e18.
- ZHENG, Y. M., WANG, N., LI, L. & JIN, F. 2011. Whole genome amplification in preimplantation genetic diagnosis. *J Zhejiang Univ Sci B*, 12, 1-11.
- ZHENG, Z. B., WU, Y. D., YU, X. L. & SHANG, S. Q. 2008. DNA microarray technology for simultaneous detection and species identification of seven human herpes viruses. *J Med Virol*, 80, 1042-50.

ZHOU, J. & THOMPSON, D. K. 2002. Challenges in applying microarrays to environmental studies. *Curr Opin Biotechnol*, 13, 204-7.